Postnatal Development of the Primate Prefrontal Cortex (areas 9 and 46): Maturation of Pyramidal Neurons and Serotonergic Innervation in Layer 3.

THESIS SUBMITTED FOR Ph.D.

by JOHN DAVID CLASSEY.

Institute of Ophthalmology.
University College of London.

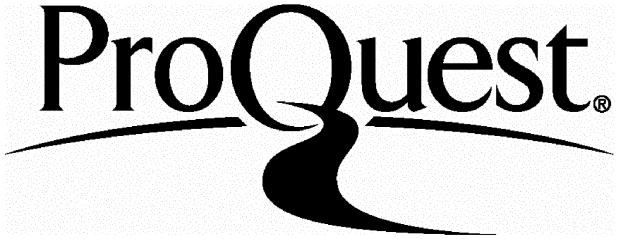

CONTENTS

LIST OF FIGURES.

Figure no. Page.

LIST OF TABLES.

1.4: Abstract.

The dorsolateral prefrontal cortex (DLPFC) of the monkey brain exhibits a unique combination of intraareal and interareal connections, as well as distinctive neuronal properties, which correlate with diverse cognitive and mnemonic behaviours. Many of these attributes are found in the homologous region of the human brain. This thesis describes and compares the developmental time courses of two important components of the cortical circuitry in the monkey DLPFC: pyramidal neurons providing extensive, elaborately-patterned intrinsic connections in the superficial layers and the serotonin (5-HT) innervation in the same region. We hope that the results from these studies will contribute to a model of the human DLPFC; aiding the understanding of complex interactions within the DLPFC during postnatal development. The layer 3 pyramidal neurons providing intrinsic lattice connectivity within layers 1-3, are also the sources and targets for efferent and afferent corticocortical connections between the DLPFC and the rest of the brain. The postnatal time course of maturation for layer 3 pyramidal neurons was quantified by means of the changes in the relative density of their dendritic spines, which represent the postsynaptic sites of excitatory (asymmetric) synapses. We compared the developmental sequence for dendritic spines to the time courses of maturation for other components of layer 3 circuitry, e.g. asymmetric synapses, inhibitory parvalbumin-immunoreactive (PV-IR) cartridges, dopaminergic (DAergic) axons and we comment on possible implications for observed temporal similarities or differences between them. Layer 3 is also the site of a dense 5-HTergic axon innervation, which originates from the mid-brain raphe nuclei and comprises 2 classes of axon fibres ("thick" and "thin"). We examined the time-scale of postnatal development for 5-HTergic axons in layer 3 and attempted to find temporal correlation's between 5-HT axon maturation and pyramidal neuron dendritic spine development, as well as with previously examined layer 3 components, including DAergic axons and 5-HT tissue concentration. Findings included the demonstration of concurrent time courses of maturation for dendritic spines and PV-IR cartridges; synchrony between rates of spine and excitatory synapse production in the first 2 postnatal months and a subsequent plateau phase, but different time periods of decline (from 1.5 and 3.0 years, respectively) and complex relationships between the stages of spine maturation and changes in density of DAergic axons coinciding with the rise (birth-2 months) and fall (1.5-4.6 years) of spine numbers. We also demonstrated temporal interrelations between 5-HTergic axon development and that of other neuropil components, including modulatory interaction between the density of 5-HTergic axons and dendritic spines as well as strong reciprocal correlation's between the 5-HTergic and DAergic axon innervations.

2.0: Introduction.

2.1: The prefrontal cortex in the primate brain.

The prefrontal cortex (PFC) of the primate brain is an anatomically and physiologically heterogeneous region, which occupies 29% of the entire cerebral cortex in humans (Brodmann, 1909; **see updated map Figure 1A**) and 11.5% of the total in non-human primates such as the macaque monkey (Brodmann, 1905, 1912; **see updated map Figure 1B**). The large size of the PFC, together with the profound functional deficits observed in patients with surgically or disease-induced prefrontal lesions, demonstrate the PFC to be an extremely important cognitively-related region of the human cerebral cortex. In the monkey brain, one major sub-region of the PFC, the dorsolateral (DL)PFC (area 46; **see Figure 1B**) has been well characterised as being the locus for working memory function as has been observed for normal human subjects, as demonstrated by performance in delayed response tasks, which are analogous to aspects of human decision making (**see section 2.3**).

The monkey PFC is composed of many cytoarchitectonically distinguishable areas or sub-regions, which have been defined by various schemes of nomenclature, each differing slightly in their cytoarchitectonic criteria (Brodmann, 1909; Vogt and Vogt, 1919; Walker, 1940; von Bonin and Bailey, 1947, **see Figure 2**). More recently the anatomical divisions have been recognised to possess their own functionally distinct physiological properties (reviewed by Fuster, 1989 and Goldman-Rakic, 1987a). In addition, continued anatomical research has led to further subdivision of the Walker-defined areas (Barbas and Pandya, 1989; Preuss and Goldman-Rakic, 1991; Carmichael and Price, 1994; Petrides and Pandya, 1994; Pandya and Yeterian, 1996a; **see Figure 1B**).

Cytoarchitectonically, the monkey PFC shows a significant diversity of structure in adjacent areas; dorsal areas tend to be granular (i.e. showing a distinct layer 4 of densely packed small cells, in Nissl-stained tissue) but the ventral areas are agranular in structure (i.e. layer 4 is not so distinct in Nissl-stained tissue). In addition, even areas within this dorsal-ventral dichotomy show subtle differences; such that caudal areas in both locations seem to be less differentiated, i.e. not so clear in their overall laminar organisation, whilst areas more rostrally located, are the most differentiated in terms of the structure and clarity of their laminae. In the mediolateral axis of the PFC, the dorsolateral areas are more differentiated than the dorsomedial and the ventrolateral areas are more differentiated than the ventromedial areas (Barbas and Pandya, 1989; Pandya and Yeterian, 1990; Barbas and Pandya, 1991; Barbas, 1992). The existence of a continuum of increasingly distinctive laminar structure progressing from the caudal to rostral PFC areas and from the medially to the laterally

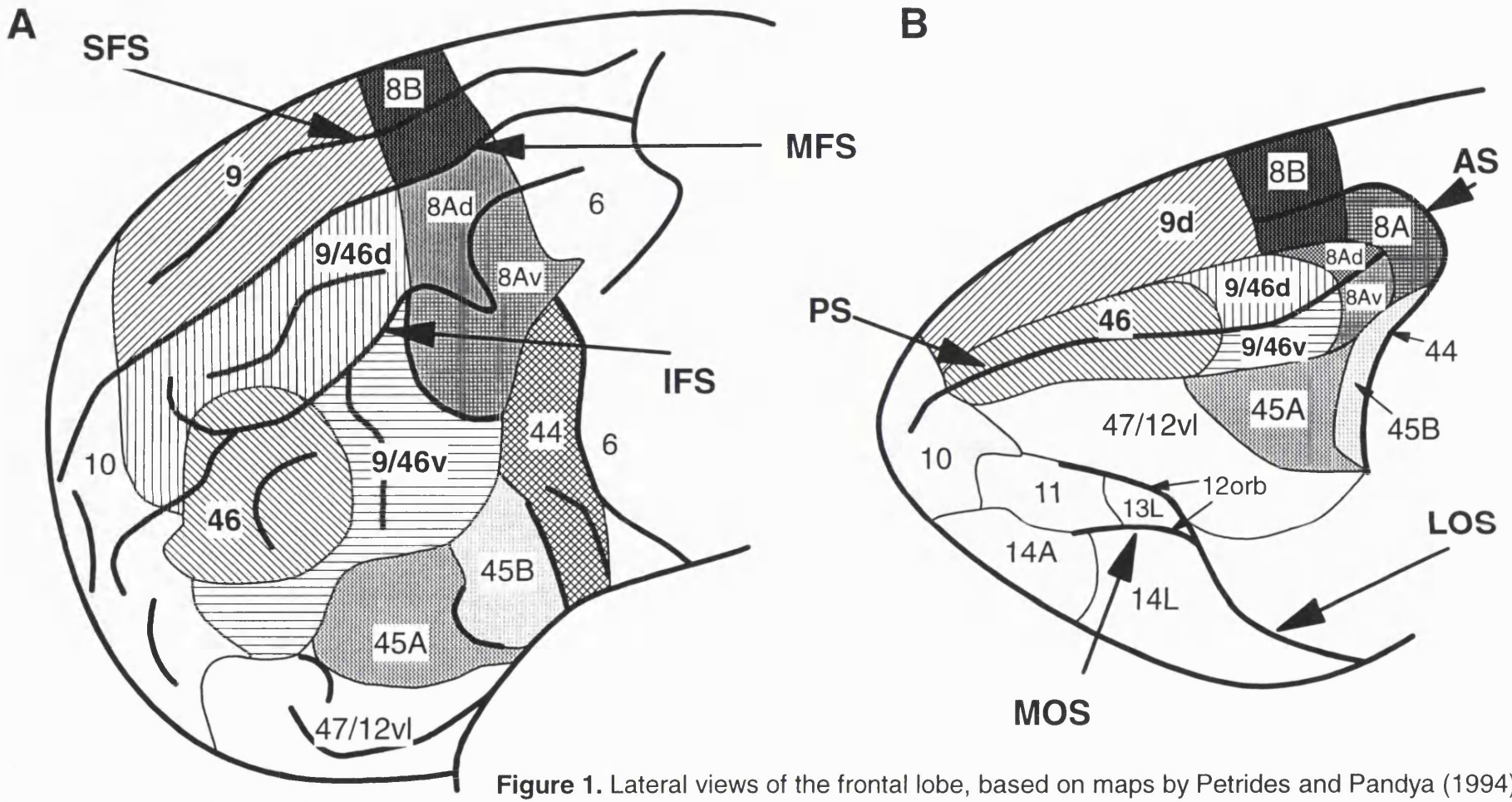

Figure 1. Lateral views of the frontal lobe, based on maps by Petrides and Pandya (1994). **(A)** The human brain and **(B)** The Macaque monkey brain, illustrating the striking similarities of the cytoarchitectonic organisation within these two primate species (based on the observation of cellular and laminar organisation in nissl-stained sections. Rostral is left and caudal is right in both diagrams. AS = arcuate sulcus. IFS = inferior frontal sulcus. LOS = lateral orbital sulcus. MFS = middle frontal sulcus. MOS = medial orbital sulcus. PS = principal sulcus. SFS = superior fromtal sulcus.

located PFC areas and from the ventral to dorsal PFC areas shows the dorsolateral PFC to be the most differentiated sub-region of the PFC and the ventromedial PFC to be the least differentiated sub-region.

With respect to this thesis, where areas 9 and 46 were examined, the cytoarchitectonic structure of these areas has previously been described to be very similar in many aspects (reviewed in Barbas, 1992). There is not a clear-cut border between the 2 areas, but rather there is evidence of a gradual change in the laminar architecture between the 2 areas, both in the human and monkey prefrontal cortex (Petrides and Pandya, 1994). For this reason, to all intents and purposes areas 9 and 46 are often viewed together as a single region - the dorsal prefrontal cortex - with lateral (areas 9/46) and medial (area 9) components. We have taken this view into account in this first study of the thesis, such that spine density measures from individual pyramidal neurons in areas 9 and 46 were pooled within each animal to obtain an overall mean value of relative spine density over postnatal development for the dorsal PFC.

2.2: Concurrent development: Same maturational time course within all cortical areas.

The "concurrent hypothesis" of development is supported by studies in the macaque monkey which have examined the time courses for maturation of synaptic density (Rakic et al, 1986; reviewed in Rakic et al, 1994); callosal axons (LaMantia and Rakic, 1990); neurotransmitter tissue concentration (Brown and Goldman, 1977; Goldman-Rakic and Brown, 1982). There is also evidence for this global synchrony of brain maturation, from studies of functional development in the monkey, as measured by levels of performance in behavioural tasks evaluating either sensory, motor or cognitive abilities individually or in combination (reviewed in Goldman-Rakic, 1987b).

The studies of synaptogenesis (Rakic et al, 1986; Granger et al, 1995) have examined the primary visual, primary motor, primary somatosensory, dorsolateral prefrontal and cingulate cortices in detailed quantitative EM analyses of the time course for the attainment of mature synaptic numbers in all cortical layers using measures of synaptic density per unit volume and per unit area (for total, asymmetric and symmetric synapses). A concurrent time course of synaptogenesis has been demonstrated for asymmetric (excitatory) synapses in cortical layers 1-6 (most clearly for layers 1-3) within all the above cortical regions.

Generally for every layer of each area, the time course for asymmetric synapse development was as follows: synaptic density began to rise in the late prenatal period and continued to increase in postnatal life until 2 months of age when levels reached a peak or

"overshoot" (except in layer 6). The peak levels of synaptic density were consolidated between 2 months and 3.0 years of age (puberty), thereafter a gradual decline in the numbers of synapses was observed throughout adult life (oldest animal in this study was 20 years of age). Levels of total synaptic density followed a similar time course to that for asymmetric synapses in all regions examined (at least 80% of all cortical synapses are excitatory), whilst the overall numbers of symmetric (probably inhibitory) synapses did not change significantly in any region across the entire period of pre- and postnatal development.

Observations of concurrent maturation were also found for the tissue concentrations of monoaminergic neurotransmitters in biochemical analyses (Brown and Goldman, 1977; Goldman-Rakic and Brown, 1982) of various cortical regions including primary visual, primary motor, primary somatosensory, parietal, premotor, orbital and dorsolateral prefrontal cortices. The levels of dopamine, serotonin and noradrenaline in each region were observed to increase dramatically within the first 5 to 8 months of life, with some variation between individual regions in the exact rate of development, as well as more considerable differences in the changes in the concentrations of these neurotransmitters between 8 months and 3 years of age (onset of puberty).

Evidence from numerous behavioural studies in both monkeys and humans (reviewed in Goldman-Rakic, 1987b) has indicated that a synchronous rather than a sequential pattern of cortical maturation occurs in primates, with emergence of diverse "critical" sensory, motor and cognitive functions during the early postnatal period when levels of synaptic density are at their highest (2-4 months in monkeys; 8 months-2 years in human infants).

In monkeys, some of these observations have included the appearance of visual cortex-dependent functions such as visual-tracking of small stimuli, visually-guided reaching and differential recognition of facial features (Mendelson et al, 1983; Boothe et al, 1985) at between 6-8 weeks after birth. It is also around this time (i.e. 2 months of age) when visual object discrimination ability - characteristic of medial temporal lobe memory systems - first becomes evident in monkeys (Goldman et al, 1974; Bachevalier and Mishkin, 1984). Infant monkeys as young as 10 weeks old, were able to demonstrate adult-like abilities of the determination of size and texture in a tactile discrimination task (Carlson, 1984) indicative of a certain degree of primary somatosensory cortex maturation. Finally, the monkey DLPFC first exhibits signs of its most distinctive function at between 2-4 months of age, with regard to working memory ability in the delayed response task, object retrieval task and Piaget's A-not-B hiding task (Harlow et al, 1964; Diamond and Goldman-Rakic, 1986, 1989).

In humans, comparable tests of cortical functional development have shown

that the development of visual acuity as subserved by the primary visual cortex exhibits a "critical period" of plasticity within the first 2 years of life (reviewed in Garey, 1984). Emergence of functions such as visuospatially guided hand orientation and visually controlled preparation for grasping of objects have been demonstrated by infants of 4.5-8.5 months and 9-13 months respectively. In the first task, rapid learning was seen in the ability to adjust hand posture to the orientation of an object on the basis of visual inspection (von Hofsten and Fazel-Zandy, 1984) and in the second task, significant improvement in the ability to modify distance between thumb and fingers prior to contact with an object rather than in reaction to it (von Hofsten and Ronnqvist, 1988), was evident during the above period of development. In the case of medial temporal lobe and hippocampal functions, the ability to perform well in a visual-paired comparison task, by comparative recognition of novel objects, is present prior to 4-6 months in human infants (Overman et al, 1993) and also the ability to perform on single- and multiple-object discrimination is present by at least 12 months of age (Overman et al, 1992) if not as early as 5-6 months of age (Diamond, 1995). There is also evidence for some degree of recognition-memory emergence in the early postnatal period, as measured by successful performance in a reaching task-with-delay in infants as young as 6 months of age (Diamond et al, 1994). DLPFC-specific functions, as measured by the delayed response task and Piaget's A-not-B task appear to emerge between 7.5 and 12 months of age in human infants (Diamond and Doar, 1989; Diamond and Goldman-Rakic, 1989).

2.3: Hierarchical development: Different rates and periods of maturation within each cortical area.

The "hierarchical theory" of cortical maturation, which has been more traditionally accepted, is that different regions of the primate brain progressively mature, both anatomically and functionally at different rates during the course of postnatal life in the manner of a hierarchically-organised sequence. Observations which would support such a theory have been observed for levels of myelination in post-mortem brains (human: Flechsig,, 1920; Yakovlev and Lecours, 1967; monkey: Gibson, 1970; Quencer et al, 1980; Quencer, 1982; reviewed in Greenfield, 1991), myelination in MRI studies of humans (infants: Girard et al, 1991; Nomura et al, 1994; adolescents and adults: Nomura et al, 1994) and grey matter volume with MRI (children and adults: Jernigan et al, 1991; children and adolescents: Reiss et al, 1996).

There have been studies of synaptic density in various cortical regions (in human: Huttenlocher, 1979; Huttenlocher et al, 1982, 1993), synaptically-related proteins (in rat:

Alvarez-Bolado, 1996). Also there is supporting evidence from the maturational time course of neurotransmitter innervations (cat: Vu and Törk, 1992; monkey: Foote and Morrison, 1984 and present observations), calcium-binding protein-labelled (PV-IR) interneurons (Condé et al, 1996), a neurochemical subtype of pyramidal neurons (Kostovic et al, 1988), axonal projection pathways (Kostovic et al, 1983; LaMantia and Rakic, 1994) and cellular metabolic enzymes (Farkas-Bargeton and Diebler, 1978). Studies of levels of glucose metabolism in humans (infants: Chugani and Phelps, 1986; Chugani et al, 1987; adolescents and adults: Chiron et al, 1992) and monkeys (infants: Kennedy et al, 1982; adolescents: Kennedy et al, 1978; and of all ages: Jacobs et al, 1995; reviewed in Raleigh et al, 1996b; Distler et al, 1996) have also shown there to be different rates of energy-usage at a given age in different cortical regions.

Finally, functionally-related studies with electroencephalography (EEG) in humans (infants to adults: Thatcher et al, 1987; Feinberg et al, 1990; Hudspeth and Pribram, 1992), measurements of glucose metabolism following cognitive enrichment (juvenile monkeys: Raleigh et al, 1995, 1996b), while behavioural tasks of DLPFC function in humans (children: Casey et al, 1995; Luciana and Nelson, 1996) would seem to be convergent with the anatomical and metabolic data (reviewed in Kostovic et al, 1995).

In primates, the more posteriorly-situated primary sensory areas, such as primary visual, auditory and somatosensory cortices are thought to reach their adult state in many aspects, both anatomically and functionally, much earlier, i.e. within the 6 months of postnatal life in monkeys (over the first 3-4 years in humans), than the more anteriorly-located higher association areas, e.g. DLPFC, ventrolateral PFC and anterior cingulate cortices which are thought to reach maturity at later ages. In the case of the DLPFC, the final stage of functional and anatomical maturity is thought to occur at around the time of puberty (3 years of age) in monkeys (anatomically: Andersen et al, 1995; Rosenberg and Lewis, 1995; present thesis studies; functionally: Goldman and Alexander, 1977; Alexander, 1982; Kubota, 1993, 1994) and in humans at around 16-18 years of age (Uylings et al, 1995; reviewed in Kostovic, 1990; Kostovic et al, 1995).

By contrast, the orbitofrontal cortex is known to mature at a much earlier time, at around 7 months-1 year of age in monkeys (functionally: Goldman, 1972; Raleigh et al, 1996a). In the case of the primary motor cortex, the maturation of its functional properties (monkey: Lawrence and Hopkins, 1976; Armand et al, 1994; Olivier et al, 1997; Human: Muller et al, 1994) and anatomical projections (monkey: Galea and Darian-Smith, 1995; Armand et al, 1994; human: Amunts et al, 1995) are found to be achieved by some time

point intermediate to those for the primary sensory and most association regions. This idea has been given credence by the observation of functional and anatomical maturation of corticospinal projections from the hand region of primary motor cortex to the spinal cord by around 8-11 months of age in monkeys (Armand et al, 1994; Galea and Darian-Smith, 1995). In humans, the conductance velocity of afferent axonal pathways between median nerve fibres in the hand and the primary motor cortex mature between 5-7 years of age (Muller et al 1994), while the functional properties of the efferent pathway from the primary motor cortex to the nerves of the hand show a slightly longer time course of postnatal maturation, i.e. by around 10 years of age (Muller et al, 1994).

3.0: Anatomical connections of the DLPFC (area 46) in the macaque monkey.

3.1: Introduction: Afferent and efferent connections.

The PFC as a whole receives inputs from cortical and subcortical areas which each demonstrate a particular involvement in every possible sensory modality and sub-modality. These afferent projections converge on distinct areas of the PFC in accordance with their particular class of sensory information. We were concerned in this thesis with 2 areas of the DLPFC (areas 9 and 46; **see Figure 1B and Figures 3A and B**). The functional roles of area 9 are not well understood, although it is thought to be involved in sensorimotor integration and is known to be heavily interconnected with somatosensory, auditory, cingulate and extrastriate visual areas (Barbas, 1992). More is known regarding the functional and anatomical structure of area 46, which is primarily appears to receive visuospatially related information. It in addition receives auditory, somatosensory and object-related visual input. Most of the extensive corticocortical afferent inputs converging on area 46, originate from pyramidal neurons in the posterior parietal cortex (Petrides and Pandya, 1984; Barbas and Mesulam, 1985; Barbas, 1988; Cavada and Goldman-Rakic,1989b) and some sectors of the superior temporal association cortex (Barbas and Mesulam, 1985; Barbas, 1988; Seltzer and Pandya, 1989a).

These two heterogeneous cortical regions are known to consist respectively, of multiple visual-, visuomotor- or somatosensory-related (parietal) and visual- or polysensory-related (temporal) areas. These regions are linked by numerous reciprocal interconnections not only with the DLPFC (area 46) and the extrastriate visual regions (Morel and Bullier, 1990; Baizer et al, 1991). They are also mutually interconnected by way of pathways between their respective areas (Seltzer and Pandya, 1984; Neal et al, 1990; Seltzer and Pandya, 1994).

In addition to the primary reciprocal pathways between the DLPFC, the posterior

parietal region, the cortex of the superior temporal gyrus and the upper bank of the STS, there are numerous other PFC connections (Alexander et al, 1986, 1990; Pandya and Yeterian 1990; Barbas and Pandya, 1991). These other PFC interconnections fall into five major classes of pathways according to their primary functional specificity: those involving general motor control functions (i.e. cingulate motor areas; frontal and supplementary eye fields; premotor cortex and primary motor cortex).

Secondly, there are interconnections with subcortical and thalamic areas with a important motor component specifically concerned with spatially-guided behaviour, involving the lateral, dorsal and medial subdivisions of the pulvinar, the parvocellular division of the mediodorsal nucleus, the central portion of the striatum (caudate nucleus and putamen) and other basal ganglia nuclei e.g. the globus pallidus; claustrum as well as the dentate nucleus of the cerebellum.

The third major group of areas interconnected with the PFC are the medial temporal lobe areas with limbic, associative and procedural memory-related roles (amygdala; hippocampus; parahippocampal, perirhinal and entorhinal cortices).

The PFC is also interconnected with the superior temporal polysensory (TPO), concerned with multiple modality integration. Lastly, there are extrathalamic neurotransmitter pathway projections from the various mid-brain nuclei to the PFC which are also reciprocated by feedback projections from the PFC: the locus coeruleus (noradrenaline, NA); the ventral tegmental area (dopamine, DA); the dorsal and median raphe (serotonin, 5-HT) and the lateral septum (acetylcholine, ACh).

Study 1 of the thesis examines the time course of maturation of a population of pyramidal neurons in mid-layer 3 of dorsal areas 9 and 46 and in study 2 the postnatal development of 5-HTergic axons which innervate this same layer in ventral area 46. Since many of the corticocortical efferent projection pathways within the macaque monkey brain arise from pyramidal neurons in this layer and also many afferents terminate in layer 3, normally as part of a columnar distribution through all layers, it is of importance to describe in summary the complexity and diversity of these various afferent (incoming) and efferent (outgoing) projections. It is these extensive interconnections with other cortical (including other prefrontal areas) and subcortical regions which are an essential factor enabling the DLPFC to play a crucial integrative role in many aspects of cognitive and mnemonic processing (see Goldman-Rakic, 1987a; Fuster, 1989; Barbas, 1992; Goldman-Rakic, 1995b; Petrides, 1996 for reviews).

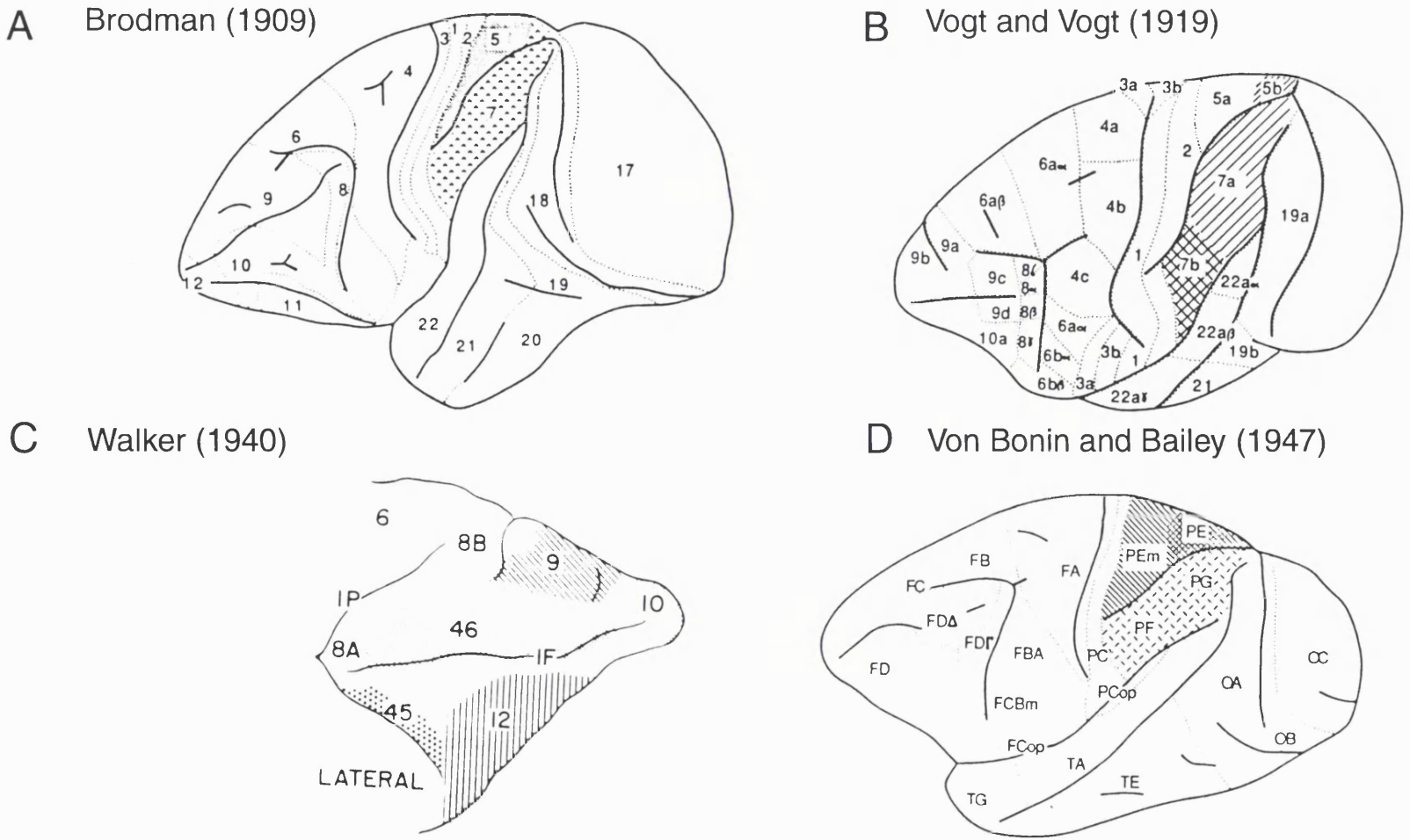

Figure 2 Lateral views of the macaque monkey brain illustrating the various early cytoarchitectonic schemes of the prefrontal cortex, (based on observations of cellular and laminar arrangements in nissl-stained sections) devised by different investigators. Walkers map **(C)** was the most widely used of these schemes until its recent revision by Petrides and Pandya, (1994). **(A), (B)** and **(D)** are orientated rostral (left) and caudal (right), whereas **(C)** is in the opposite orientation showing only the frontal lobe.

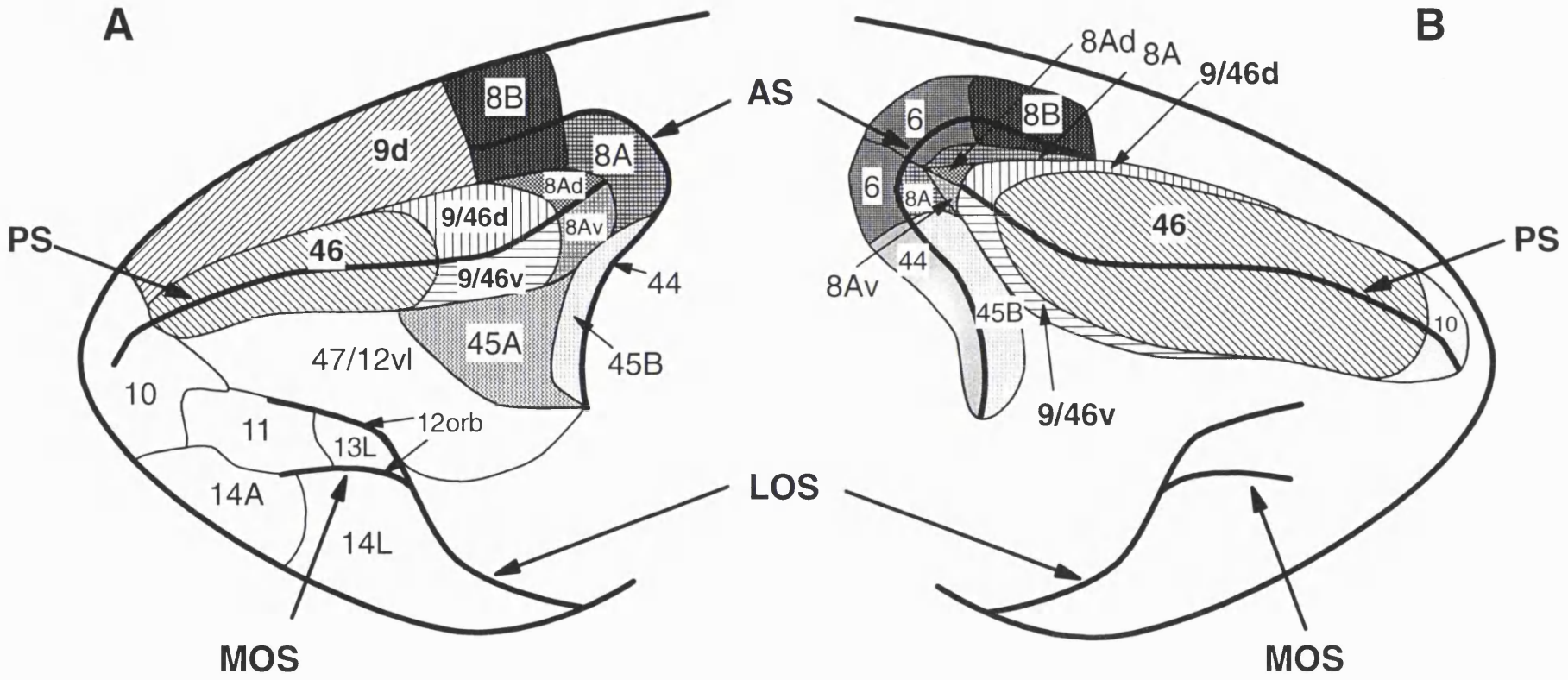

Figure 3. The subdivisions of the lateral prefrontal cortex in the macaque monkey brain. **(A)** A lateral view of the frontal lobe, showing the most recent cytoarchitectonic subdivisions of the dorsolateral and ventrolateral prefrontal cortex as seen on the lateral surface. (Preuss and Goldman-Rakic, 1991; Petrides and Pandya, 1994). **(B)** A lateral view of the frontal lobe, showing the borders of the various areas hidden within the depths of the arcuate sulcus (AS) and principal sulcus (PS). (Petrides and Pandya, 1994).LOS = lateral orbital sulcus, MOS = medial orbital sulcus.

Afferent terminations of projections from posterior parietal regions to the PS region (using anterograde tracing methods) Petrides and Pandya (1994)

Figure 4

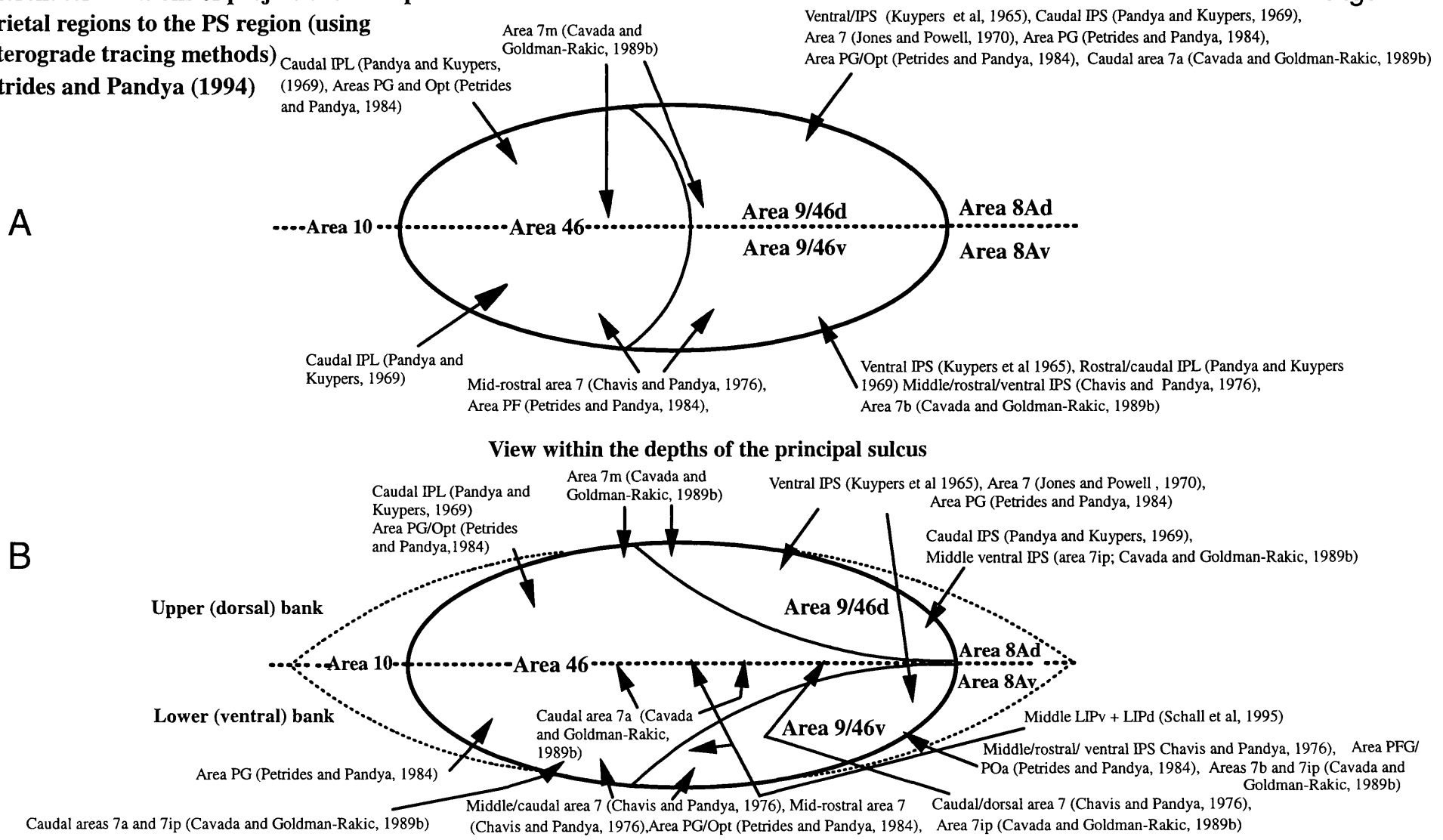

Efferent cell origins of projections from posterior parietal cortex to PS region (using retrograde tracing methods) Petrides and Pandya (1994)

Figure 5

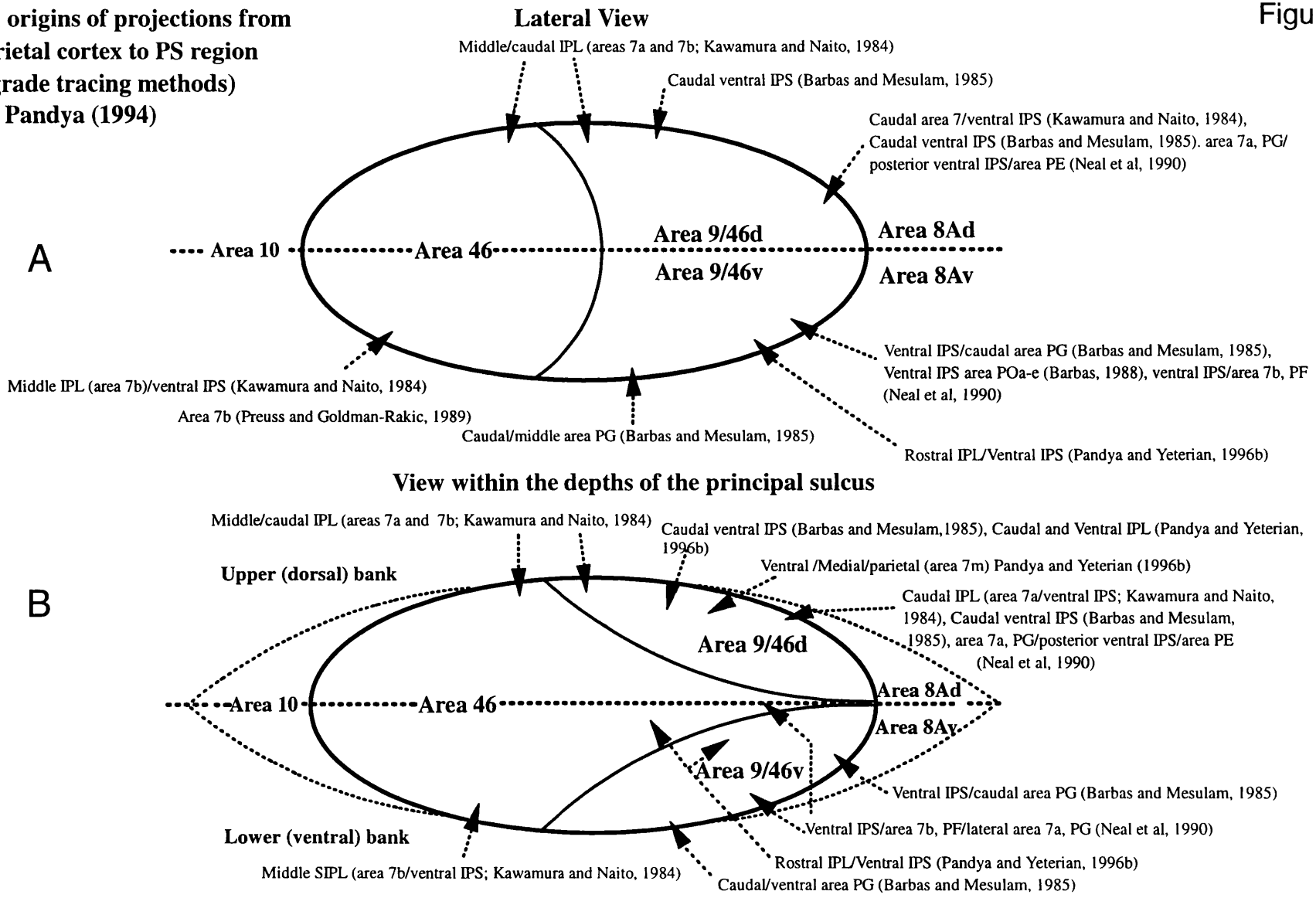

Figure 6

Afferent terminations in posterior parietal cortex of PS projections (using anterograde tracing methods) Petrides and Pandya (1994)

Lateral View

A

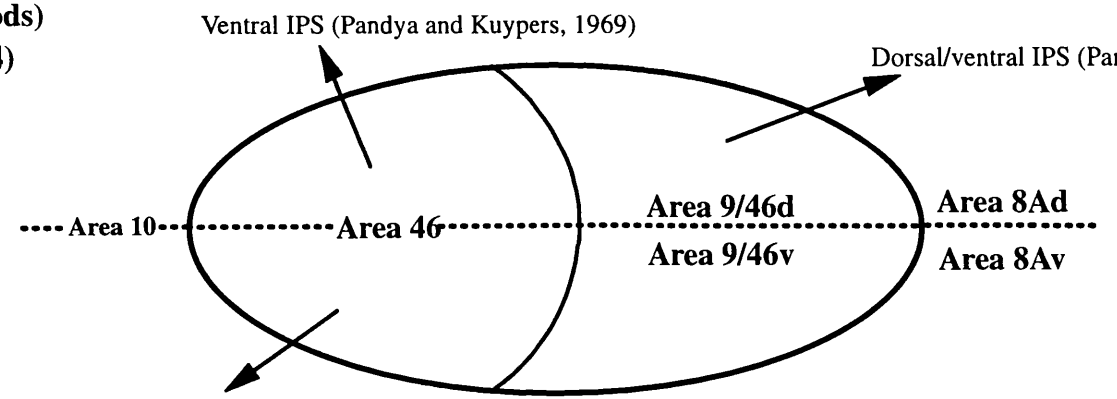

View within the depths of the principal sulcus

B

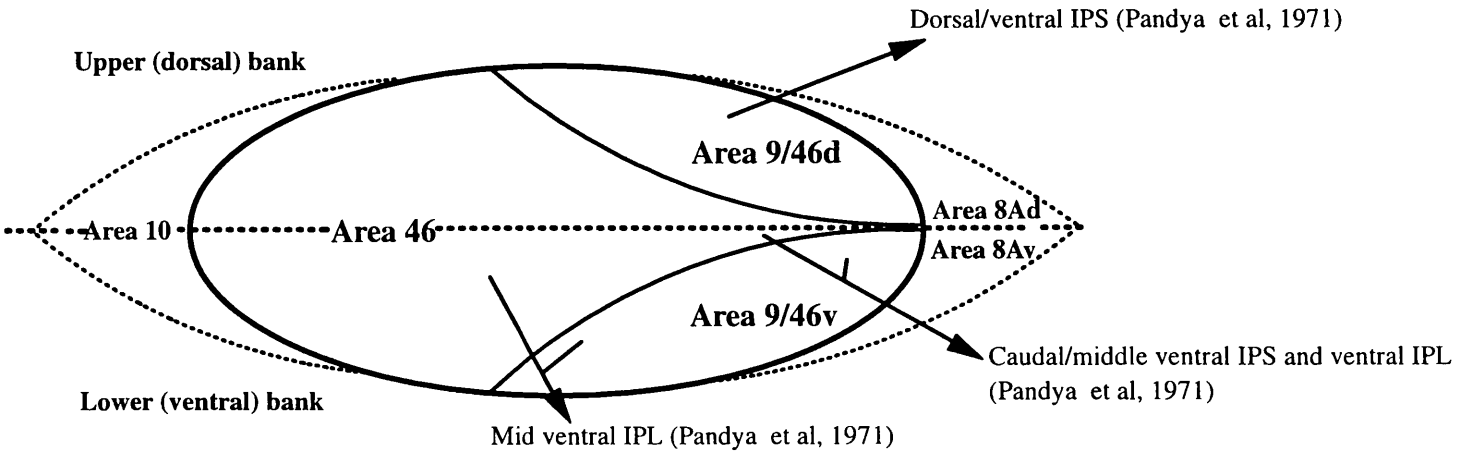

Efferent cell origins of projections from the PS region to posterior parietal areas (using reterograde tracing methods). Petrides and Pandya (1994)

Figure 7

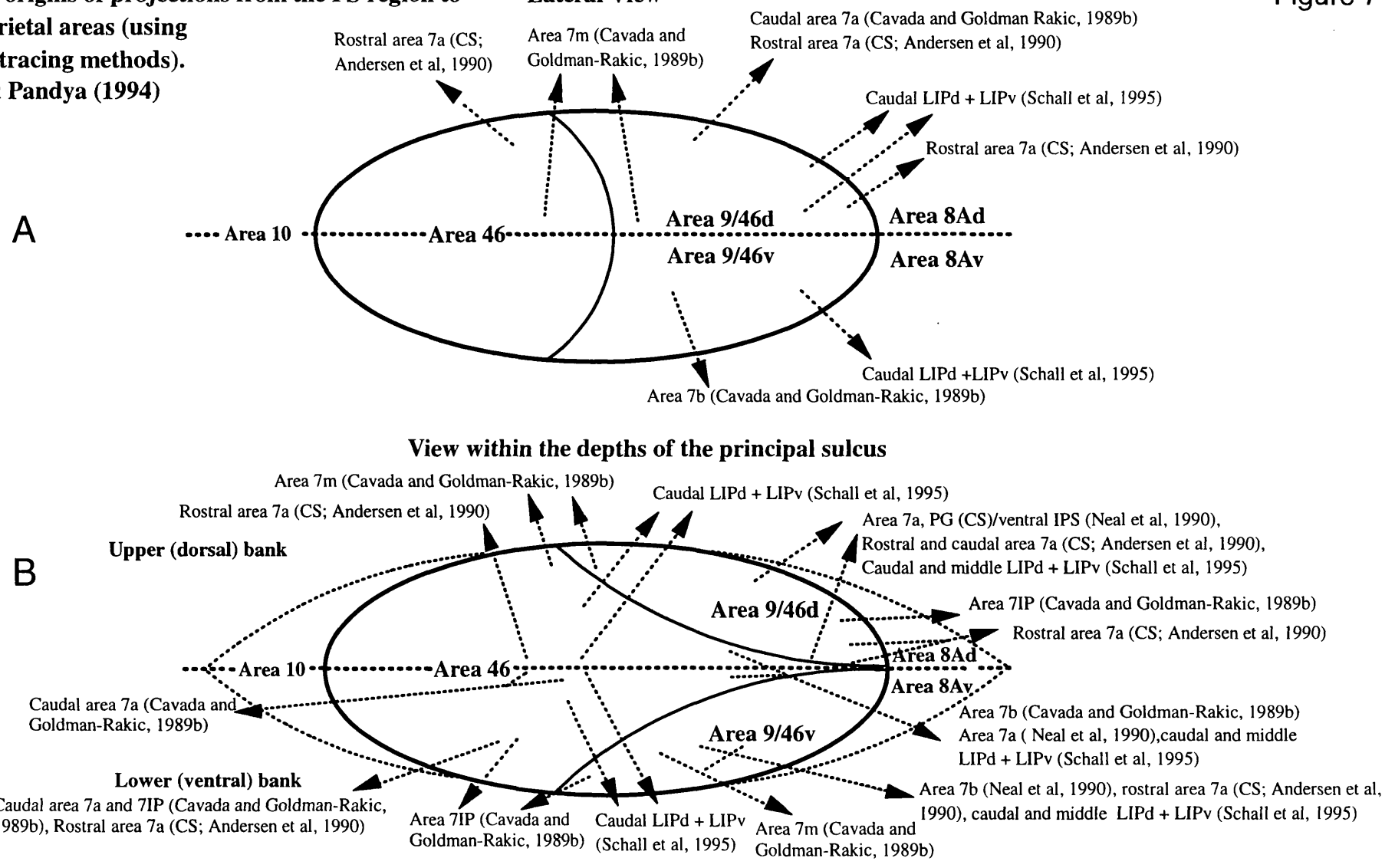

Afferent terminations of projections from superior temporal cortex to the PS region (using anterograde tracing methods)
Petrides and Pandya (1994)

Lateral View

Figure 8A

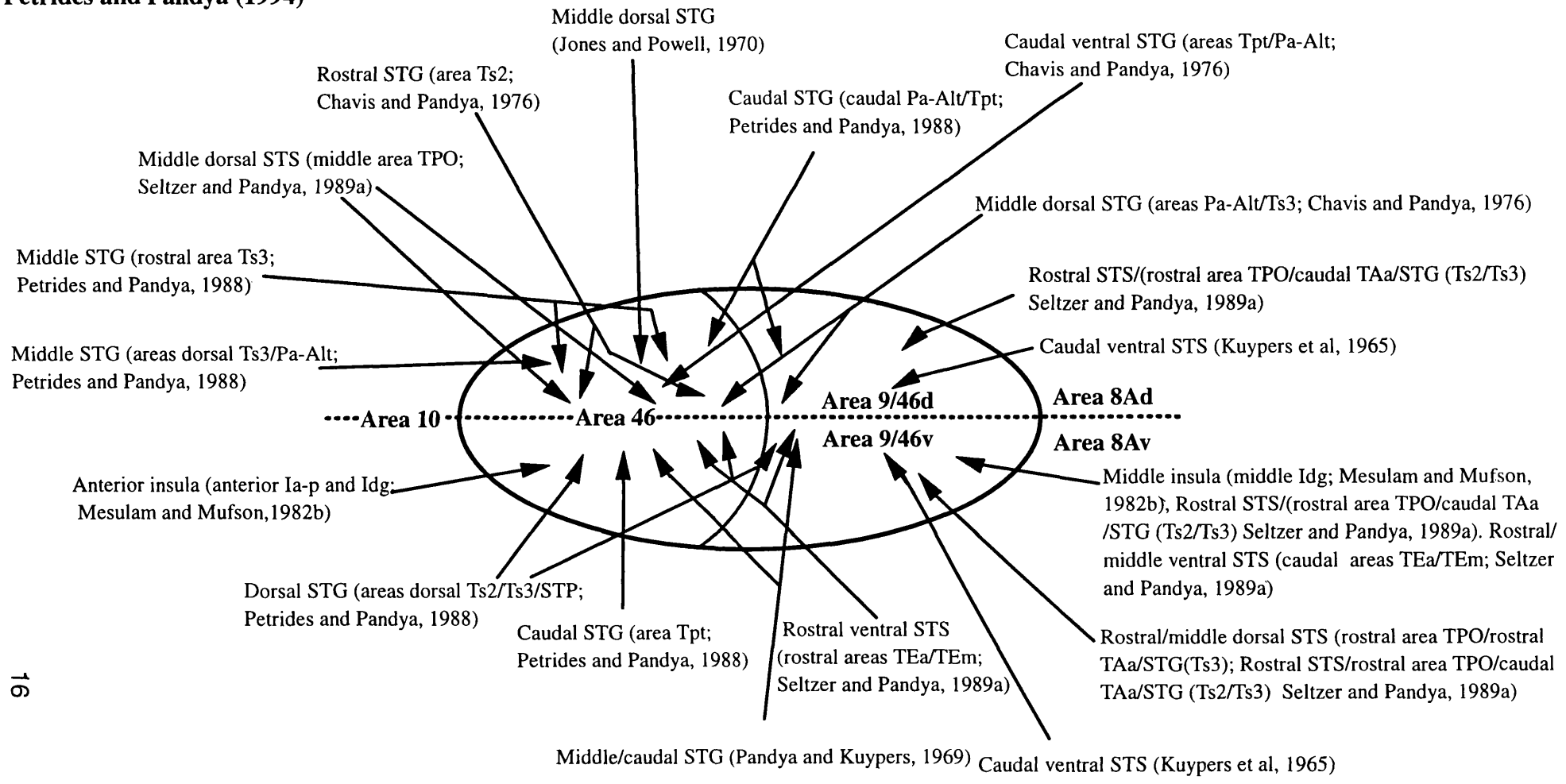

Afferent terminations of projections from superior temporal cortex to the PS region (using anterograde tracing methods)
Petrides and Pandya (1994)

Lateral View

Figure 8B

View within the depths of the principal sulcus

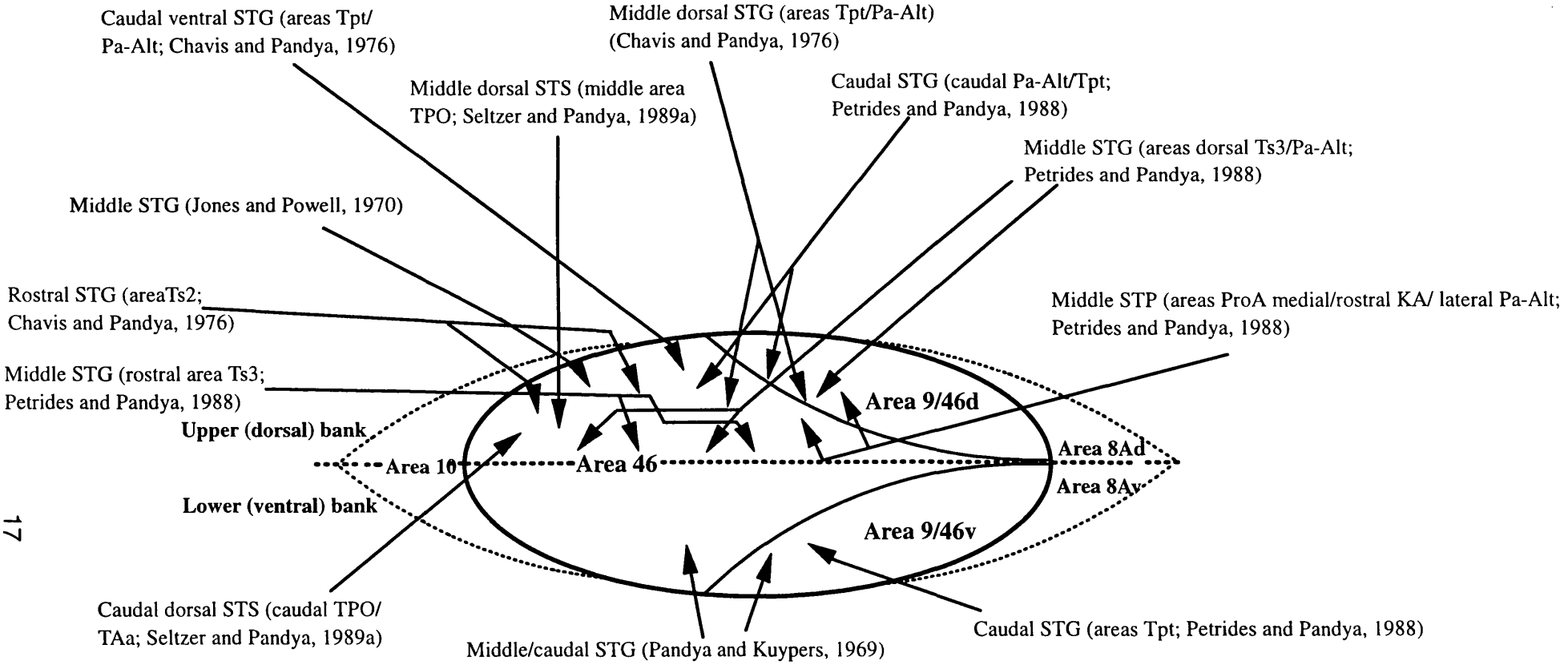

Efferent cell origins of projections from superior temporal cortex to PS region (using retrograde tracing methods). Petrides and Pandya (1994)

Figure 9

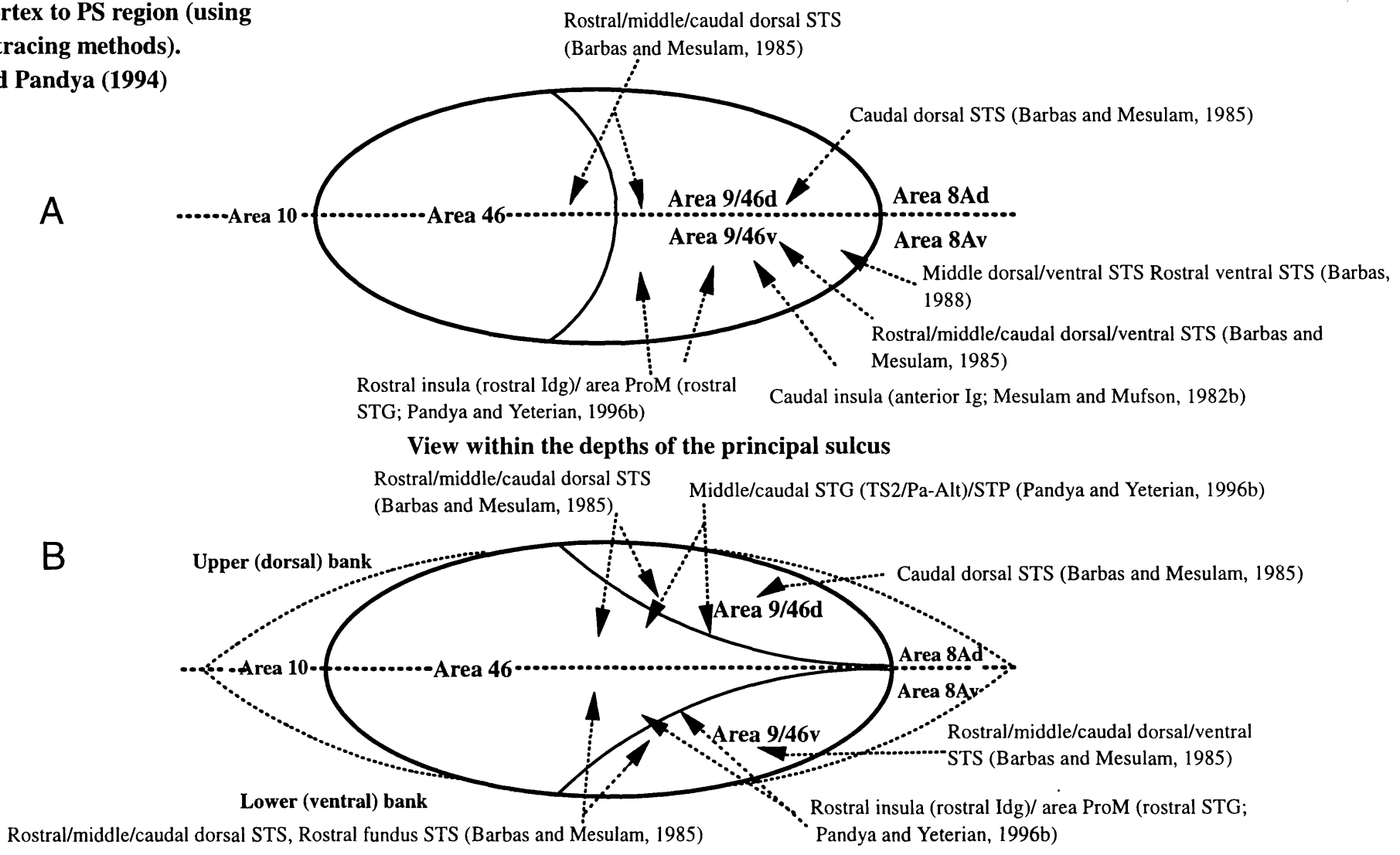

Afferent terminations in superior temporal cortex of PS projections (using anterograde tracing methods)
Petrides and Pandya (1994)

Figure 10

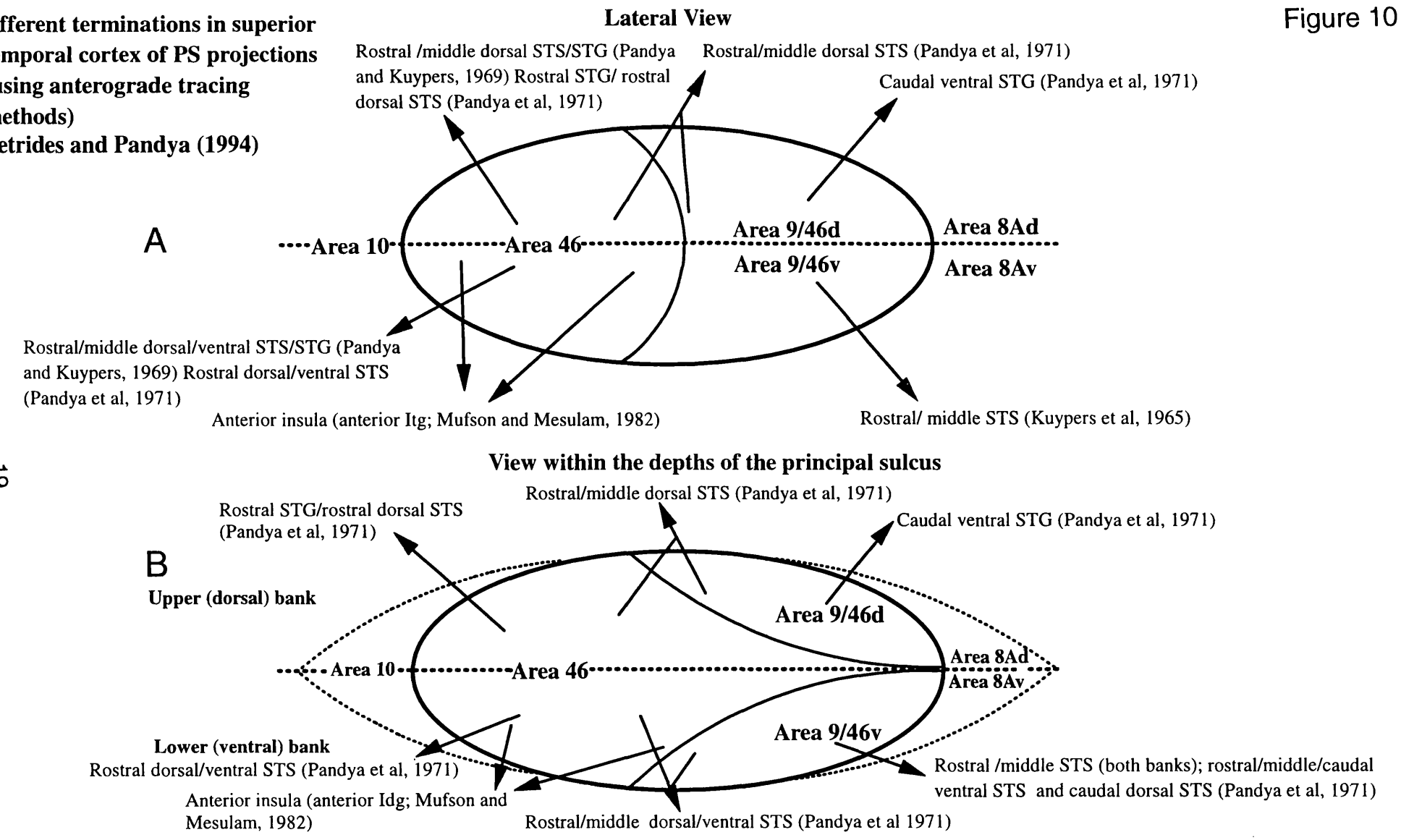

Figure 11

Efferent cell origins of projections from the PS region to the superior temporal cortex (using retrograde tracing methods). Petrides and Pandya (1994)

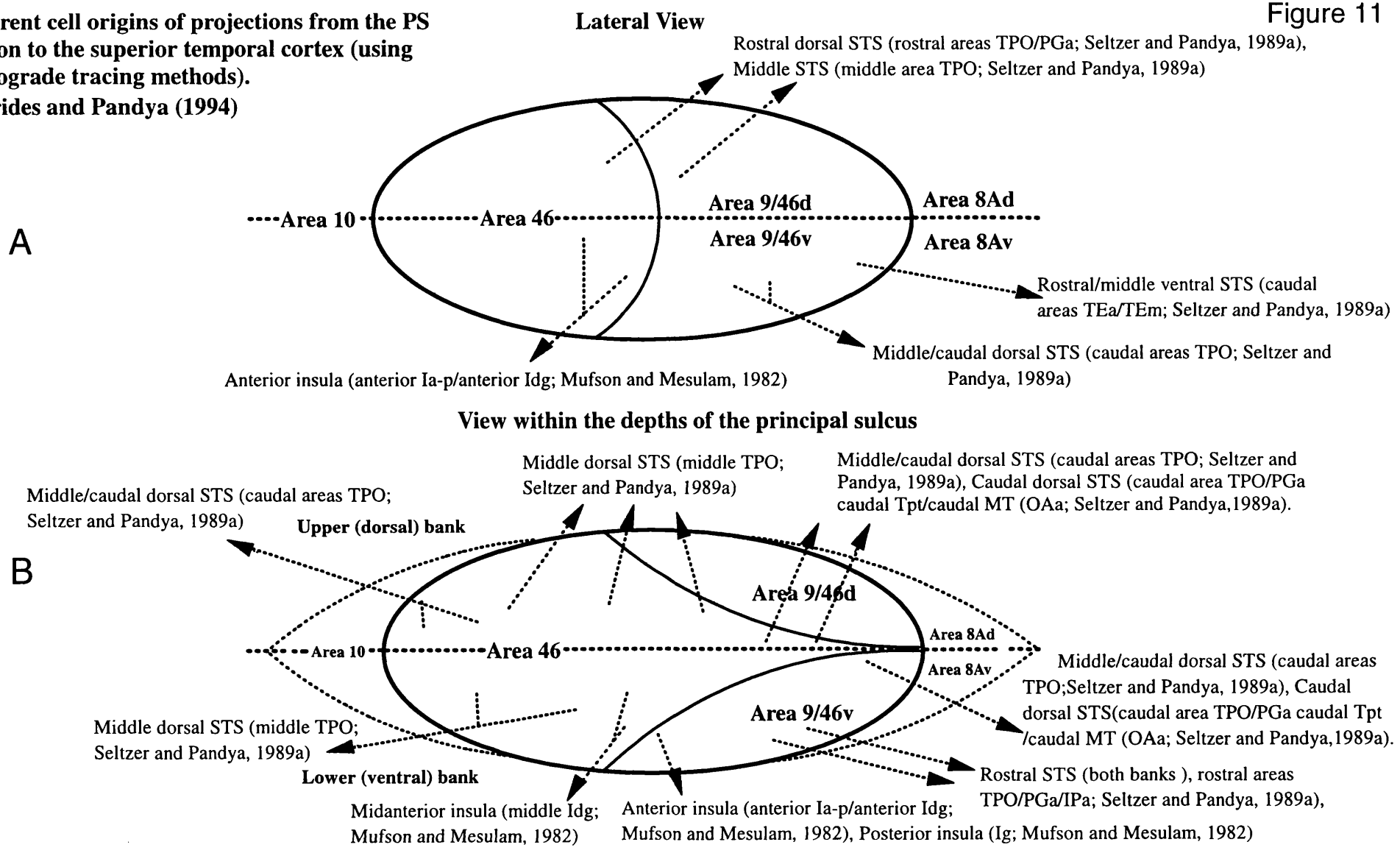

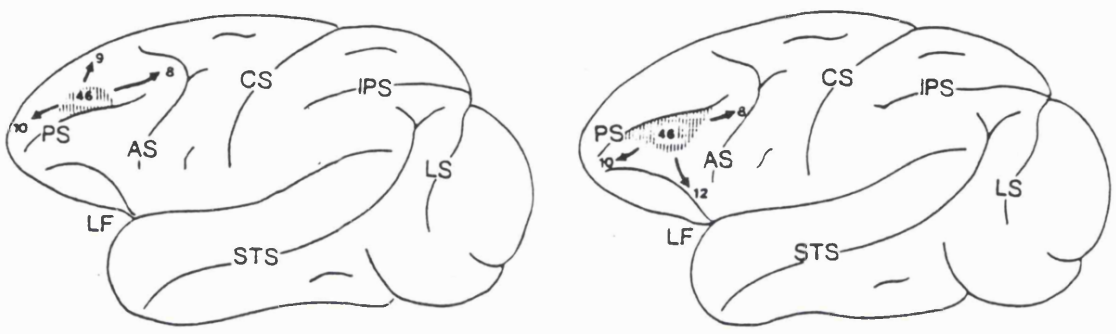

12A **12B**

Figure 12 Lateral views of the macaque monkey brain illustrating the connections of dorsal and ventral portions of area 46 (on the surface of the lateral convexity) with other prefrontal cortical areas. Afferent projections of **(A)** dorsal area 46 and **(B)** ventral area 46 are shown in simplified form based on the data of Barbas and Pandya (1989). Figures **(A)** and **(B)** from Pandya and Yeterian (1990).

Afferent terminations of projections from the thalamic and pulvinar nuclei to the PS region (using anterograde tracing methods) Petrides and Pandya (1994)

Figure 13

A

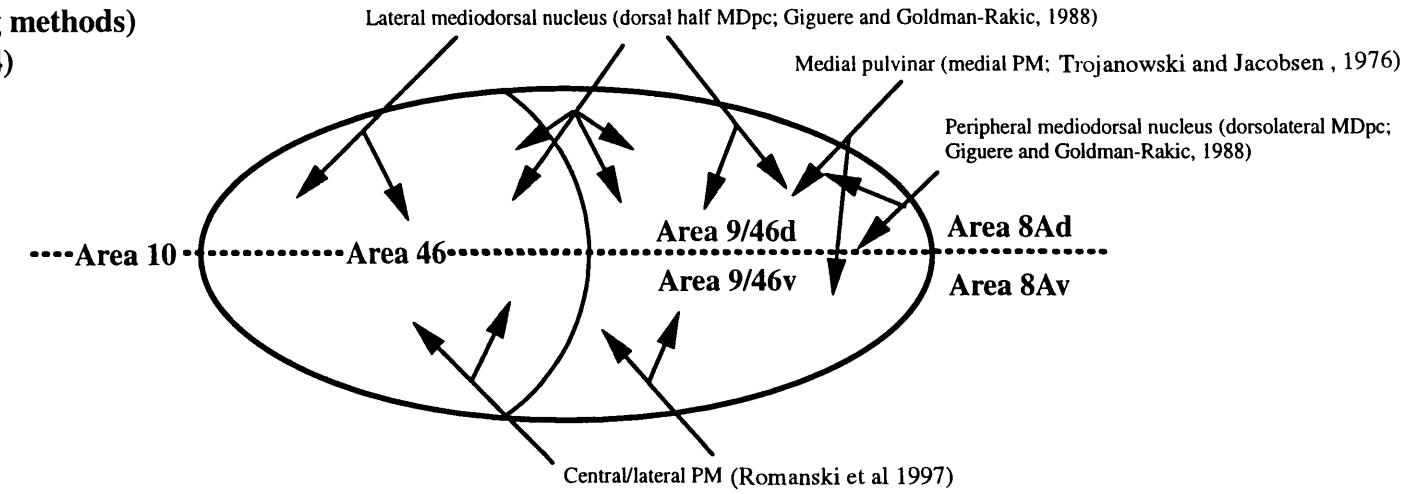

B

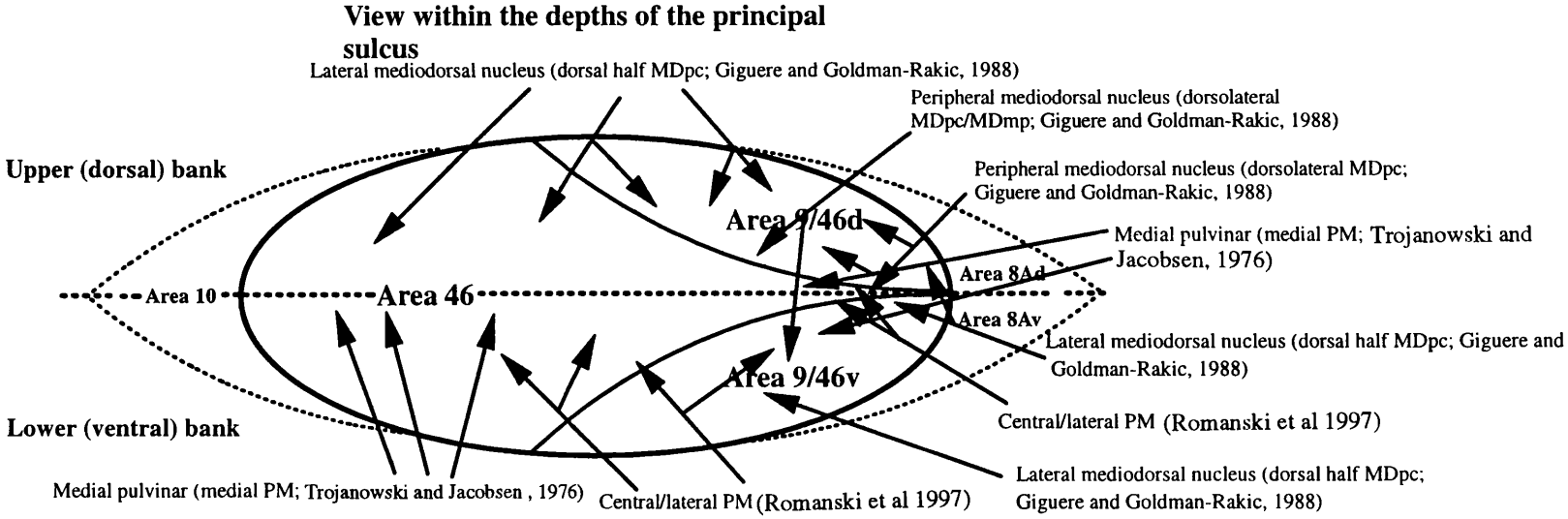

Efferent cell origins of projections from the thalamic and pulvinar nuclei to the PS region (using retrograde tracing methods) Petrides and Pandya (1994)

Figure 14

Lateral View

Mediodorsal nucleus (dorsolateral half MDpc), dorsal portion of medial pulvinar (PM), border of ventral anterior nucleus (VAmc, dorsal), ventral anterior nucleus (VA, ventral) and anteroventral nucleus (AV dorsal half); Goldman-Rakic and Porrino (1985).

Medial pulvinar (medial PM; Jacobsen, 1975; Trojanowski and Jacobsen, 1976; Asanuma, 1985) Mediodorsal nucleus (MDmf and MDpc; Asanuma, 1985)

A

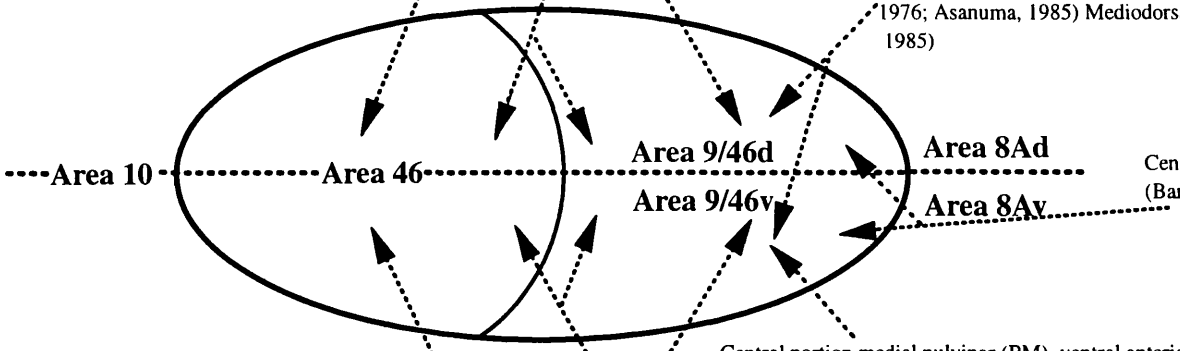

Central/ rostral MDpc, central/rostral MDmc; (Barbas et al, 1991)

Central portion medial pulvinar (PM), ventral anterior nucleus (VAmc); Barbas et al (1991)

Mediodorsal nucleus (Ventral medial half MDmf and MDpc); central portion of medial pulvinar (PM), ventral anterior nucleus (VAmc, dorsomedial half); border of anteroventral nucleus (AV, ventral) and anteromedial nucleus (AM, dorsal); Goldman-Rakic and Porrino, 1985).

View within the depths of the principal sulcus

Mediodorsal nucleus (MDpc, dorsolateral half), dorsal portion of medial pulvinar (PM), border of VAmc (dorsal), VA (ventral) and AV (dorsal half): Goldman-Rakic and Porrino, 1985)

B

Medial pulvinar (PM, medial); Jacobsen (1975); Trojanowski and Jacobsen (1976); Asanuma et al (1985). Mediodorsal nucleus (MDmf and MDpc; Asanuma et al, 1985)

Upper (dorsal) bank

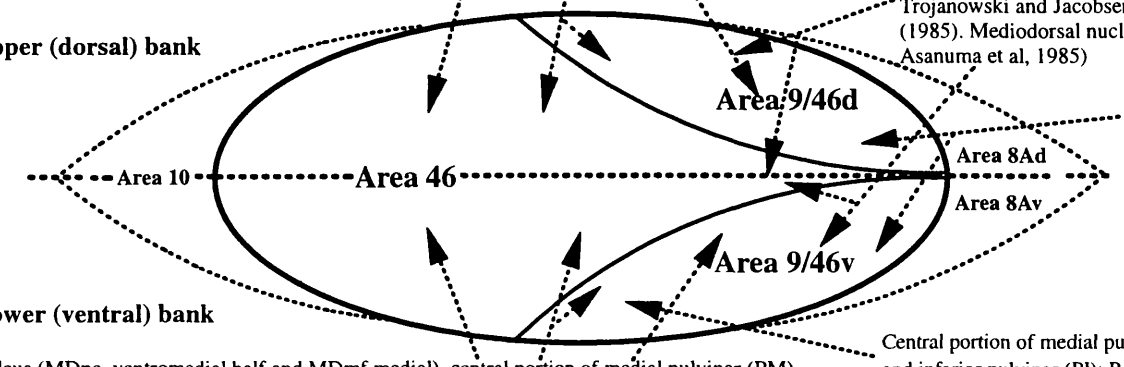

Central/rostral MDmc, central/rostral MDpc (Barbas et al, 1991)

Lower (ventral) bank

Central portion of medial pulvinar (PM), rostral lateral pulvinar (PL) and inferior pulvinar (PI); Romanski et al (1997).

Mediodorsal nucleus (MDpc, ventromedial half and MDmf,medial), central portion of medial pulvinar (PM), VAmc (dorsomedial half), border of AV (ventral) and AM (dorsal); Goldman-Rakic and Porrino (1985).

Afferent terminations in the thalamus and pulvinar nucleus of PS projections (using reterograde tracing methods). Petrides and Pandya (1994)

Figure 15

A

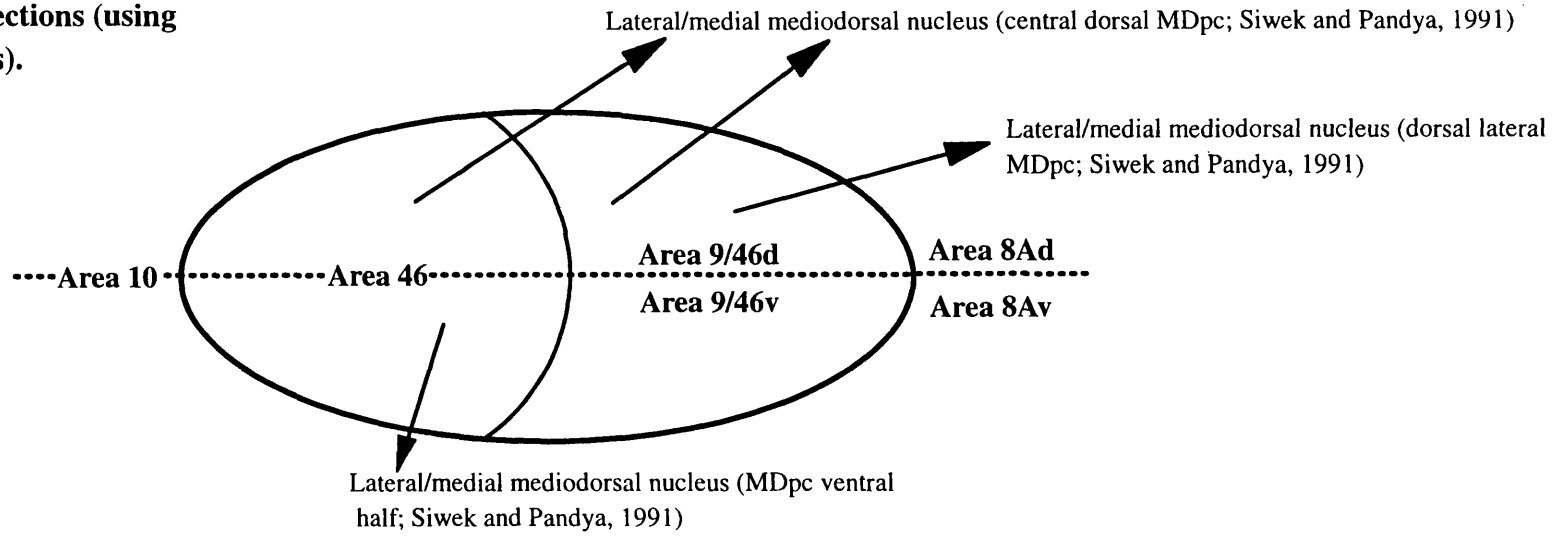

B

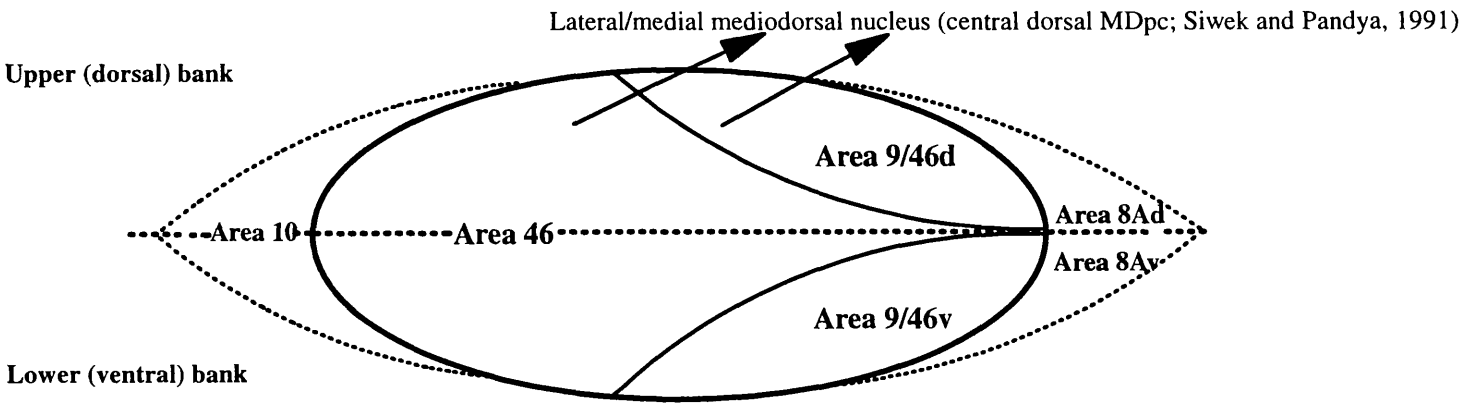

Efferent cell origins of projections from the PS region to the thalamus and pulvinar nucleus (using reterograde tracing methods). Petrides and Pandya (1994)

Figure 16

A

Lateral View

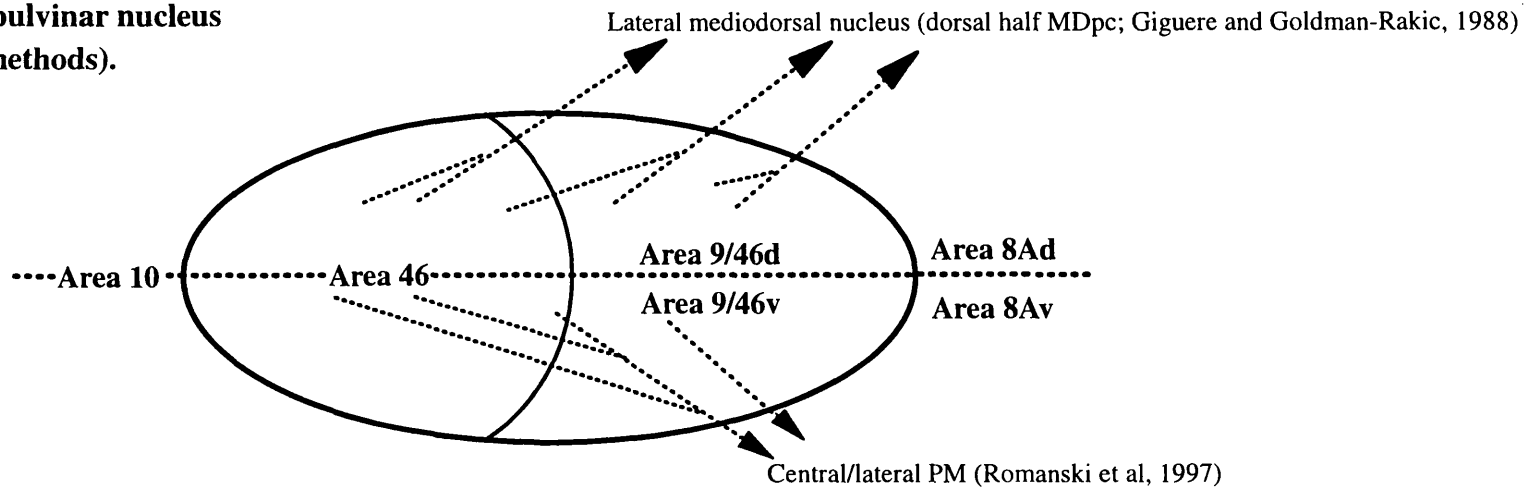

B

View within the depths of the principal sulcus

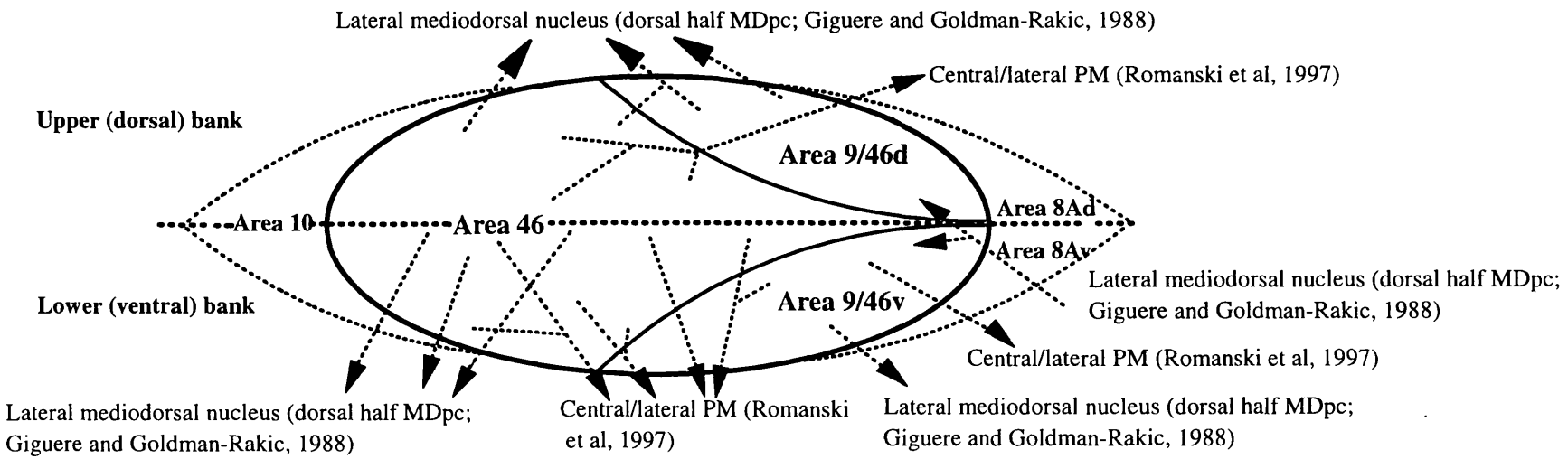

4.0: Functional and behavioural studies of the primate DLPFC.

4.1: Introduction: Functional roles of the PFC and those unique to the DLPFC (areas 9 and 46).

The functional picture that emerges from the wealth of non-human primate and human neuropsychological, neuroanatomical and neurophysiological data, is one of a massive convergence of information occurring throughout the PFC, originating from all sensory modalities. Thus one broad major role for the PFC is in the interrelation and sorting of sensory information - using a process of selective attention to those stimuli relevant at that point in time.

The PFC appears to be able to suppress or juggle more than one item of information in "short-term" or working memory so that each can be rapidly evaluated and either acted upon, ignored or conveyed for storage into "long-term" memory. This is achieved via the many pathways connecting the prefrontal cortex indirectly with the various nuclei of the hippocampus and other medial temporal lobe structures, where declarative or long term memories are thought to be located in a distributed manner, i.e. information is rendered into its most basic constituent parts, each being coded for by the activity of cells in different regions or sub-regions, perhaps coding for a wide range of attributes in a specific sensory modality or for a single attribute across all modalities.

The PFC is also implicated in humans, with playing roles in abstract thought, lexical formulation and speech, decision making, motor behaviour, organisational planning and emotional association. On the evidence of PET and fMRI studies in humans, the DLPFC in particular can probably lay claim to being significantly involved in the "higher association" processing, merging and mnemonic encoding of information in the visuospatial, visuomotor, somatosensory, speech and auditory domains. Many of these attributes, some perhaps uniquely human, have been examined in as direct a way as possible in the macaque monkey, using indirect methods, such as electrophysiology, lesion studies, behavioural psychological testing and various combinations of two or all three of these approaches.

Recent PET and functional magnetic resonance imaging (fMRI) studies in normal human subjects have shown the importance of the DLPFC in many higher order mnemonic (memory-related), executive (goal- and planning-related), cognitive (thought-processing) and motor-related functions. Several recent PET imaging studies in normal volunteers have examined the effects of administrating various neurotransmitter antagonists or agonists (specific for particular receptor subtypes, especially those for the neurotransmitters serotonin and dopamine) on the performance of tasks particularly sensitive to prefrontal cortical

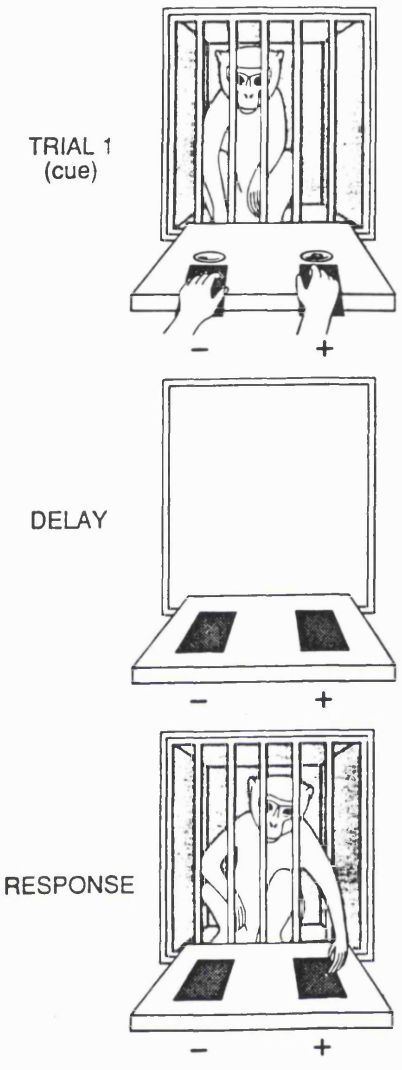

Figure 17

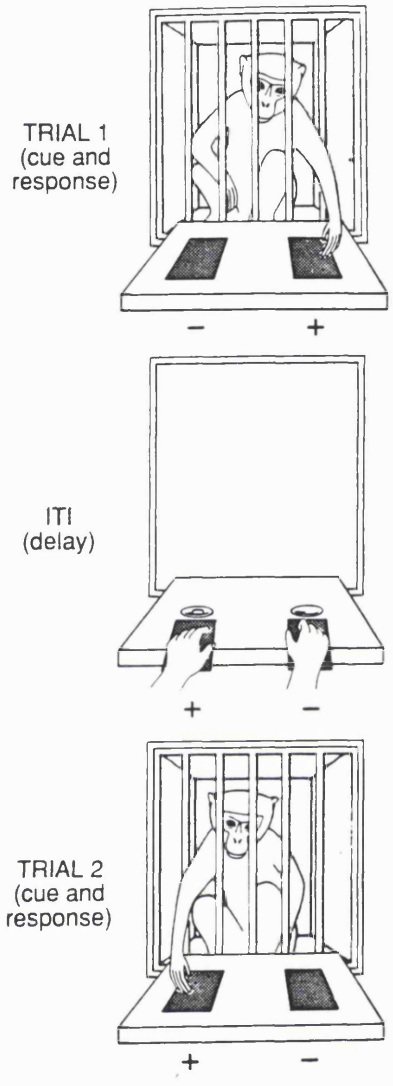

Figure 18

Figure 17 A cartoon illustrating the basic sequence of events in the spatial delayed response task as commonly used in neuropsychological and neurophysiological studies in non-human primates. Figure from Friedman and Goldman-Rakic (1988).

Figure 18 A cartoon illustrating the basic sequence of events in the spatial delyaer alternation task as commonly used in neuropsychological and neurophysiological studies in non-human primates. Figure from Friedman and Goldman-Rakic (1988).

function such as the Wisconsin card-sorting task (Mattay et al, 1996) and sub- and supra-span auditory-verbal memory tasks (Grasby et al, 1992, 1995).

The thesis concentrates on areas 9 and 46 of the DLPFC in the macaque monkey. These areas together represent the best overall characterised region of the PFC so far, both in terms of functional roles and anatomical organisation. This region receives its major cortical inputs from areas within the posterior parietal and superior temporal visual association regions. It has been found that several forms of cellular activity occur in the DLPFC during the performance of visuospatial working memory tasks in non-human primates (reviewed in Goldman-Rakic, 1987a; Fuster, 1989 and Funahashi and Kubota, 1994); each pattern of neuronal activity appears to be specifically related to particular stages of the sequence of task behaviour. Pronounced deficits are observed in the performance of these working memory tasks when portions of the DLPFC have been lesioned in monkeys (Petrides, 1991b, 1995; reviewed in Passingham, 1993) particularly following lesions located in and around the principal sulcus (area 46) where the form of cellular activity is most strongly temporally related to the various stages of delayed response (DR) task behaviour (Fuster and Alexander, 1971; Kubota and Niki, 1971; Fuster, 1973; Niki, 1974a). **See Figure 17.**

It has been possible to examine the mechanism by which these cells implement a response to a stimulus in area 46 by means of a revised version of the classic delayed response task; this uses eye movements rather than manual reaching movements - the oculomotor delayed response (ODR; reviewed in Goldman-Rakic et al, 1990 and Goldman-Rakic, 1996). A certain population of the prefrontal cells recorded, has been found to possess a so-called "memory field" (Funahashi et al, 1989), which is analogous to the receptive field of a cell in visual cortex, except the area 46 cells code for the memory of the spatial location of a visual cue, rather than for the sensory perception of the position as represented by the angle subtended by the stimulus on the retina.

The complexity of the structure and function of the PFC in the monkey is reflected by the diversity and number of hypotheses that have been proposed to describe the various functional roles of this region (reviewed in Fuster, 1989; Goldman-Rakic, 1987a; Passingham, 1993). The breadth and development of ideas and discoveries in this field are briefly reviewed, before some specific examples are examined in more detail, to illustrate the range of functions attributable to the DLPFC and its interactions - via extensive reciprocal anatomical connections - with multiple cortical and sub-cortical areas elsewhere in the primate brain.

The functional and behavioural aspects of the DLPFC, especially the PS region (area 46) are of fundamental importance when considering the organisation of the anatomically

unique lattice pattern of intrinsic circuitry in the superficial layers of this region. Also, equally important are the extensive connections of the DLPFC with the rest of the brain, via reciprocal corticocortical and cortico-subcortical pathways which individually are thought to represent overlapping sectors of the large and extensive multiple distributed networks of projections between areas of similar functional-relations.

It is thought that mnemonically distinct but temporally-overlapping patterns of behaviour may be achieved via the topographically arranged sub-level pathways of these different sectors being recruited as required, in a kaleidoscope of constantly changing permutations over time, with swapping and switching of information occurring such that it travels along the widest/fastest available sub-pathways between a variety of dedicated networks each enabling the integrative recording from sensory modality to mnemonic template to motor action and vice versa with variations on all the intermediate stages in between.

4.2: Methodological advances and diverse studies of the DLPFC in the adult non-human primate.

By the early 1970's, a large body of literature had accumulated of studies both in monkeys and in humans, which had examined the relationship between the removal or permanent inactivity of a particular PFC area or region and the resulting changes in behavioural and psychological performance on delayed response tasks in monkeys and on the Wisconsin Card Sorting Test in humans. Many studies were concerned specifically with examining the DLPFC (area 46; cortex within and immediately around the principal sulcus region), believed to be the site of spatial memory (Milner, 1964; Mishkin, 1964; Goldman and Rosvold, 1970; Goldman et al, 1971; Butters et al, 1972; Passingham, 1972a,b; Goldman-Rakic, 1987a; Fuster, 1989). In human studies, experimenters were only able to test patients with large, uncontrolled, variably located lesions of disease origin or resulting from surgical treatment for neurological disorders, comparing their task performances with those of normal subjects. In studies using experimental monkeys, relatively circumscribed, surgical lesions could be made and it was thus possible to compare the post-surgical results of these monkeys on certain tasks, compared to their pre-surgical ability (i.e. acting as their own control). The results from these behavioural studies strongly supported the case that lesions of the equivalent DLPFC regions in monkeys and humans could result in comparable deficits on analogous tests of spatial memory.

Despite the large numbers of investigations that had been conducted on the

neuropsychological aspects of the PS region in the monkey DLPFC, there still remained many unanswered questions even after nearly 40 years of research and many groups held equally compelling evidence to explain the differences which arose despite identical lesions and testing with the same performance tasks. One aspect of functional specificity which was clearly reinforced over many different studies was the general idea of the PS as the functional locus of the "spatial engram" (Butters et al, 1972), i.e. the anatomical location of visuospatial memory, essential to the successful completion of a delayed response task.

Neurophysiological recordings carried out in the intact normal monkey DLPFC have related the various behavioural stages in delay task performance to the simultaneous changes occurring in the activity of single cells during the performance of these tasks (Fuster and Alexander, 1971; Kubota and Niki, 1971; Fuster, 1973). In these electrophysiological studies, awake behaving monkeys with an implanted electrode - directed into the PS region of the DLPFC - were required to perform visually-guided manual delay tasks such as spatial delayed alternation (**see Figure 18**; Kubota and Niki, 1971) and spatial delayed response (Fuster, 1973; Fuster and Alexander, 1971). Continuous recording of single unit neuronal activity before, during and after the delay stage of the task, for each trial, enabled a comparison of that activity (based on mean data for many neurons) with the distinct stages of the task performance.

The task stages were divided into: presentation of the stimulus, delay period and active response (i.e. reaching for the food reward). The various alterations in neuronal activity during the course of each trial appeared to reflect the temporal sequence and duration of these behavioural subdivisions. It was demonstrated that during a delayed alternation task some units were more active after the delay period (i.e. just before the response was made) than during it and others were more active during the delay period than just before the onset of the response (Kubota and Niki, 1971). Alternatively, during the performance of the delayed response task, DLPFC neurons could be classed into 6 different types, on the basis of the temporal relation of their activity to the delay period of the trial (Fuster, 1973; Fuster and Alexander, 1971). In either case, the anatomical location of the recorded types of neurons appeared to show no clear relation to their particular pattern of electrical activity during the performance of the task. Instead all types of units were apparently randomly distributed throughout the extent of the sampled region of the PS.

Neurophysiological and neuropsychological studies of delayed response task performance were not solely restricted to the DLPFC alone; areas known to be interconnected with the DLPFC, such as the posterior parietal cortex (Fuster, 1973) and

the medial dorsal (MD) nucleus of the thalamus (Fuster and Alexander, 1973) were also examined for evidence of task-related neuronal activity or lesion-induced deficits, during task performance.

Both these regions were found to show temporally-related activity - comparable to that found in the DLPFC - with respect to the delay period of the spatial delayed response task. These observations provided further support for the view that the mutual anatomical connections linking these widely spaced regions, facilitate the essential integration of sensory and mnemonic information from the various processing levels in the brain, as a necessary component of the complex organised motor behaviour needed to correctly accomplish the task.

From the early 1970's to the early 1980's, many of the experimental studies carried out were still based on the use of the traditional lesioning methods (either surgical ablation or reversible cooling) (Passingham, 1978; Kojima et al, 1982; reviewed in Fuster, 1989). It was only with the advent of more sophisticated investigative techniques (beginning in the early 1980's), that significantly new discoveries were made concerning the specific relations between the anatomical organisation of the DLPFC and its range of functional attributes, along with their eventual *in vivo* visualisation. These included more complex computer-based testing apparatus (leading to less chance of experimenter-induced bias), more specific lesioning made possible by knowledge acquired from the more detailed pathway tracing of the anatomical connections between the PFC and a host of other cortical and thalamic areas (**see review section 3.0 on the anatomical connections of the DLPFC**).

Gradually with the development of more sophisticated behavioural single unit recording techniques, the neurophysiological study of monkey DLPFC diversified to include the examination of more sophisticated neuronal properties such as visuokinetic activity during delayed visual discrimination, i.e. delayed response with visual light cues (Kubota et al, 1974), direction of response activity in the delay period i.e. directed towards left or right (Niki, 1974a), absolute versus relative direction of response in the delay period i.e. the literal location of left and right response keys versus their relation to each other (Niki, 1974b) during the performance of the spatial delayed alternation task.

The same paradigm was examined for the spatial delayed response task as well (Niki, 1974c) and overall for both tasks about 5-6% of DLPFC cells recorded showed this response-direction dependent activity during the delay period, hinting at a possible likelihood of cells exhibiting this property during the cue period (light spot stimulus) also. The relative importance of the light stimulus or key pressing response towards the cellular

activity during the delay period in a visually guided key pressing task was also investigated (Sakai, 1974) and it was found that increased cellular activity prior to the light cue were indicative of the animal's "expectancy".

Some studies concentrated upon the properties of prefrontal neurons in and around the principal sulcus (area 46) in "timing" behaviour, i.e. changes in neuronal activity relative to the events during the performance of a long latency task (Niki and Watanabe, 1979).Whilst others investigated cellular activity in the DLPFC during the performance of a task which tests the relative significance of the stimulus to the animal, beyond its physical attributes, e.g. using the delayed conditional discrimination task paradigm (Watanabe, 1981). The increasing numbers of physiological studies, combined with the development of new varieties of behavioural tasks, was bringing to light, new and diverse properties of DLPFC neurons and allowing the formulation of new theories on how the DLPFC could initiate and functionally interact in structured behaviour via its connections with a multitude of cortical and thalamic areas (reviewed in Kubota, 1978).

From the middle 1980's until the present day, the use of lesioning methods has continued and the results obtained by this basic, but ambiguous method still warrant attention. The results of lesion studies in monkeys can still be highly informative when they are augmented by more specific studies involving the pharmacological manipulation of neurotransmitter systems in the DLPFC and the subsequent effects on psychological tests of spatial memory and other paradigms. The development of the measurement of local cerebral glucose uptake (LCGU) - using the 2-[^{14}C]-deoxyglucose (2DG) technique in monkey brain slices (Kennedy et al, 1978) enabled the functional contributions of a variety of cortical (in particular the DLPFC) and subcortical regions in the performance of spatially-related tasks to be evaluated on a quantitative scale (reviewed in Goldman-Rakic and Friedman, 1991). This technique is based on the hypothesis that an increase in the levels of energy usage during the performance of a sequence of task behaviour is a reflection of raised neuronal activity and hence an increased demand for metabolic precursors, i.e. radio-labelled glucose, which can be measured by rapidly perfusing the animal immediately following the end of the task and visualising the levels of 2DG present prior to sacrifice, with autoradiography.

The catecholaminergic neurotransmitter dopamine (**see Neurotransmitter review section for more detail**) has long been associated with an important role in normal DLPFC function and its deficit or overabundance (as reflected by receptor density) has been hypothesised to be a major factor in the cognitive dysfunction observed in some neuropsychiatric disorders such as Parkinson's disease and schizophrenia,

respectively. The initial identification of DA as the crucial neurotransmitter in cognitive/motor-related mechanisms in the DLPFC came from a biochemical/behavioural study (Brozoski et al, 1979) which examined the cognitive (i.e. DLPFC) effects of administering various neurotoxins specific to either DA, NA or 5-HT in monkeys, by subsequently testing them on the spatial delayed alternation task. It was found that only the depletion of DA produced a substantial deficit on task performance, leading to the premise that DA was particularly important in normal DLPFC cognitive functioning.

Following this significant finding, studies using more sensitive techniques to measure the specificity of DAergic mechanisms in DLPFC function i.e. at the cellular or receptor level, were used to examine the exact locus of involvement of dopamine in the performance of cognitively-related tasks, e.g. the oculomotor version of the delayed response task (ODR). Firstly, the effects of DA at the cellular level have been examined in the DLPFC (Sawaguchi, 1987b; Sawaguchi et al, 1986, 1990a,b) during the performance of various delay tasks and more recently with the development of specific antagonists, at the level of the selective effects modulated by specific DAergic receptor subtypes (Arnsten et al, 1994, 1995; Sawaguchi and Goldman-Rakic, 1991, 1994; Williams and Goldman-Rakic, 1995).

Recent investigations, using a combination of anatomy, neurophysiology and experimental psychology, have emphasised a role for the DLPFC (area 46 in particular) in the cellular and circuit basis of working memory function in the monkey (Goldman-Rakic, 1995b; Goldman-Rakic et al, 1990a). Area 46 has emerged to be an integral part of a functionally distributed network (Goldman-Rakic, 1988) made up of multiple interconnected cortical and sub-cortical areas (also including posterior parietal cortex, cingulate cortex, the striatum and various thalamic nuclei) as determined by dual anterograde tracing studies (Selemon and Goldman-Rakic, 1988). Others using predominantly neurophysiology and neuropsychology have found DLPFC (area 46) to be essential for the temporal structuring (integration or organisation) of behaviour (reviewed in Fuster, 1985a, and 1989), imbuing the DLPFC with the roles of "mediator of cross-temporal contingencies" (reviewed in Fuster, 1985b) and the "bridging of temporal gaps in the perception-action cycle" (reviewed in Fuster, 1990b).

The employment of new tracer substances has enabled the further unravelling of the anatomical connectivity of the DLPFC with a complex network of other cortical areas, including its immediate neighbours in the rest of the PFC. The intensive neurophysiological study of many behavioural tasks in awake behaving monkeys has led to the reappraisal of how the DLPFC might be uniquely functionally and anatomically organised to be able to meet the demands of the roles which it seems to be involved in (Passingham, 1993). There has

been a recent attempt to further clarify the role of areas 9 and 46 in object and spatial memory processing, by making separate as well as combined lesions of these 2 adjacent areas in adult monkeys (Petrides, 1991a,b). The subsequent testing of the animals on a delayed-matching-to-sample task has revealed there to be an unexpected performance deficit, which may suggest that the DLPFC is not strictly confined to the processing of visuospatial information as traditionally thought (Petrides, 1995). Instead, perhaps the mid-DLPFC region, where lesions produce this non-spatial deficit most profoundly - in addition to possessing a spatially-coding subset of neurons - could also be specialised for particular non-spatial aspects of visual processing involving memory for self-ordered behaviour, guided from within the PFC on the basis of an internal representation rather like the hypothesis of "on-line" working memory (Goldman-Rakic, 1987a), only not restricted to the spatial domain, but more diversely including mnemonic-coding for the colour, form and shape as well as for the spatial location or relative position of stimuli (Petrides, 1996).

There is then good reason to suppose that the DLPFC may be sub-divisible into a variety of functional and anatomically distinct sub-domains whereby various neuronal attributes of spatial and object-related memory coding are differentially distributed, but as a whole the DLPFC may integrate these diverse processing modules into a single memory "trace" which could form the basic unit of memory and cognition in the same way as the receptive fields of different neurons in V1 (area 17) code for a selective variety of diverse stimulus properties.

The applications of the 2DG technique were further extended by its modification for combined use with two radioactive labels [^{14}C] and [^{3}H] (Friedman et al, 1987), enabling the simultaneous observation of colocalised metabolic activation in 2 cortical regions, measured sequentially for a distinct experimental condition, in the brain slices of the same animal (Friedman et al, 1989). This was then applied to the functional examination of the distributed cortical circuitry thought to be involved in a working memory role, the most prominent of these being the principal sulcus region of the DLPFC (area 46) and the posterior parietal areas (7a, 7b, 7ip and 7m). These 2 cortical regions as well as being heavily reciprocally connected anatomically (Cavada and Goldman-Rakic, 1989), are found to be very closely functionally related, as revealed by their concurrent metabolic activation during the performance of a spatial DR task in monkeys (Friedman and Goldman, 1994).

The approach of localised pharmacological manipulation of the DLPFC in monkeys, involving the application of neurotransmitter-specific receptor antagonists or agonists (e.g. for neurotransmitters: GABA, DA, NA) has made it possible to potentially differentiate

the distinct functional contributions of individual receptor subtypes: $GABA_Ar$ (Sawaguchi et al, 1988), D_1- and D_2-DAergic (Sawaguchi and Goldman-Rakic, 1991, 1994), a_2r-adrenergic (Cai et al, 1993; Li and Mei, 1994) to the biochemical processes necessary for the successful performance of certain behavioural tasks, as indicated by the deficits when their normal receptor function is disrupted. These studies have brought about a much clearer understanding of the wide range of modulatory events occurring within the complex cortical circuitry of the DLPFC which are an essential component in the shaping of the unique functional roles of this particular cortical region.

Many approaches, both old and new are currently being employed to probe the detailed anatomical, neurophysiological and pharmacological aspects of the DLPFC and the areas with which it is intimately connected, i.e. posterior parietal cortex. So far, no one general theory can be said to account for the organisation of the diverse functional attributes which have been found to be exhibited by the various behaviourally-related neuron populations which are arranged in an as yet unknown manner within the complex anatomical framework of the DLPFC.

5.0: The cortical pyramidal neuron.

5.1: Introduction: Postnatal development of the dorsolateral prefrontal cortex.

The DLPFC is known to reach functional maturation at quite a late stage in postnatal development in monkeys and humans. It is generally agreed that the mature adult state is reached shortly after puberty, i.e. at around 3.0 years of age in macaque monkeys and at about 16.0-18.0 years of age in humans. Between birth and the achievement of the mature adult state, many alterations are thought to occur in the circuitry of the DLPFC. This hypothesis is supported by the changes observed in synaptic density for dendritic spines of layer 3 pyramidal neurons in humans which are found to rise rapidly in the early neonatal period to a peak value at 1.0 year of age, which is maintained until around 7.0 years postnatal, when the first sign of a drop in synaptic numbers becomes evident (Huttenlocher, 1979, 1984; reviewed in Huttenlocher, 1993). Thereafter, a gradual decline in the numbers of synapses continues until around 16.0 years of age (i.e. puberty), when stable adult-like levels of synapses are found for layer 3 pyramidal neurons.

The first part of this thesis examines the postnatal development of monkey DLPFC (areas 9 and 46) and shows that a comparable time course is observed for early changes in layer 3 pyramidal neuron dendritic spine density during the equivalent postnatal period to that in the human DLPFC (Anderson et al, 1993; Classey et al, 1994; Anderson et al, 1995), when

an apparently stable level of adult spines is achieved by around 3.0 years of age (i.e. puberty).

The process of pyramidal neuron excitatory synapse overproduction in layers 2 and 3 (most spines are contacted by the lateral projections of the same pyramidal neuron population) and their subsequent attrition at puberty serves as an indicator of the degree of functional maturation of the intrinsic lattice connections in these layers. Since this lattice organisation would appear to be an essential anatomical component in the framework providing the basis for the unique functional attributes exhibited by the DLPFC, it is of particular importance to be able to indirectly establish the time course of its probable functional development, using the timing of its primary postsynaptic points of interaction, i.e. dendritic spines, as a reflection of the degree of overall intrinsic lattice development. By understanding the normal process of postnatal anatomical maturation for layer 3 in the monkey DLPFC, it may be possible to extrapolate this to the timing of events presumed to occur during the normal postnatal development of DLPFC anatomy and function in humans.

The time course of pyramidal neuron maturation is compared with that of a subset of local circuit neurons in layer 3, the chandelier neurons, which form multiple inhibitory synapses with the axon initial segments of these pyramidal neurons. As well, the temporal maturation of the DAergic and 5-HTergic innervations (**see Study 2**) of the same layer of the monkey DLPFC are compared for the degree of synchrony and reciprocity in the timing of the various stages of their postnatal development.

Layer 3 in the DLPFC is the site of an rich dopaminergic (DAergic) innervation originating from the ventral tegmental nucleus in the mid-brain. This DAergic innervation shows dynamic changes in its density during postnatal development, finally resulting in a lower level of innervation in adulthood than is found in either the infant or adolescent animal. These DAergic axons are known to form synaptic interactions with the spines and dendritic shafts of pyramidal neurons (Goldman-Rakic et al, 1989) and GABAergic interneurons (Smiley and Goldman-Rakic, 1993).

Also forming contacts with pyramidal neurons are the characteristic axon terminal arrangements of several GABAergic inhibitory interneurons. The varicosities of one particular class of these local circuit neurons, the chandelier neuron, are observed to form cartridge arrangements in synaptic contact with the axon initial segments of pyramidal neurons (Somogyi et al, 1982; Williams et al, 1992; Lund and Lewis, 1993). They can be distinguished by their intense levels of parvalbumin-immunoreactivity PV-IR during certain periods of postnatal development (Anderson et al, 1995). The time course of development of layer 3 pyramidal neuron dendritic spines will be compared with the development of the

DAergic innervation (Rosenberg and Lewis, 1995) and PV-IR axon cartridges with which they are known to closely interact in the developing and adult primate (Anderson et al, 1995).

These various components of the cortical circuitry in layer 3 of the adult monkey DLPFC are spatially closely related and in some cases exhibit synaptic associations. It is therefore likely that there is interaction via both synaptic and non-synaptic neurochemical and electrophysiological mechanisms during postnatal development. If there is found to be temporal coincidence in the relative time courses of maturation for these components during postnatal development it may assist in our understanding of how complex cellular interactions occur during the development of the normal primate. From the evidence available, it is probable that in the DLPFC the mature adult circuitry is attained by a gradual maturational process featuring a combination of simultaneous and consecutive acquisition and removal of synaptic or other components, until the adult state is achieved.

The first study in the thesis focuses on the development of a particular pyramidal neuron population located in mid-layer 3 of the monkey DLPFC (areas 9 and 46). Layer 3 - in particular its middle and deep portions - is known to be the site of pyramidal neurons whose axon collateral's provide a complex, stripe-like excitatory intrinsic lattice network of intraareal interconnections (Levitt et al, 1993; Kritzer and Goldman-Rakic, 1995; Pucak et al, 1996). Any given point in cortex appears to connect reciprocally to a series of other points arrayed in a discontinuous stripe-like fashion. This relationship can be thought of as a combination of divergence, i.e. in the case of pyramidal neuron axon collateral's projecting intrinsically to many other pyramidal neurons. Conversely, there is a convergence of intraareal projections, i.e. with a single pyramidal neuron receiving intrinsic innervation from the axon collateral's of multiple pyramidal neurons (Kritzer and Goldman-Rakic, 1993; Pucak et al, 1996.

This particular organisation of excitatory intrinsic connectivity in layers 1-3 of the DLPFC, is unique to the prefrontal cortex in the monkey (Levitt et al, 1993; Kritzer and Goldman-Rakic, 1995; Pucak et al, 1996) and in humans (Kritzer and Goldman-Rakic, 1993; Kritzer, 1994) and may make an important contribution to the many neuronal properties and functions known to be specific to this cortical region. These wide lateral intralaminar projections spread in a tangential fashion throughout layers 1-3 and less extensively in layer 5 (Levitt et al, 1993; Pucak et al, 1996).

The discontinuous stripe-like organisation of intrinsically-projecting pyramidal neurons was also observed to be comparable in dimensions to that of the similarly stripe-like arrangement of the afferent termination's of association projections to other PFC areas

(e.g. areas 10 and 24), as well as to distant portions of areas 9 and 46 (Pucak et al, 1996). These association connections were also found to be reciprocal in nature (Pucak et al, 1996), with areas 9 and 46 being targeted by association projections from pyramidal neurons in some of the same PFC sectors (i.e. areas 9, 10, 24 and 46) which were found to receive association projections from the DLPFC.

The important roles which pyramidal neurons are hypothesised fulfil in their furnishment of both reciprocal intrinsic and extrinsic excitatory projections in adult primates, as well as the developmental changes in their morphological characteristics (e.g. dendritic spines, excitatory synapses and axonal termination's), merit a comprehensive examination of this most numerously distributed class of cortical neurons.

5.2: Morphology of cortical pyramidal neurons.

Pyramidal neurons represent the single most ubiquitous neuronal population in the mammalian cerebral cortex, making up approximately three-quarters of the total neuronal complement and fulfilling a role as the primary mediators of both local and long-distance excitatory communication within the cortex. Their axon varicosities are known to terminate onto both other pyramidal neurons and non-pyramidal (mainly GABAergic) neurons (Hendry et al, 1983c; Kisvarday et al 1986; McGuire et al, 1991). Although at first sight, cortical pyramidal neurons in different cortical regions may appear to be almost identical in their morphology, they are in fact an extremely heterogeneous neuronal class in terms of their laminar location, dendritic tree arrangements, numerical complement of dendritic spines, axon trajectories, projection targets and sources of incoming afferent inputs; as well as they can differ markedly in their biochemical content - structural proteins, enzymes and neurotransmitter molecules - and possible functional attributes (reviewed in Feldman, 1984 and DeFelipe and Farinas, 1992).

The basic structure of a pyramidal neuron consists of a pyramidal shaped cell body (soma) with a single prominent apical dendrite most commonly found to extend towards the pial surface and a set of shorter basal dendrites which emanate from the soma (or cell body). Pyramidal neurons are absent from layer 1 and only rarely found in layer 4 of most cortical regions. The apical dendritic trunk passes upwards through the cortical neuropil - with oblique branches arising along its length and sometimes it bifurcates into 2 secondary trunks away from the cell body. The apical dendrite terminates in a tuft of terminal branches within a more superficial layer - generally layer 1 in the case of layer 3 pyramidal cells. In addition to these primary distinguishing features the basal dendritic tree generally emanates from

the lower half of the soma and the dendrites radiate outwards, exhibiting an extensive degree of (first, second, third order etc) branching along the way, within a hemispheric field - although quite often in individual pyramidal cells there are basal dendrites travelling in all directions from the cell body.

5.3: Types of projections formed by cortical pyramidal neurons.

Cortical pyramidal neurons can exhibit 3 basic types of connectivity: **(i)** long interareal association (intrahemispheric) or callosal (interhemispheric) projections, **see Figure 19**, **(ii)** local or longer intraareal intrinsic projections and **(iii)** subcortical projections. Individual pyramidal neurons may contribute to all three or only one or two of these 3 types of projection patterns in the primate brain. We shall concentrate on the first 2 types of projection which are mainly (>70%) provided by layer 3 pyramidal neurons - the subject of the first study in this thesis - whereas sub-cortical projections primarily arise from pyramidal neurons in layers 5 and 6.

5.4: Organisation of excitatory intrinsic connections in the primate cerebral cortex.

Pyramidal neuron projections distributed within the same area and even the same layer as that of the projecting cells are known as intrinsic, intrareal connections and derive from laterally spreading collateral branches emerging from the primary axon in close proximity to the cell soma. Collateral branches are known to terminate on the dendritic shafts (5%) and spines (75%) of other pyramidal neurons and the smooth dendritic shafts (20%) of interneurons in the primary visual cortex (McGuire et al, 1991). In the DLPFC (Melchitzky et al, 1995, 1996), a large proportion of the synaptic targets of intrinsic pyramidal neuron collateral's are dendritic spines (95%) of other pyramidal neurons, while only 5% are smooth dendritic shafts of interneurons.

5.5(A): Pyramidal neuron excitatory intrinsic lattice circuitry in the monkey DLPFC.

The intraareal intrinsic connectivity of pyramidal neurons has been examined in areas 9 and 46 of the adult monkey DLPFC using small, focal (200-400 μm wide) injections of biocytin in layers 2-6 and mapping the location of the resultant local labelling of anterograde axon fibres and terminals within these same areas (Levitt et al, 1993). A stripe-like pattern of clustered axon fibres and terminals was observed in layers 1-3, surrounding the injection site. Narrow bands of terminal labelling (200-400 μm wide; **see Figure 20A**), were seen to be interspersed by regular, similarly sized, label-free bands surrounding the injection site. Overall,

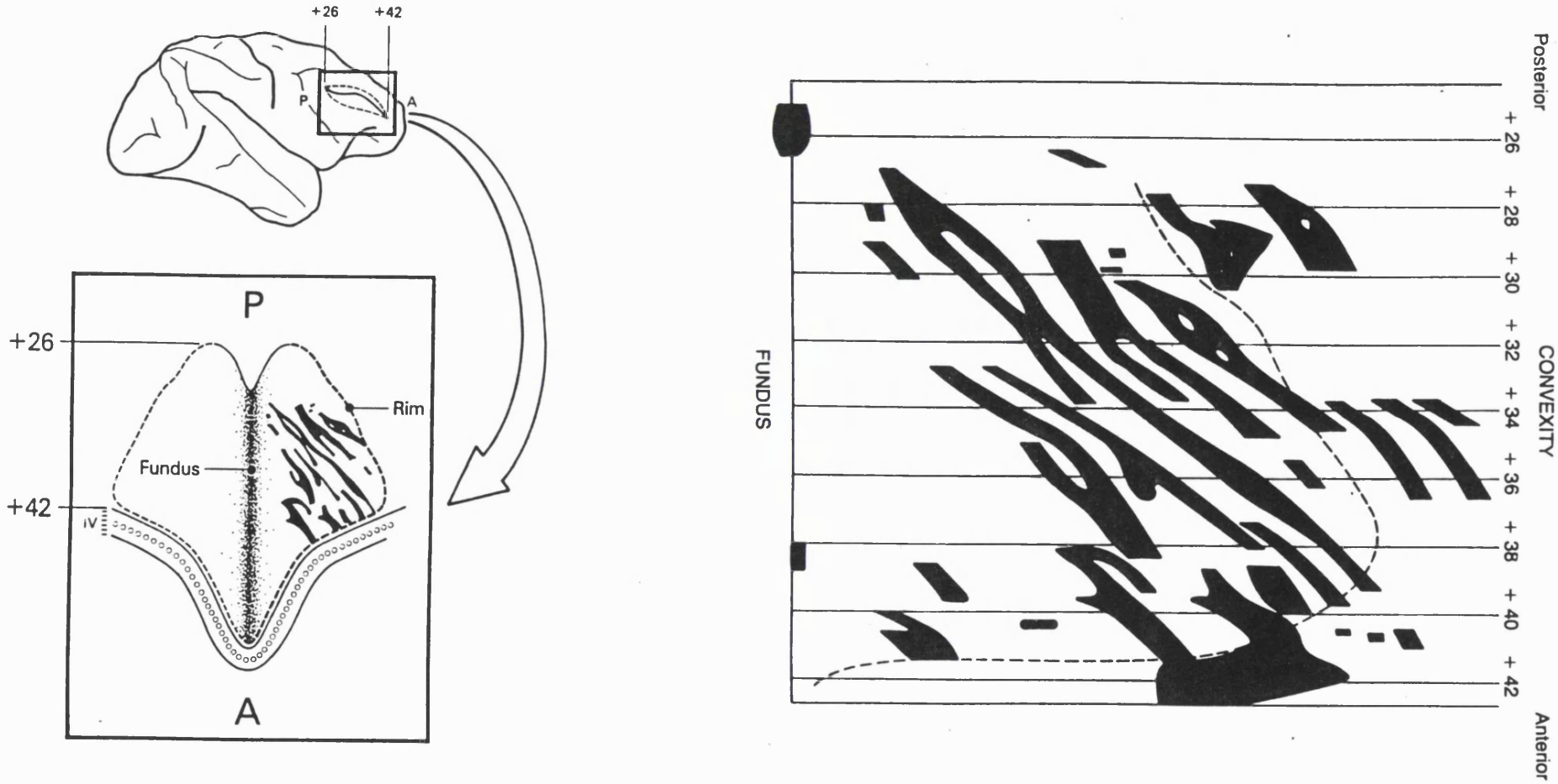

Figure 19 The organisation of callosal (from a contralateral area 46 injection) cortical afferent terminations in the PS region (area 46) of the DLPFC in the monkey. **(A)** shows an opened-up view of the inner surface of the PS (i.e. ventral bank = left, dorsal bank = right, A = anterior, P = posterior), with the pattern of afferent terminations within layer 4 plotted on the surface as a flat tangential map constructed from serial coronal sections through the PS region. **(B)** shows an enlarged version of the same tangential map of afferent terminations as seen in **(A)** allowing a greater appreciation of the overall stripe-like pattern, with cross-junctions, blind-endings and Y-shaped overlaps. The rostrocaudal extent of the reconstruction in proportion to the rest of the cortex is indicated on the small lateral view of the macaque monkey brain (top) in **(A)**. Figure **(A)** from Goldman-Rakic (1981a) and figure **(B)** from Goldman-Rakic (1984).

these labelled domains occupied an elongate slab of cortex (2-4 mm in length) tangentially parallel with the pial surface and oriented such that the long axis of the labelled terminal fields was approximately at right angles to the nearby principal sulcus. These stripes extended in a parallel vertical arrangement through and within layers 1-3 of areas 9 and 46, maintaining their discrete separated lattice-like organisation in all 3 dimensions in tangential reconstruction's of serial coronal sections.

The terminal fields of pyramidal neuron axons furnishing the superficial layer intrinsic lattice connectivity within the DLPFC cover a larger area with clusters of terminals distributed in the form of discontinuous elongated stripes (Levitt et al, 1993; Pucak et al, 1996). These stripes are almost identical in size for the distribution of both the terminal fields (Levitt et al, 1993; Lund et al, 1993; Pucak et al, 1996; **see Figure 21B**) and the projecting neurons of origin within layer 3 of areas 9 and 46 (Kritzer and Goldman-Rakic, 1995; Pucak et al, 1996; **see Figure 21A**). These stripe domains of anterogradely-labelled axon terminals or retrogradely-labelled pyramidal cells run tangentially across layers 2 and 3 of both areas 9 and 46 with no obvious disruption in their organisation at the border region between these 2 areas.

The dimensions of stripe-like arrangements of intrinsically-connected pyramidal cells and their axon collateral's and terminals in the DLPFC have been described in some detail (Levitt et al, 1993; Kritzer and Goldman-Rakic, 1995; Pucak et al, 1996). It has been observed that the horizontal (tangential) distribution of neurons or terminals fields within the superficial layers (less clear in layer 5) shows a distinct preference for extending further along the mediolateral axis than the anteroposterior axis (anisotropy or asymmetry), for example sometimes producing a ratio of 7 mm : 700 μm, respectively for the most distant clusters of intrinsically-labelled layer 3 pyramidal cells (Kritzer and Goldman-Rakic, 1995; Pucak et al, 1996).

Tracer injections placed in layers 2 and 3a resulted in a pattern of labelled cell or terminal clusters with a lateral extent that exhibited a minor difference of a few hundred mm between the medial and lateral extent of labelling on either side of the injection locus. By contrast layer 3c injections could produce very significant asymmetry in the mediolateral distribution of labelled cells with for example a lateral extent of 7 mm and a medial extent of 3 mm for the discontinuous, tangentially-oriented elongated patch domains of labelled neurons (Kritzer and Goldman-Rakic, 1995). Less extensive connections spread from the injection sites placed in layer 5 of the DLPFC with recurrent axon collateral's ascending into the superficial layers (Levitt et al, 1993; Pucak et al, 1996).

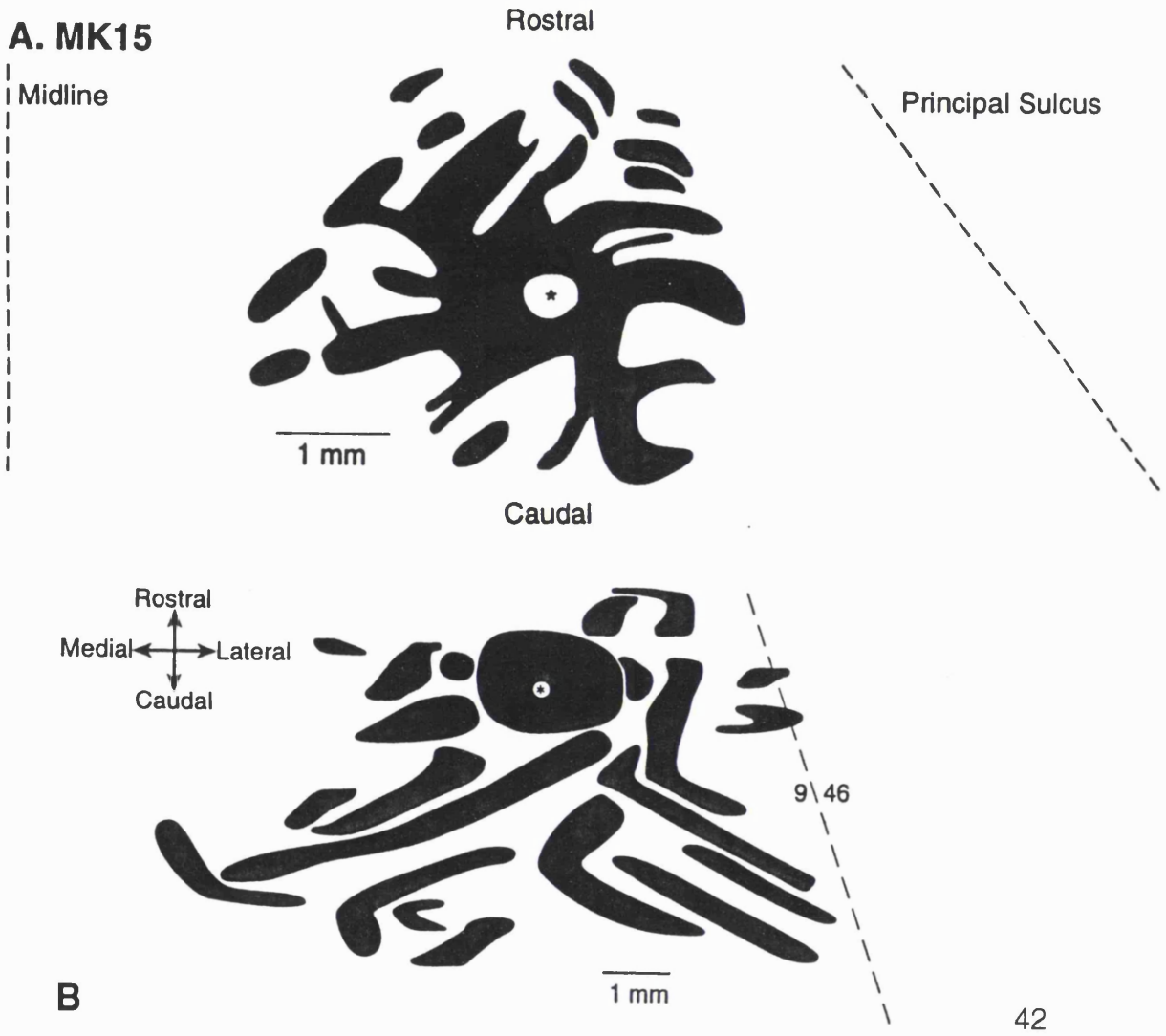

Figure 20 Tangential organisation of intrinsic lattice circuitry in the monkey DLFPC (areas 9 and 46). **(A)** shows a flat-map reconstruction from serial coronal sections of anterogradely-labelled axon/terminal clusters distributed in area 9 (on dorsal surface) near the border with area 46. **(B)** shows a flat-map reconstruction from serial coronal sections of retrogradely-labelled neurons distributed in area 9 (on dorsolateral surface) near the border with area 46. Note the roughly orthogonal orientation of stripes as they near the the principal sulcus **(A)** or the 9/46 border **(B)**. In both **(A)** and **(B)**, the asterisk represents the injection site in area 9, following an injection of in **(A)** biocytin, 450 µm core size and in **(B)** cholera toxin subunit-B, 400 µm core size. **N.B.** slightly different scales of **(A)** and **(B)**. Figure **(A)** from Levitt et al (1993) and figure **(B)** from Pucak et al (1996).

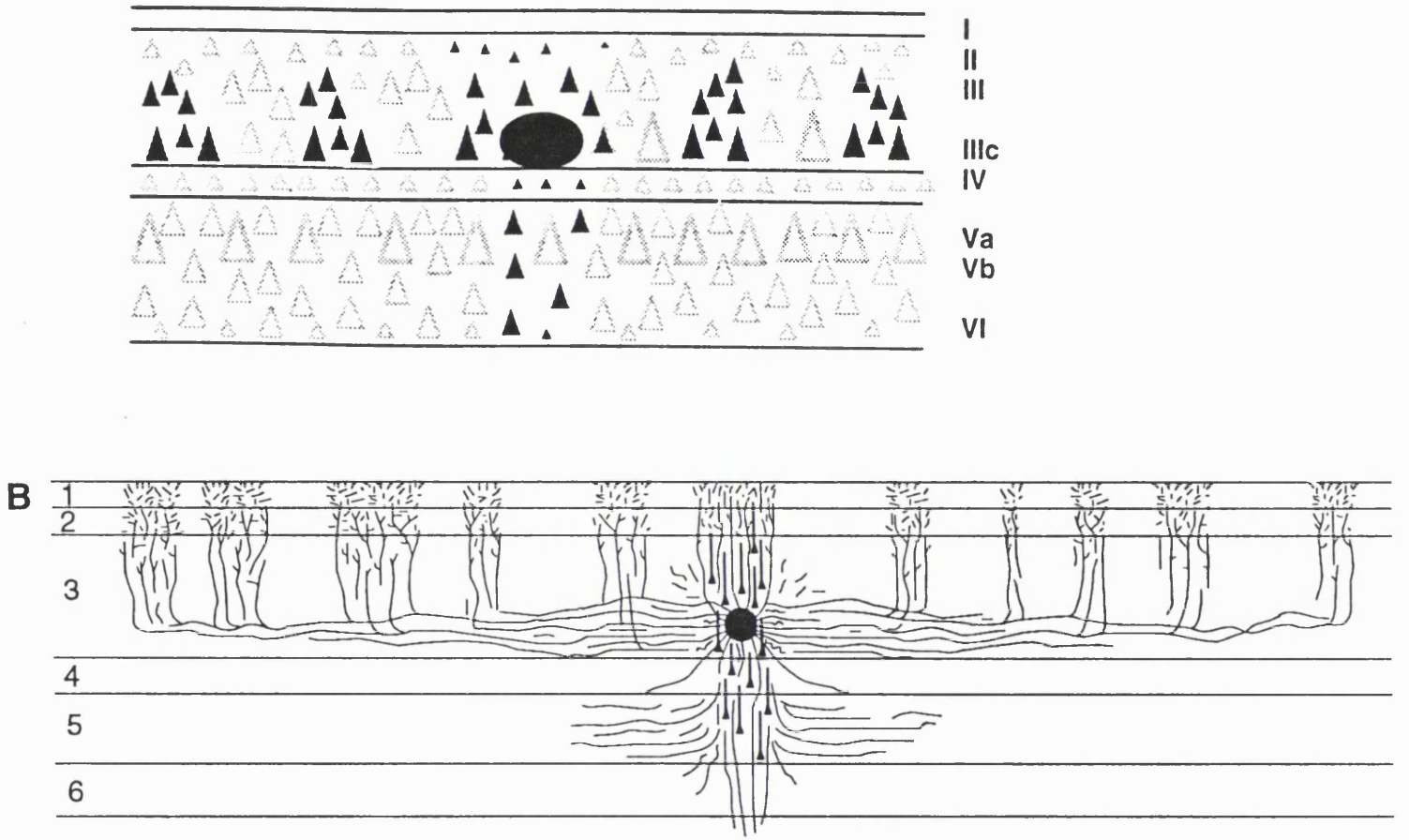

Figure 21 Schematic drawings (N.B. not to exactly the same scale) showing the comparative dimensions of intrinsic lattice circuitry in the monkey DLFPC (areas 9 and 46). **(A)** Retrogradely-labelled pyramidal neurons originating from an injection site in layer 3c, give rise to intrinsic lattice circuitry. These intrinsically-projecting pyramidal neurons are arranged in clusters within layer 3c (deep layer 3) in the coronal plane and form a discontinous pattern of parallel stripes across the DLPFC in the tangential plane (mediolaterally). **(B)** Anterogradely-labelled axons and terminals resulting from an injection site in layers 3b/3c furnished by intrinsically-projecting pyramidal neurons in the same layer. These intrinsically-derived axons and terminals form ascending columns which pass through layers 2 and 3 and form terminal tufts in layer 1. They also form a discontinous pattern of parallel stripes across the DLPFC in the tangential plane (mediolaterally). Figure **(A)** from Kritzer and Goldman-Rakic (1995). Figure **(B)** from Levitt et al (1993).

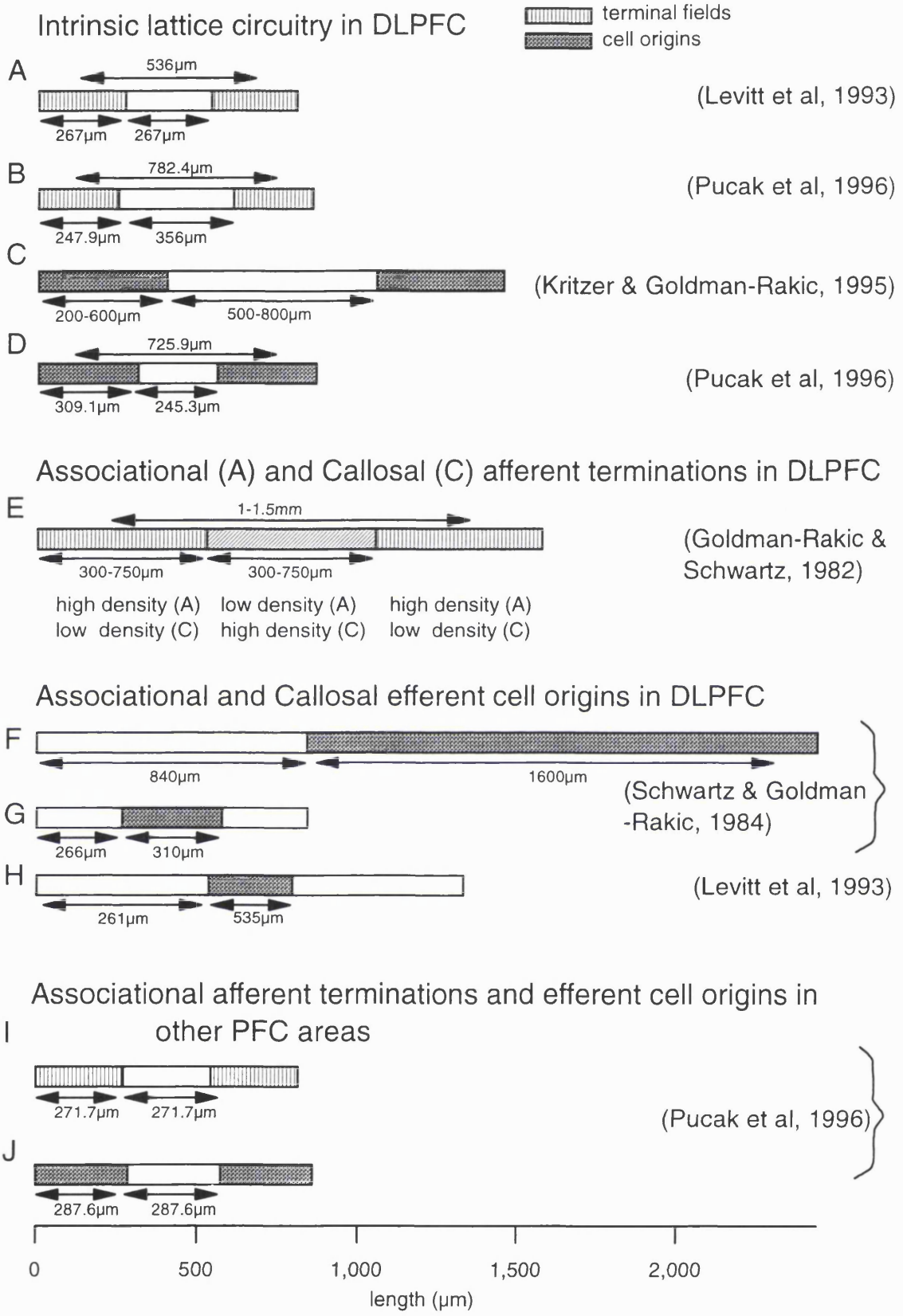

Figure 22 A schematic diagram showing the scale of intrinsic lattice circuitry (**A-D**) in the monkey DLPFC, with a comparison of the distribution of terminations and cell origins for short-range callosal projections in the same region (**E, G** and **H**) and long-distance associational pathways in the same (**E** and **F**) and other PFC regions (**I** and **J**). The lengths of the bars illustrate the widths of stripe (dense distribution of terminals or cells) and interstripe (sparse distribution of terminals or cells) compartments in each case. Also shown are the mean centre-to-centre distances between stripes, where available, which represent the maximal separation between stripe-centres at their narrowest point in the coronal, pial-to-white matter or tangential axes, where appropriate. Figure based on an original diagram in Levitt et al (1993) while the data was compiled from the literature (references indicated above).

5.5(B): Comparison of intrinsic pyramidal neuron axon/terminal domains and cell body domains in the DLPFC.

The dimensions of clusters made up of retrogradely-labelled intrinsically-projecting pyramidal neurons in areas 9 and 46 (200-600 μm wide, 5-7 mm long; Kritzer and Goldman-Rakic, 1995) were observed to be of the same order of magnitude, in width and length as those of the pyramidal neuron intrinsic terminal clusters (100-600 μm wide, 3.5-8.0 mm long; Levitt et al, 1993).

In the most recent study of pyramidal neuron intrinsic lattice connections (Pucak et al, 1996), elongated stripes composed of clusters of either anterogradely-labelled axon fibres/terminals or retrogradely-labelled pyramidal neurons, resulting from separate injections of different tracers, were observed to be of comparable size to those observed in the 2 previous studies (Levitt et al, 1993; Kritzer and Goldman-Rakic, 1995). In the tangential plane i.e. parallel to the pial surface, the lateral extent of the overall alternating pattern of labelled and unlabelled stripe domains was of the order of (1.0-7.4 mm for anterograde, 0.8-6.0 mm for retrograde) on either side of the injection site, with between (9-17 for anterograde, 9-21 for retrograde) stripes resulting from a single injection case (**see Figure 20B**). Both types of stripes, composed of either anterogradely-labelled axons/terminals or retrogradely-labelled neurons were found to be oriented in all directions surrounding an injection site, but were predominantly aligned length-ways along the mediolateral plane of the cortex, as previously observed (Levitt et al, 1993; Kritzer and Goldman-Rakic, 1995).

Specifically, using the tracer BDA Pucak et al (1996) found that the mean width of stripes composed of clusters of anterogradely-labelled intrinsic pyramidal neuron axons/terminals through layers 1-3 in the DLPFC (247.9 μm; **see Figure 22**) was found to compare favourably with the previous finding of 267 μm for the width of axon/terminal stripes labelled with biocytin in the DLPFC (Levitt et al, 1993; **see Figure 22**). Also, in the same study (Pucak et al, 1996), the width of stripes composed of clusters of CtB retrogradely-labelled intrinsic pyramidal neurons (309.1 μm; **see Figure 22**) was within the range of that found by Kritzer and Goldman-Rakic (1995), i.e. between 200-600 μm in width (**see Figure 22**).

5.6: Maturation of the corticocortical projections of the monkey DLPFC.

Since study 1 of the thesis concerns the postnatal development of dendritic spines located on layer 3 pyramidal neurons in the DLPFC, we shall review the maturational time

course of the associational and callosal connections of layer 3 pyramidal neurons in the monkey DLPFC. In the adult monkey, these extrinsic projections are known to contact the dendritic spines present on the dendrites of pyramidal neurons; these same pyramidal cells in turn sending efferents to other cortical areas.

As a consequence of the primarily layer 3 location of their input and output, these interareal connections are likely to be in close association with the intrinsic lattice connections of layers 1-3 in the DLPFC. Therefore, the developmental time course of afferent termination's to and efferent neuronal projections from the DLPFC, are presumed to have a significant impact on the maturation of the intrinsic circuitry within this region.

The well-defined columnar arrangements of afferent terminal input found in the dorsolateral PFC and in other cortical association regions were first demonstrated by making injections of radio-labelled amino acids into the appropriate areas. Radio-labelled terminals and fibres were visualised by autoradiography for each of the homotopic regions in the hemisphere contralateral to the injection site (Goldman and Nauta, 1977). Terminal labelling was found to be distributed in a periodic fashion, composed of vertically-oriented stripes or columns: 200-500 μm wide, with terminals and fibres present throughout layers 1 to 6 in all areas. This form of afferent distribution was observable in monkeys of all ages examined, i.e. 4 days through to 5.5 months. This columnar organisation of labelled afferents was most clearly seen in neonatal animals, while the clarity of their distribution was observed to decrease and become more diffuse with increasing age.

Very few studies have been carried out which investigate the time course of formation of connections between area 46 and other cortical areas during pre- and postnatal development and whether the immature organisation of corticocortical connectivity varies greatly from that of the adult pattern of connections. It is of particular importance to discover how the maturation of DLFPC corticocortical afferents and efferents is related to the functional maturation of the region and the complex sensory-integrative behaviours it mediates. Those studies conducted, have been restricted to autoradiographic tracing with large injections of radioactive amino acids placed into the PS of foetal or young infant monkeys, with examination of the resulting arrangement of terminal labelling in the contralateral PS (Goldman-Rakic, 1981; reviewed in Goldman-Rakic, 1982 and Goldman-Rakic, 1987b).

5.7: The maturation of layer 3 pyramidal neuron morphology in the monkey DLPFC.

The unique organisation of the complex intrinsic stripe-like lattice circuitry

which has been shown to exist in the superficial layers of the primate DLPFC (areas 9 and 46), is thought to be the major distinguishing component of an elaborate anatomical and neurochemical milieu mediating the diverse functional properties exhibited by this cortical region. It is important to establish the time course for the anatomical and functional development of this intrinsic lattice organisation, to be able to determine whether it is coincident with or distinct from that of other cortical regions. This knowledge would assist in answering the questions of how large-scale distributed networks of areas each with their own form of intrinsic circuitry, may provide substrates for the gradual emergence of particular aspects of functional behaviour at different stages of development and if these go awry, e.g. as may occur in the schizophrenic brain, how the formation of abnormal circuitry may bring about the diverse symptomatology observed in this disease.

The postnatal changes occurring for pyramidal neurons in the primary visual cortex (area 17) in the macaque monkey have been examined in some detail and they appear to show a close relation in their time course to the emergence of the mature functional properties of this sensory cortical region in primates. The numbers of dendritic spines on pyramidal and stellate neurons in layers 3 and 4, respectively, of the macaque monkey striate cortex (area 17), have been observed to change substantially during postnatal development (Boothe et al, 1979). The number of asymmetric synapses in all layers of area 17 have also been observed to show an identical time course (Bourgeois and Rakic, 1993). A rapid rise in spine numbers occurs between birth and 8 weeks of age (during which the spine number doubles) followed by a plateau phase of stable levels between 8 weeks and 36 weeks and then a gradual decrease in spine numbers occurs throughout puberty and into adulthood.

These changes have been found to closely coincide with the various stages of critical events involved in the maturation of visual function. These events have been documented in neurophysiological, anatomical and behavioural studies and primarily consist of the final stages of ocular dominance column segregation in area 17 (LeVay et al, 1980). There appears to be a correlation between the sharp rise in the numbers of dendritic spines and the timing of the critical or "sensitive" period of visual plasticity, i.e. the early stage of the neonatal period during which monocularly-deprived monkeys still demonstrate the ability to recover their normal functional and anatomical ocular dominance properties when the deprived eye is reopened or they show additional changes when the conditions for the deprived and normal eyes are reversed (Lund et al, 1991).

Changes in spine numbers have been found to vary for different neuron populations according to their laminar environment (Mates and Lund, 1983a,b). More

specifically, these differences have also been observed for neurons of the same class targeted by different types of afferent input in adjoining layers (Lund and Holbach, 1991). Even different portions of the dendritic tree of a single pyramidal neuron may exhibit variation in the maturational time course of spine populations during postnatal development, depending on their particular laminar surroundings (Boothe et al, 1979).

Changes in synaptic density for all cortical layers, have been quantitatively analysed in several different areas of the monkey cerebral cortex, for animals ranging in age from the early prenatal period through postnatal development and into the period of middle adulthood (Rakic et al, 1986). Samples were made from the visual, motor, somatosensory and prefrontal cortices. The shape of the time course of synaptogenesis was found to be identical for all these functionally distinct areas and in all but the primary visual cortex (area 17) - where values reached maximum earlier in development than for any of the other regions - the absolute densities of synapses (per 100 μm^2 of neuropil) were also the same for all areas sampled. For both these parameters, there also appeared to be no significant differences between the values for the individual layers of any given area, apart from area 17.

This type of analysis has also been carried out in specific layer-by-layer study of the DLFPC (area 46; Bourgeois et al, 1994). In this study, measures of absolute number, density and proportion of synapses per unit area and per unit volume of neuropil were acquired for each layer of each area in monkeys of ages ranging from E (embryonic day) 47 through to 20.0 years of age. The densities were also described in terms of the 2 main types of synaptic thickening's, i.e. asymmetric (excitatory, Gray's type 1; Gray, 1959) or symmetric (inhibitory, Gray's type 2; Gray, 1959) and the proportion of synapses situated on dendritic spines or shafts across the time-scales of prenatal and postnatal development. Synaptogenesis was divided into 5 distinct periods or phases (in synapses per μm^2 of neuropil; **see Figure 23C**), the "pre-cortical" phase (between E47-E78) was characterised by the presence of synapses both above and below the cortical plate and the "early cortical" period (E78-E104) was distinguished by a low-level accumulation of synapses within the cortical plate itself. Thirdly, the "rapid" phase (E104-2 months postnatal) was marked by a dramatic increase in mean synaptic density (per μm^2) over this period which reached a peak at around the end of the second postnatal month. The peak "rate" of synaptic acquisition was at E165 just prior to birth, when levels of synapses equalled that found in the adult animal. The fourth "plateau" period of synaptogenesis occurred between 2 months and 3.0 years of age, when the high

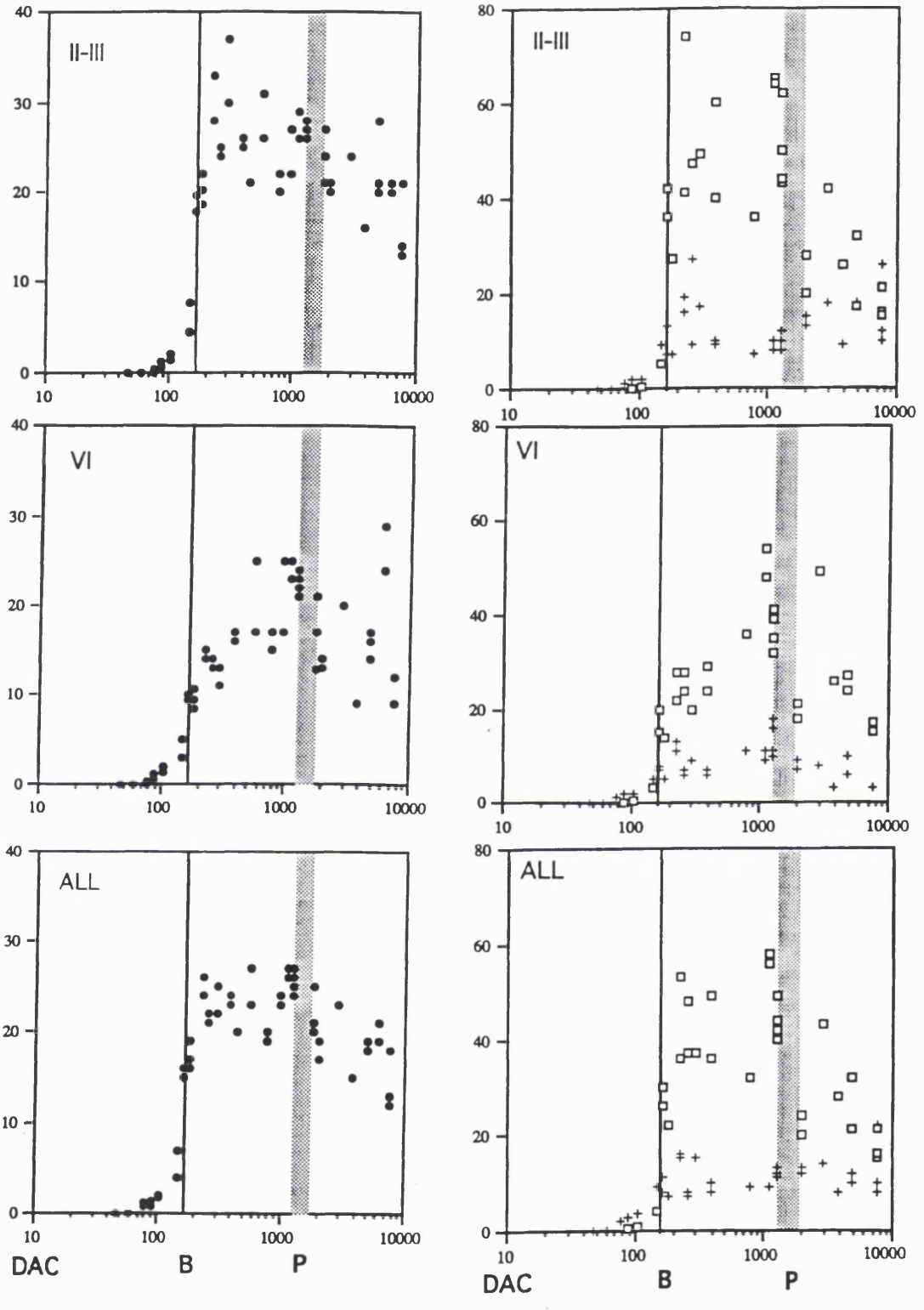

Figure 23 Histograms showing the timescale of changes in the density of synaptic contacts (per 100 μm^2 area) of synaptic contacts in the neuropil of **(A)** layers 2-3, **(B)** layer 6 and **(C)** all cortical layers in area 46 of the monkey DLPFC. Pooled values for all types of synapses = filled circles. Histograms showing the timescale of changes in the density (per 100 μm^3 volume) of synaptic contacts in the neuropil of **(D)** layers 2-3, **(E)** layer 6 and **(F)** and all cortical layers, in area 46 of the monkey DLFPC. Axospinous synapses = open squares, axodendritic synapses = crosses. In **(A)-(F)**, B = birth, DAC = days after conception and P = puberty. Figures from Bourgeois et al (1994).

mean synaptic density (per μm^2) attained in the previous phase appeared to be maintained at the same constant level throughout this period. Finally, the last "declining" phase of synaptic development was observed between 3.0 years and 20.0 years of age, in which there was a slow and gradual, but sustained reduction in the density of synapses throughout adulthood.

The overall finding was that the superficial layers 1-3 (**see Figure 23A**), all exhibited the same overall time course of maturation, magnitude of total synaptic density and were synchronous in terms of their rates and patterns of total synaptic accumulation and reduction. The excessive level ("overshoot" in the initial portion of the rapid phase) of mean synaptic density (per μm^2) observed in the superficial layers was found to be of a lesser magnitude in layers 4 and 5 and was not observed in layer 6 (**see Figure 23B**). The authors considered these results to be unsurprising since almost three-quarters of all cortical synapses in area 46 were located in the superficial layers, together with the majority of corticocortically projecting cells and incoming afferent terminals and so these layers were concluded to make a considerable contribution to the shape of the overall cortical synapse distribution. When the total synaptic density was expressed in terms of number per 100 μm^2 of neuropil (taking into account the length of synaptic profiles in section thickness'; **see Figure 23D-F**) it still retained the same pattern and time-scale of events as that seen for the area per 100 μm^2 of neuropil (**see Figure 23A-C**).

The classification of synapses, at various developmental stages, into distinct classes on the basis of their target locus, i.e. either dendritic spines, shafts or cell somata, varied according to the particular time point sampled, across both prenatal and postnatal development. The 3 kinds of synapses defined by their postsynaptic targets were found to represent between: 25-40% (axodendritic), 60-75% (axospinous) and < 1% (axosomatic) of total synapses (**see Figure 23F**), across the entire range of ages examined. The earliest synapses to appear in the prenatal monkey were identified as those contacting dendritic shafts, increasing gradually in number between E60 and 2 months of age, they showed no further change in their density throughout adolescence or adult life. A constant population of synapses would therefore appear to be sustained on neuronal dendritic shafts, with no evidence of either overproduction, plateau or depletion during the animal's life-span. It has been proposed (Bourgeois et al, 1994) that this stability in numbers may be the result of the conversion of many of these synapses to the axospinous type during the "rapid" phase of synaptogenesis.

Axospinous synapses were first observed approximately 2-4 weeks following the appearance of axodendritic synapses, i.e. at between E78-E89 and gradually accumulated

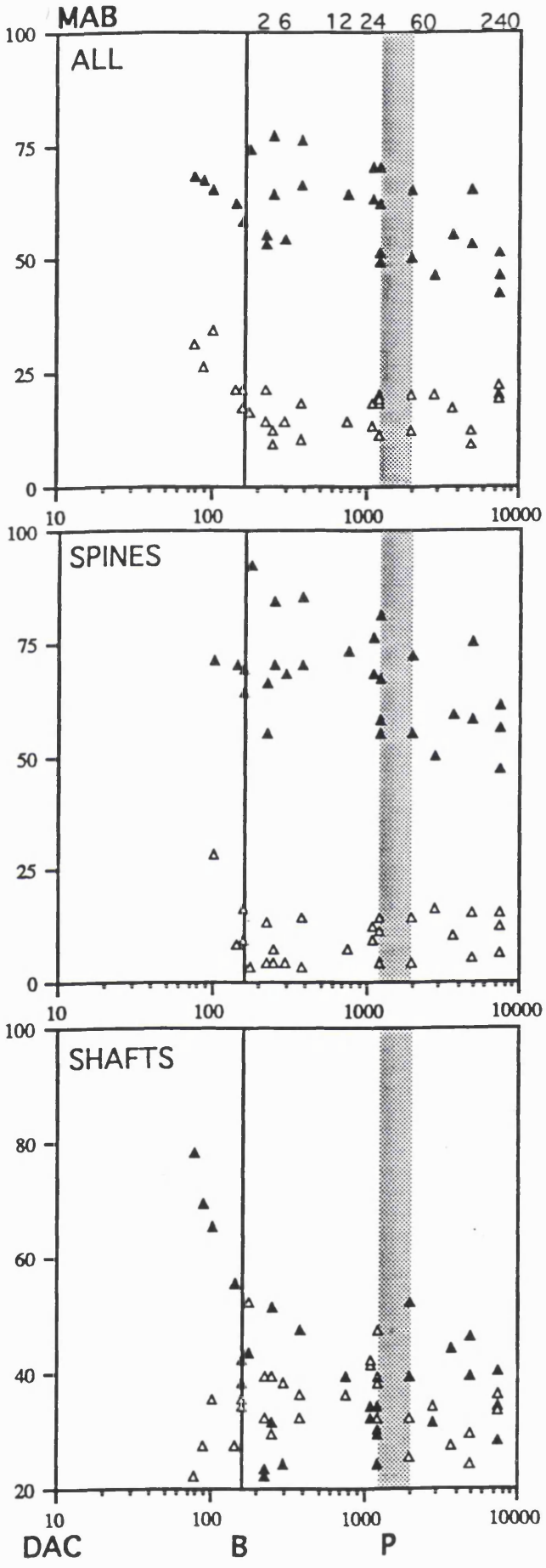

Figure 24 Histograms showing the percentage representation of asymmetric and symmetric synapses within the overall numbers, respectively of **(A)** all, **(B)** axospinous and **(C)** axodendritic classes of cortical synapses, pooled for all cortical layers during the course of pre- and postnatal development, in area 46 of the monkey DLPFC. Asymmetric synapses = filled triangles and symmetric synapses = open triangles. In **(A)-(C)**, B = birth, DAC = days after conception, MAB = months after birth, P = puberty. Figure from Bourgeois et al (1994).

from thereon. Between E104 and E149, the early part of the "rapid" phase of synaptic acquisition began. The levels of axospinous synapses accelerated postnatally, attaining a peak by the end of the second postnatal month a level which was maintained until 3 years of age and beyond, as the onset of puberty occurred. From then on, through puberty and into adulthood, the numbers of these synapses slowly, but consistently declined, eventually reaching 50% of their peak value as seen at the beginning of adolescence. Synapses terminating on dendritic spines make up most of the total synaptic complement in area 46 at all stages of development and as such are mainly responsible for the dynamic changes in synaptic density that are exhibited by this region during synaptogenesis.

Further subdivision of synapses in area 46 into those of either the symmetric or asymmetric type in the adult monkey, revealed the former to account for 20% and the latter to represent 80% of the total synaptic complement (**see Figure 24A**). The same values were also found at early, middle and late stages of prenatal development (E78-E149), it could be assumed that these proportions remain unchanging across the life of the animal, reflecting consistent proportional rates of production for each synaptic class at all stages of development. The respective contribution of each type of synaptic morphology to each of the 2 major types of postsynaptic contact, was such that approximately 60-80% of axospinous synapses consisted of the asymmetric class while < 10% were of the symmetric type (**see Figure 24B**), the rest were unclassified due to their being obliquely sectioned. In the case of synapses terminating onto dendritic shafts, this population split roughly into equal subpopulations of the symmetric and asymmetric forms (**see Figure 24C**). In both cases, either for synapses contacting dendritic spines or shafts, all layers of area 46 individually exhibited an identical proportion and pattern of distribution for symmetric and asymmetric forms of synapses in both prenatal and adult stages of development and these were comparable in relative levels to the overall proportions found for the pooled values for all layers.

5.8: Summary.

The cortical pyramidal neurons of the DLPFC are not a homogeneous class of cell they may be distinguished on an individual basis by their dendritic morphology (including spine number), local or long-distance axonal projection targets, synaptic inputs, developmental time course, neurochemical signature and functional properties. It appears that pyramidal neurons are as heterogeneous in their anatomical, biochemical and functional

properties as the morphologically and neurochemically diverse (reviewed in DeFelipe, 1993) cortical non-pyramidal class of neurons.

In terms of postnatal development of pyramid neuron circuitry dendritic spines, which are each the postsynaptic half of an asymmetric synapse show dynamic changes in density within all cortical layers of the DLPFC during the postnatal period. An examination of the time course of maturation in the density of these markers of excitatory synapses on individual pyramid neurons of layer 3, where intrinsic and extrinsic projections converge and diverge, will provide important information regarding the anatomical and functional development of the intraareal and interareal cortical circuitry furnished by these neurons.

6.0: Neurotransmitter Systems.

6.1: Introduction: Organisation of neurotransmitters in the monkey PFC.

The functional heterogeneity of the PFC is best illustrated by the diversity and specificity of the distribution patterns of various neurotransmitters across its constituent areas, as measured by immunohistochemical staining of their synthetic enzymes or the transmitter molecules themselves. All the major modulatory neurotransmitters are represented throughout the PFC, albeit to varying degrees, whereas in the primary sensory cortical areas these neurotransmitters may either be almost totally absent or alternatively they may predominate. For example, in monkey primary visual cortex (V1), the 5-HTergic and noradrenergic (NAergic) innervations are strongest , the cholinergic input is moderate, whilst dopaminergic axons are virtually absent. By contrast, in the DLPFC, axons of the 5-HTergic, NAergic, AChergic and DAergic systems are all well represented within the 6 cortical laminae, with their own distinctive patterns of density distribution and fibre orientation within the various layers.

All 4 neurotransmitters achieve many of their functional effects via their binding to various receptor subtypes specific for each neurochemical. These receptors are distinguishable by their differences in molecular structure, cortical areal, laminar and cellular location (somatic, dendritic, axonal, i.e. pre- or postsynaptic locus) and in their mechanisms of action (i.e. G-protein linked, phosphoinositide-linked etc). In this way the 4 major modulatory neurotransmitters are able to exert a whole host of diverse effects on various components (even distinct portions of the same neuron may express different subtypes of the same or another neurotransmitter receptor) of the cortical circuitry in the DLPFC. In various studies of cortical areas, the density distribution of a particular neurotransmitter receptor subtype has been observed not to coincide exactly with that of the axon innervation which conveys

the neurotransmitter itself. This so-called "mismatching" of neurotransmitter release sites and receptors seems to hold true for the DLPFC and for 5-HT and DA specifically.

Neurotransmitter receptors can be located either pre- or postsynaptically; a significant proportion, if not the vast majority, of modulatory neurotransmitter-containing axons appear not to form synaptic contacts in the monkey prefrontal cortex (Smiley and Goldman-Rakic, 1993, 1996; Mrzljak et al, 1995) and so are not restricted to the confines of localised "classical" synaptic neurotransmission. It has been hypothesised that these terminals release their transmitter by a diffuse "volume transmission" mechanism (reviewed in Descarries et al, 1991). In order for this latter mechanism of neurotransmitter release to be effective and to justify the heterogeneous anatomy of the various neurotransmitter systems, it would be highly dependent on there being a variety of different receptor subtypes and diverse locations for them on different classes of cells and axons (even on the terminal axons of other transmitter systems). By this means they would be able to exert specific effects and enable temporally coherent action, perhaps at the level of a population of neurons in a certain layer in each area. On the basis of the low synaptic frequency for their axons (Smiley and Goldman-Rakic, 1993, 1996) both the 5-HTergic and DAergic systems appear to be prime candidates for this form of neurotransmission in the DLPFC.

There is significant evidence to implicate DA and its receptors with an important modulatory role in the mechanisms of cognitive functions such as working memory in the primate DLPFC, in monkeys (Sawaguchi and Goldman-Rakic, 1991; Williams and Goldman-Rakic, 1995). There is also evidence in visual cortex that 5-HT can exert a profound modulatory influence on sensory processing and although its effects have not been examined to the same extent or in the same detail as dopamine, it may well emerge to be making as important a contribution as DA in the mechanisms of DLPFC function. Preliminary pharmacological studies have been conducted in the primate DLPFC and many PET studies have been carried using specifically designed ligands to localise the various 5-HT receptor subtypes in the human brain; it has been found that as in the monkey (for 5-HT_1 and 5-HT_2 receptors) they have distinctive distribution patterns in different layers and areas, including in the DLPFC. There is also much evidence to suggest that serotonin and dopamine may act reciprocally towards each other, either directly via their partial antagonistic effects on each others receptors or indirectly via their binding to their own receptors which may be localised on the same cellular components and might have opposing fine regulatory control over the same functional mechanism, e.g. working memory in the monkey DLPFC.

In addition, 5-HT and its receptors have been well characterised with an

important modulatory role in the development of circuitry in several areas of the cerebral cortex in many mammalian species (Bennett-Clarke et al, 1995; Matsukawa et al, 1995; Rörig and Sutor, 1996; reviewed in Lauder, 1993; Killackey et al, 1995; Whitaker-Azmitia et al, 1996).

It is of interest, where possible to compare the developmental time courses for different neurotransmitters in the primate DLPFC, in order to explore the possible parallels which can be drawn between the permanent modulatory/regulatory interactions which they show in the adult monkey and human DLPFC. In this way it might be possible to relate the pattern and time course of axon development to the transient or cycling nature of the neurotransmitters, with their potentially trophic or neuromodulatory roles during the prolonged developmental maturation of the unique cortical circuitry and functional attributes of the primate DLPFC.

6.2: Dopamine (DA).

6.2(A): Introduction.

Dopamine is a catecholaminergic neurotransmitter, localised within an afferent system of projections originating from several subcortical nuclei, namely the substantia nigra (SN; pars reticulata and pars compacta subdivisions) and the ventral tegmental area (VTA) of the mid-brain. These nuclei contain large numbers of DA synthesising neurons which send out long distance axon projections to innervate various regions within the cerebral cortex. Dopamine is produced via a synthetic biochemical pathway common to all catecholamines (noradrenaline and adrenaline), its major rate limiting synthetic enzyme being tyrosine hydroxylase (TH).

The DLPFC (areas 9 and 46) is thought to receive the bulk of its extrinsic DAergic axon projections from the ipsilateral anterior two-thirds of the VTA and in addition to receive only a very sparse input from the ipsilateral medial third of the pars compacta (pc) subdivision of the SN (Porrino and Goldman-Rakic, 1982). A recent study using a combination of retrograde tracer injections in area 46 and double-labelling with a TH-specific antibody in the SN-VTA region (Goldman-Rakic and Williams, 1995), has revealed that not all prefrontally-projecting DAergic neurons are restricted to the VTA as previously thought; showing that the DLPFC receives a significant DAergic input via the direct projection it receives from the lateral-medial extent of the dorsal SNpc as well as from the VTA (2/3 of double-labelled cells distributed equally through both nuclei) and also from the dorsal retrorubral area (1/3 of double-labelled cells).

The DAergic innervation of the DLPFC has been characterised at both light and electron microscope level and is probably the best understood of all neurotransmitters, in terms of its actions and interactions with other components of the cortical circuitry. DAergic axon terminals have been shown to synapse with the dendritic spines of pyramidal neurons in the DLPFC (a subject of study in this thesis); often they are accompanied by unlabelled axon terminals forming asymmetric (excitatory) synapses onto the same spines. These inputs are presumed to be corticocortical or thalamocortical afferent projections as well as intracortical connections, which are thought to use glutamate as their modulatory neurotransmitter. The localisation of glutamate immunoreactivity in the PFC has not yet been examined, but it is reasonable to assume that glutamate plays an important role in corticocortical, intracortical and thalamocortical neurotransmission to and from the DLPFC. The possible interaction of DAergic afferents with major excitatory inputs to pyramidal neurons is thought to be an integral part of the cellular mechanism for modulating their internal cellular activity levels; perhaps placing DA in a position to control and mediate the interactions between multiple cortical areas. In addition, the cellular and sub-cellular locations of various subtypes of DAergic receptors have been determined in the DLPFC and it is thought that their specific distribution enables the DAergic system to have a powerful influence over both the intrinsic, corticocortical and corticothalamic connectivity of the DLPFC in the primate brain. Dopamine is also known to be subject to complex modulatory interactions with other neurotransmitters, e.g. serotonin (studied in this thesis), acetylcholine, neuropeptides such as CCK and excitatory amino acids such as glutamate and aspartate via the synergistic actions of some of their respective receptor subtypes.

The postnatal maturational time course of the DAergic innervation in layer 3 of the monkey DLPFC (Rosenberg and Lewis, 1994, 1995; **see Spine study Discussion**) is hypothesised to correlate with certain stages in the postnatal development of spines located on the dendrites of layer 3 pyramidal neurons (Anderson et al, 1995 and this thesis). In this thesis we also examine a similar hypothesis, for the possible relationship of the postnatal time course of development of the 5-HTergic innervation in layer 3 of the monkey DLPFC, to developmental of connections to layer 3 pyramidal neurons, as well as other components of the neuropil.

6.2(B): Distribution of TH-labelled and DAergic axons.

6.2(B).(i): TH-labelling.

Studies using an antibody against tyrosine hydroxylase (TH), the synthetic

enzyme of dopamine production, have found the DLPFC (area 46) to have an intermediate to sparsely distributed TH axon innervation in terms of the overall density of the innervation across the entire cerebral cortex, primary motor cortex having the greatest density (Lewis et al, 1987, 1988). Although TH-immunoreactivity is found to be present in all layers, layers 1 - superficial 3 and layers 5 and 6 show the densest TH-axon innervation in area 46, producing a characteristic bilaminar pattern (Lewis et al, 1987). Area 46 on the dorsal and lateral surface is relatively densely innervated whilst the density of TH-axons is much lower in both banks of the principal sulcus (PS) and lower still in the fundus of the PS (Lewis et al, 1988). By contrast, area 9 is described as being heavily innervated in terms of the overall TH-axon distribution in the cerebral cortex, the medial portion, 9M being more densely innervated than the lateral portion, 9L (Lewis et al, 1988). A bilaminar innervation pattern of TH-axons is seen in area 9, as in area 46 (Lewis et al, 1987, 1988).

6.2(B).(ii): DA-labelling.

In the last few years antibodies to the dopamine molecule itself have been developed and with one such antibody a similar distribution of dopaminergic (DAergic) axons has been seen in areas 9 and 46, to that observed with the TH-antibody, i.e. a bilaminar innervation pattern. However, DAergic axons were described as being more densely distributed in the dorsal as opposed to the ventral bank of the PS in area 46, mainly due to a greater innervation of layer 3 (Williams and Goldman-Rakic, 1993).

6.2(C): Distribution of DAergic or TH-labelled varicosities and their postsynaptic targets.

In an electron microscopic (EM) study of the PFC (Goldman-Rakic et al, 1989), DAergic and TH-labelled synapses have been found in large numbers in the dorsal bank of the PS, their density distribution is equivalent to that of the bilaminar organisation of presynaptic axons as seen in light microscopic studies of DAergic immunoreactive axons. Symmetric synaptic contacts are observed to be made by TH-labelled varicosities with the cell bodies, dendrites and spines of Golgi-impregnated pyramidal neurons (N.B. contacts between DAergic varicosities and pyramidal neurons are not readily visualised in Golgi material). Synapses between DAergic axons and dendritic spines as seen in EM material, are normally accompanied by an asymmetric unlabelled bouton (indicative of glutamatergic input) contacting the same spine in a so called synaptic "triad" or complex (Goldman-Rakic et al, 1989).

A serial section EM study in monkey prefrontal cortex in the dorsal bank of the PS (Smiley and Goldman-Rakic, 1993) has shown that on average, 39% of DAergic varicosities through all layers form synapses (40% in layer 3). The mean overall distribution of synapses is as follows: 2% on somata; 34% on dendritic spines and 64% on dendritic shafts (0% on somata; 50% on spines and 50% on shafts in layer 3). The identity of all observed postsynaptic dendrites is: 42% spiny (pyramidal) dendrites; 29% smooth (interneuron) dendrites and 42% are of uncertain dendritic identity (of the 2 dendritic shafts receiving DAergic synapses in layer 3, both were of uncertain origin).

In layers 1-3 of monkey DLPFC (area 9), the synaptic incidence of TH-labelled varicosities on GABA-labelled dendrites is found to account for 44% of all TH-labelled synaptic contacts; 56% of synapses are formed with unlabelled dendrites (Sesack et al, 1995a). Also in area 9, a negative result has shown that although some TH-labelled boutons synapse onto the GABA-labelled dendrites of some local circuit neurons, the GABAergic, calretinin-positive (CalR) subclass are exempt from this synaptic input (Sesack et al, 1995b). A mean 26% of total TH-labelled varicosities were said to be closely associated with GABA-labelled postsynaptic dendrites but only 13% of the total number of TH-labelled varicosities formed actual synaptic contacts; 12% of the total TH-labelled varicosities were observed to be closely associated with CalR-positive dendrites, but no synaptic contacts were observed.

A more recent preliminary EM-level immunohistochemical study by the same group (Lewis et al, 1996) has identified at least one of the calcium-binding protein (CBP) subtypes of GABAergic interneurons which form the postsynaptic targets of TH-labelled axon terminals. Using a double-labelling EM procedure with antibodies specific for the CBP parvalbumin (PV) and tyrosine hydroxylase (TH) to label DAergic axon terminals in monkey DLPFC (area 9), it was observed that TH-labelled varicosities were apposed to PV-immunoreactive dendrites. About 33% of these contacts were found to represent symmetric synapses, but many TH-labelled varicosities contacted unlabelled dendrites in close proximity to PV-IR structures. It is likely that DAergic axons form synaptic contacts on one or other or both of either wide arbour (basket) neurons or chandelier neurons in the monkey DLPFC. These EM-level observations of DAergic/GABAergic circuitry interaction suggest that DAergic afferents are in a position to indirectly modulate the levels of inhibitory control exhibited by PV-IR interneurons which are known to target pyramidal neurons in the DLPFC.

6.3: Gamma-aminobutyric acid (GABAergic) and/or calcium-binding-protein-positive local circuit interneurons in monkey DLPFC.

6.3(A): Introduction.

Non-pyramidal cells of the cerebral cortex, can be broadly divided into those that are GABAergic i.e. they express immunoreactivity for the inhibitory neurotransmitter GABA, presumably reflecting their use of it to carry out their modulatory functions, and those that are non-GABAergic, i.e. they do not appear to use GABA as their neurotransmitter - or it is present at levels below the threshold of immunocytochemical detectability - and instead contain one or more of various neuropeptide molecules. Other populations of non-pyramidal cells have been found to express both GABAergic and neuropeptide molecules. In recent years, interest has grown regarding the morphological diversity and local circuitry of inhibitory GABA-containing interneurons in the cerebral cortex of the primate brain (Somogyi et al, 1981,1983; DeFelipe and Jones, 1985; reviewed in Jones and Hendry, 1984; Peters, 1984; Somogyi and Cowey, 1984).

Of the 13 classes of local circuit interneuron found in areas 9 and 46 (Lund and Lewis, 1993), we shall be examining only those which either have their cell bodies and axons in layer 3 or whose cell bodies are outside layer 3 but whose axon arbours pass through layer 3 (sometimes furnishing lateral projections) and terminate in other layers.

These generally inhibitory cells have been further subdivided into subpopulations of GABAergic interneurons, on the basis of their content of one or more of 3 distinct calcium binding proteins - CBP; calbindin (CalB), calretinin (CalR) and parvalbumin (PV) - as well as in some cases one of numerous neuropetide molecules (see later in this review). The distribution and morphology of these interneurons has been described most notably for the primary visual cortex (V1) of the monkey brain (Hendry et al, 1989; Van Brederode et al, 1990; reviewed in Jones et al, 1994), but some studies have also been conducted which examine the biochemistry and morphology of these cells in the PFC (Lewis and Lund, 1990; Williams et al, 1992; Lund and Lewis, 1993, Condé et al, 1994; Gabbott and Bacon, 1996a,b).

The study by Lund and Lewis (1993) identified the Golgi-impregnated morphological characteristics of 13 distinct classes of local circuit interneurons in the DLPFC (areas 9 and 46). This catalogue was then used to identify the observed morphologies of CBP-specific (calbindin, CalB-IR; calretinin, CalR-IR and parvalbumin, PV-IR) or neuropeptide-specific (CCK and prosomatostatin) interneurons in the same region, thus providing further subclasses of interneurons on the basis of their biochemical heterogeneity. No significant

differences were observed between interneurons in area 9 or area 46, so both their populations were pooled together.

Three well described inhibitory neuronal subtypes (based on their distinct morphologies) present throughout all regions of the cerebral cortex, are chandelier, large basket and double-bouquet neurons (Jones and Hendry, 1984; Peters, 1984; Somogyi and Cowey, 1984). In the DLPFC, they are found throughout the depth of the cortex from layers 2 to 6 (Williams et al, 1992; Lund and Lewis, 1993; Condé et al, 1994).

6.3(B): Chandelier neurons.

Lewis and Lund (1990) have examined the morphology of chandelier neurons and their content of parvalbumin in areas 9 and 46 of monkey DLPFC. Using the Golgi-rapid technique they identified chandelier neurons throughout layers 2-5, as possessing small cell bodies of 12-15 μm diameter, from which emerged fine vertically arranged dendrites. These dendrites were found to be arrayed in columnar-shaped arbours (50-75 μm wide, 200-300 μm length), sometimes spreading into layer 1. Cells in layers 2-3, were observed to give rise to axons, either from the base of their soma or sometimes from a proximal dendritic segment, which spread beyond the dendritic field in deep layer 3, but which did not enter layer 1. The axon's thickness varied along its extent, but upon reaching the vertical cartridge arrangements of varicosities, unique to chandelier neurons, the intervaricose segments between these columns of varicosities were often very fine.

Axon cartridges were found in all layers except layer 1, many were found to be comprised of the axon contributions from several chandelier neurons, since the numbers of varicosities traced in cartridges arising from the axons of single neurons were fewer than for those free cartridges seen to be associated with individual pyramidal neurons in the neuropil as had been previously shown for the chandelier neurons in other cortical regions by Somogyi et al (1982). The varicosities contained within axon cartridges were occasionally observed to contact the axon initial segments (AIS) in Golgi-impregnated pyramidal cells but in immunohistochemical preparations (with an antibody specific for PV) of tissue they could be observed to enclose the shadows of un-impregnated pyramidal cell AIS's and somata. In Golgi preparations, axon cartridges were most commonly seen in layers 2-4, but were also present in layers 5-6.

Using an antibody against parvalbumin (PV), Williams et al (1992) and Lund and Lewis (1993) observed PV-immunoreactive (PV-IR) vertical arrangements of densely

labelled boutons (sometimes connected with intervaricose segments) of 1-2.5 μm width and 15-40 μm length. In adult monkeys, these PV-IR cartridges were mostly seen in deep layer 2-superficial 3, were present at a lower density in superficial layer 2 and deep layer 3 and even less commonly observed in the other cortical layers (absent in layers 1 and 6). It was assumed from the similarities between the Golgi and the immunohistochemical observations that the PV-IR processes were chandelier neuron axon cartridges. However, PV-IR cannot be regarded as a wholly reliable marker of chandelier neurons and their axon cartridges in the monkey DLPFC, due to the absence of labelling in the superficial and deep layers seen in the adult monkey; however these neurons may be clearly seen in all layers in Golgi preparations of both infant and adult material. In addition PV-IR is present in other GABA cell subtypes such as basket neurons, in areas 9 and 46 (Lewis and Lund, 1990).

PV-IR chandelier neurons are known to form symmetric synaptic contacts onto the axon initial segments (AIS, DeFelipe et al, 1989: motor cortex, area 4; Williams et al, 1992: DLPFC, area 46) of pyramidal neurons in monkey cerebral cortex. It has been noted that the number of termination's made by GABAergic chandelier neuron axon terminals contacting the AIS's of pyramidal neurons in monkey somatosensory (area 3b) and motor (area 4) cortices (DeFelipe et al, 1985), varies widely perhaps in relation to the inhibitory regulation of particular functional properties exhibited by those pyramidal neurons, with a sub-population of large callosally-projecting pyramidal cells in layer 3 receiving an especially dense innervation compared to their associational and/or intrinsic projecting neighbours. This observation has also been made for commissural-projecting pyramidal neurons in layer 3 of the primate supplementary motor area (Williams et al, 1990), where these neurons were seen to be densely innervated by PV-IR varicosities and it is presumed that the same is true for callosally-projecting pyramidal neurons of the PFC (area 46).

The time course of development for PV-IR axon cartridges - representing the terminal inhibitory inputs of a sub-population of GABAergic chandelier neurons - will be compared - (**in section 13**) with the rate of development for their postsynaptic targets, the pyramidal neurons of layer 3, which are known to receive inhibitory synaptic inputs onto their AIS's from these PV-IR cartridges.

6.3(C): Basket neurons.

Another morphologically distinct PV-IR cell class is evident in the DLPFC, namely the wide arbour "basket" neuron. PV-IR wide arbour "basket" neurons are known to form symmetric synaptic contacts with the proximal dendrites, axon hillocks and the cell

bodies of pyramidal neurons in the DLPFC (area 46) as well as other cortical regions (DeFelipe et al, 1985; Hendry et al, 1989; Williams et al, 1992. As in the case of GABAergic chandelier neuron axon terminals contacting AIS's, GABAergic basket cell axon terminals have been observed to vary in the number of contacts which they make with the axon hillocks of layer 3 and 5 pyramidal neurons, in line with the particular class (callosal, associational, intrinsic) of their projection trajectory (DeFelipe et al, 1985: somatosensory and motor cortices). Similar observations have been made in the primate supplementary motor cortex for PV-IR synaptic varicosities (Williams et al, 1990).

It has been proposed that the dimensions and shapes of the axon arbours of wide arbour "basket" cells may ideally suit them to the role of selectively mediating the inhibition of sub-populations of pyramidal neurons in layer 3 (Lund et al, 1993) which furnish excitatory intrinsic lattice connections, which in the DLPFC are organised in a discontinuous elongated stripe-like pattern across the surface of the cortex in the tangential plane (Levitt et al, 1993; Kritzer and Goldman-Rakic, 1995; Pucak et al, 1996). The width of an average "basket" neuron is at least 3 times greater (900-1000 μm) than the largest of pyramidal neuron basal dendritic field diameters (mean 355 μm) in the DLPFC (Lund et al, 1993). It is thought that these parameters enable the cell body of a "basket" neuron situated closely to that of a given pyramidal neuron to be in a position to influence - via its elongated axonal arbour - only the pyramidal cells in the surrounding mediolateral portion of cortex (**see Figure 25**). This would still permit the local axon collateral's of the pyramidal neuron - which arise horizontally in layer 3, but arbourise in the plane orthogonal (i.e. vertically) to that of the "basket" cell axon - to excite other pyramidal neurons within layers 2-3 located in the nearest parallel stripe domains situated on either side of the intrinsically-projecting pyramidal neuron.

6.3(D): Distribution of interneurons containing calcium-binding proteins (CBP's).

Condé et al (1994) have examined the morphology and the laminar distribution of neurons expressing each of 3 CBP's (calbindin, CalB, calretinin, CalR and parvalbumin, PV) in areas 9 and 46 of the monkey DLPFC. The laminar distribution of CalR-IR neurons spread through all cortical layers, but most were concentrated in layers 2 and 3 and they were rarely seen in layer 6. For CalB-IR neurons the expression was again present in all layers, predominantly in layers 2 and 3, but also with some concentration in layers 5 and 6. PV-IR neurons were present throughout layers 2-6 (although layer 2 was sparsely populated)

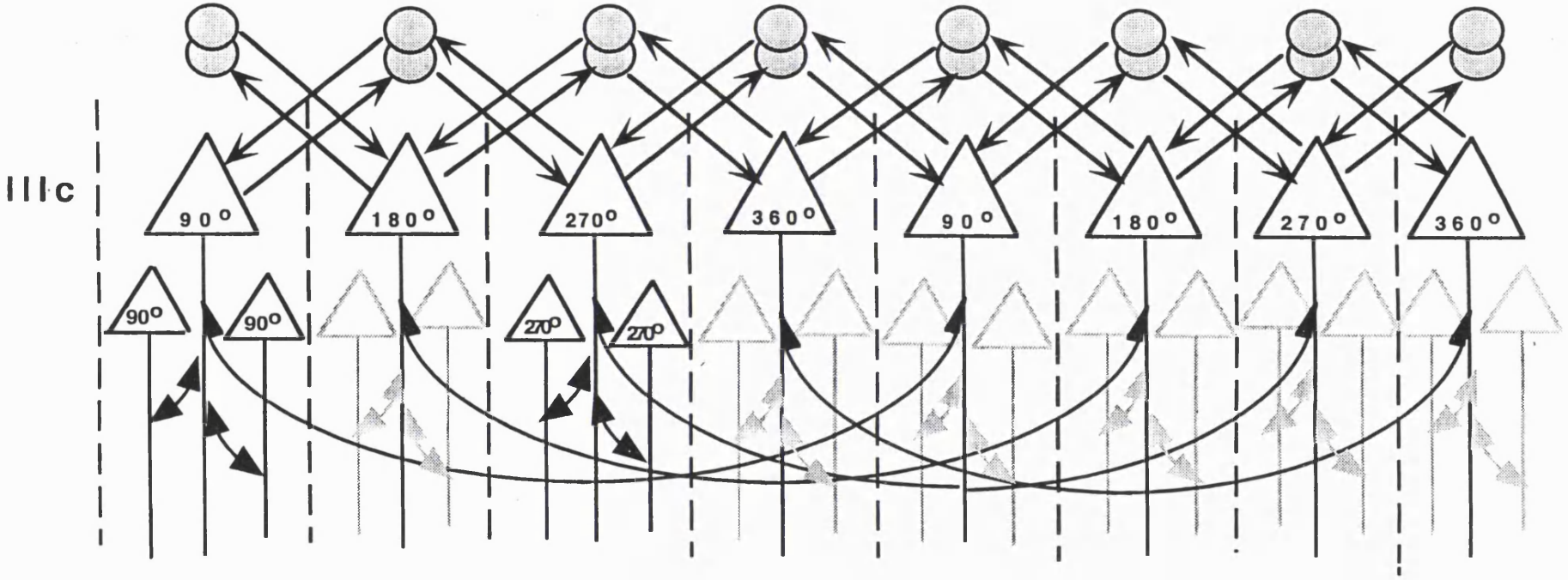

Figure 25 A model of working memory circuitry in deep layer 3 of the monkey DLPFC (area 46). The schematic diagram (coronal section) shows a population of reciprocally-linked (via their axon collaterals; bottom of figure) intrinsically-projecting pyramidal neurons (centre) which may be the best candidates for the neuronal loci of "memory" fields specific for the different portions of visual space as shown in neurophysiological studies (Goldman-Rakic et al, 1990). These neurons may interconnect on the basis of their mnemonic-coding for like-orientations visual space Also shown are the "basket" neurons which may be reciprocally-connected with these intrinsic pyramidal neurons and may modulate their coordinated activity in the lateral axis(see text for extra details)while the intrinsic pyramidal neurons and their axon terminations are arranged in clusters which are organised in vertical stripes in the tangential and mediolateral planes. Figure from Goldman-Rakic (1995, 1996).

and highest numbers were seen in layer 4 and the adjacent parts of deep layer 3 and upper l.

Quantitative analysis of the laminar distribution of CalB, CalR and PV immunoreactive neurons supported the qualitative observations, with no significant differences in the laminar level of expression of each CBP between areas 9 and 46. Within each region, the overall number of CalR-IR neurons was consistently almost twice that of the CalB-IR and PV-IR neurons, although care should be taken in comparing the expression of different antibodies (there may be as yet unknown differences in antibody penetration and sensitivity for these CBP's). In layers 2-3, the percentage of CalB-IR and CalR-IR neurons was significantly greater than that of PV-IR neurons, in areas 9 and 46 (being 58.5%: 61.9%: 49.1% for area 9 and 68.3%: 66.7%: 49.1% for area 46, respectively).

For each CBP (except maybe PV) the density of labelled neurons was invariant across PFC regions, perhaps providing a consistent framework of intrinsic local neuron circuitry for the functional role of each CBP in the PFC. This observation is contrasts with the representation of neuropeptides - which are all GABAergic (Hendry et al, 1984) and are also often co-localised with CBP's in other brain regions (DeFelipe et al, 1990: a few large CalB-IR/tachykinin-IR unidentified cells in primary auditory).

The synaptic relationship of the majority of local circuit neurons with pyramidal neurons in the DLPFC, remains so far unexamined at EM level. It is possible that particular subpopulations of pyramidal neurons (on the basis of morphology, efferent targets and biochemical heterogeneity) may be preferentially innervated by particular sub-classes of local circuit neurons. It is also evident that certain CBP-defined subclasses of interneuron in the DLPFC may also contact other interneurons as well as interacting with pyramidal cells (Gabbott and Bacon, 1996a).

It appears that the general activity of a layer 3 pyramidal neuron is regulated by synaptic contacts from a range of local circuit neurons, each targeting different portions of the pyramidal neuron dendritic tree, soma or axon initial segment. Each interneuron has its own discrete distribution pattern of synaptic innervation interacting with other cells (both pyramidal and non-pyramidal types), a distinctive biochemical identity (usually as a co-transmitter with GABA) and axonal arbour architecture, with differing and specific functional roles subserved by particular neuronal subclasses.

7.0: Anatomy and functions of the serotonergic neurotransmitter System in the macaque monkey.

7.1: Introduction: Serotonin and the prefrontal cortex.

The second part of the thesis, examines the development of the serotonergic (5-HTergic) innervation in mid-layer 3 of the monkey DLPFC (area 46) which originates predominantly from cells in the dorsal and median raphe nuclei in the brainstem (Porrino and Goldman-Rakic, 1982; Wilson and Molliver, 1991b). The existence of this dual origin for the 5-HTergic axon innervation has been thought to account for the observation of 2 morphologically distinct subpopulations of 5-HTergic axons with differential laminar distributions throughout the cerebral cortex, including the DLPFC (Kosofsky et al, 1984; Wilson and Molliver, 1991a). The premise for the existence of these 2 types of 5-HTergic axon projections, perhaps fulfilling distinct functional modulatory roles, has been based mainly on observations originally made in rodents (Kosofsky and Molliver, 1987; Mamounas and Molliver, 1988) and cats (Mulligan and Törk, 1988, 1993). However, this differentiation of 2 axon morphologies is not always clearly seen in monkeys (see Smiley and Goldman-Rakic, 1996, as well as present observations), although they have been seen in post-mortem human neocortex (Kosfsky and Kowall, 1989; Hornung and Celio, 1992).

Although the three-dimensional anatomical arrangement of the 5-HTergic axon innervation has not been examined in detail in the monkey cerebral cortex, a study employing small injections of 5,7-dihydroxytryptamine to ablate localised portions of the cortical 5-HT axon population produced restricted spherical regions of 5-HT denervation in the cortex (Wilson and Molliver, 1986). This result demonstrated that the 5-HTergic innervation of the monkey cerebral cortex is unlikely to be arranged such that individual dorsal or median raphe axons follow a tangential course through the anteroposterior extent of the cortical axis of the brain, which is observed for the rat cortical serotonergic (Lidov and Molliver, 1982) and noradrenergic (Morrison et al, 1978, 1981) axon innervations, or like the noradrenergic (Morrison et al, 1982) innervation in the monkey neocortex. Instead it is more likely that the 5-HT innervation of the primate cerebral cortex is arranged in a discretely topographic fashion with single 5-HT parent axons from raphe neuron groups projecting only as far as their target region before ramifying and branching intrinsically, with very little evidence of extrinsic collateralisation of long distance projections to more than one area from a single cell group.

The synaptic associations of 5-HTergic axons in the monkey prefrontal cortex have not been examined in great detail, but from preliminary observations it appears that only

about a fifth of all 5-HTergic varicosities form synaptic contacts, and most of these (approx. 90%) are associated with the smooth dendritic shafts of interneurons in area 46 of prefrontal (Smiley and Goldman-Rakic, 1996) and in primary visual cortex (De Lima et al, 1988), whilst only about 10% of 5-HTergic varicosities contact pyramidal neuron dendrites. The similarity of the synaptic frequencies in these 2 different regions is unexpected, since there is a much greater overall density of 5-HTergic innervation in area 17 than in area 46. A much higher synaptic frequency has been determined for the varicosities of 5-HTergic axons in non-primate species such as the rat, where at least 50% of [^{3}H]-5-HT-bound (visualised by autoradiography) varicosities sampled in a serial-section EM analysis, were demonstrated to form asymmetrical synaptic contacts with the spines and shafts of pyramidal neuron dendrites in visual cortex (Parnavelas et al, 1985).

Serotonin (5-hydroxytryptamine or 5-HT) is one of the 4 major monoaminergic neurotransmitters found in the mammalian brain, along with acetylcholine, dopamine and noradrenaline. Each of them demonstrate distinctly individual innervation patterns, both across different areas and within the boundaries of individual areas of the cerebral cortex.

Although most research investigating the anatomy, physiology and pharmacology of the serotonergic (5-HTergic) system has been carried out in the rat, a sizeable literature has now accumulated on the equivalent system in the non-human primate, in particular the old world monkey genus *Macaca* (reviewed in Foote and Morrison, 1987a). It is this system in the macaque monkey that will provide the focus for the present review.

We shall review the literature up to the present on the anatomical architecture of the cerebral cortical 5-HTergic system, concentrating on the morphology and distribution of the extensive 5-HT axon innervation in the monkey neocortex. We shall focus particularly on the principal sulcus (area 46) region of the DLPFC, as examined in this thesis. The importance of the 5-HTergic input to the normal functioning of these cortical areas will be examined, especially in area 46. Possible functional roles for 5-HT during the development of the cerebral cortex in primates will also be discussed.

7.2: Different serotonergic projections from the raphe nuclei each exhibiting a distinctive axonal morphology for their innervation of the cerebral cortex.

Having established the evidence for the existence of 2 distinct pathways from the DRN and the MRN, to thalamic/basal ganglia structures and the neocortex respectively in the monkey; it is now appropriate to describe studies which have characterised the regionally-specific terminal innervation of these projections in the monkey cerebral cortex.

Studies carried out have examined whether any differences in morphology could be related to differences in the raphe nuclei of origin, or whether different cell types within both raphe nuclei are the source of the heterogeneous cortical 5-HT innervation.

The organisation of a dual 5-HTergic innervation of the cerebral cortex has been hypothesised in primates (Wilson et al, 1989; Wilson and Molliver, 1991b), i.e. an extensively distributed pathway of fine-calibre axons, originating from the DRN and a sparsely distributed pathway of coarse-calibre axons, stemming from the MRN. This hypothesis was inferred from a combination of observations in the monkey, where 5-HT immunohistochemistry was used to label 2 morphologically distinct populations of 5-HTergic axons in the neocortex, whose projection origins in the raphe nuclei were known from a retrograde tracing study (Wilson and Molliver, 1991b) as has also been seen in the rat (Kosofsky and Molliver, 1987). Also, in the monkey neocortex, administration of amphetamine derivatives appears to eliminate the fine axon population (60-90% of the total axon population, compared to controls) but not the beaded axons (Wilson et al, 1989), as previously seen in the rat (Mamounas and Molliver, 1988 and Mamounas et al, 1991). All this evidence has enabled a conclusion to be reached, that the same arrangement of 2 differential 5-HT projection pathways exist to the neocortex, in the 2 species, which share comparable degrees of innervation pattern and functional roles and may be anatomically represented by the same 2 groups of morphologically distinctive axon terminals (Wilson and Molliver, 1991b). Compared to the rat, however primates including humans exhibit a greater degree of regional heterogeneity in the organisation of their cortical 5-HTergic innervation, with widely varying axon fibre densities in one area relative to another.

7.3: The 5-HTergic innervation of the DLPFC.

The earliest study to examine the presence of 5-HT in the DLPFC of the adult monkey, used biochemical analysis of the gross tissue content of 5-HT and its catabolic breakdown product 5-hydroxyindoleacetic acid (5-HIAA) and also measured the *in vivo* synthesis rate of its synthetic precursor 5-hydroxytryptophan (5-HTP; Brown, et al, 1979). The tissue level of 5-HT in the DLPFC were regarded as low compared to that of other cortical areas examined (namely somatosensory, anterior inferotemporal and superior temporal cortices). The same was true of the levels of 5-HIAA - primary 5-HT metabolite - although in this case levels increased steadily along a rostro-caudal gradient from the DLPFC to the occipital cortex. The estimates of *in vivo* synthesis rate of 5-HTP in DLPFC, were only measurable in monkeys pre-treated with an aromatic amino acid decarboxylase inhibitor

NSD 1015. Samples of tissue taken at 15, 30 and 45 minutes following the administration of the inhibitor, showed a linear increase in accumulation of 5-HTP with time. It was concluded that the 30 minute measure would be an accurate reflection of rate of 5-HT synthesis. The rate of 5-HTP accumulation for the DLPFC was low compared to that of the parietal and occipital cortices and the brainstem; rate constant of 0.41/hour for DLPFC and 0.66/hour for parietal cortex. In terms of overall cortical distribution, 5-HTP synthesis rates were equivalent for the PFC (including DLPFC and orbital PFC), premotor and primary motor cortices but much higher in somatosensory, parietal and visual cortices.

Up until the early 1990's the immunohistochemical staining of 5-HTergic axons in the adult cynomolgus monkey PFC had only been described in brief (Lewis, 1990; Lewis et al, 1985). In these studies, using a 5-HT specific antibody (raised in rabbits or guinea pigs) the overall PFC 5-HTergic innervation, was described as being homogeneous and of moderate density; concentrated in layers 1 and 4, with some areas e.g. area 9, where the infragranular layers were slightly denser than the supragranular layers. In addition, 5-HT "basket" arrangements of 5-HTergic axons were observed and 5-HTergic axons were described as being morphologically heterogeneous. More extensive observations were reported by Wilson and Molliver (1991a), where the distribution of 5-HTergic axons in the DLPFC of the adult monkey (cynomolgus and rhesus) was examined using a rabbit 5-HT specific antibody. The 5-HTergic innervation of DLPFC was described as being moderate in density relative to other cortical areas, with the ventral bank of the principal sulcus (area 46) being slightly more densely innervated than the dorsal bank, especially in layer 1.

In the cynomolgus monkey, 5-HTergic axons were quite evenly distributed throughout all cortical layers. While the same pattern was generally true for the rhesus monkey, it was noted that there was a sparseness in the innervation of layer 3, as characterised by a clustering or patchiness in the distribution of 5-HTergic axons. In both species there were similar differences in the orientation of 5-HTergic axons in different layers through the cortical depth. In layer 1, tangentially directed axons were pre-eminent, whilst in layers 2 and 3, 5-HTergic axons were generally radial in their trajectory. In layers 4-6, most 5-HTergic axons were obliquely arranged in a tortuous fashion, although some long tangential axons were also seen, mainly in layer 6. In layer 1, 5-HTergic axons were mainly of the large type, whilst the 5-HTergic axons in layer 2-6 were predominantly of the fine type.

7.4: Localisation of 5-HTergic axons to particular neuronal subtypes (synaptic and non-synaptic relations).

Recently, an estimation of the synaptic incidence of 5-HTergic axon terminals on putative interneurons or pyramidal cells was carried out for the adult monkey DLPFC (area 46) using a rabbit anti-5-HT antibody (Smiley and Goldman-Rakic, 1996). The-light-microscopic observations in one monkey, revealed a complex network of 5-HTergic axons, which was particularly dense in layers 1 and 4, as seen in previous studies of adult primate DLPFC (rhesus and cynomolgus monkey: Wilson and Molliver, 1991a and marmoset: Hornung et al, 1990). Serotonergic axons were described as showing a diverse range of morphologies, both in terms of calibre and the shape, size and presence of terminals. Entire axons or even the portions of a given axon could vary between-non-varicose and smooth, varicose, with small terminals (thin axon type) or highly varicose with large terminals (thick axon type). Many axons demonstrated this range of variability in their appearance and were thus hard to classify strictly into one or other type of 5-HTergic axon and were thought of as an intermediate class of serotonergic axon. Layers 3-6 were observed to be populated mainly by non-varicose, smooth axons, although they were also seen in layers 1-2 as well.

The authors also observed basket arrangements in the superficial cortical layers, as seen previously in primate DLPFC (rhesus monkey: Wilson et al, 1989), but they were very rarely encountered, with between 1-3 being seen in any one section of the PS.

At EM level the appearance of 5-HTergic axons in the DLPFC of 2 monkeys was equally heterogeneous, most being less than 0.2 μm in diameter (these were too fine to be included in the analysis of synaptic frequency) and others, which were less in number, ranged from 0.2 μm up to 1 μm in calibre (these were surveyed for synaptic interactions). The thinner axons were characterised by their content of synaptic vesicles, these were mainly of the clear type, but occasionally dense core vesicles were also seen, along with microtubules. Within the thicker axons, microtubules were the main components, with clear synaptic vesicles being less common and sometimes absent for long stretches of serial-sectioned axon. This larger type of axon was most prevalent in layer 1 and could exhibit vesicle-containing protuberances or varicosities which formed synaptic contacts; dense core vesicles were also encountered in these axons.

Typical varicosities exhibited by either thick or thin type 5-HTergic axons were distinguished by their content of many clear synaptic vesicles, which could vary in shape depending on the perfusion fixation used for that animal (either glutaraldehyde alone or a glutaraldehyde and paraformaldehyde mixture), being more spherical in the latter

case and more aspherical in the former. Thus overall, 70% of varicosities were described as containing dense core vesicles; some varicosities only possessed 1-2 vesicles, while others contained between 10-20 vesicles. In the animal perfused with the mixed fixation medium, dense core vesicles were found in 85% of varicosities, whilst in the glutaraldehyde-only perfused animal, they were found in only 60% of varicosities. These 2 types of synaptic vesicles were prominent features of 5-HTergic axon morphology, but there did not appear to be any relation between the 2 morphologically distinct types of axon and their proportional content of vesicles. This was supported by the observation that dense core vesicles were present in both large and small numbers within both axon types, but for any one axon the densities were comparable for each individual varicosity, across the range of different sized varicosities.

The synaptic frequency for 5-HTergic axon varicosities was much less than that previously observed for other neurotransmitter innervations in the primate DLPFC. Only 23% (48/213) of serotonergic varicosities analysed forming unequivocal synapses in layers 1, 3 and 5 of area 46, compared to 39% (59/153) for dopaminergic varicosities in all layers (Smiley and Goldman-Rakic, 1993) and 44% (44/100) for cholinergic (as represented by ChAT labelling) varicosities also in all cortical layers (Mrzljak et al, 1995). This low frequency of 5-HTergic synapses was observed ,despite the fact that most varicosities contained large numbers of synaptic vesicles, hinting that unconventional forms of 5-HTergic synapses may exist, which are not detectable by present methods. This was supported by the occasional appearance of faint membrane darkening's at associations between 5-HTergic varicosities and cellular processes, but these were not pronounced enough to be regarded as synapses in the normal sense. Observed 5-HTergic synapses were asymmetric (Gray's type 1) in form, with prominent postsynaptic densities and were quite small in terms of this synaptic class, being detectable through the course of between only 2-5 (mean = 2.83) serial sections (mean width = 70 nm) or 0.21 μm in diameter at their thickest part. These dimensions are much smaller than those for other asymmetric synapses - such as glutamatergic synapses formed between corticothalamic or corticocortical afferents and pyramidal neuron dendritic spines - in area 46 of the monkey DLPFC.

The postsynaptic targets of 5-HTergic axon synapses have also been characterised by complete serial-section analysis and found to be almost exclusively dendritic shafts. Dendritic shafts were classified as previously described (Smiley and Goldman-Rakic, 1993) into 3 main types smooth, interneuron (S), pyramidal (P) and those of uncertain classification (U). In the 3 layers examined, 48% (23/48) of all labelled 5-HTergic varicosities which formed

synapses in area 46 were most commonly found to contact the S-type of postsynaptic process, 8% (4/48) contacted the P-type processes and over two-fifth's i.e. 42% (20/48) of all synapse-forming 5-HTergic varicosities contacted processes of the U-type. The observation of the latter population resulted from half not being distinguishable into either S- or P-type processes and the other half being too fine to trace through sufficient numbers of-serial-sections.

For layer 3, where we examined in this thesis, the maturational time course of 5-HTergic axons across development, the percentage of synapses formed by 5-HTergic varicosities (Smiley and Goldman-Rakic, 1996) was of the order of 21%, with all postsynaptic targets having the characteristics of S-type, interneuron dendrites and none having the features of P-type, pyramidal neuron spiny dendrites. Overall for the synaptic contacts that were identifiable in layers 1, 3 and 5 in area 46 of the monkey DLPFC (Smiley and Goldman-Rakic, 1996), over 85% of 5-HTergic synapses were found to contact the dendrites of interneurons and only 15% of postsynaptic targets were made with the dendrites of presumed pyramidal neurons.

7.5: The postnatal development of the serotonergic innervation of the cerebral cortex: Maturation of layer 3.

The second part of the thesis examines the postnatal maturation of the serotonergic (5-HTergic) innervation of layer 3 in area 46 of the monkey DLPFC. In the adult monkey, the 5-HTergic innervation, originating from the mid-brain raphe nuclei, is known to be distributed throughout the cerebral cortex as well as sub-cortical regions. It is most densely distributed within the primary visual cortex (area 17) of the macaque monkey, and exhibits an extremely varied areal and laminar pattern of innervation, both within and across different cortical areas, including DLPFC (areas 9 and 46), (Morrison et al, 1984; Foote and Morrison, 1987a; Wilson and Molliver, 1991a). Biochemical studies have revealed that the tissue concentration of 5-HT achieves its adult levels by about 5 months postnatally in the DLPFC, compared to between 2-5 months of age in area 17 (Goldman-Rakic and Brown, 1982).

It has been demonstrated from pharmacological and neurophysiological studies in the adult nervous system, that serotonin has a primarily, inhibitory modulatory role (although unequivocal excitatory-type properties have also been observed for 5-HT in various neural systems) in the functioning of various cortical and thalamic areas. Serotonin has also been also been found to show evidence of an important modulatory role during the early stages of both pre- and post-natal development in diverse brain regions in several species, e.g.

during the early cortical period in the cat primary visual cortex, both 5-HT_1 and 5-HT_2 receptors are known to be mutually essential for the plasticity which facilitates the postnatal rearrangement of ocular dominance columns (Gu and Singer, 1995). In the layer 4 barrel fields of the developing rat primary somatosensory cortex (S-I), normal serotonergic innervation of the vibrissae-specific patches are necessary for the correct timing of the pattern formation of thalamic inputs to these compartments (i.e. 5-HT might be playing a trophic role; Blue et al, 1991) and for the attainment of normal patch size, as dictated by the in-growth of these thalamocortical afferents (Bennett-Clarke et al, 1994, 1995). The thalamocortical and 5-HT innervations to the barrel fields may in fact mutually influence each other's maturation, during early postnatal development (Rhoades et al, 1990).

Additional evidence which supports the crucial involvement of the 5-HT system in the development of cortical circuitry comes from the observation that 5-HT_{1B} receptors are specifically and transiently expressed on thalamocortical axon terminals in S-I and primary visual cortex in the developing rat (Bennett-Clarke et al, 1993), coinciding with the time course of a dense 5-HT axon innervation in these areas (D'Amato et al, 1987). It is therefore possible that serotonin in conjunction with its various receptor subtypes might play an important role in the functional plasticity of DLPFC circuitry during early development. It might be involved in functional development e.g. increased levels of DR task performance and/or in anatomical maturation e.g. formation of the intrinsic lattice arrangement of lateral connections in the superficial layers. Disruption of the maturational process of the growth of the 5-HT innervation within the DLPFC, might therefore perhaps adversely affect functional performance in adolescent and adult humans, which may possibly occur in the case of the schizophrenia.

The rationale for studying the postnatal development of the 5-HT innervation in layer 3 of area 46, was to examine how the maturation of numbers of putative 5-HT release sites (i.e. 5-HTergic axon varicosities) might be temporally related to the development of excitatory postsynaptic inputs (i.e. dendritic spines; **see first thesis study**) between pyramidal neurons providing intrinsic lattices in this region. Since the dorsal and median raphe nuclei in the mid-brain have been shown to provide separate inputs in the form of fine axons with small varicosities and coarse axons with large varicosities, respectively in the DLPFC of the macaque monkey (Wilson and Molliver, 1991a,b), these two systems might be expected to exhibit different developmental time courses as well. So the thesis also examines the issue of the possibly differential developmental aspects of these 2 components of the 5-HT system. The developmental time course of the 5- HTergic innervation could then be expected

perhaps to relate to other developmental events which are known to take place in other cortical systems which also contribute to the intrinsic circuitry of the DLPFC. The different systems for which time course was compared to that of 5-HTergic axons included, the DAergic axon innervation (Rosenberg and Lewis, 1995), 5-HT and DA neurotransmitter tissue concentrations (Goldman-Rakic and Brown, 1981, 1982), the parvalbumin-immunoreactivity present within axon cartridges of inhibitory local circuit chandelier neurons (Anderson et al, 1995; Condé et al, 1996) and levels of excitatory (asymmetric) synapses (Bourgeois et al, 1994).

So far, to our knowledge, no qualitative or quantitative studies have previously examined the prenatal or postnatal time course of serotonergic axon development in the monkey DLPFC - or in any cortical area, except for a qualitative study within the primary visual cortex (area 17) carried out by Foote and Morrison (1984). It was our intention to fill this major gap in the knowledge regarding the maturational time course of the 5-HTergic system during the postnatal period that we carried out an immunohistochemical investigation, which forms study 2 of this thesis. Although immunohistochemical studies of 5-HT development have not been conducted in the monkey PFC, there has been some examination using biochemical methods, of the gross endogenous tissue content of 5-HT and its synthetic and catabolic precursor and by-product in the PFC from birth to the onset of adulthood (Goldman-Rakic and Brown, 1982) and in ageing monkeys (Goldman-Rakic and Brown, 1981).

In the first study (Goldman-Rakic and Brown, 1982), the brains of new-born monkeys up to the age of 3.0 years of age, were examined for 5-HT tissue content, the levels of the metabolic precursor of 5-HT (5-hydroxytryptophan, 5-HTP) and the catabolic by-product of 5-HT degradation (5-hydroxyindoleacetic acid, 5-HIAA) in the PFC. The "adult" value for tissue levels of 5-HT in the PFC as a whole was attained as early as 5 months of age, whilst for the other cortical regions sampled the mean age was 2 months (i.e. for the occipital, parietal, somatosensory and motor cortices). The maximal statistically significant difference in the 5-HT levels between different ages was observed between the new-born monkeys and those of 2.0-3.0 years of age. However, in the PFC, the eventual adult value was not achieved simply through a process of uninterrupted growth in the 5-HT tissue levels across postnatal development, since a significant decrease in 5-HT was observed to occur between the ages of 5 and 8 months. The value for the 8-month-old animals was significantly lower than that for the 2-month-old and 3.0-year-old animals, whilst the 5-HT levels of the 5 month old animals were not significantly different from those of the 3.0-year-old's.

Following this drop in 5-HT concentration between 5 months and 8 months of age, the tissue levels of 5-HT were observed to rise again, between 8 months and 3 years of age to the same high levels that they had initially shown at 5 months of age. This pattern of postnatal maturation for 5-HT tissue content was similarly observed for DA tissue content in the PFC, with a parallel rise and fall in 5-HT and DA concentrations being observed between 2 and 18 months of age. The tissue content of 5-HTP in the PFC, over the same period of postnatal development was found to remain relatively stable, with no significant differences between the levels present at any age between birth and 3.0 years of age.

In a study of an older age group of animals, Goldman-Rakic and Brown (1981) used the same methods of biochemical analysis to determine the gross tissue content of 5-HT and 5-HTP in the PFC of monkeys between 2.0 and 18.0 years of age. The striking observation for 5-HT and 5-HTP content, was that there were no significant differences in either the tissue levels of 5-HT or the levels of its synthetic precursor, 5-HTP, during either the late pubertal period or throughout adult life in the monkey PFC. Thus, levels of 5-HT were identical for animals of 2.0 years of age and for those of 18.0 years of age, with no divergence in 5-HT levels for the animals of ages in between. In addition, levels of 5-HT synthesis as quantified by 5-HTP tissue content were also invariant over the same age range. So 5-HT activity in the monkey PFC, as measured by the tissue content and levels of synthetic precursor, would appear to remain constant throughout adult life and would seem not to be affected in the process of normal ageing, as measured in this study.

7.6: Functional roles of 5-HT in the cerebral cortex.

Serotonin has been attributed with significant involvement in numerous aspects of brain functioning in most major mammalian species including a significant role as a developmental signal or trophic factor in both pre- and postnatal development (Lauder and Krebs, 1978; reviewed in Whitaker-Azmitia et al, 1996). E.g. an intact serotonin innervation appears to be necessary for the correct somatotopic patterning of thalamocortical axons in the rat primary somatosensory cortex (Bennett-Clarke et al, 1994a); the activities of certain 5-HT receptor subtypes (5-HT_{1C} and 5-HT_{2C}) have been shown by *in vitro* and *in vivo* electrophysiological and pharmacological studies to be essential in the facilitation of the developmental plasticity necessary for the formation of ocular dominance columns in layer 4 of the kitten visual cortex (Wang et al, 1994; Gu et al, 1995; Gu and Singer, 1995) and hypothesised to be invoked through the medium of increased intracellular Ca^{2+} levels in turn achieved via a 5-HT-induced (binding at 5- HT_2 receptors in layer 4) opening of L-type

Ca^{2+} voltage-gated channels and/or the activation of NMDA receptors (Kojic et al, 1996).

The maturation of GABAergic cortical neurons has been shown to be dependent on the activity state of particular 5-HT receptor subtypes, as shown by *in vitro* studies in neonatal rat slices (Köstner and Hornung, 1995). There is also evidence from chemical lesioning of the 5-HT innervation, that 5-HT fulfils a modulatory role which is necessary for the partial developmental refinement of excessive callosal and claustral projections to areas 17 and 18 of the kitten visual cortex (Turlejski and Djavadian, 1996). In addition, serotonin has been shown in the same way as dopamine (Rörig et al, 1995a, 1995b) to have an important role as a regulator of gap junction coupling between layer 2/3 pyramidal neurons during early postnatal development as observed by the technique of *in vitro* dye coupling in slices of the neonatal rat prefrontal, frontal and somatosensory cortices (Rörig et al, 1995a, 1996).

Several studies in the rat hippocampus (Haring et al, 1995; Ogawa et al, 1995; Yan et al, 1995) and cerebral cortex (Matsukawa et al, 1995; Varela et al, 1995; Whitaker-Azmitia et al, 1995) have shown 5-HT to be important as a modulator of synaptogenesis along with either noradrenaline (Matsukawa et al, 1995) or acetylcholine (Ogawa et al, 1995). *In vitro* slice preparations of the rat visual cortex have demonstrated that 5-HT inhibits the induction of long-term potentiation in layers 2/3, implying a role for 5-HT in the modulation of synaptic plasticity in early development (Edagawa et al, 1996). In rat hippocampal cell cultures, 5-HT activity as modulated via the somatodendritic 5-HT_{1A} receptor, appears to be a major regulating factor (along with the neuronal extension factor: S100ß and the hormone corticosterone, via its receptors) in the levels of expression of the synaptic vesicle protein: synaptophysin, particularly on surface of the neuronal cell body (Nishi et al, 1996).

In adult animals, serotonin has also been found to play an important part in the maintenance of several functional systems (reviewed in Jacobs and Azmitia, 1992), including the sleep-wake cycle, states of anxiety, attention, appetite and arousal (mediated by thalamic and brainstem nuclei) as well as being integral to the regulation of cognitive and mnemonic or limbic-associative functions (mediated through the higher association cortices: e.g. the dorsolateral prefrontal and orbitofrontal cortices, respectively).

Experimental studies have been conducted in vervet monkeys (*Cercopithecus aethiops* , of both sexes, differeing in their social status. In these groups it was observed that changes in social behaviour were evident for subordinate adult males who had received pharmacological manipulation of their brain 5-HT levels (reviewed in Raleigh et al, 1996a). The brain serotonin levels of these animals were found to alter chronically (over a period of 4 weeks), after treatment with tryptophan (5- HT precursor) or fluoxetine (5-HT re-uptake

inhibitor) which increased their serotonin production and functioning, resulting in their exhibition of dominant behaviour (Raleigh et al, 1991). When these previously subordinate males were treated with fenfluramine (non-specific 5-HT agonist in acute doses, but an antagonist in chronic doses) or cyproheptadine (5-HT_2 antagonist) over a period of time, they did not become dominant. This difference of effect may have been due to the inhibitory actions of these chemicals acting as 5-HTr antagonists, especially in the case of fenfluramine (Muckseler and Diksic, 1996) which caused a significant decline in the animal's levels of 5-HT synthesis over time and reduced 5-HT-dependent behavioural functioning. A study in the rat (Muckseler and Diksic, 1996) has shown that fenfluramine acts at 5-HTergic terminals by increasing the rate of 5-HT release in acute doses, but with more chronic administration, the 5-HTergic neurons in the raphe nuclei - the source of 5-HT - become depleted of the neurotransmitter.

It has also been shown that an animal's social status is reflected by its levels of whole blood serotonin (WBS), with dominant monkeys having much higher levels of WBS (almost 2x greater) than subordinate animals, although this could change for an individual when its social status is reversed (Raleigh et al, 1984). Status-linked differences have also been found between animals in terms of their ability to become behaviourally affected by the administration of either tryptophan (5-HT precursor) or the 5-HT re-uptake inhibitor, fluoxetine or the 5-HT agonist, quipazine (Raleigh et al, 1985). In each case, dominant males exhibit significantly increased levels of WBS, coupled with an increase in the number of affiliative actions and decreased aggressive behaviour, than the subservient males undergoing the same treatment. These diverse behavioural and physiological observations were attributed to differences between the 5-HT systems of the 2 groups of animals, resulting in differential effects of increased 5-HT synthesis, blocking of 5-HT re-uptake sites and occupation of 5-HT_{2A} receptor sites by the actions of tryptophan, fluoxetine and quipazine, respectively. One hypothesis proposes that 5-HT_{2A} receptors might be present in higher numbers or have a increased binding-affinity for 5-HT in dominant animals.

To test this hypothesis, the levels of 5-HT_{2A} receptors (using [^{3}H]-ketanserin as a binding-ligand) were compared in various brain regions for dominant and subordinate adult males. No significant differences in the densities or affinities of 5-HT_{2A} binding sites were found for the 2 groups of animals, despite their behaviourally disparate social states (Brammer et al, 1987).

A long-term study was conducted for a group of adult male vervet monkeys whose levels of 5-HT system activity were analysed in terms of 5-HT_{2A} receptor density in the

same brain regions as the Brammer et al (1987) study, to see if there was a correlation between 5-HT_{2A} receptor levels and the behavioural attributes of dominance or subordination for individual animals over their life-span until sacrifice (Raleigh et al, 1996a). Significantly higher mean levels of 5-HT_{2A} receptors were found in the posterior orbitofrontal, medial prefrontal and the amygdala of animals who very seldom displayed unprovoked destructive or aggressive behaviour and vice versa. Whilst animals who demonstrated pronounced, pro-social behaviour were significantly more likely to exhibit higher levels of 5-HT_{2A} receptors in the posterior orbitofrontal and temporal pole cortices as well as in the hippocampus compared to monkeys who didn't engage in positive behaviour patterns. Thirdly, co-operative behaviour among animals was correlated with higher values for 5-HT_{2A} receptor binding in the posterior orbitofrontal and temporal pole cortices than animals which didn't exhibit these attributes. It is likely that the consistently increased levels of 5-HT_{2A} receptors in the posterior orbitofrontal cortex of dominant animals plays an important contribution along with other cortical and subcortical regions and somehow confers them with an increased ability to show mutually beneficial behaviour in social engagements with other vervet monkeys.

7.7: Summary.

The monoaminergic neurotransmitter serotonin with its varied distribution both as a free transmitter in the neuropil or within its extensive network of axonal innervation in the cerebral cortex is likely to play many roles in normal cortical functioning as well as being vulnerable in disease conditions such as schizophrenia, autism and depression. The diversity of physiological and pharmacological interactions with other components of the cortical circuitry, throughout the mammalian neocortex in several species (rat, cat and monkey) may be easily attributed to the existence of the complex array of 5-HT receptor families and subtypes. These different receptors appear to be able to act as effector mechanisms in various ways depending on their cellular location (i.e. presynaptic effects at axon terminals or on en passant varicosities or postsynaptic effects at cell bodies and dendrites) enabling 5-HT to trigger-off second messenger systems and so put into operation cascades of events which ultimately bring about large-scale changes in the behavioural state of the animal, either cognitive, emotional or attentional in their nature.

8.0: Study 1. A quantitative Golgi study of the postnatal maturation of mid-layer 3 pyramidal neuron basal dendritic spines in the monkey DLPFC (areas 9 and 46).

8.1: Introduction.

We have seen from the functional and behavioural review (**section 4.0**) that the structural and biochemical integrity of the DLPFC in the monkey, is essential to the correct performance of important cognitive behaviours. In humans, the disruption of the DLPFC region (by head injury or disease processes) is commonly results in a profoundly cognitive dysfunction, e.g. such as that seen in schizophrenia, while motor and affective systems seem to remain relatively unaffected. This mentally-debilitating disease, usually has its onset during late adolescence (18.0 years of age) and has been considered to be a neurodevelopmental disorder, whereby the DLPFC is a major focus for the disturbance of working memory function, a hypothesis suggested by many of the symptoms exhibited in such patients. In this first study of the thesis, using the macaque monkey DLPFC as a model for the equivalent region in humans, we shall attempt to define the time course of normal development for a crucial population of pyramidal neurons situated in the mid-portion of cortical layer 3.

The review of pyramidal neurons (**section 5.0**) has shown that the superficial layers (2-3) of the DLPFC in the macaque monkey are known to contain large numbers of pyramidal neurons, which participate in extensive intrinsic intraareal connections. Many of these same pyramidal cells also project extrinsically to other cortical areas, either callosally to the other hemisphere or associationally within the same hemisphere. These pyramidal neurons projecting intrinsically within the DLPFC are known to possess axons with an extensive horizontal spread, which form abundant periodically-spaced collateral branches that are directed vertically upwards and possess profusely arbourising terminal branches throughout the superficial layers (1-3). This intrinsic excitatory lattice circuitry, is organised so that any given local cluster of pyramidal neurons (150-300 μm in width) possesses a projection field which is arranged mediolaterally as a sequence of stripe-like terminal-fields observable in tangential sections of the superficial layers following small (200-300 μm wide) micro-injections of anterograde tracer in layers 2/3.

The cell bodies of pyramidal neurons which furnish connectivity to individual points injected with retrograde tracer are also themselves arranged in the same regularly-spaced organisation of stripes in layers 2/3 across the cortex and the cell bodies, dendritic shafts and spines of these cells are known to be the targets of these intrinsic projections from other pyramidal neurons in the same layer. An analysis of the numbers of dendritic spines on pyramidal neurons in mid-layer 3 is likely to sample many of those pyramidal neurons

which participate in the intrinsic lattice circuitry and an examination of the changes in relative spine complement should provide an indication of the time course of maturation for the intrinsic lattice circuitry as a whole.

Postnatal development from birth until adulthood, in all regions of the primate (including human) cerebral cortex is characterised by substantial changes in the numbers of asymmetric (excitatory) synapses which are primarily associated with the dendrites and spines of pyramidal neurons. The time course for these changes is characteristically one of initially rapid overproduction of synapses during infancy, a plateau phase when levels of synapses remain maximal until puberty - or sometimes slightly earlier in adolescence - then a period of gradual decline in numbers is observed to occur on through into adulthood. Dendritic spines could be considered to be a useful marker for the analysis of changes in the relative density of excitatory synapses on any population of pyramidal neurons at the light microscope level. While electron microscopic studies have examined the detailed changes which occur for the densities of asymmetric synapses during development, within all cortical layers in several cortical regions; the technical limitations of sampling synapses in the neuropil, rather than being able to identify the specific type of synapses associated with the dendrites of pyramidal neurons located in that same layer, inevitably means sampling populations of spines belonging to pyramidal neurons in deeper layers. For example, the sampling of synapses in layer 3 would necessarily also include spines on the apical dendrites of cells in layers 5 and 6, which very often pass through the superficial layers. It is known that individual variants of the same neuronal class, within a layer or sub-layers may exhibit slightly different time courses of development for their synaptic components, e.g. as seen for the spiny stellate cells in layers 4Cα and 4Cß of the primary visual cortex (area 17).

The unique intrinsic excitatory lattice structure of connections within the superficial layers of the DLPFC has been hypothesised to represent an anatomical substrate essential for the particular kind of functional organisation exhibited by this cortical region. From observations in behavioural, neurophysiological and pharmacological studies, the DLPFC has been consistently implicated in the guidance of goal-directed behaviour, the temporal organisation of diverse sensory inputs and their integration with programmes of motor responses. Also, it as been found by cell recordings in the DLPFC, that neurons within area 46 appear to provide an internalised representation of the outside world, termed visuospatial working memory, whereby the mnemonic "trace" of an object's location in space (memory field) is retained "on-line" during a delay period. Ensembles of neurons have been found which share a specificity of memory-coding for a particular angle or position of a

remembered stimulus, while groups of other neurons are omnidirectional and code for the memory traces of all orientations equally. By assessing the relative changes during postnatal development for the postsynaptic sites of excitatory synapses in layer 3, presumed to be part of the intrinsic lattice connections found in the superficial layers of the DLPFC, we hoped to be able to attain a quantitative measurement, representative of the degree of functional maturation achieved by the DLPFC at each developmental stage, as implied by the levels of anatomical refinement characterised by changes in spine density.

The evaluation of the functional maturation of a region as inferred from the levels of anatomical refinement of the underlying cortical circuitry in a particular layer during postnatal development has been studied previously in primary visual cortex. The circuitry of area 17 in the monkey has been found to show changes in the density of dendritic spines and synapses in layer 3, which are in general agreement with the observations for the emergence of functional development in this region. In area 17, functional plasticity of neurons coding for both eyes is demonstrated during the early period of rapid spine acquisition on spine-bearing neurons. The disappearance of spines correlates with the final formation of alternating ocular dominance columns containing cells coding for each eye. While the emergence of the characteristically patchy distribution of clusters of terminals making up the intrinsic excitatory circuitry located in the superficial layers of this region is present prenatally, function in the superficial layers is initially plastic in the postnatal period, then matures during adolescence losing plasticity in step with spine loss.

Therefore, in the DLPFC, the maturation of intrinsic lattice circuitry, i.e. the levels of pyramidal neuron dendritic spines, should correlate with the emergence (rapid phase of synaptogenesis or spine growth) and the ability to learn to be able to correctly perform in the spatial delayed response or delayed alternation tasks. Correspondingly, the refinement (declining phase of synaptogenesis or spine loss) should correlate with the loss of the ability to significantly modify behavioural organisation in these tasks. The exceptions to the latter, are found in the cases of traumatic head injury or disease processes, when reorganisation of circuitry can occur in one region to compensate for loss of function in another. Repeated testing on these tasks provides an indication of the growth in "buffer" capacity of working memory over time, as represented by increasing the length of the delay period during which an animal can retain a "memory trace" and still provide the correct response for the reward at the end of the delay. The length of delay period over which an animal can sustain working memory function, can vary between animals according to the length of prior training received on the task or may be due to acquired genetic factors. However, the times of emergence

and refinement of this function would be expected to be dictated by the degree of maturation of the underlying cortical circuitry, particularly the intrinsic lattice connections of the superficial layers, furnished by the spine-bearing pyramidal neurons, whose development we have examined in study 1 of this thesis.

This study has been previously published as Golgi study 2 in a paper addressing the development of excitatory and inhibitory inputs onto layer 3 pyramidal neurons in prefrontal cortical areas 9 and 46 of the macaque monkey (see Anderson et al, 1995). It has also been presented in abstract form (Anderson et al, 1993, Classey et al, 1994, Anderson et al, 1995). The following **Materials and Methods (8.2) and Results (9.0) sections** are concerned with work undertaken by J. Classey, while the contribution by S. Anderson will be described separately in **Results section 10.0**.

8.2: Materials and Methods.

8.2(A). Animals.

Ten rhesus monkeys (*Macaca mulatta*) of both sexes and of an age range from 4 days postnatal to 7.0 years were used in this investigation (**see Table 1**); four of the male animals had been previously castrated, three at 14 months and one at birth (as part of another study). Animals were deeply anaesthetised with ketamine hydrochloride (25 mg/kg, intramuscularly) and pentobarbital sodium (30 mg/kg, intraperitoneally) and perfused transcardially with cold 4% paraformaldehyde in phosphate buffer (n = 6) as described previously (Lewis and Lund, 1990) or with 4% paraformaldehyde and 0.2% glutaraldehyde in phosphate buffer (n = 4). Immediately after perfusion, the brain was removed, sliced into 2-5-mm thick coronal blocks and placed in fixative. Tissue from brains perfused with the 4% paraformaldehyde/0.2% glutaraldehyde mixture were transferred to 4% paraformaldehyde several weeks before Golgi processing.

8.2(B): Golgi Study.

For each monkey, 2 mm blocks of PFC were prepared by the Golgi rapid technique (see Lund, 1973) and 90 μm coronal sections were subsequently cut for analysis. The basal dendritic trees of mid-layer 3 pyramidal neurons, in Walker's areas 9 and 46 (Walker, 1940; **see Figure 26**) of the dorsal lateral prefrontal cortex (DLPFC) were reconstructed and their

Table 1. Rhesus monkeys used in the 2 studies

Animal number	Age[1]	Sex	Weight (kg)	Golgi study	5-HT study
Rh109	4d	F	0.50	X	X
Rh105	8d	M	0.54		X
Rh106	22d	M	0.60	X	X
Rh131	37d	F	0.70		X
Rh130	67d	F	0.75	X	X
Rh117	72d	F	0.58	X	X
Rh104	78d	F	0.63		X
Rh134	5m	F	1.2		X
Rh128	7m	F	1.3		X
Rh133	1.0yr	F	1.9		X
Rh135	1.5yr	F	2.8		X
Rh2107[3]	1.5yr	M		X	
Rh127[2]	2.3yr	M	N.A.[5]		X
Rh111	2.5yr	M	2.9		X
Rh118	2.7yr	M	3.2	X	X
Rh2007[3]	2.7yr	M		X	
Rh2091[3]	2.8yr	M		X	
Rh145[4]	3.0yr	M	6.0		X
Rh1975[2]	4.2yr	M		X	
Rh119[2]	4.5yr	M	6.4		X
Rh114	5.7yr	F	4.4		X
Rh103	7.0yr	M		X	
Rh143	15.9yr	M	8.4		X
Rh112	16.7yr	F	7.0		X

[1]d,Days; m, months; yr, years. [3]Castrated at 14 months (60 weeks).
[2]Castrated neonatally [4]Undergone GnRH treatment. [5]N.A., not available.

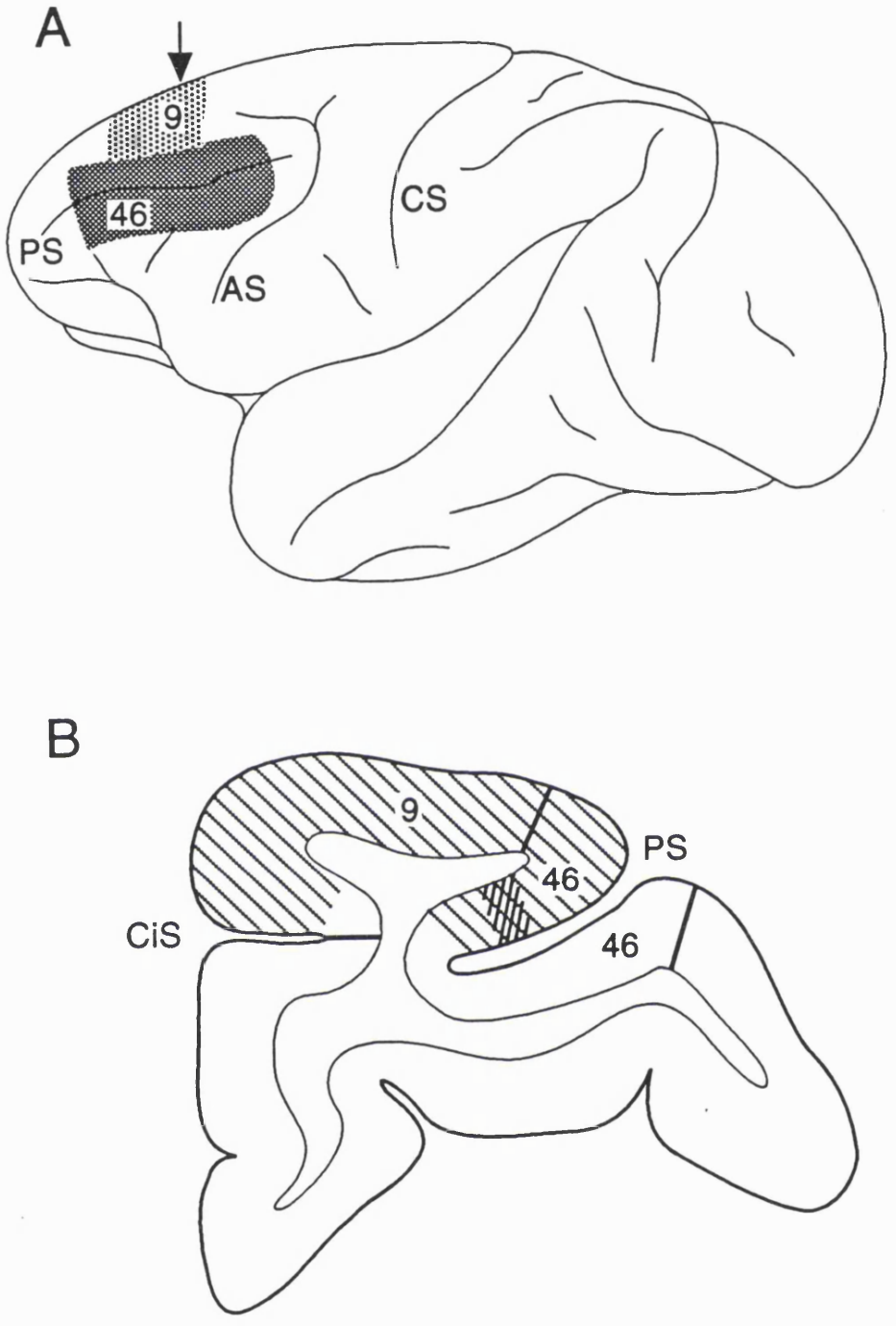

Figure 26 (A) A lateral view of the rhesus macaque monkey (Macaca mulatta) brain, with the shaded regions showing the locations of areas 9 and 46 (Walker, 1940; DLPFC). **(B)** A representative coronal section through the PFC, with the hatching indicating the limits of the sampling region within areas 9 and 46, from which mid-layer 3 pyramidal neurons from each animal were selected in the analysis of dendritic spine density, apical dendritic length and the degree of basal dendritic branching. The cross- hatched region in the dorsal bank of the PS, represents the sampling region for the PV-IR chandelier neuron axon cartridges (from Andersen et al, 1995; as compared with spine density in the Discussion section of the Spine study in the thesis). (Figure from Andersen et al, 1995). Abbreviations: AS = arcuate sulcus, CS = central sulcus, CiS = cingulate sulcus and PS = principal sulcus.

dendritic spines counted. Only pyramidal neurons located between the dorsal bank of the cingulate sulcus and the ventral bank of the principal sulcus were considered. The 10 animals used in the study were split into 5 age groups: < 4 weeks (n = 2), 10 weeks (n = 2), 1.5 years (n = 1), 2.6 years (n = 3) and > 4.5 years (n = 2).

Since the laminar boundaries in depth of areas 9 and 46 could not be easily determined directly in Golgi-impregnated material and the method of impregnating tissue blocks prevented alternate section Nissl-staining, a less direct method of establishing laminar borders was adopted. A scheme was devised, whereby the initial 30% of the cortical depth from the pial surface was hypothetically split into 3 bands of equal width (**Figure 27B**). Laminar divisions were then determined from Nissl-stained sections of blocks contiguous with the Golgi-reacted ones and from homologous portions of the contralateral hemisphere of each animal. It was found that the first 10% of cortical depth was equivalent to layer 1 and the next 6% to layer 2. Thus the first 10% band in the Golgi-tissue was regarded as layer 1, the second 10% band as layer 2 and upper layer 3 and the third 10% band as lower and mid-layer 3. (**see Figure 28**).

The population of pyramidal neurons chosen for this study were defined by the following criteria:

1. Ten layer 3 pyramidal neurons per animal from areas 9 and 46 were selected, on the basis that at least 3 of their basal dendrites came to a natural end within the extent of the 90 μm thickness of the section.
2. Each cell soma was located in mid-layer 3 (**see Figure 27A**).
3. The cell had a basal dendritic tree that was restricted to layer 3 (**see Figure 27C**).

The basal dendritic trees of each pyramidal neuron were then drawn using a 50x oil immersion objective lens and a camera lucida (drawing tube). A Sholl ring analysis was then carried out on the drawing (Sholl, 1953; **see Figure 27D**) whereby a transparency of 10 concentric circles spaced 20 μm apart, was placed over each drawing, centred on the cell soma. This enabled an estimation to be made of the degree of dendritic branching and the width of the dendritic arbour for each pyramidal neuron, by counting the number of dendritic intersections with each ring and estimating the distance from the cell soma to the last ring making contact with each dendrite. For each neuron 3 basal dendrites were then selected that were at least 40 degrees apart and continued to a natural ending within the confines of the tissue section. The dendritic spine density for each of these basal dendrites was then

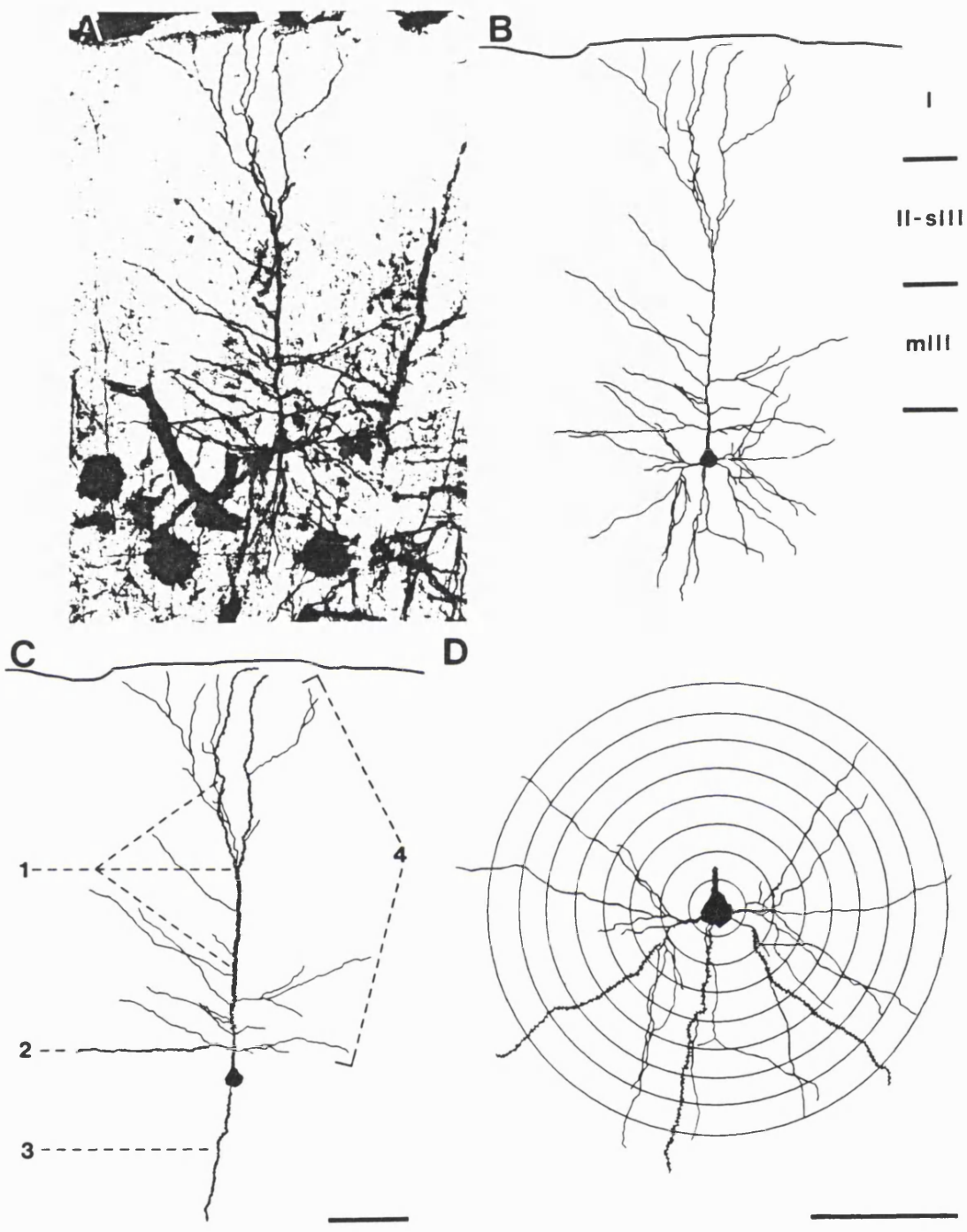

Figure 27 Golgi studies in monkey DLPFC. (**A**) Bright field photomontage showing a Golgi-impregnated mid-layer 3 pyramidal neuron in the 72-day-old animal. (**B**) The same neuron as reconstructed by the Eutectics neuron tracing system in Golgi study 1 (Andersen et al, 1995). Three equal bands each representing 10% of the total cortical depth are indicated (as used in the spine density analysis), with the laminae included within these bands: sIII=superficial layer3, mIII = mid-layer 3. (**C**) A portion of the reconstructed mid-layer 3 pyramidal neuron from (A) and (B) showing the various dendritic fields for which spine densities were measured in Golgi studies 1 and 2 in Andersen et al (1995) and study 1 of the thesis. (1) the main apical dendritic trunk and 2 side branches entering layer 1, (2) an apical oblique dendritic branch, (3) a basal dendrite (thesis study 1) and (4) indicates the total length of the apical dendritic tree. (**D**) For each mid-layer 3 pyramidal neuron, in study 1 of the thesis, 3 basal dendrites were analysed for spine density (per µm) as well as for the number of basal dendritic branch intersections (20 µm apart) made by the entire basal dendritic tree, using the Sholl ring method. (Figure from Andersen et al, 1995). Scale bars, (**A-C**) = 100 µm and (**D**) = 100 µm.

determined under a 100x oil objective lens by the counting spines contained within 10 μm segments every 20 μm along the dendrite, starting from the cell soma.

The objective of this investigation was to ascertain whether there were differences in the relative density of dendritic spines on mid-layer 3 pyramidal neuron basal dendrites confined to layer 3, across different age groups. There was no attempt made to determine the absolute numbers of spines on each dendrite across postnatal development. Since, equivalent portions of each dendrite were examined for every pyramidal neuron in each animal, no correction factors were applied for spines hidden behind dendritic shafts. While uncorrected spine measures obviously underestimate the absolute spine density of a dendritic population (Feldman and Peters, 1979), it has been found that both corrected and uncorrected spine counting methods provide equally good surveys of relative spine density when similar dendritic populations are being examined (Horner and Arbuthnott, 1991) as in the present study.

The rationale for conducting 2 separate studies of layer 3 pyramidal neurons in Golgi material (that by S. Anderson will be reported separately in the **Results section 10.0**) was due to the fact that only rarely were there found to be intact (i.e. both apical and basal dendritic trees) single pyramidal neurons in any one 90 μm thick Golgi-section. This was mainly due to the angle of cut being somewhat off that of the pia-to-white matter plane of the pyramidal neurons. It was decided to conduct separate analyses of the 2 portions of the dendritic tree of pyramidal cells and to compare the studies in terms of the relative time course for observed changes in spine density for apical and basal dendrites. To further ensure that the pyramidal neurons selected for analysis, were comparable in both cases, a second sample of basal dendritic measures were made by S. Anderson using the Eutectics method (**see Results section 10.0**). The use of data from two independent investigators employing different methods reduced the chances of observer and method bias in the results. It was also useful to be able to examine whether the same sequence of maturation occurred for different portions of the mid-layer 3 pyramidal neuron dendritic tree.

8.2(C). Statistical analyses.

The statistical significance of variations in Sholl ring measurements between animals of different ages was examined using a least-squares analysis of linear regression. The statistical significance of variations in relative spine density during postnatal development, was assessed using the non-parametric Kruskal-Wallis test. Animals were grouped by age and the measures were compared between age groups using the Bonferroni correction.

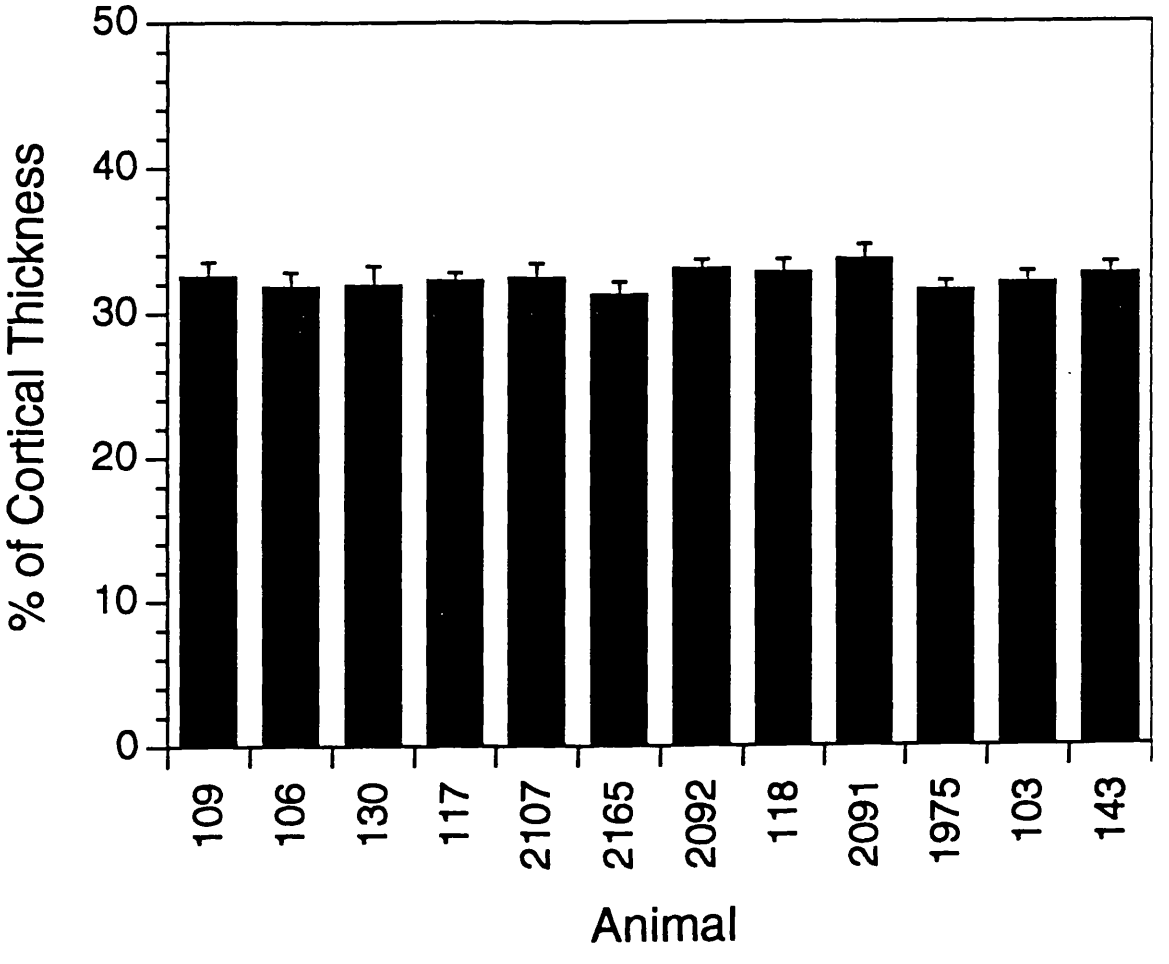

Figure 28 A bar plot illustrating the location by depth (as percentage of cortical pia-to-white -matter distance), for each animal in age, for the cell bodies of pyramidal neurons in mid-layer 3 of areas 9 and 46. As used in apical, basal and apical oblique dendritic spine density analysis (from Golgi study 1 in Andersen et al, 1995). The plot shows that there was minimal variation between the locations of pyramidal neurons for different ages. The same rationale for selecting pyramidal neurons was adopted in the present Golgi study (study 2 in Andersen et al, 1995), with the cell bodies of pyramidal neurons, whose basal dendrite spines were counted, being located at between 31-33% of cortical depth.

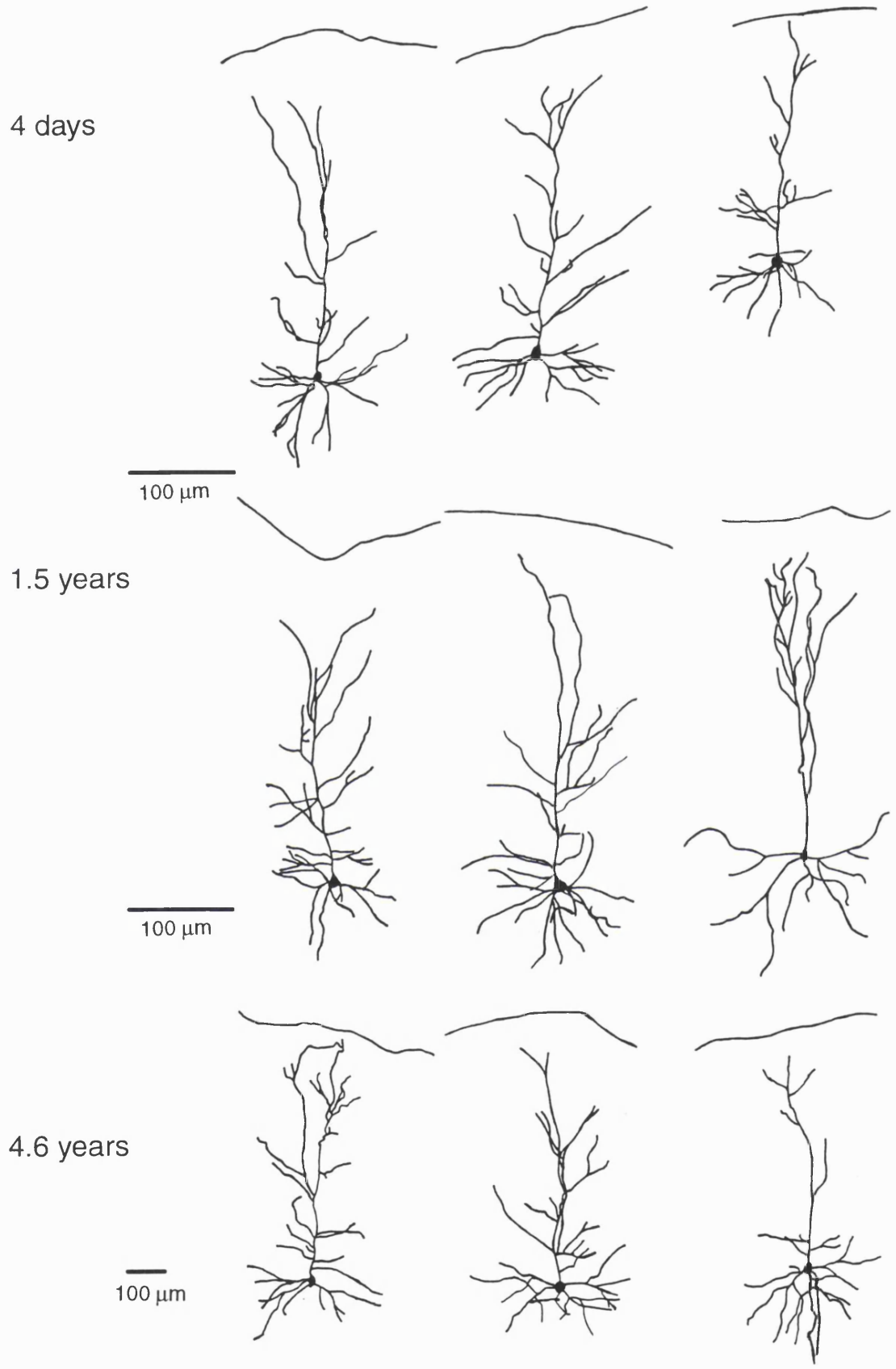

Figure 29 Examples of the different morphologies observed for Golgi-impregnated mid- layer 3 pyramidal neurons in areas 9 and 46 (DLPFC) used in the spine density and Sholl branching analyses, at different ages during postnatal development.

9.0 Results.

Study 1: A quantitative Golgi study of the postnatal maturation of mid-layer 3 pyramidal neuron basal dendritic spines in the monkey DLPFC (areas 9 and 46).

This study forms the basis of Golgi study 2 in Anderson et al (1995), the contribution to that paper made by J. Classey.

9.1(A): Qualitative observations of mid-layer 3 pyramidal neurons.

As described in the **Methods section 8.2**, mid-layer 3 pyramidal neurons were defined as having their cell soma located within the middle third of layer 3 in areas 9 and 46, their apical dendrite ascending into layer 1 and their basal dendritic tree confined to layer 3 and not extending into layer 4 (**see Figure 27**). Although, all mid-layer 3 pyramidal neurons examined in this study conformed to these basic criteria, there was a degree of morphological variation between individual pyramidal neurons, both between animals of different ages, but also within mid-layer 3 of any given animal (**see Figure 29A, B and C**; 4 days, 1.5 and 4.6 years). There were a large variety of apical dendritic and basal dendritic tree formations found in animals at all ages: some apical dendrites ended with terminal tufts only in layer 1, whilst others branched within layer 2 and furnished several major branches up into layer 1. Basal dendritic fields were also noted for their different architectures, with some pyramidal neurons possessing primarily downwardly-oriented dendrites, many had predominantly laterally-spreading dendrites, whilst others had a more uniformly distributed basal dendritic field.

9.1(B): Quantitative observations of mid-layer 3 pyramidal neurons.

9.1(B):(i). Changes in length and degree of branching for basal dendrites across postnatal development.

Using the Sholl ring analysis (**see Methods 8.2**), the mean number of dendritic ring intersections was measured for the basal dendritic fields of mid-layer 3 pyramidal neurons for cells in animals from 7 of the 10 ages (not the 22 day, 67 day or 2.5 year-old animals) employed in the study (**see Table 1**). There was found to be no significant difference in the mean number of dendritic intersections for the basal dendritic trees of mid-layer 3 pyramidal neurons at the various stages of postnatal development (**see Figure 31B and Table 2, for raw data**). Using a least sum-of-squares form of linear regression analysis, there was also found to be no significant difference between the mean total numbers of Sholl intersections for pyramidal neurons in each animal across the course of postnatal development.

Table 2. Sholl plots, i.e. number of intersections made by basal dendrites crossing each part of a circular grid aligned on the centre of the cell soma as shown for each animal age.

Distance from soma in (μm)	4 days	72 days	1.5yr	2.6yr	2.7yr	4.6yr	7.0yr
20	10.0	7.6	9.5	7.2	10.4	9.4	9.4
40	17.7	11.1	14.0	12.7	14.2	18.6	13.3
60	18.0	12.7	16.2	13.1	13.1	20.8	14.1
80	15.3	12.2	13.9	12.3	11.7	18.7	12.2
100	12.4	10.9	13.0	10.0	8.5	16.1	10.5
120	11.5	8.7	11.4	8.2	5.9	12.6	8.7
140	8.0	7.4	8.4	6.1	4.0	7.7	6.7
160	5.4	5.2	6.6	4.0	2.2	3.8	4.2
180	2.5	3.9	4.7	2.8	1.5	1.6	4.5
200	-------	2.2	2.5	2.0	------	1.0	1.0
Mean	11.2	8.2	10.0	7.8	7.9	11.0	8.5

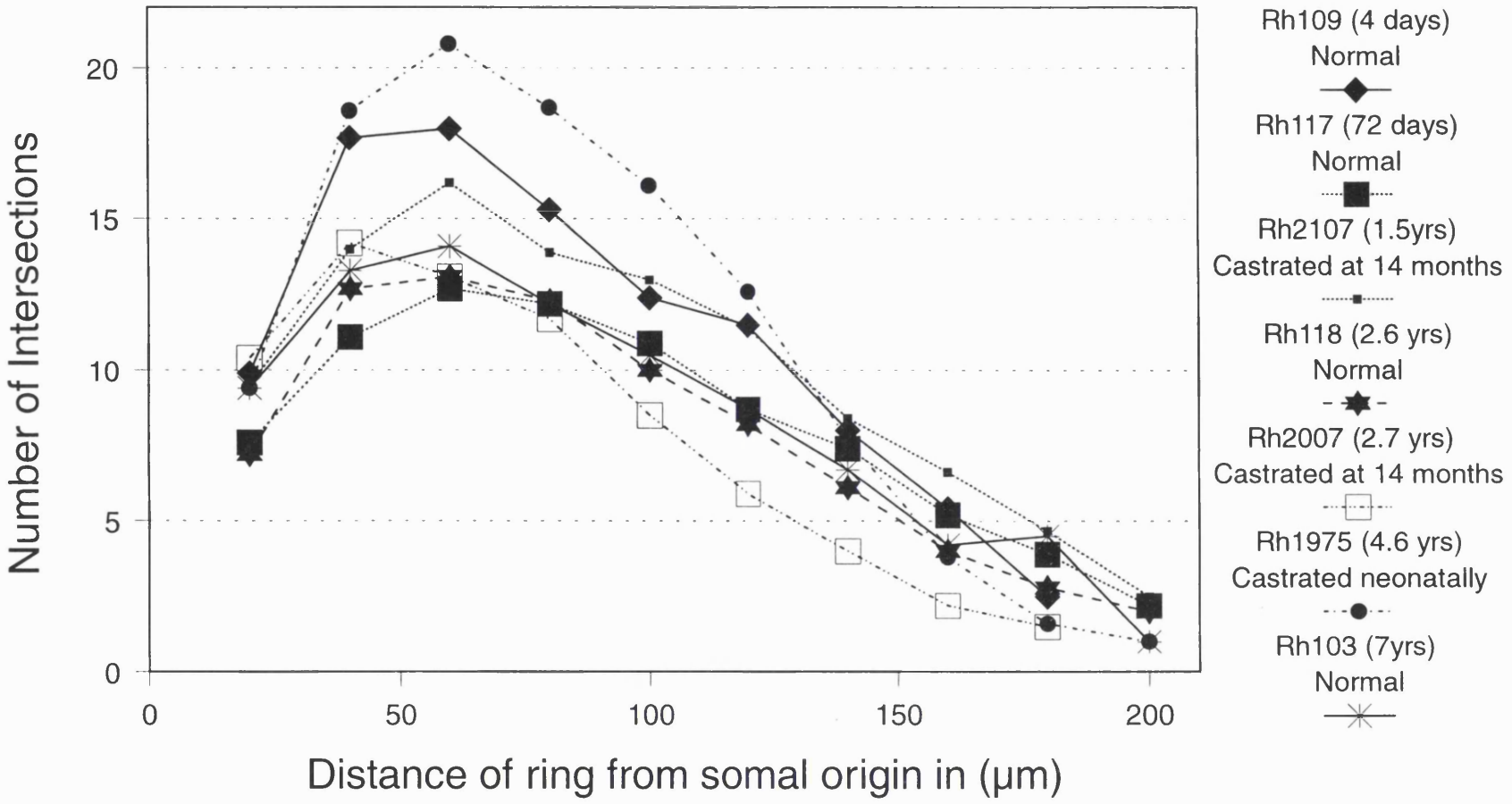

Figure 30 A chart showing the stable relationship with age (for 7 out of the 10 animals used in the study), for the mean extent of dendritic branching at various distances from the cell soma for the basal dendritic fields of mid-layer 3 pyramidal neurons during postnatal development in areas 9 and 46 (DLPFC).

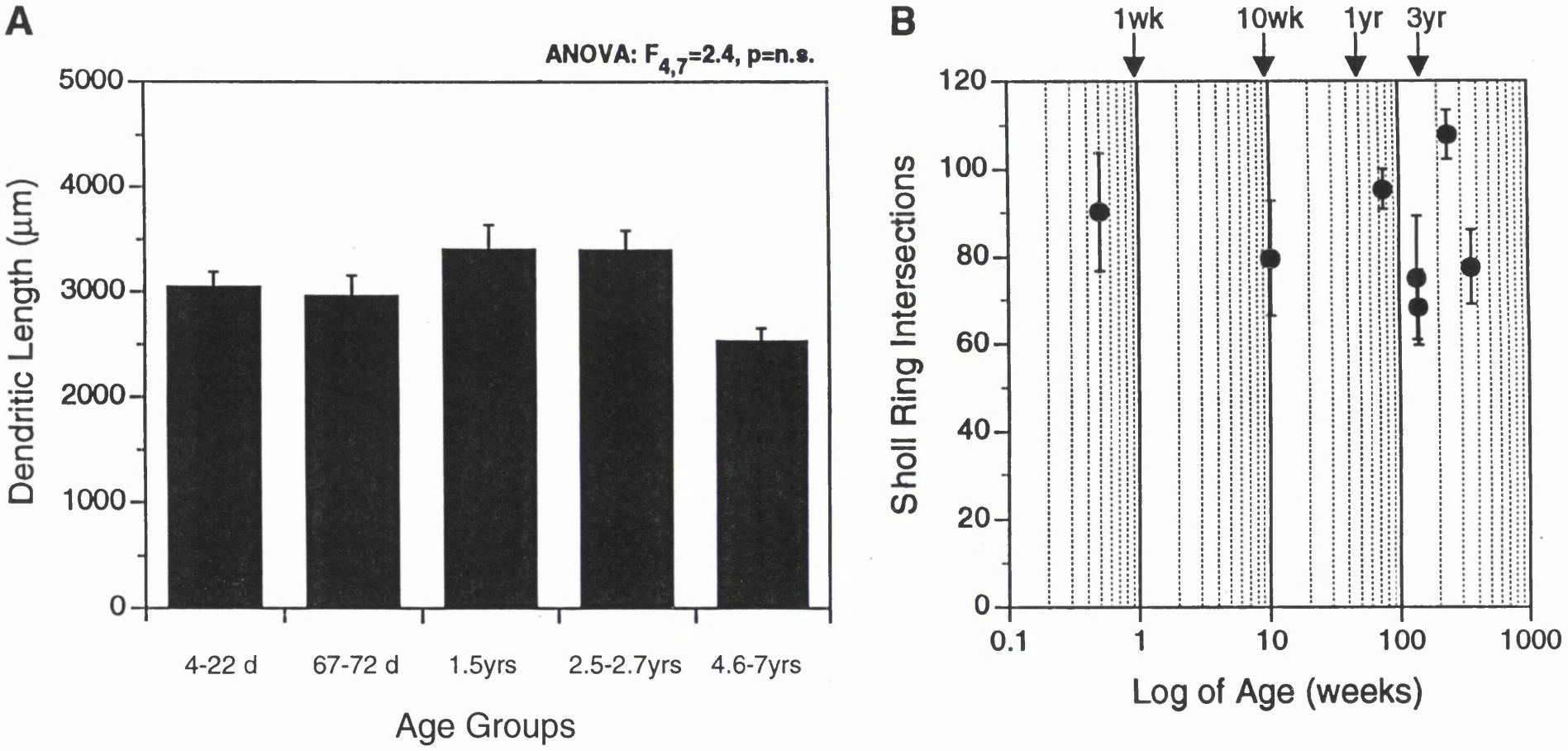

Figure 31 Measurements of dendritic length and dendritic branching. **(A)** Mean total apical dendritic length (in µm) for the mid-layer 3 pyramidal neuron sample used for the spine density analysis in Golgi study 1 of Andersen et al (1995), arranged in 5 age groups. **(B)** Mean number of Sholl ring intersections made by the basal dendritic fields of the mid-layer 3 pyramidal neuron sample - for 7 of the 10 animals - used in Golgi study 2 of Andersen et al (1995) - i.e. study 1 in the thesis. Standard errors indicated. N.B. the absence of an effect of age on apical dendritic length or the number of basal dendritic branches for mid- layer 3 pyramidal neurons. (From Andersen et al, 1995).

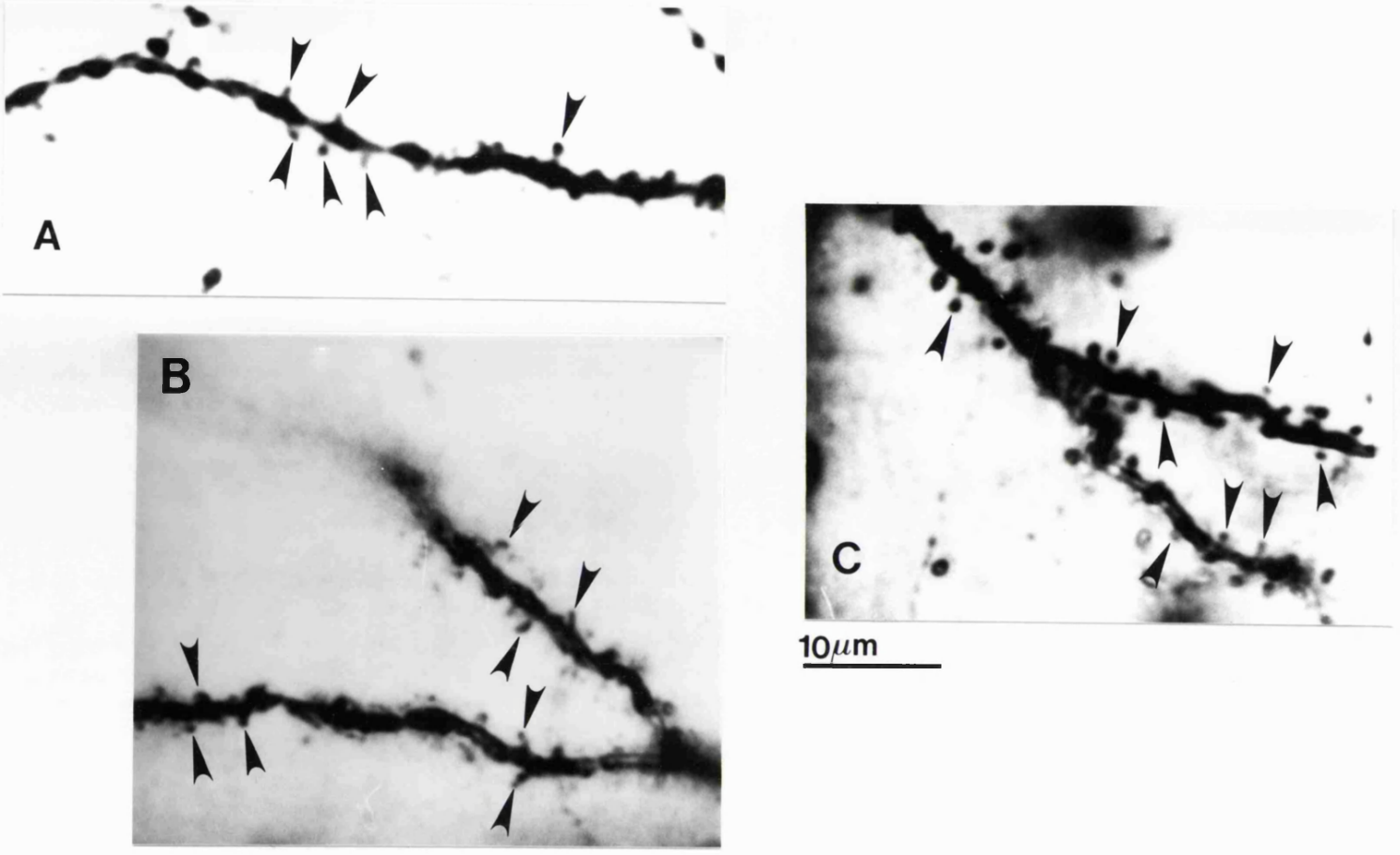

Figure 32. Bright-field photomicrographs illustrating the varied morphology of dendritic spines (indicated by arrow-heads), located on the basal dendrites of pyramidal neurons within mid-layer 3 of areas 9 and 46, in animals of various ages: **(A)** 4 days, **(B)** 78 days and **(C)** 7.0 years.

The distribution of dendritic branches around cell soma was found to be relatively invariant across development, in terms of their pattern, order of branching and their individual lengths. There were no statistically significant differences between animals, in terms of the dendritic length (**see Figure 30**), the mean number of basal dendritic branches or mean diameter of basal dendritic fields (**see Figure 31B**) for mid-layer 3 pyramidal neurons during the entire period of postnatal development between birth and 7.0 years of age, i.e. adulthood.

9.1(B).(ii): Changes in relative spine density for basal dendrites during postnatal development.

Regarding the spine density analysis conducted for selected basal dendrites of mid-layer 3 pyramidal neurons (**see Figures 33A, B and Table 3 for raw data**), values were initially found to be at low levels in the early neonatal animal (4 days of age) and were only slightly higher in the 22 day-old animal. Between 22 days and 10 weeks of age (in the 67 and 72 day-old animals) a dramatic rise in spine density was observed with an approximately 75% increase in values over this period of postnatal development. This high level of spine density for basal dendrites remained at a plateau until a 41% decrease occurred sometime between the animals of 2.5 and 2.6 years of age, bringing spine density values back down to levels close to that seen in the 22 day-old animal. This low level of spine density was maintained with a slight degree of variation from adolescence into adulthood (as seen for the 2.7, 4.6, 5.7 and 7.0 year-old animals).

The spine density data from the 10 animals examined, was originally grouped into 5 age groups in Anderson et al (1995), which when applied in this thesis using the non-parametric Kruskal-Wallis test as opposed to the parametric ANOVA test used in the original paper, resulted in a finding of no significant difference between the 5 age groups during postnatal development. However when the animals were grouped into just 2 age groups (4 days-22 days/4.6 yrs-7.0 yrs: $n = 4$ and 67 days-2.8 yrs: $n = 6$) for this thesis, on the basis of the similarity in values for the youngest and oldest animals and again the Kruskal-Wallis test was applied, a significant level (asymptotic) of $P < 0.055$, was found between the 2 groups of animals. That is between the youngest and mid-range animals and also between the oldest and mid-range animals. This was further confirmed by the use of the Mann-Whitney U test, which in addition to providing a 2-tailed (asymptotic) significance level of $P < 0.055$, also gave an exact significance level of $P < 0.067$. By grouping the results for the 10 animals used in the study in various ways, in terms of their ages, it was possible to find even more significant changes occurring for spine density during postnatal development. Maximally significant

Table 3. Mean spine density for basal dendrites of layer 3 pyramidal neurons.

4d

Distance (μm)	Cell 3A	Mean	Cell 3B	Mean	Cell 5A	Mean
20	4 3 7	4.67	7 11 4	7.33	6 6 7	6.33
50	7 10 9	8.67	9 12 9	10.00	10 8 8	8.67
80	9 9 10	9.33	7 9 10	8.67	7 7 12	8.67
110	8 4 11	7.67	6 7 8	7.00	- 0 9	6.50
140	8 4 6	6.00	4 - 6	5.00	------	-----
170	-------	-----	4 - 5	4.65	------	-----

Distance (μm)	Cell 7A	Mean	Cell 7B	Mean	Cell 9A	Mean
20	4 6 8	6.00	5 4 8	5.00	6 6 6	6.00
50	9 11 11	10.33	11 9 11	10.33	8 6 9	7.67
80	10 11 10	10.33	8 6 9	7.67	10 8 6	8.00
110	9 6 10	8.33	6 4 9	6.33	7 7 6	6.67
140	7 3 8	6.00	6 - 5	5.50	7 - -	7.00

Distance (μm)	Cell 9B	Mean	Cell 4B	Mean	Cell 6B	Mean
20	8 6 8	7.33				
50	10 8 10	9.33	16 12 11	13.00	10 9 6	8.33
80	- - 7	7.00				
110	- - -	---------	9 5 8	7.33	6 8 4	6.00
140	- - -	---------				
170	- - -	---------				

Distance (μm)	Cell 5B	Mean
20		
50	6 11 5	7.33
80		
110	10 9 4	7.67
140		
170	- - -	---------

22d

Distance (μm)	Cell 3A1	Mean	Cell 3A2	Mean	Cell 3B	Mean
20						
50	13 11 12	12.00	7 10 8	8.33	8 7 11	8.67
80						
110	12 10 10	10.67	10 12 12	11.33	10 7 8	8.33
140						
170	8 6 2	5.33	10 5 8	7.67	9 7 6	7.33

Distance (μm)	Cell 5A	Mean	Cell 7A	Mean	Cell 9A	Mean
20						
50	9 8 6	7.67	10 8 9	8.00	8 14 10	10.67
80						
110	7 11 11	9.67	12 10 11	11.00	9 11 9	9.67
140						
170	5 9 8	7.33	9 12 7	9.67	9 6 -	7.50

Distance (μm)	Cell 9B	Mean	Cell 11A	Mean	Cell 11B	Mean
20						
50	5 6 10	7.00	10 11 10	10.33	10 10 11	10.33
80						
110	11 8 8	9.00	8 9 9	8.67	9 8 7	8.00
140						
170	4 - -	4.00	5 - 8	6.50	9 - -	9.00

Distance (μm)	Cell 7B	Mean
20		
50	10 11 8	9.67
80		
110	9 9 13	10.33
140		
170	6 6 9	7.00

67d

Distance (μm)	Cell 3B	Mean	Cell 3C	Mean	Cell 5A	Mean
20						
50	7 5 10	7.33	11 16 16	14.33	11 16 13	13.33
80						
110	13 8 8	9.67	15 18 11	14.67	17 18 18	17.67
140						
170	10 11 8	9.67	12 - 13	12.5	14 15 16	15.00

Distance (μm)	Cell 5B	Mean	Cell 7A	Mean	Cell 7B	Mean
20						
50	11 12 19	14.00	12 16 10	12.67	21 14 17	17.33
80						
110	15 15 15	15.00	15 18 12	15.00	17 20 21	19.33
140						
170	12 - 7	9.50	11 12 -	11.50	14 14 -	14.00

Distance (μm)	Cell 7C	Mean	Cell 9A	Mean	Cell 10C1	Mean
20						
50	17 17 15	16.33	15 14 15	14.67	18 14 17	16.33
80						
110	15 20 14	16.33	14 16 14	14.67	12 14 13	13.00
140						
170	11 18 12	13.67	12 18 13	14.33	- - -	---------

Distance (μm)	Cell 10C2	Mean
20		
50	14 15 13	14.00
80		
110	15 12 11	12.67
140		
170	15 10 -	12.50

72d

Distance (μm)	Cell 6B	Mean	Cell 8B	Mean	Cell 9B	Mean
20	7 8 14	9.67	9 8 12	9.67	10 7 9	8.67
50	17 17 14	16.00	14 13 12	13.00	12 12 15	13.00
80	14 15 16	15.00	12 11 18	13.67	15 13 17	15.00
110	11 16 13	13.33	11 12 16	13.00	14 15 11	13.33
140	9 12 15	12.00	- 10 11	10.50	17 12 13	14.00
170	- 11 9	10.00	- - 20	20.00	14 18 11	14.33
200	- 7 -	7.00	- - 16	16.00	14 9 -	11.50

Distance (μm)	Cell 11A	Mean	Cell 12C	Mean	Cell 13B	Mean
20	7 9 8	8.00	17 17 11	15.00	6 10 11	9.00
50	9 6 6	7.00	16 15 15	15.33	14 15 14	14.33
80	5 - 11	8.00	14 20 16	16.67	11 17 20	16.00
110	9 - 13	11.00	13 15 17	15.00	13 13 16	14.00
140	7 - -	7.00	10 11 -	10.50	15 12 -	13.50
170	- - -	---	- - -	---	16 - -	16.00

Distance (μm)	Cell 13C1	Mean	Cell 13C2	Mean	Cell 14A1	Mean
20	13 13 13	13.00	11 20 25	18.67	8 6 8	7.33
50	15 14 16	15.00	24 15 11	16.67	10 12 12	11.33
80	19 12 17	16.00	20 22 22	21.33	10 10 7	9.00
110	17 16 16	16.33	16 - 17	16.50	8 12 9	9.67
140	20 - -	16.00	17 - 15	16.0	12 13 7	10.67
170	- - -	---	10 - -	10.0	- 12 -	12.00
200	- - -	---	- - -	---	- 9 -	9.00

Distance (μm)	Cell 14A2	Mean
20	17 14 8	13.00
50	17 8 8	11.00
80	14 10 12	12.00
110	12 8 12	10.67
140	10 6 -	8.00

1.5yr

Distance (μm)	Cell 7A1	Mean	Cell 7A2	Mean	Cell 12A	Mean
20	8 6 16	10.00	8 4 9	6.00	10 5 8	7.67
50	14 13 14	13.67	12 15 9	12.00	14 8 15	12.00
80	14 12 12	12.67	11 13 10	11.33	13 11 11	11.67
110	12 12 12	12.00	11 12 16	13.00	8 9 10	9.00
140	8 12 12	10.67	9 12 12	11.00	6 7 8	7.00
170	9	9.00	8 9 10	9.00	- 7 -	7.00
200	--------	---------	8 8 -	8.00	----------	---------

Distance (μm)	Cell 8A1	Mean	Cell 8A2	Mean	Cell 8B1	Mean
20	10 8 10	9.33	4 12 12	9.33	4 3 10	11.67
50	16 15 16	15.67	10 14 14	12.67	11 9 13	12.67
80	15 13 12	13.33	12 10 11	11.00	13 9 15	11.67
110	16 13 12	13.67	8 - 11	8.00	8 10 12	14.00
140	15 15 13	14.33	----------	------	----------	14.50
170	10 - -	10.00	----------	------	----------	---------

Distance (μm)	Cell 10A2	Mean	Cell 10B2	Mean	Cell 10A1	Mean
20	10 11 8	9.67	5 4 6	5.00	10 16 9	11.67
50	13 20 16	16.33	14 13 15	14.00	12 14 12	12.67
80	16 19 14	16.33	15 19 17	17.00	14 7 14	11.67
110	13 18 12	14.33	16 17 19	17.33	16 - 12	14.00
140	10 16 11	12.33	14 14 15	11.00	16 - 13	14.50
170	- 13 11	9.00	13 11 13	12.33	9 - 12	10.50
200	----------	---------	- - 12	12.00	- - -	---------

Distance (μm)	Cell 7B	Mean
20	6 11 4	7.00
50	14 18 15	15.67
80	16 16 16	16.00
110	15 14 19	16.00
140	17 13 17	15.67
170	18 9 15	14.00
200	15 - -	15.00

2.5yr

Distance	Cell 4A1	Mean	Cell 4A2	Mean	Cell 4B1	Mean
20						
50	17 15 24	18.67	16 14 18	16.00	15 22 19	18.67
80						
110	22 21 22	21.67	21 16 15	17.33	21 20 16	19.00
140						
170	- - 12	12.00	11 12 13	12.00	- 14 10	12.00

Distance (μm)	Cell 8C	Mean	Cell 4A3	Mean	Cell 4B2	Mean
20						
50	9 12 11	10.67	9 14 12	11.67	15 17 10	14.00
80						
110	12 10 13	11.67	10 16 15	13.67	19 17 8	14.67
140						
170	8 8 8	8.00	- - 11	11.00	15 -	15.00

Distance (μm)	Cell 8B	Mean	Cell 8A1	Mean	Cell 8A2	Mean
20						
50	11 14 9	11.33	10 16 12	12.67	21 22 21	21.33
80						
110	17 8 12	12.33	13 14 15	14.00	17 20 23	20.00
140						
170	5 - -	5.00	- 4 12	8.00	- 16 14	15.00

Distance (μm)	Cell 8A2	Mean
20		
50	15 13 14	14.00
80		
110	14 19 12	15.00
140		
170	12 15 -	13.50

2.7yr

Distance (μm)	Cell 3B1	Mean	Cell 3B2	Mean	Cell 4A	Mean
20	5 4 5	4.67	5 - -	5.00	11 3 6	6.67
50	8 9 7	8.00	8 - -	8.00	16 10 9	11.67
80	10 6 10	8.67	7 - -	7.00	9 15 18	14.00
110	2 7 8	5.67	- - -	---	- 10 10	10.00
140	8 - 8	8.00	- - -	---	- 8 -	8.00
170	- - -	---	- - -	---	- - -	---

Distance (μm)	Cell 5A	Mean	Cell 5B	Mean	Cell 6A	Mean
20	5 5 4	4.67	9 10 5	8.00	9 11 7	7.00
50	7 6 8	7.00	11 10 12	11.00	13 13 15	13.67
80	8 - 6	7.00	11 11 10	10.67	17 18 19	18.00
110	6 - 5	5.50	8 8 11	9.00	15 17 14	15.33
140	- - -	---	8 - 6	7.00	8 12 9	9.67
170	- - -	---	- - 8	8.00	- 4 9	6.50

Distance (μm)	Cell 7B1	Mean	Cell 7B2	Mean	Cell 9B	Mean
20	10 13 13	12.00	1 5 7	4.33	11 13 14	12.67
50	18 12 12	14.00	9 10 10	9.67	19 18 16	17.67
80	12 11 13	12.00	10 13 8	10.33	17 14 13	14.67
110	15 8 12	11.67	- 11 10	10.50	15 11 11	12.33
140	- - -	---	- 10 8	9.00	12 4 4	6.67
170	- - -	---	- 8 -	8.00	11 - -	11.00
200	- - -	---	- - -	---	2 - -	2.00

Distance (μm)	Cell 13B	Mean
20	6 7 5	7.00
50	10 9 10	9.67
80	12 13 11	12.00
110	12 11 10	11.00
140	11 6 10	9.00
170	6 - 7	6.50
200	- - -	-------- --

2.8yr

Distance (μm)	Cell 7A	Mean	Cell 7C	Mean	Cell 8B	Mean
20	4 2 2	2.67	2 7 6	5.00	5 10 7	7.33
50	9 9 7	8.33	9 7 12	9.33	8 14 9	10.33
80	9 10 8	9.00	9 9 9	9.00	9 11 7	9.00
110	8 - 8	8.00	9 9 9	9.00	6 7 11	8.00
140	10 - 6	8.00	6 10 7	7.67	6 - -	6.00
170	----------	--------	6 8 -	7.00	----------	-------

Distance (μm)	Cell 8D	Mean	Cell 9A	Mean	Cell 9C	Mean
20	6 9 3	6.00	6 5 5	5.33	2 3 6	3.67
50	10 11 9	10.00	- 10 -	10.00	7 5 8	6.67
80	15 11 11	12.33	11 10 8	9.67	8 7 11	8.67
110	10 - 12	11.00	13 10 6	9.67	7 7 6	6.67
140	10 - 11	10.50	14 13 8	11.67	10 7 -	8.50
170	----------	--------	11 11 -	11.00	6 - -	6.00
200	----------	--------	8	8.00	5 - -	5.00

Distance (μm)	Cell 10B	Mean	Cell 10C	Mean	Cell 11A	Mean
20	4 2 4	3.33	1 0 3	1.33	7 7 7	7.00
50	6 9 6	7.50	11 10 4	8.33	9 11 10	10.00
80	5 7 -	6.00	14 8 7	9.67	12 15 14	13.67
110	8 8 -	8.00	12 9 4	9.67	12 11 11	11.33
140	5 7 -	6.00	12 12 -	12.00	5 8 11	8.00
170	----------	-------	11 7 -	9.00	11 6 9	8.67
200	----------	-------	13 9 -	11.00	8 - 9	8.50
230	----------	-------	- 6 -	6.00	- - 9	9.00

Distance (μm)	Cell 8A	Mean
20	6 3 3	4.00
50	6 9 6	7.00
80	7 6 7	6.67
110	7 9 9	8.33
140	4 4 6	4.67
170	4 - -	4.00

4.6yr

Distance (μm)	Cell 8A	Mean	Cell 4B1(1)	Mean	Cell 4B2(1)	Mean
20	8 6 7	7.00	5 5 6	5.33	7 4 6	5.67
50	16 11 13	13.33	7 11 9	9.00	- 12 18	15.00
80	15 13 14	14.00	10 8 11	9.67	10 11 16	12.33
110	11 13 13	12.33	- 7 8	7.50	9 11 14	11.33
140	11 12 10	11.00	- 6 6	6.00	9 9 9	9.00

Distance (μm)	Cell 6A	Mean	Cell 4A	Mean	Cell 6B	Mean
20	4 2 2	2.67	4 9 7	6.67	10 8 11	9.67
50	7 11 8	8.67	7 11 9	9.00	16 13 15	14.67
80	12 9 10	10.33	11 11 9	10.33	15 11 13	13.00
110	11 9 10	10.00	12 10 -	11.00	13 11 11	11.67
140	- - -	10.00	9 10 -	9.50	9 8 -	8.50
170	- - -	---	---	---	---	---

Distance (μm)	Cell 10A2	Mean	Cell 4B1(2)	Mean	Cell 4B2(2)	Mean
20	7 9 7	7.67	7 4 5	5.33	6 6 5	5.67
50	10 11 10	10.33	10 7 7	8.00	11 8 13	10.67
80	8 13 10	10.33	10 7 9	8.67	12 10 12	11.33
110	8 10 10	9.33	9 7 7	7.67	11 10 12	11.00
140	- - 8	8.00	9 6 7	7.33	11 - 9	10.00
170	- - 6	6.00	- - -	---	- - -	---

7.0yr

Distance (μm)	Cell 4A	Mean	Cell 5B	Mean	Cell 8A	Mean
20	12 7 5	8.00	3 4 6	4.33	4 5 9	6.00
50	10 11 14	11.67	15 12 6	11.00	10 15 12	12.33
80	9 8 10	9.00	12 13 7	10.67	9 10 10	9.67
110	6 6 8	6.67	8 11 8	9.00	11 8 12	10.33
140	8 6 8	7.33	8 9 -	8.50	8 10 9	9.00
170	6 5 -	5.50	7 5 -	6.00	5 5 8	6.00

Distance (μm)	Cell 9A	Mean	Cell 11A	Mean	Cell 11B	Mean
20	3 10 11	8.00	9 10 10	9.67	10 5 8	7.67
50	11 13 10	11.33	12 12 15	13.00	10 6 9	8.33
80	10 10 9	9.67	10 8 9	9.00	14 11 9	11.33
110	9 10 9	9.33	14 8 11	11.00	14 7 9	10.00
140	12 6 -	6.00	5 11 11	9.00	6 - -	6.00
170	11 - -	11.00	- - -	---	- - -	---
200	7 - -	7.00	- - -	---	- - -	---

Distance (μm)	Cell 13A1	Mean	Cell 13A2	Mean	Cell 13A3	Mean
20	6 9 5	6.67	6 10 7	7.67	6 8 8	7.33
50	7 13 7	9.00	11 11 12	11.33	5 13 10	9.33
80	9 9 8	8.67	7 14 8	12.33	10 8 11	9.67
110	10 8 11	9.67	---	9.67	6 7 9	7.33
140	12 7 -	9.50	---	---	9 7 8	8.00
170	- - -	---	---	---	- 9 -	9.00
200	- - -	---	---	---	---	---

Distance (μm)	Cell 13B	Mean
20	8 13 10	10.33
50	11 15 13	13.00
80	12 12 11	11.67
110	13 7 8	9.33
140	11 12 -	11.50
170	----------	---------

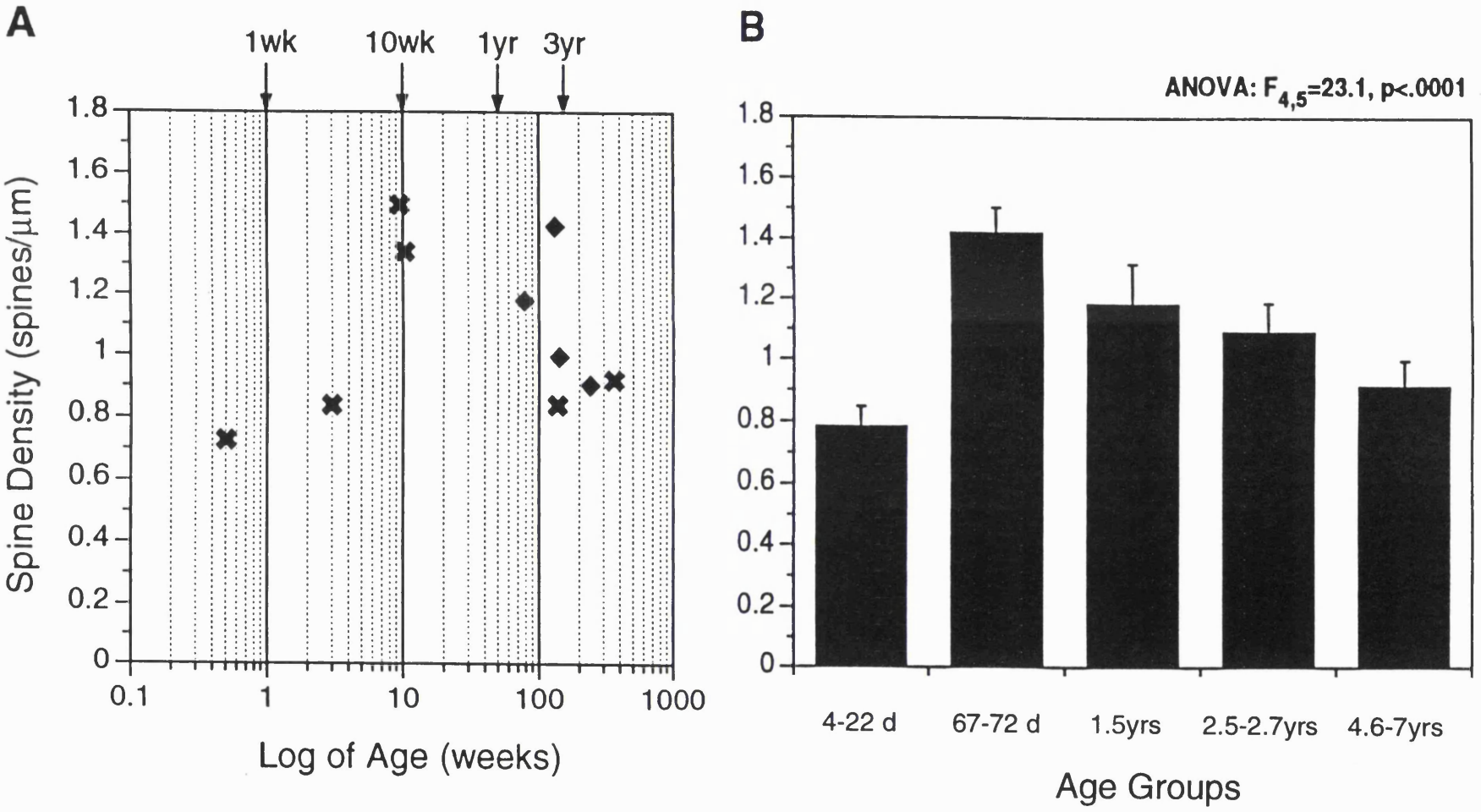

Figure 33 Mean relative spine density (per µm) on basal dendrites of mid-layer 3 pyramidal neurons (Golgi study 2 in Andersen et al (1995). **(A)** histogram showing results for individual animals on a proportional logarithmic time scale and **(B)** bar plot showing the results plotted in 5 age groups used for Golgi studies 1 and 2 in Andersen et al (1995). Standard errors indicated. (From Andersen et al, 1995).

differences were found to occur between the age groups containing the 4 youngest (4 days-72 days), 4 mid-age (1.5 yrs-2.8 yrs) and the 2 oldest (4.6 yrs and 7.0 yrs) animals: (asymptotic) significance, $P < 0.036$, with the strongest difference between the youngest and mid-age animals ($P < 0.001$) and equally when grouped together as the 2 youngest (4 days and 22 days), 4 mid-age (67 days-2.5 yrs) and 4 oldest (2.7 yrs-7.0 yrs) animals: (asymptotic) significance, $P < 0.036$, with the strongest difference between the mid-age and oldest animals ($P < 0.001$).

There were also significant variations in absolute spine density between proximal, medial or distal portions of basal dendrites (graph not shown, but see raw data in **Table 3**) the highest density occurring on the medial segment. However the relative differences in spine density along the extent of single dendrites were very similar at different ages, so there was not found to be a statistically significant age-related change in the overall mean proximal-to-distal distribution of spines along basal dendrites.

9.1(C): Summary.

The time course of postnatal development for basal dendritic spines on pyramidal neurons in mid-layer 3 of areas 9 and 46, although showing a broadly-defined pattern of rise, plateau (stable values) and decline, only the stages of rising and falling spine density could be substantiated by statistical means, due to the small numbers of animals used in this study.

10.0: S. Anderson contribution to Anderson et al, 1995, (i.e. Golgi study 1).

10.1: The postnatal maturation of apical dendritic spines of mid-layer 3 pyramidal neurons in the monkey DLPFC.

The above results (**Golgi study 2**) have been published as part of an investigation (Anderson et al, 1995), which also included an independent analysis (by S. Anderson) of spine density on the apical dendrites (**Golgi study 1**) of PFC layer 3 pyramidal cells. Many cells were analysed from the same sections from the same animals in both analyses (but systematic dual analysis of the same neurons was not possible for reasons stated previously; **see Methods 8.2 for details**). The developmental time course for apical dendritic spine maturation showed a strong correlation with that seen for the basal dendritic spines seen in this thesis study.

A quantitative analysis was carried out for spine density on the apical dendrites of a comparable population of mid-layer 3 pyramidal neurons in area 9 and 46 of animals of various ages, several being the same animals used in the basal dendritic spine analysis. The

rationale for 2 comparable studies using different methods is discussed in the **Methods section 8.2**. Like the findings of changes in spine density across postnatal development for basal dendrites, apical dendrites showed a rapid rise in values within animals ranging from birth until 10 weeks of age when they reached their maximum and remained at this high density (plateau period) until at least within the 1.5 year-old animals (**see Figure 56A in the appendix**). Beyond this age, spine density dropped below the maximal level for the animal of 2.6 years of age and appeared to decrease steadily, initially reaching lowest values in the 4.6 year-old animal, when stable mature adult values were first observed. This mature level of apical dendritic spine density remained relatively constant throughout the rest of adult life, until at least 15.9 years of age (the oldest animal for which spine density was assessed in the apical dendritic analysis).

Statistically significant differences were found (**see Figure 56B in the appendix**) for the apical dendritic spine density of mid-layer 3 pyramidal neurons ($F = 65.5$, $P < 0.0001$). Specifically, there was a rise in spine density between the < 3-(0.49±0.02) and 10-week-(0.75 ±0.02) old age groups, a decrease between the 1.5-(0.74 ±0.01) and 2.6-year-(0.63 ±0.02) old age groups. Also there were reductions between the 10-week (0.75 ±0.02) and > 4.5-year-(0.45 ±0.01) old and between the 1.5-(0.74 ±0.01) and > 4.5-year-(0.45 ±0.01) old age groups. All differences were observed at a significance level of $P < 0.05$.

Also, differences were observed in the distribution of spines on the proximal, medial and distal portions of apical dendrites, corresponding with the ascending passage of the apical dendrite through-mid-layer 3, superficial layer 3 to layer 2 and layer 1, respectively (**see Figure 57A, B and C in the appendix**). The proximal portion of the apical dendrite, corresponding to a 10% band of cortical depth, from the soma in mid-layer 3 to the base of superficial layer 3, was shown to consistently possess the greatest absolute values for spine density during development; whilst the distal portion situated in layer 1, always demonstrated the smallest contribution to the overall spine density of apical dendrites at all ages. The medial portions of apical dendrites in layers 2 and superficial 3, initially exhibited high absolute levels of spine density (10 weeks age group), comparable to those for the proximal portions, but in the adult animals (> 4.5 years age group) the levels of spine density were much lower than the equivalent for the proximal dendritic portions.

10.2: Comparison of postnatal time courses of maturation for changes in basal dendritic spine density in Golgi study 1 (J. Classey's work) with those in Golgi study 2 (S. Anderson's work from Anderson et al, 1995).

Changes in spine density for basal dendrites in Golgi study 1 were comparable to those seen for the basal dendritic analysis of Golgi study 2 with a similar time course and significant differences (study 1: $P < 0.0001$; study 2: $P < 0.055$) between almost identical age groups, but with lower absolute values for spine density in Golgi study 1 (**compare figures 33A and B with Figure 58B in the appendix**), due to the different sampling techniques employed for analysing spine density.

10.3. Summary: The postnatal time courses of maturation for pyramidal neuron basal and apical dendritic spines.

Over the course of postnatal development, apical dendritic spine density had much lower values than those observed for the basal dendritic spine analysis (e.g. 0.8 compared to 1.5 spines per μm at peak levels in the 72-day-old animal). Several factors account for this discrepancy, firstly the differences in the neuron reconstruction employed in each study (and different levels of magnification used) and secondly the variation in the methods of quantitative analysis. The basal dendritic spine analysis omitted the most proximal (0-10 μm) and very distal (mean = 10 μm) portions of the dendrites where spine densities are lower than for the rest of the dendrite. Despite these differences in methods and hence the absolute spine density values for the basal and apical dendrites of mid-layer 3 pyramidal neurons, the age-related changes in relative spine density with which we are primarily concerned were remarkably similar for both apical and basal dendrites of the mid-layer 3 pyramidal cells across the entire period of postnatal development.

11.0: Discussion.

Study 1: A quantitative Golgi study of the postnatal maturation of mid-layer 3 pyramidal neuron basal dendritic spines.

11.1: Introduction.

It is concluded that all dendritic compartments of mid-layer 3 pyramidal neurons in areas 9 and 46 share a generally concurrent pattern of refinement for the acquisition and loss of their spines, the sites of potential excitatory postsynaptic inputs, during the postnatal period (birth to 7.0 years of age, **see extrapolated curve in Figure 34A**). The only exception to this general rule was the variation between proximal and distal portions of both apical

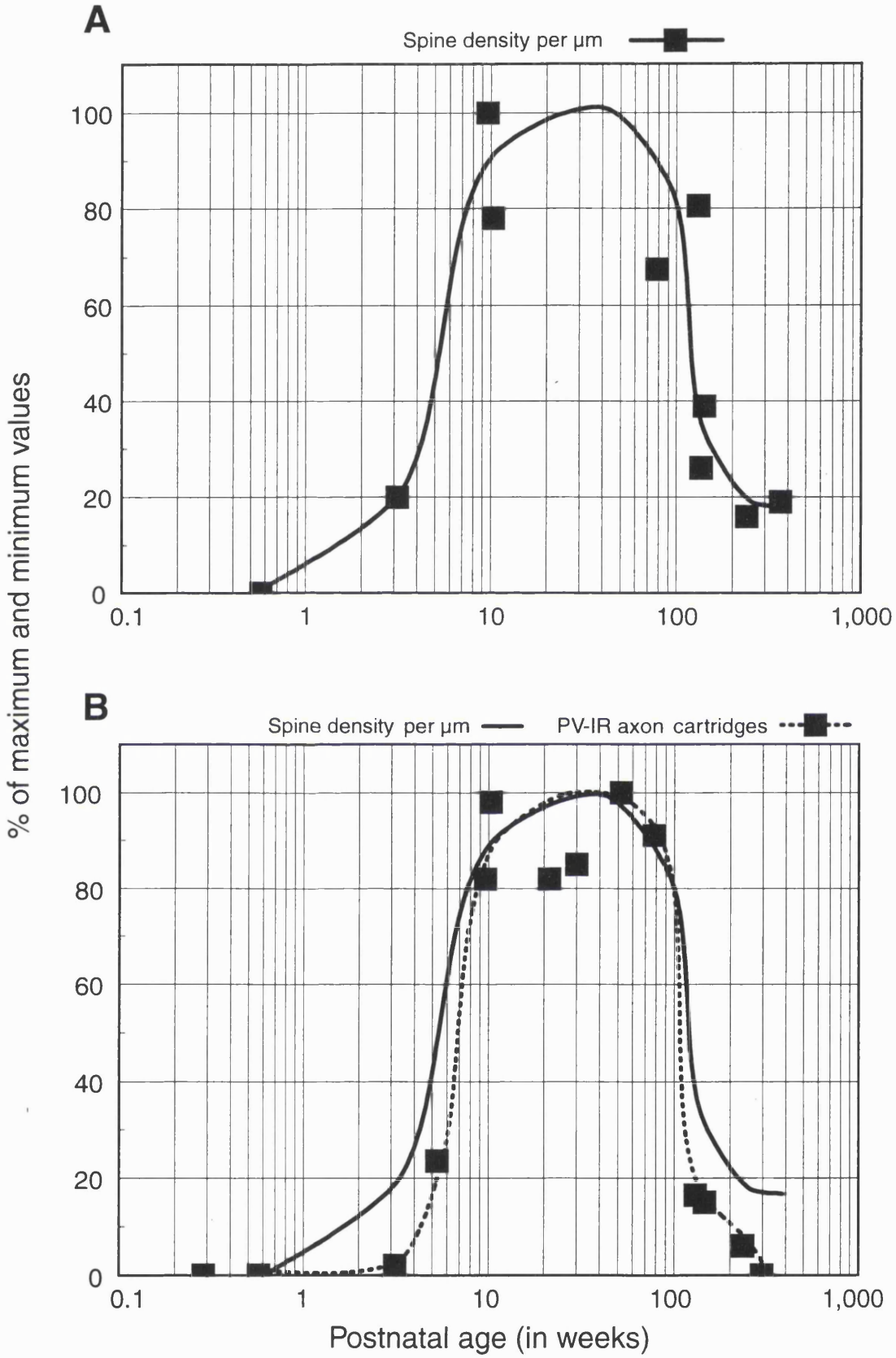

Figure 34. Schematic summary curves illustrating the percentage of maximum and minimum values for spine density on the dendrites of mid-layer 3 pyramidal neurons during postnatal development, with a comparison to the density of chandelier neuron axon cartridges in deep layer 3 which exhibit PV-IR (data from Anderson et al, 1995). **(A)** Spine density (per µm), **(B)** Spine density (per µm) and PV-IR chandelier neuron axon cartridges (per μm^2).

and basal dendrites in terms of their spine density. In the case of the apical dendrites (**in S. Anderson's work**), this was manifested in terms of a more protracted plateau phase and a later refinement of maximal spine numbers for the proximal dendritic portions (decline between 10 weeks and 1.5 years age groups) situated in mid-layer 3 (**see Figure 58C in the appendix**) relative to the remainder of the apical dendrite located more superficially in layers upper 3, 2 or 1 (**see Figure 58A and B in the appendix**). The latter portions followed the general postnatal pattern of basal dendritic spine maturation (decline between 1.5 and 2.6 years age groups).

These changes in the relative density of dendritic spines located on a particular population of pyramidal neurons in mid-layer 3 of the DLPFC during postnatal development, may be related to the maturational time course of the unique intrinsic lattice circuitry which exists in the superficial layers of this region, including mid-layer 3 - where the majority of pyramidal neurons furnishing this circuitry are found to be located (Kritzer and Goldman-Rakic, 1995; Pucak et al, 1996. The postnatal refinement during puberty of the width of intrinsic lattice stripes in the superficial layers of areas 9 and 46, formed by the distribution of clusters of anterogradely-labelled axons and terminals been reported in a preliminary study (Woo et al 1997). There appeared to be a significant difference (30% > in size) in the both the length and width of stripes in pre-pubertal compared to young adult monkeys, when tangential reconstruction's were made of axons in layers 1 and 3. In addition, a 50% loss in the numbers of varicosities and branch points of the pyramidal neurons axons was observed between the 2 age groups, demonstrating that significant changes in the intrinsic lattice circuitry of the DLPFC occurs during puberty, when overall numbers of axospinous synapses primarily associated with pyramidal neurons, are also declining.

11.2: Comparison of changes in dendritic spine density with other developmental events in layer 3:

11.2(A): Comparison with the time course of changes in density of parvalbumin immunoreactive (PV-IR) axon cartridges.

The time course of postnatal developmental changes in the inhibitory axon cartridges associated with GABAergic chandelier neurons as demonstrated by the density of PV-IR axon cartridges in mid-layer 3 can be compared to the changes in pyramidal neuron spine density in the same layer and region. These axon cartridges are constructed of a series of PV-IR varicosities forming a elongated columnar array below the unlabelled outlines of pyramidal neuron cell bodies (DeFelipe et al, 1989a; Akil and Lewis, 1992b). Comparative

immunohistochemical and Golgi studies in area 46 of monkey prefrontal cortex (Lewis and Lund 1990; Lund and Lewis, 1993) have identified these PV-IR cartridges to be the terminal portions of the axon arbours belonging to the chandelier class of inhibitory local circuit interneuron, as earlier described (Somogyi, 1977, 1979; Somogyi et al, 1982; DeFelipe et al, 1985, 1989a) to terminate on the initial axon segments of pyramidal neurons in other regions of rat, cat and monkey cerebral cortex. When observed at EM level in area 46 (Williams et al, 1992), these PV-IR axon cartridges can be seen to form symmetric (inhibitory) synapses with the axon initial segments of pyramidal neurons.

A quantitative analysis was conducted of the developmental changes in the density of PV-IR axon cartridges in the deep half of layer 3 in area 46 for a set of animals encompassing a similar age range (2 days-5.7 years) to that used in the dendritic spine study. A pattern of changes in density of PV-IR axon cartridges occurred that showed a rapid rise in numbers between the animals of 22 days and 10 weeks of age, a plateau phase present in 10-week- an 1.5-year-old animals, then a period of dramatic decline in density for the animals aged 1.5 years and 2.6 years of age and an almost entire loss of cartridges within deep layer 3 by the stage of adulthood represented in the 5.7-year-old animal.

The time course of changes in the density of chandelier neuron PV-IR axon cartridges during postnatal development, appears to follow the same time course of rise and fall (**see Figure 34B**) as that for spine density changes on their postsynaptic pyramidal cells (Anderson et al, 1995).

These events may reflect an increased activity by inhibitory inputs onto pyramidal neurons during the period when they concurrently possess elevated levels of excitatory synapses contacting their dendritic spines. That is mid-layer 3 pyramidal neurons may require greater regulatory control, by way of an increased level of release of the inhibitory modulatory neurotransmitter GABA, perhaps in order to balance the increased number of excitatory synapses. As a result, this may trigger the increasing of levels of PV, in a compensatory response to the overall increase in neuronal activity, whereby this specific calcium-binding protein can fulfil its neuroprotective role, acting to prevent - by intracellular buffering and ion transport - levels of calcium ions from rising to neurotoxic levels (Celio, 1986, 1990; reviewed by Rogers, 1989). This hypothesis (and the second one below) has been cited as possible explanations for the increased levels of PV-IR observed in layer 3 chandelier axon cartridges - known to terminate on pyramidal neuron AIS's - during the early postnatal period in DLPFC; showing a time course concurrent with that for an increase in the numbers of layer 3 pyramidal neuron dendritic spines - the sites of excitatory

synapses (Anderson et al, 1995). Likewise, both these components of DLPFC circuitry show parallel time courses during puberty when they decrease, in the case of PV-IR to levels below detectability and in the case of dendritic spines down to a level as low as that seen in the neonatal animal (Anderson et al, 1995).

11.2(B): Comparison with the postnatal maturation of dopaminergic (DAergic) axon varicosities in deep layer 3.

The density of TH-immunoreactive (IR) axons and varicosities in deep layer 3 of area 46 in the monkey prefrontal cortex has been observed to change markedly during the course of postnatal development (Rosenberg and Lewis, 1995). TH-IR and DAergic axons are distributed in a bilaminar pattern of innervation in area 46 at all ages with the highest density in layers 1-superficial 3 and a moderate density in layers 5 and 6 (Lewis et al, 1988; Williams and Goldman-Rakic, 1993). TH-IR and DAergic axons have been shown at EM level to primarily form symmetric (inhibitory) synapses with the somata and distal dendritic spines and shafts of pyramidal neurons in superficial layers of area 46 in the adult monkey prefrontal cortex (Goldman-Rakic et al, 1989; Smiley and Goldman-Rakic, 1993).

These observations have lead to the conclusion that there is likely to be close a functional relationship between the DAergic innervation and pyramidal neurons in layer 3 of the adult monkey DLPFC (Goldman-Rakic et al, 1989; Smiley and Goldman-Rakic, 1993). Correspondingly, during postnatal development it would not be surprising if there was a close relation between the time courses of maturation for pyramidal neuron basal dendritic spines and DAergic axon varicosities in layer 3 of the DLPFC.

However, a significant minority of symmetric synapses made by TH-IR varicosities have been observed at EM level associated with the distal dendrites of GABAergic interneurons in the superficial layers of lateral area 9 in the adult monkey DLPFC (Sesack et al, 1995b) which have been confirmed not to belong to the calretinin subclass of interneurons (Sesack et al, 1995a). Also, DAergic symmetric synaptic contacts have been found on the smooth, synaptically populous dendrites of presumed GABAergic interneurons (Smiley and Goldman-Rakic, 1993) in area 46 of adult monkey prefrontal cortex. Another recent EM-immunohistochemical double-labelling study of area 9 in monkey DLPFC (Lewis et al, 1996) has confirmed that TH-IR varicosities form close appositions with the PV-IR dendrites of either or both presumed chandelier or wide arbour "basket" neurons. One third of these contacts were concluded to be symmetric synapses, whilst other synapses were observed onto unlabelled dendrites in close proximity to PV-IR dendrites.

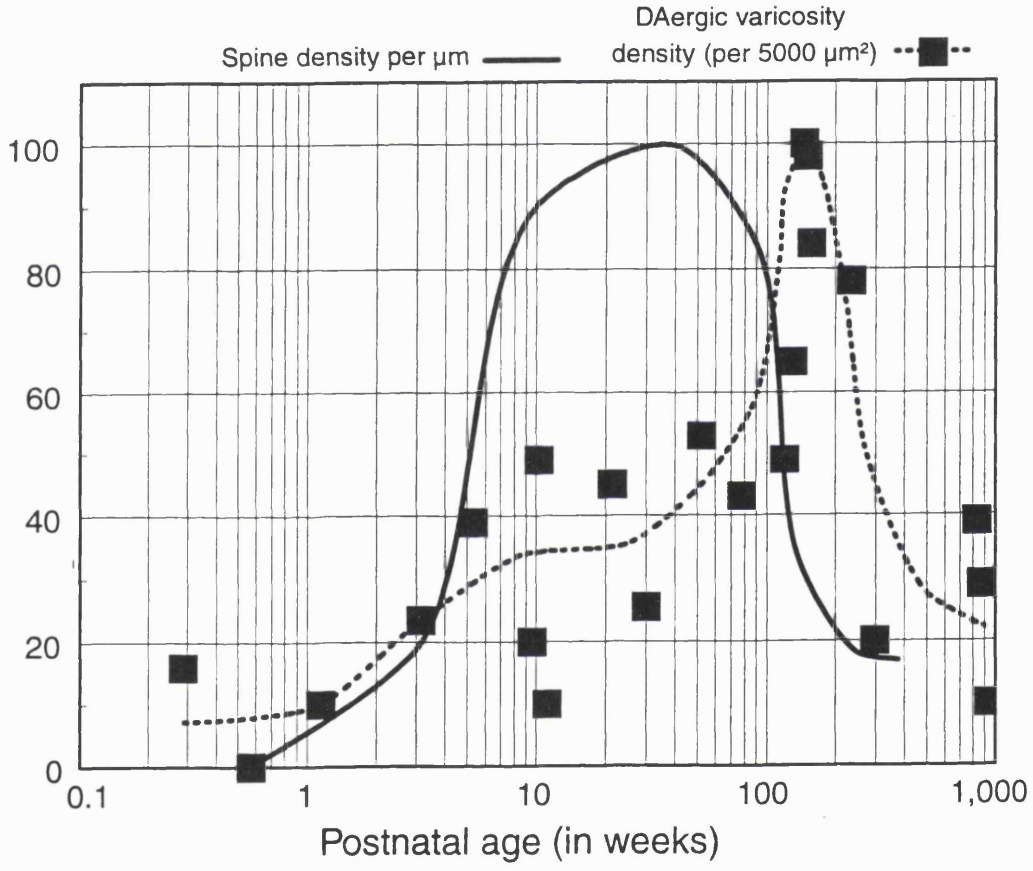

Figure 35. Schematic summary curves illustrating the maximum-minimum range of values for spine density (per µm) on mid-layer 3 pyramidal neurons, compared to the varicosity density (per 5000 μm^2) for DAergic axons in deep layer 3 (data from Rosenberg and Lewis, 1995).

The time course for the changes in the varicosity density (per 5000 μm^2) associated with DAergic axons in deep layer 3 of area 46 (from Rosenberg and Lewis, 1995) during postnatal development showed a pattern of progression which began with a small rise and plateau between birth and around 10 weeks of age, before rising considerably between 10 weeks and 2.0 years of age to reach a peak which was maintained between 2.0-3.0 years of age, before rapidly declining until a low stable level was achieved in the adult animals. The highest levels of DAergic varicosities for those animals aged between 2.0-3.0 years was found to be statistically significant compared to the levels in younger and older animals.

The time course of postnatal maturation for DAergic axon varicosities appeared to show a complex relationship (**see Figure 35**) to that for pyramidal neuron dendritic spines in layer 3 of DLPFC (Anderson et al, 1995). Firstly, between birth and approximately 10 weeks (or 2 months) of age both cortical components exhibited a rapid parallel increase in numbers, which in the case of the DAergic varicosities slowed to a less dramatic rate of growth once the spines had reached their maximum levels. High levels of spines were maintained between 10 weeks and 1.5 years of age before declining; prior to this decrease the levels of DAergic varicosities began to climb markedly once more, reaching their peak at around or just after the initiation of the down-turn in spine numbers has occurred. The levels of DAergic varicosities remained at peak values between 2.0-3.0 years, the same period during which the numbers of spines was observed to fall significantly, only once the levels of spines appeared to be slowing in their rate of decline did the numbers of DAergic varicosities begin to fall as well, so that both cellular components achieved a stable mature circuitry at about the same time in the adult monkey.

It is pertinent to mention here, that the time period over which the refinement of pyramidal neuron dendritic spines occurs, i.e. during puberty (around 3.0 years of age in the monkey) is likely to mark the crucial developmental stage for the emergence of the mature adult intrinsic lattice circuitry furnished by pyramidal neurons in the superficial layers of the DLPFC. This stage of development may be regarded as the "critical period" for DLPFC anatomical circuitry and the maturation of cardinal functions (i.e. working memory), comparable to that found in the monkey primary visual cortex and would hence be equally vulnerable to both experimental perturbation or to complex mechanisms of disease, in this case schizophrenia.

11.2(C) Comparison with the time course of maturation in asymmetric synaptic density in layer 3 of the DLPFC.

As described in detail in the pyramidal neuron review (**section 5.8**), a study has been conducted of the changes in density of synapses occurring in the different layers of area 46 during postnatal development in the monkey DLPFC (Bourgeois et al, 1994). A similar pattern of changes was observed in both the present thesis study and the Bourgeois et al (1994) study (**see Figures 23A-C in section 5.7**), with an initially rapid rise in spines or asymmetric (excitatory) synapses observed during the first 2 months or so of postnatal development, followed by a plateau period of high synaptic or spine density between 2 months and 1.5-2.5 years (spines) or 3.0 years (synapses) and finally a phase exhibiting either a gradual decline in the numbers of synapses from puberty through into adulthood (Bourgeois et al, 1994) or in the case of spines (present thesis study) a steady decline between 1.5 years of age (adolescence) and 4.6 years of age (early adulthood). The major difference between the time course of decline for spines and synapses shown by this present thesis study is that the period of decline begins earlier for the dendritic spines known to be located specifically on layer 3 pyramidal neurons than it appears to do for synapses generally located in the neuropil of layer 3 (Bourgeois et al, 1994), with no knowledge of the location of their parent cells.

The observation that synapses in layer 6 of the DLPFC did not show the same pattern of overshoot and decline in density as synapses in the superficial layers during postnatal development (Bourgeois et al, 1994), means that those synapses associated with the spines of apical dendrites passing through layer 3 which originate from layer 6 cells will contribute to the overall synaptic milieu sampled in that layer and provide an inaccurate representation of the changes occurring for pyramidal neurons whose cell body is actually present in layer 3. The majority of layer 3 pyramidal neurons are involved in providing and receiving corticocortical and corticothalamic (deep layer 3)/thalamocortical projections or they participate in intrinsic lattice connections, whereas layer 5 pyramidal neurons primarily project to sub-cortical targets such as the thalamus, superior colliculus and pulvinar etc, although they contribute 20% or more of corticocortical pathways and receive afferent input from other cortical areas. The differences between the projection targets and presumably in the functional influence of these 2 populations of pyramidal neurons, whose cell bodies and principal axon origins are located in different cortical layers, invalidates any suggestion that cell populations in all cortical layers show a concurrent time course in the maturation of their asymmetric synapses or dendritic spines. These considerations are found to be especially true, if no account has been taken of the fact that the different dendritic portions of the same

cell located in different cortical layers are likely to exhibit the same common patterns of change in the levels of their postsynaptic sites and synaptic contacts during development, irrespective of their laminar location. The only exception to this observation, seen in the work related to the current thesis study (contribution of S. Anderson) was for the different portions of the apical dendrites of layer 3 pyramidal neurons at their various levels in layers 1-3. The proximal portions of these dendrites demonstrated a slightly later attainment of their peak levels of spine density than the middle and more distal portions, thus the exact timing of the initial rise was varied, but there was a similar overall pattern of change in the amplitude of changes and a concurrence in the timing of the period of decline in spine density for all 3 portions of these apical dendrites.

The above implications along with the evidence for changes in spine density specific to layer 3 pyramidal neurons in this thesis study, show that various sub-populations of pyramidal neurons in different layers may exhibit distinct time courses of maturation both in terms of their levels of dendritic spines and asymmetric synapses during postnatal development. These changes in circuitry might correlate closely with the particular stages of emergence, consolidation and refinement of functional behaviours unique to the DLPFC, during the course of normal development in the macaque monkey. In humans, the same processes have been hypothesised to take place - albeit over a longer time scale - at the equivalent stages of postnatal development and the disruption of any one of these maturational stages may be an important clue to the underlying causes of the acute, florid symptoms (hallucinations, delusions and working memory deficits) of schizophrenia typically emerging in the late teenage years.

11.2(D) Other aspects of developing circuitry which may be relevant to the maturation of pyramidal neuron dendritic spines and the intrinsic lattice circuitry.

Extrapolation of the observations concerning dynamic biochemical changes occurring in dendritic spines during development and in adulthood (**see Section 5.9**) to the present study 1 of the thesis enables us to predict that similar phenomena may occur in the monkey DLPFC for the dendritic spines of mid-layer 3 pyramidal neurons. The 2 major forms of synaptic plasticity, i.e. long-term potentiation (LTP) and long-term depression (LTD) are triggered respectively by the opposed effects of Ca^{2+} ions flowing through NMDA activated glutamate receptor channels. LTP is thought to result from high-frequency stimulation facilitating high levels of postsynaptic NMDA receptor activation, while LTD is modulated by

low-frequency stimulation, e.g. resulting in low levels of postsynaptic NMDA receptor activation (Kirkwood et al, 1996). It is possible that the ongoing process of LTP could account for the rapid growth of spine numbers during early postnatal development (birth to 2-4 months postnatal), while during adolescence (2.5-3.0 years) and puberty (3.0-3.5 years) the conversely-acting process of LTD could provide a mechanism for synaptic activity to be "toned down" as a signal for individual excess spines and their postsynaptic contacts to be selectively detached from one another and retracted into their parent dendritic or axonal processes or perhaps engulfed by nearby glial cells. Spines and presynaptic processes which are either genetically-programmed to remain synaptically-active or which through a process of competitive inhibition via multicellular interactions (i.e. GABAergic neurons modulating pyramidal neurons and DA and 5-HT modulating both cell types) are not removed, are as a result incorporated into the mature adult cortical circuitry.

Since NMDAR1 and AMPA, AMPA/kainate and kainate receptor subunits have all been localised to various portions of pyramidal neurons in the monkey DLPFC as well as other cortical regions (**see Section 5.10**). It is likely that the activity state of these receptors plays an important role in enabling synaptic plasticity via changes in the density of dendritic spines, to occur during early development as well as in the normal mediation of excitatory neurotransmission between individual pyramidal neurons and their feedback influence on GABAergic interneurons (which also differentially express these glutamate receptors; **see section 5.10**). Observations of the involvement of NMDA receptors and non-NMDA receptors in visual plasticity in the cat and rat visual cortex provides a useful indication of what may occur in the monkey visual cortex and perhaps by a similar electrobiochemical mechanism, but with a different form of behavioural correlation (i.e. cognitive rather than sensory processing) in the monkey DLPFC.

Thus in the monkey DLPFC, plasticity of function is observed in the period of rapid synaptogenetic growth in the first 2 postnatal months and has been found to be accompanied by the ability to learn the delayed response (DR) task (Kubota, 1994). After 2 months of daily training beginning at 2 months of age, normal 4 month-old monkeys could perform with a 3 second delay on the DR task. This period of learning ability has been demonstrated to continue until around 2.5-3.0 years of age, when lesions of the DLPFC are first shown to produce profound deficits on DR task performance (reviewed in Goldman, 1972), which cannot be overcome even despite intensive retraining attempts. Infant or juvenile monkeys receiving DLPFC lesions seem to exhibit functional plasticity (Goldman, 1971) showing an initial deficit on the task, which with learning can be almost entirely reversed, so that in

adulthood they perform as well as do control unlesioned animals on a 10 second delay version of the DR task. Even lesions inflicted prenatally in monkeys (Goldman and Galkin, 1978), do not seem to prevent the emergence of DLPFC functions at their normal time in early postnatal development and their subsequent maturation at puberty, albeit in a region of cortex adjacent to that ablated.

It would appear that this contiguous region of cortex is modified at the cellular and connectional level - **see section 5.6(C)**, to enable the appropriate cellular processes of anatomical and functional development to occur, including re-routing of thalamic pathways, which would seem to be important to the success of this functional sparing. Reversible cryogenic lesioning used in infant, juvenile and peri-pubertal monkeys (Alexander and Goldman, 1978), produces significant deficits (25% more errors) on DR task performance in the animals of around 3.0 years of age (puberty), compared to only minimal effects (7-8% more errors) in the 1.5-2.0 year-old animals, while there was no observable disruption of normal levels of correct responses for the youngest animals (9 months-1.5 years of age). These cooling experiments support the hypothesis that the maturation of DLPFC function is a gradual process, which does not begin to reach its full potential until around puberty (or between 3.0-4.0 years of age), although clearly the functional ability to learn tasks is present from early in the first few months of life, but there appears to be a requirement of 2.5 years of behavioural experience and anatomical refinement before the mature functional level of performance is possible.

The observation in this thesis study that levels of dendritic spines associated with pyramidal neurons in layer 3, begin to decline in their numbers earlier in development (from 1.5 years) than the asymmetric synapses (3.0 years), for which they are the postsynaptic contacts, may correlate with the findings of the behavioural studies that a certain level of functional maturation is detectable during early adolescence (1.5-2.0 years), prior to full functional maturation after 3.0 years of age, which would coincide with the start of the decrease in synaptic density in all layers at this time. Thus developmental events occurring in layer 3 may play an especially important role in this initial phase of the functional maturational sequence of the DLPFC and act to lay the anatomical framework of the intrinsic lattice circuitry (**see section 8.1**) which will eventually become the substrate for the mature diversity of fully-fledged DLPFC functions.

In summary, the functional and behavioural maturation of the primate DLPFC would appear to closely follow certain aspects of anatomical development including the formation, stability and loss of asymmetric synapses and also the time course of pyramidal neuron

dendritic spine growth, plateau and decline in layer 3, the site of intrinsic lattice connections, the maturation of which is thought to be instrumental in the fulfilment of normal adult functional ability in the monkey DLPFC. If a similar process of overproduction, consolidation and refinement of the excitatory pyramidal neuron circuitry occurs in the human DLPFC, then disruption of these process, either prenatally and/or postnatally, would be expected to have profound effects on the subsequent ability of the individual concerned to utilise the diverse aspects of DLPFC function such as involvement in behavioural patterns, requiring the "holding in mind" ability of working memory, multisensory integration with cognitive and motor schedules, goal-direction and planning of the future. All these functions are often found in one form or another to be disrupted in schizophrenia, in patients with lesions of the frontal lobe and to a lesser and more variable degree in subjects suffering Parkinson's disease, Alzheimer's disease, epilepsy and autism.

The synaptotrophic activity of steroid hormones as observed in rat hippocampal cell cultures (**see section 5.9**), may play a similar role in the initiation and/or maintenance of the rapid increase in spine numbers observed during neonatal development in the monkey DLPFC, when the mother's hormones (having crossed via the placenta prior to birth) are likely to be still active and still of major influence to the immature offspring. In later development when the maturation and refinement of dendritic spine complement is occurring on cortical pyramidal neurons, the reverse effect might come into play by means of the sexual maturation of the animal occurring concurrently with spine loss, when the levels of different intrinsic hormones are in a state of change, so that the most prevalent hormone would act with deleterious effects on spine density together with NMDA (LTD) mechanisms. There is also evidence to support hormonally controlled up-regulation of synapse numbers in adult animals (**see section 5.9**) as demonstrated by changes in sizes and types of presynaptic axon varicosity and axospinous synaptic interactions in the hippocampus of ovariectomised female rats.

As mentioned in **Table 1** in the **Methods section 6.0,** several of the monkeys used in the study had previously undergone castrations for use in unrelated endocrinological studies. Examination of the data for the Spine study, showed that these animals did not appear to exhibit levels of spine density, dendritic length or degree of branching, outside the normal range of values either for the basal (thesis study) or apical (S.A. Andersen contribution) dendrites of layer 3 pyramidal neurons. For example, the castrated animals in the 2.6 years and 4.5 years age groups (**see Figures 33A and B**), possessed relative mean spine densities which were well within the overall range of values for the other animals in those age

groups. Therefore, we draw the conclusion from these observations, that there is little evidence to suggest that gonadal hormones have a significant influence over the changes in spine density which we have observed for layer 3 pyramidal neurons in the monkey DLPFC in this study. However, in view of the findings of sex differences for several aspects of development in the literature for both rodents and monkeys, larger samples of animals and a comparison of values for both sexes across postnatal development (which was not possible in this thesis study, due to lack of age-matched males and females) need to be conducted before this issue can be resolved satisfactorily

11.3: Final conclusions.

Thesis study 1, has examined the time course of development for dendritic spines on a population of pyramidal neurons in mid-layer 3 of the monkey DLPFC, as part of a wish to define the parameters of anatomical and presumably functional maturation in this important cortical region in primates. The study's findings indicate that the sequence of spine growth, stability and decline is intimately related to the presence of high densities and rapid acquisition of spines in the infant animal, consolidation of these high levels in the juvenile stage followed by a steady loss of spines from adolescence and through puberty, so by early adulthood low numbers of spines characterise the anatomical structure of the mature primate DLPFC.

Also, it was shown that the time course of changes in spines closely follows that for one form of inhibitory input that is known to contact pyramidal neurons in this layer, namely PV-IR chandelier neuron axon cartridges; whose levels of immunoreactivity for PV follow almost exactly the same amplitude and time frame of development as that for the density of dendritic spines.

The maturational development of pyramidal neuron dendritic spines in mid-layer 3 of the DLPFC was compared with the postnatal development of DAergic axons and varicosities in the same layer and a striking correlation was found to be shown by both markers. There appeared to be an intimate relation between the period of greatest rate of spine growth and raised DAergic activity (indicated by moderately increased levels of varicosities and axons between birth and 10 weeks of age). The rise in the density of the DAergic innervation in layer 3, continued during the period of highest spine density and then just prior to the decline in spine number, there was another rapid climb in the levels of DAergic axons and varicosities, whose peak levels coincided with the loss of spines and DAergic axons only decreased in density once spine number had matured to low adult levels.

Finally, we compared the time courses for dendritic spines and asymmetric

synapses in layer 3 and found that there was a coincidence for both markers of pyramidal neuron maturation in the first half or development, i.e. from birth to about 1.5 years, whereby both exhibited a rapid increase in their numbers in the first 2 postnatal months or so, which was maintained for spines until 1.5 years of age and for the synapses until 3.0 years of age. Since, the measures for excitatory synapses were not strictly limited to pyramidal neurons, nor to those with their cell bodies in layer 3 (layer 5 apical dendrites included), while spine density measures were restricted on both these counts, this could help explain the discrepancy between the 2 closely-linked quantities during the second half of their developmental time courses, although there might also be a genuine time-lag in the shedding of excitatory synapses compared to that for their postsynaptic sites on pyramidal neuron dendrites.

Therefore, Study 1 of this thesis has demonstrated by comparison with other data in the literature, for the same layer of the same region, that pyramidal neuron dendritic spine development in layer 3 during the postnatal period in the monkey, is closely related to the development of PV-IR inhibitory contacts on the same pyramidal neurons and also to DAergic axons which are known to contact both pyramidal neuron dendritic spines and shafts as well as PV-IR (GABAergic) interneurons in adult monkeys, whose axons terminate in the PV-IR axon cartridges which contact the axon initial segments of pyramidal neurons - again in adult monkeys. These closely related time courses are not surprising in view of the apparent synaptic relationships between these 3 cortical components of layer 3 circuitry in the adult monkey DLPFC, but the anatomy of these synapses has not yet been examined in developing animals. It thus remains to be seen whether there is in fact a direct functional synaptic mechanism which exists to co-ordinate events between these components or whether it is simply due to the common action of trophic factors or large scale "volume transmission" release of DA, GABA and glutamate, acting at DA (expressed on pyramidal cells and PV-IR neurons), GABA (on pyramidal cells and interneurons) and NMDA/non-NMDA receptors (on pyramidal cells and interneurons), respectively.

All of the issues discussed here are of major importance to the understanding of the normal time course of development in the DLPFC of the macaque monkey, which at the beginning of this thesis study we proposed as an animal model for the DLPFC in the human brain (many of the cortical anatomical similarities between the two species have been covered in the review sections). In this regard, it is likely that the disruption at any time-point of such impeccably synchronised time frames for the development of the 4 (spines, PV-IR cartridges, DAergic axons and asymmetric synapses) markers of layer 3 cortical circuitry in the DLPFC which we have examined and compared in this thesis study, would lead to an

exceptional disturbance of the normal structure of anatomical circuitry and patterns of functional behaviour in adult life, as would seem to be exhibited in schizophrenic subjects.

We shall see in the next part of the thesis (Study 2; **sections 12.0, 13.0 and 14.0**) how the time course of development for another monoaminergic (like dopamine) neurotransmitter, serotonin, in layer 3 of the monkey DLPFC, may be related to the changes in spine density and the other components of the cortical circuitry examined in study 1 of the thesis. There will also be further discussion concerning the possible disruption of these maturational events in humans and their implication for the aetiology of schizophrenia (**see General Discussion section 15.0**).

12.0: Study 2. A quantitative immunohistochemical study of the postnatal development of 5-HTergic axons in mid-layer 3 of the ventral bank of area 46 in the monkey.

12.1: Introduction.

This study examines the maturation of the serotonergic innervation of layer 3 in the ventral bank of area 46 in the dorsolateral prefrontal cortex of the macaque monkey during postnatal life. We chose to examine the development of the serotonergic innervation in mid-layer 3 for this study, because it is the location of important intrinsic excitatory connectivity between pyramidal neurons and many of its pyramidal cells are the major source of corticocortical connections to other regions of the brain. Previous studies by our laboratory (**study 1 in this thesis**) had examined the postnatal development of other components of the cortical circuitry in layer 3 and we wished to compare how the time course of the mid-layer 3 serotonergic innervation might relate to these other developmental events.

In this study we used a quantitative analysis to examine whether there were significant changes in the density of the mid-layer 3 serotonergic innervation in the ventral bank of area 46 (visualised using a 5-HT-specific antibody) during the course of postnatal development. The study makes use of measures of total axon length (per 5000 μm^2), varicosity density (per 5000 μm^2) and varicosities per mm of axon to evaluate the degree of anatomical maturity at various ages, from birth into middle adulthood, for the overall population and for thick and thin varieties of 5-HTergic axons. These quantitative analyses are then used to reconstruct the time course of development for the 5-HTergic axon innervation in mid-layer 3 of the DLPFC. This time course is then related to the known functional roles of the serotonergic system during development and its interactions with the other anatomical circuitry and receptors in the prefrontal cortex of both adult and developing monkeys as well as for other species and other brain regions.

We also wished to establish whether the maturational time course of 5-HTergic axon development in mid-layer 3 was the same as or distinct from the time course of maturation for dendritic spines on Golgi-impregnated pyramidal neurons in mid-layer 3 of areas 9 and 46 (**study 1 in this thesis**; Anderson et al, 1995). In addition we wished to determine whether the time course of any changes in the 5-HT innervation during postnatal development, occurred in alignment with changes previously observed for other neurotransmitter-containing axons or chemically-defined neuronal populations, using quantitative immunohistochemistry, e.g. dopaminergic axons (Rosenberg and Lewis,1995), and PV-IR axon cartridges (Anderson et al, 1995).

It seemed especially important, in view of the variation in the density of 5-HT innervation across the monkey cerebral cortex and in different layers within a given area (Takeuchi and Sano, 1983; Berger et al, 1986, 1988; Morrison and Foote, 1986; Hornung et al, 1990; Wilson and Molliver, 1991a; reviewed by Foote and Morrison, 1987a) to investigate how the serotonergic innervation of a particular PFC area develops during the postnatal period and within that area, to examine closely the time course of maturation for a specific layer - in this case layer 3 - since each cortical laminae contains neuron populations with distinctive morphological and immunohistochemical characteristics as well as unique functional attributes and intrinsic and extrinsic anatomical connectivity.

Serotonin acting via its many receptor subtypes, has been implicated in many diverse functional aspects of cortical and subcortical processing (reviewed in Spoont et al, 1992; Sirviö et al, 1994; Cassel and Jeltsch, 1995; Buhot, 1997), including associative learning (marmoset: Harder et al, 1996; rat: Meneses and Hong, 1997), spatial working memory (human: Grasby et al, 1992; rat: Buhot et al, 1995; Herremans et al, 1995; macaque monkey: Williams et al, 1996), visual recognition memory (squirrel monkey: DeNoble et al, 1991) and object discrimination (marmoset: Carey et al, 1992). Of particular relevance to Study 2 of the thesis are the observations of Williams et al (1996) in the DLPFC of the macaque monkey. In this study, the authors examined the effects of the 5-$HT_{2A/2C}$ receptor antagonist ritanserin by iontophoresis on the firing properties of neurons in the DLPFC during the performance of the ODR task (a test of spatial working memory function; **see Functional review section 4.0 for details**). The overall activity of pyramidal neurons was shown to be reduced for 57% of recorded task-related cells, 75% of which exhibited memory fields and 14% of recorded task-related cells increased their firing activity in response to the antagonist, all of which demonstrated inhibitory activity during the delay period. This kind of modulatory action by serotonin probably via a restricted number of synapses and also by way of 5-HT receptors

located on GABAergic interneurons, supports the extensive evidence in clinical studies with various antipsychotic drugs in schizophrenic humans, that 5-HT via its receptors can act to mediate cognitive behaviour in regions such as the DLPFC in primates. Abnormal alterations in the 5-HT receptor expression or in the density of the 5-HT innervation in the DLPFC triggered during the course of their maturation during postnatal development, may be an instrumental part of the complex pathophysiology which generates the diversity and extent of the cognitively-disabling, delusional and hallucinatory symptoms commonly found in schizophrenic patients.

To our knowledge, this is the first quantitative immunohistochemical study to examine the postnatal development of 5-HTergic axons in the macaque monkey cerebral cortex. Qualitative studies have been conducted previously of the postnatal development of the 5-HTergic innervation in the cerebral cortex of the marmoset monkey (Hornung, 1992a) and in the primary visual cortex (area 17 or V1) in the macaque monkey (Foote and Morrison, 1984; reviewed in Morrison et al, 1984; Foote and Morrison, 1987b). Biochemical studies have been carried out for the tissue levels of serotonin and its breakdown-product 5-HIAA in blocks encompassing the entire PFC in developing and ageing macaque monkeys (Goldman-Rakic and Brown, 1981, 1982), but not for area 46 or the DLPFC specifically. This is despite the fact that moderate differences were seen between the tissue concentrations and *in vivo* synthesis rates of 5-HT in the dorsolateral and the orbital prefrontal cortices of adult monkeys in a previous study by the same group (Brown et al, 1979) i.e. their use of total PFC block tissue samples may have obscured a variability in the time course of changes occurring within different regions of the PFC during postnatal development.

12.2: Materials and Methods.

12.2(A): Animals.

This study includes analysis of tissue from 18 macaque monkeys, including many of the same animals used previously in the pyramidal neuron dendritic spine density study, (**see Table 1 for details**), thus giving the opportunity for within-animal comparisons between the two studies.

Eighteen rhesus monkeys (*Macaca mulatta*) of both sexes, covering an age range from 4 days postnatal to 16.7 years, were used in this study. Sixteen of the animals had undergone no prior experimental procedures. The 2.3-year-old (Rh127) and 4.5-year-old (Rh119) males were castrated at between 6-10 days after birth. The 3.0-year-old (Rh145) male had received 2-4 injections of gonadotrophin releasing hormone (GnRH)

over a period of time, the final injection being given not less than 8 months prior to perfusion as part of another study. In previous studies of prepubertal monkeys that have been through the same procedure, it is clear that even following protracted hypothalamic GnRH neuronal stimulation, discontinuation of that stimulation usually leads to a resumption of the animals original stage of sexual development (Gay and Plant, 1987, 1988). This was confirmed from 4 weekly measures of morning and evening plasma testosterone sampled just before perfusion. It was thus found that the 3.0-year-old had a level of testosterone secretion, characteristic of late puberty (which was appropriate for its calendar age, i.e. it was a normal monkey - see Rosenberg and Lewis, 1994, 1995 for further details). We could find no evidence to suggest that the procedures had altered any aspect of the development of the 5-HTergic system in these animals.

Animals were deeply anaesthetised with ketamine hydrochloride (25 mg/kg, intramuscularly) and pentobarbital sodium (30 mg/kg, intraperitoneally) and then perfused transcardially with cold 4% paraformaldehyde in phosphate buffer (buffer pH = 7.4) as described previously (Noack and Lewis, 1989, Anderson et al, 1995, Rosenberg and Lewis, 1995). The brain was removed immediately and the left frontal lobe cut into coronal blocks 3-5 mm thick. Tissue blocks were immersed in the same fixative for 6 hours; washed in a series of cold, graded sucrose solutions; and then sectioned (40 μm) on a cryostat. Tissue for the present study was obtained from stored sections of these animals which were stored in ethylene glycol as a cryoprotectant at -20 degrees C immediately subsequent to sectioning.

Appropriate sections which included (Walker's area 46, principal sulcus region) were chosen with the aid of a 1-in-4 series of interleaved Nissl-stained sections prepared immediately subsequent to sectioning. The rostral-caudal position of the sections was chosen to coincide with a region between the appearance of the caudate and putamen caudally and the start of area 10 rostrally. Stored sections from the 2.3-year-old (Rh127) animal were taken from the right frontal lobe due to unavailability of sections from the left frontal lobe.

12.2(B): Immunocytochemical procedures.

Before any immunocytochemical procedures the sections were removed from the ethylene glycol storage solution, allowed to warm to room temperature before further processing and then given six 3-minute washes in phosphate-buffered saline (PBS). Sections were then pre-treated for 30 mins at room temperature on a shaker with PBS containing 0.3% Triton X-100 and 450 ml normal serum per 10 ml of solution. Since the secondary antibody was raised in goat, goat normal serum was used. For the primary antibody

stage, the pre-treatment solution was poured off and the sections were given a further six 3-min washes, before being incubated for 24-48 hours at 4 degrees centigrade in PBS containing 0.3% Triton X-100, 0.5 mg/ml bovine serum albumin (BSA), 300 ml normal serum per 10 ml of solution and a rabbit anti-5-HT antibody (diluted 1:8000).

The anti-5-HT antibody (obtained from Incstar Corp, Stillwater, MN) was generated in rabbit serotonin conjugated to BSA with paraformaldehyde. The serotonin molecule identified by the antibody was 5-HT creatinin sulphate provided by Sigma. This antibody has been previously shown to specifically recognise 5-HT in studies of rat (Barr et al, 1987; McClean and Shipley, 1987a,b) and monkey (Smiley and Goldman-Rakic, 1996) brain. For the secondary antibody stage, the primary antibody solution was poured off and the tissue washed 3 times, 8 mins each time. The secondary antibody solution was used to incubate the sections at room temperature for 1 hour, consisting of PBS, 0.3% Triton X-100, 300 ml normal serum per 10 ml solution and 1 drop vectastain biotinylated antibody per 10 ml solution. Sections were then processed with the avidin-biotin method of Hsu et al (1981), using a standard Vectastain ABC kit (Vector Laboratories, Burlingame, CA) and diaminobenzidine (DAB). After the DAB reaction, sections were mounted on subbed (gel-coated) slides and cover-slipped with TTX.

To control for potential variability of immunocytochemical staining between separate experiments, sections from all the animals were processed together, three sections from different animals were placed in each reaction compartment, in order to ensure equivalent exposure to the antibody and hence eliminate age-specific processing bias. In a pilot study, sections from animals of 3 widely spaced ages (2 days, 1.5 years and 16.7 year) were reacted together. Different sets of sections from each animal were tested at 3 different dilution's of the anti-5-HT antibody in order to determine the optimum dilution at which to use for the main experiment. The ideal dilution of antibody was determined to be between 1:6000 and 1:12000, thus a compromise of 1:8000 was settled on for optimum staining intensity of both 5-HT axons and uniformity of background neuropil staining, indicating an equivalent uptake of antibody throughout the tissue section. Two complete sets of sections from all the animals were then reacted in separate experiments, in order to control for variability in the absorption of the anti-5-HT antibody. There was found to be an overall difference in intensity of staining between the 2 reacted series' of sections. Thus for the quantitative analysis, sections from different animals were only used from the more intensely stained reaction series.

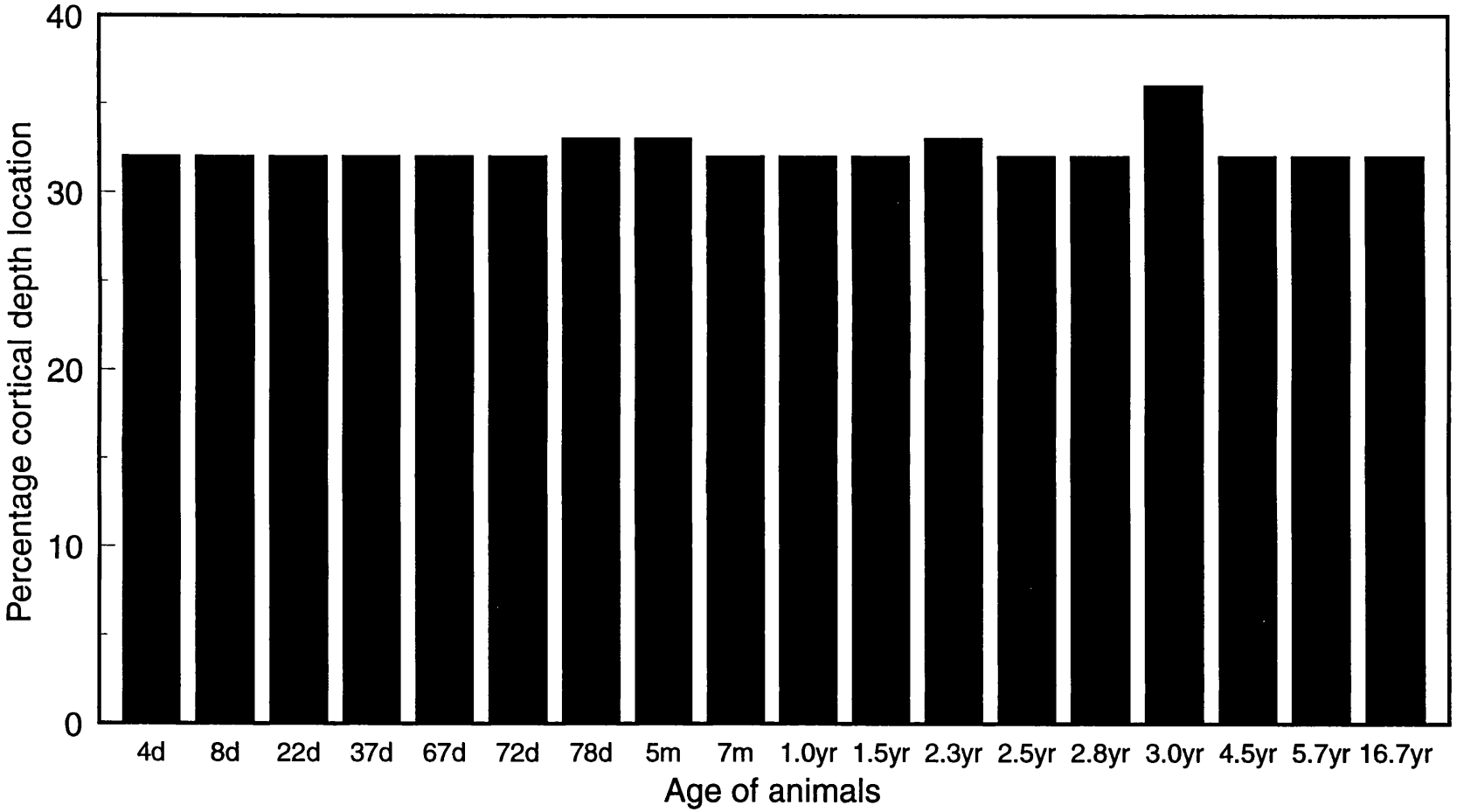

Figure 36. A bar plot illustrating the cortical depth location (as percentage of cortical pia-to-white-matter distance), for each animal age, of the topmost edge of the sampling box (100μm wide by 50μm depth) within which tracings were constucted of 5-HTergic axons (3 boxes per animal) in mid- layer 3 of the ventral bank of the principle sulcus (area 46). The plot shows that there was minimal variation between the locations of the 5-HTergic axons for different ages, with the topmost edge of tracing at all ages located within a cortical depth of between 32-36%, so the 5-HT axons would be at the equivalent percentage depth as the basal dendritic fields of the mid-layer 3 pyramidal neurons in the spine study.

12.2(C): Quantitative analyses.

The laminar locations of 5-HT immunoreactive (IR) axons in Walker's area 46 were ascertained by referring to the Nissl-stained sections mentioned previously, which occupied comparable (to within a few sections) rostral-caudal positions in the brain. Variations in the density of 5-HT-IR axon processes and varicosities across development, were determined by computer-tracing the labelled structures using the Eutectic Neuron Tracing System (Eutectic Electronics, Inc, Raleigh, SC). Three reconstruction's of 5-HT labelled axon processes were made in mid-layer 3 of area 46 in the ventral bank of the principal sulcus in each animal. Tracings were located at a position which represented a consistent percentage of the cortical depth, determined in all Nissl-stained sections to be reliably within mid-layer 3. This percentage depth, 32-36% (**see Figure 36**) was comparable to the 31-33% of cortical depth which represented the range of locations of mid-layer 3 pyramidal neuron cell bodies examined in Golgi study 1 (Anderson et al, 1995, **see Figure 28**) and similarly the locations of pyramidal neurons in Study 1 of this thesis.

Each tracing reconstructed the extent of all the axons and marked all the varicosities along those axons, located within the confines of a rectangular line-image, 50 μm high by 100 μm wide, which was superimposed over a bright-field image of the 5-HT-IR stained section at a total magnification of 630x. Three outlined reconstruction's were traced for each layer in each animal and the three outlines were positioned 100 μm apart in mid-layer 3 so as to avoid overlap in the reconstruction's. Since it was only practical to trace a very limited area of tissue in this study, three separated sampling areas were judged to give a more accurate representation of axon length and varicosity density in each layer than tracing within 3 contiguous outlines placed end-to-end. This was important since the axon processes were observed to be unevenly distributed across the lateral extent of layer 3, a clustering effect was often seen in some parts of the layer, producing alternately dense and sparse patches of 5-HT innervation. By spacing the sampling areas some distance apart, it was hoped to overcome tracing just low or just high density patches and to achieve an overall representative density measurement.

The criterion used for an axon varicosity was: an enlargement of the diameter of a fibre which was bordered by a smaller calibre intervaricose segment on at least one side, but preferably on both sides (Oeth and Lewis, 1993). The total 5-HTergic axon length was calculated for each box (per 5000 μm^2), by summing the lengths of individual axon processes. Likewise, the total density of 5-HTergic varicosities (per 5000 μm^2) was found for each box

and from these two measures a third could be quantified, i.e. varicosity density/ total axon length (in μm) = varicosities per μm of 5-HTergic axon length. The results were then presented in terms of total axon length (per 5000 μm^2), density of varicosities (per 5000 μm^2) and varicosities per μm of axon length, respectively, for each reconstructed box area. A mean value for all three parameters was calculated from the 3 box reconstruction's traced per animal. These measures provided a means of quantifying the postnatal maturation of the 5-HT innervation within mid-layer 3 in area 46 of the monkey dorsolateral prefrontal cortex. All measures were conducted in sections from animals of different ages, which were processed together in the same immunohistochemical reaction. The 5-HT axon innervation reconstruction's were made on coded slides, such that the age of the animal was unknown to the investigator at the time of tracing.

12.2(D): Morphological criteria for 2 distinct classes of 5-HTergic axons.

To establish whether there may be changes during postnatal development in the proportions of 2 different classes of 5-HTergic axons, every effort was made to assign each 5-HTergic axon in the analysis to one or other of two main groups, i.e. the thick or thin axon classes. This was achieved by evaluating the size and shape of the varicosities, the calibre of the intervaricose segments and the overall impression of the thickness of each individual 5-HTergic axon in relation to those others surrounding it in the neuropil. This judgement was made for the convenience of the analysis and also on the basis of the previous observations in the literature of 2 populations of varicose 5-HTergic axons in adult animals (**see Serotonin review section 7.0, for background and references**). The other possibilities are that there may be more than two populations of varicose 5-HTergic axons or alternatively these morphological differences may be the manifestation of temporally differential maturational changes occurring within a single 5-HTergic axon population.

The choice to quantitatively evaluate the total 5-HTergic axon sample as the two separate thick and thin 5-HTergic axon sub-populations, made on the basis of their different morphological characteristics, was made despite the fact that the postnatal time courses of the varicosity density (per 5000 μm^2) for each appeared very similar. The 2 sub-populations of 5-HTergic axons were also present in the tissue examined in the present thesis study. As shown in the **Results, sections 13.1(C)(i), (iv) and (vi)**, we quantitatively evaluated the contribution of each fibre type on the basis of its morphological characteristics.

However because of the apparent heterogeneity of many 5-HTergic axons it was often difficult to assign them categorically to one type or another, so in order to justify

presenting the results for each type separately we decided to conduct a further statistical analysis comparing the concurrence or distinctions of the time courses for each 5-HTergic axon type.

12.2(E): Statistical analyses.

The statistical significance of changes across postnatal development in terms of total axon length for 5-HTergic axons, the density of 5-HTergic varicosities and the number of varicosities per μm of axon length, were all determined for the total 5-HTergic population in mid-layer 3 of prefrontal cortical area 46, as well as specifically for the morphologically distinguishable thick and thin types of 5-HTergic axons that make up this population. The non-parametric Kruskal-Wallis test was used to examine the statistical significance of changes in the 5-HTergic innervation over postnatal development. Between-group comparisons for age were carried out using the Bonferroni test.

13.0: Results. Study 2. A quantitative immunohistochemical study of the postnatal development of 5-HTergic axons in mid-layer 3 of the ventral bank of area 46 in the monkey DLPFC.

13.1(A): Morphology of 5-HTergic axons.

Three morphologies of 5-HTergic axons were observed throughout area 46 of the macaque monkey prefrontal cortex for each of the different ages examined, in agreement with previous observations in various regions of the adult rat, cat, ferret and primate cerebral cortex (Lidov et al, 1980; Mulligan and Törk, 1987, 1988; Blue et al, 1988; De Lima et al, 1988; Wilson et al, 1989; Hornung et al, 1990; Mamounas et al, 1991; Voigt and De Lima, 1991a; Wilson and Molliver, 1991a; Mulligan and Törk, 1993; Smiley and Goldman-Rakic, 1996; reviewed by Kosofsky and Molliver, 1987). The first variety of axon was termed the "thick" or "beaded" class of 5-HTergic axon and was characterised by large bead-like (round) varicosities interlinked by fine intervaricose segments. Secondly, there were the "thin" or "fine" class of 5-HTergic axon which was distinguished by its generally smaller, pleomorphic (many-shaped) varicosities and fine intervaricose segments. The third kind of axon (not quantified in this study) was termed the "thick non-varicose" type of 5-HTergic axon, on account of its lack of varicosities and very thick smooth appearance; they are presumed to represent the parent or pre-terminal trunks of the varicose terminal 5-HTergic axons i.e. the thick and thin types of 5-HTergic axons.

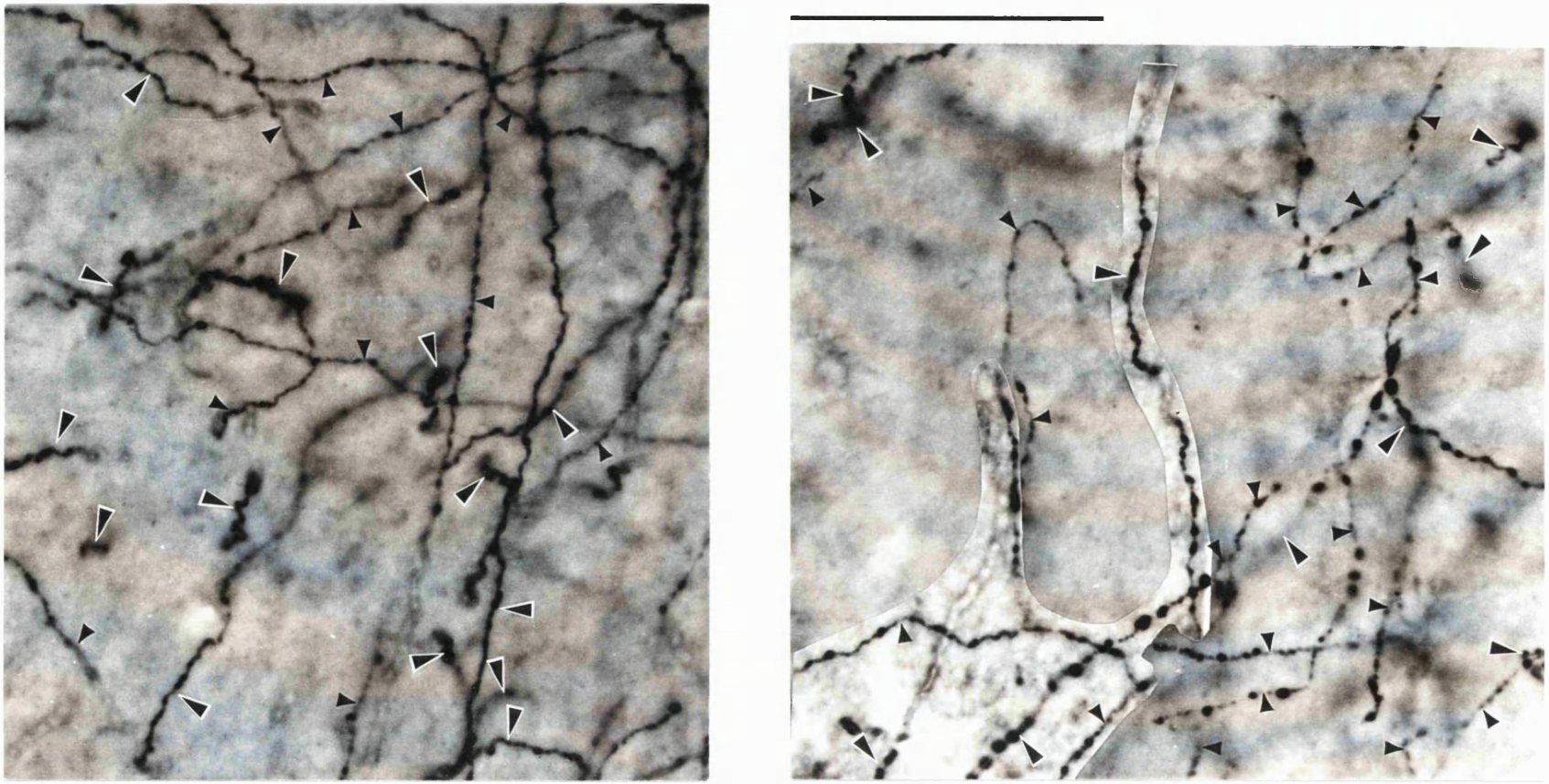

Figure 37. Bright-field photomicrographs, showing examples of the thick (large arrowheads) and thin (small arrowheads) types of 5-HTergic axon in area 46 of the monkey DLPFC at various ages during postnatal development: **(A)** 8 day-old animal, **(B)** 67 day-old animal. Scale bar represents 50 μm.

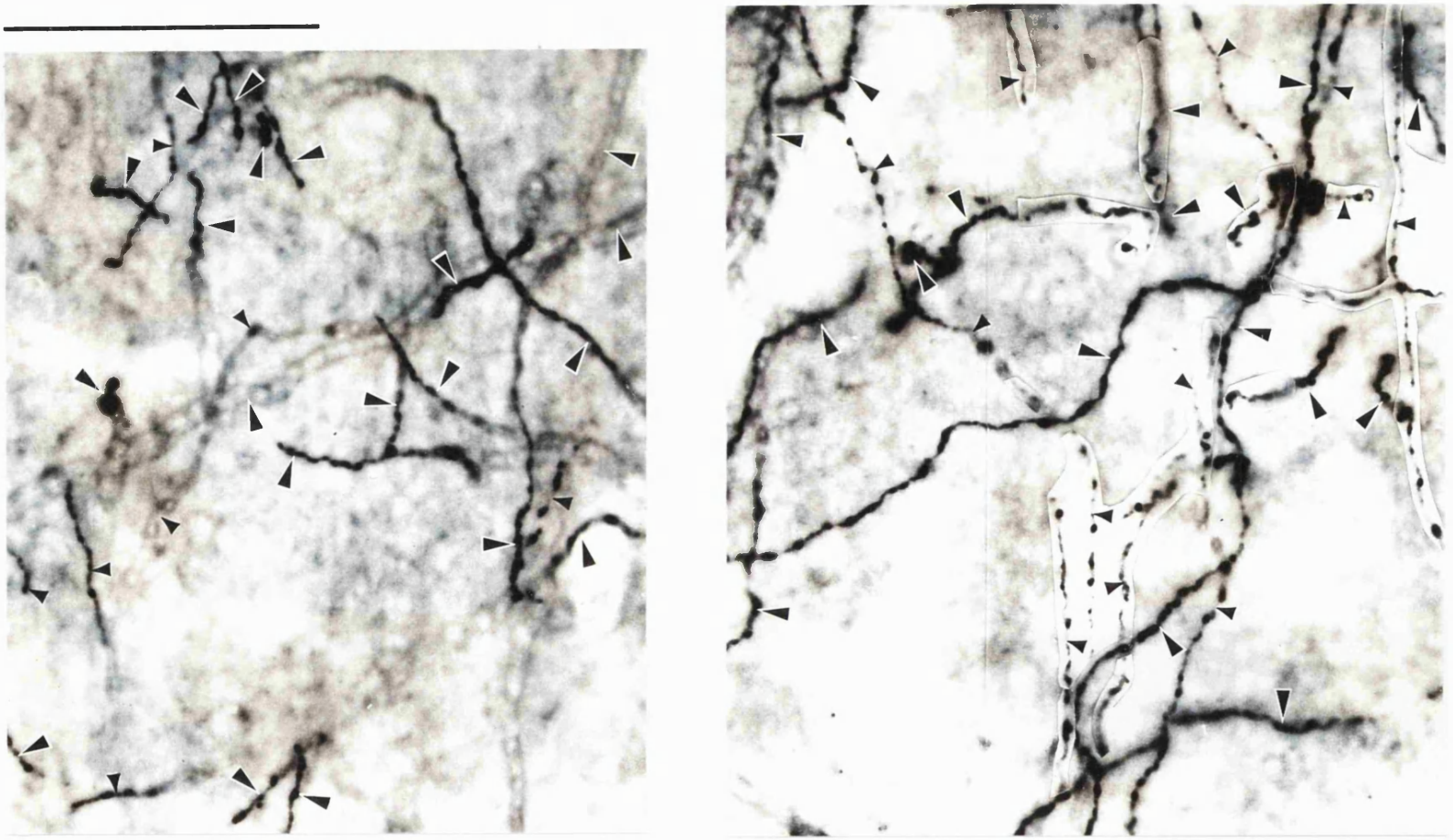

Figure 37. Bright-field photomicrographs, showing examples of the thick (large arrowheads) and thin (small arrowheads) types of 5-HTergic axon in area 46 of the monkey DLPFC at various ages during postnatal development: **(C)** 5 month-old animal **(D)** 1.5 year-old animal. Scale bar represents 50 µm.

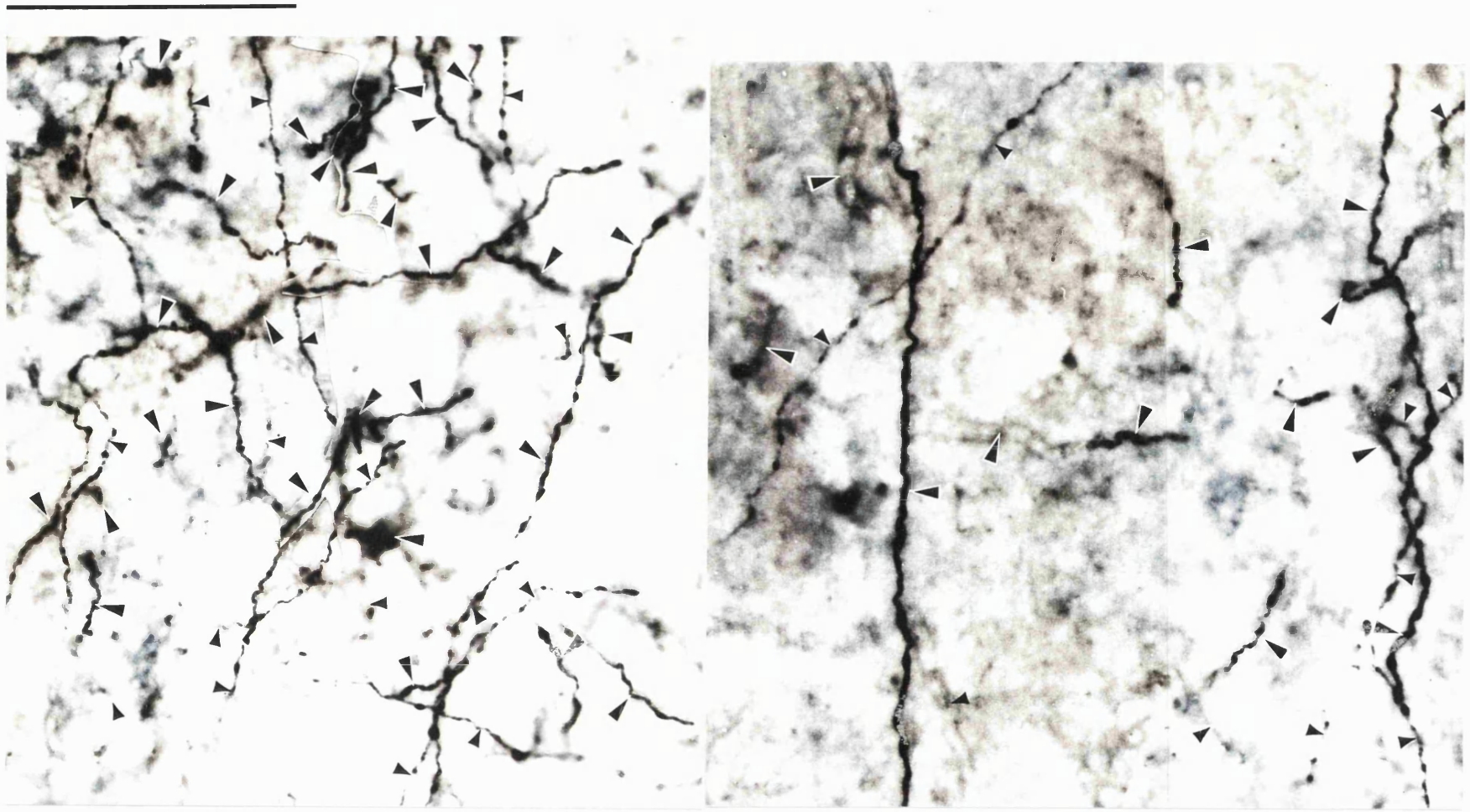

Figure 37. Bright-field photomicrographs, showing examples of the thick (large arrowheads) and thin (small arrowheads) types of 5-HTergic axons in area 46 of the monkey DLPFC at various ages during postnatal development: **(E)** 2.5 year-old animal **(F)** 3.0 year-old animal. Scale bar represents 50 μm.

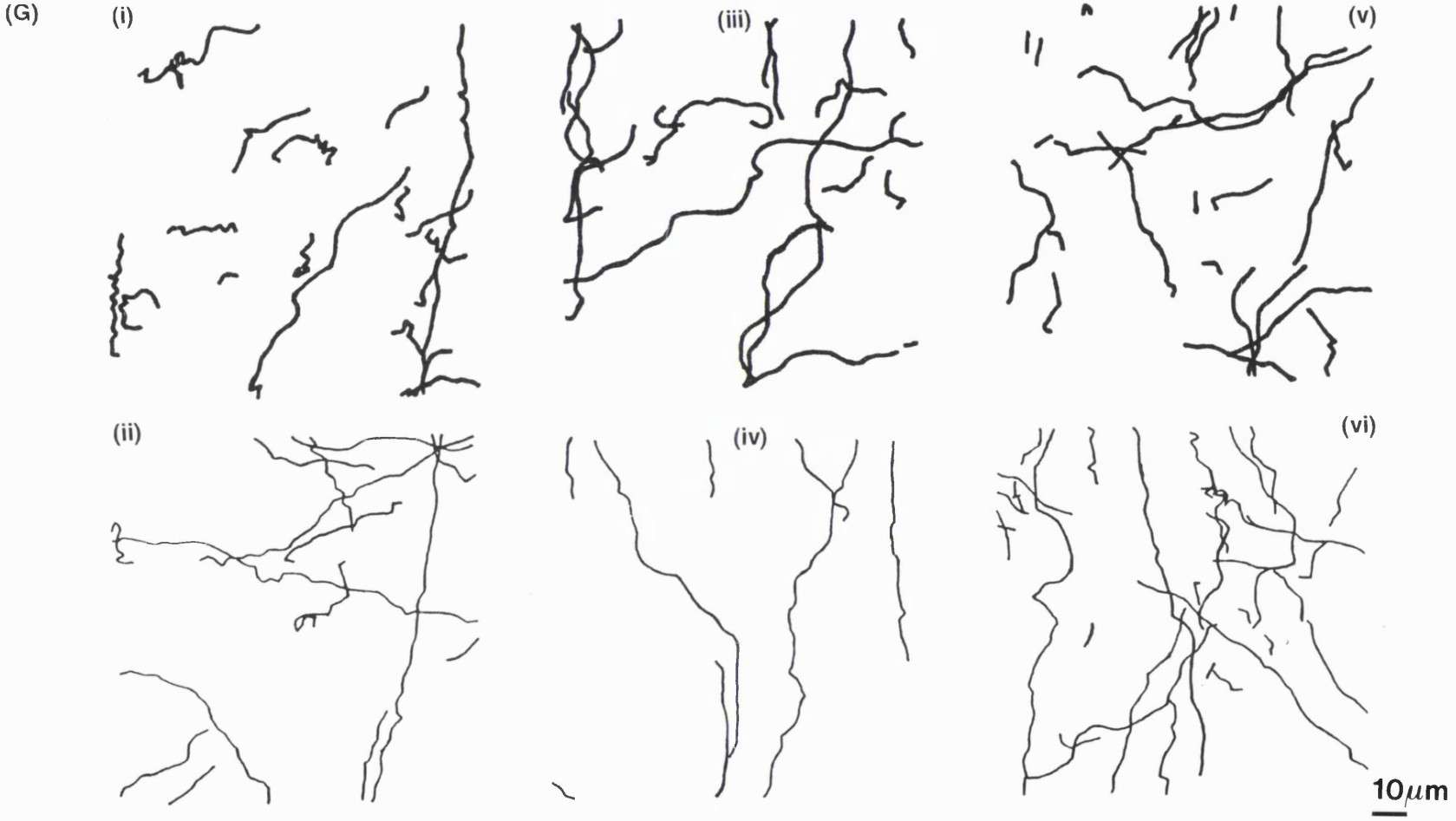

Figure 37. Illustrations of thick and thin varieties of 5-HTergic axons in area 46 of the monkey prefrontal cortex at various stages of postnatal development. **(i)** thick and **(ii)** thin 5-HTergic axon in an 8-day-old animal; **(iii)** thick and **(iv)** thin 5-HTergic axons in a 1.5-year-old animal and **(v)** thick and **(vi)** thin 5-HTergic axons in a 2.5-year-old animal. N.B. these tracings represent reconstructions of axons seen in photomicrographs: **(A), (D) and (E),** respectively.

As commented in a previous study of adult macaque monkey prefrontal cortex (area 46) at the light and electron microscope level (Smiley and Goldman-Rakic, 1996), the distinction between the first and second varieties of 5-HTergic axon were not always clear-cut. Their morphology seemed to form a continuum, ranging from the characteristics of the thick axons through to those of the thin variety, with many 5-HTergic axons being of intermediate morphology combining aspects of both sets of morphological criteria. For example, a single 5-HTergic axon process with large beaded varicosities may sometimes be observed to become finer and exhibit smaller pleomorphic varicosities further along its extent. This continuum of 5-HTergic axon morphologies was particularly evident in the tissue of the many immature animals examined in the present study, suggesting that perhaps the characteristics of the thick and thin 5-HTergic axon varieties develop over time, but even in the adult animal their morphological distinction is not always absolute.

13.1(B): Qualitative observations of 5-HTergic axons in mid-layer 3 .

All sections of monkey PFC which were reacted for 5-HT immunohistochemistry were initially examined without knowledge of the age of the animal; then later, after quantitative data had been obtained, they were again observed now arranged in order of ascending age, in order to form a qualitative impression of the density and arrangement of 5-HT axons over postnatal development. The main objective was to compare the overall pattern of the maturing 5-HT axon organisation throughout layer 3 of the entire ventral bank of the principal sulcus, since it was only practical to sample a restricted area of this portion of the PS in the quantitative part of the study (**see Methods section 8.2**). This was evaluated in terms of the general density, morphology and orientation of 5-HT axons in layer 3 of the ventral PS of each animal and any evidence of patchiness, unevenness or clustering in the 5-HT axon distribution was also noted.

The 5-HTergic innervation of layer 3 was observed to show some common characteristics which were clearly evident at all stages of postnatal development:

(i) A pronounced radially and/or obliquely oriented criss-cross network of 5-HTergic axons was observed to extend through the dorsal-ventral extent of layer 3, with many axons often spanning across adjacent layers as well.

(ii) Long tangentially-aligned 5-HTergic axons could sometimes be observed to traverse hundreds of micrometers in some animals, most notably seen in layers 2-3 of the 2.8-year and 16.7-year-old animals and in layer 6 of the 1.0-, 2.8-, 3.0-, 5.7-year-old animals.

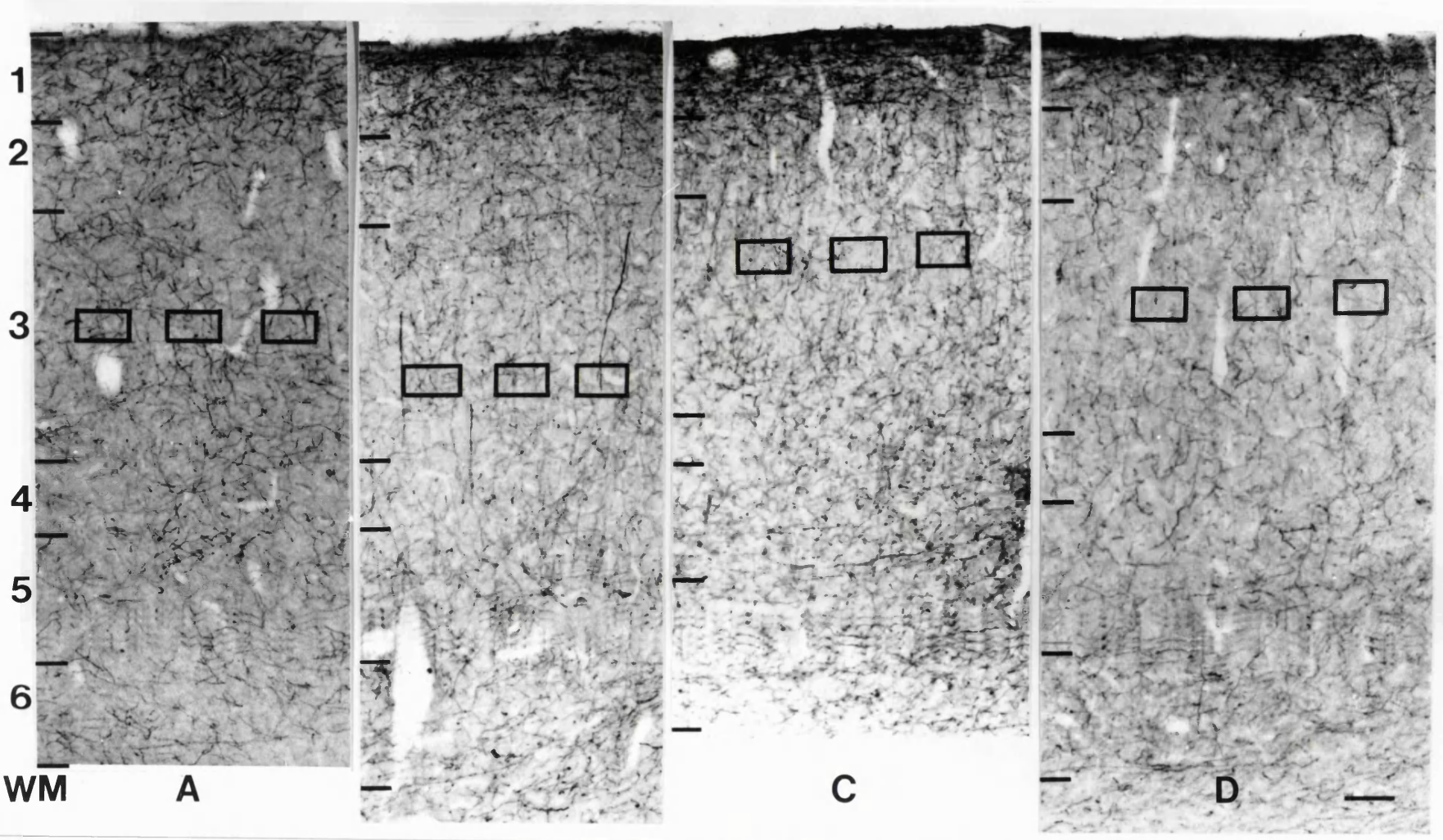

Figure 38 Low-power bright-field photomicrographs, showing a pia-to-white matter view of the developing serotonergic (5-HTergic) innervation in the ventral bank of the principal sulcus (area 46), as visualised by an anti-5-HT antibody in the neonatal, juvenile, adolescent and adult macaque monkey DLPFC, respectively at ages: **A.** 4 days, **B.** 5 months, **C.** 2.5 years and **D.** 4.5 years. Also shown are representations of the 3 sampling frames (100μm by 50 μm) used to conduct a quantitative analysis of 5-HTergic axons (**see Materials and Methods section 11.2(C)** for more details). Scale bar represents 100 μm.

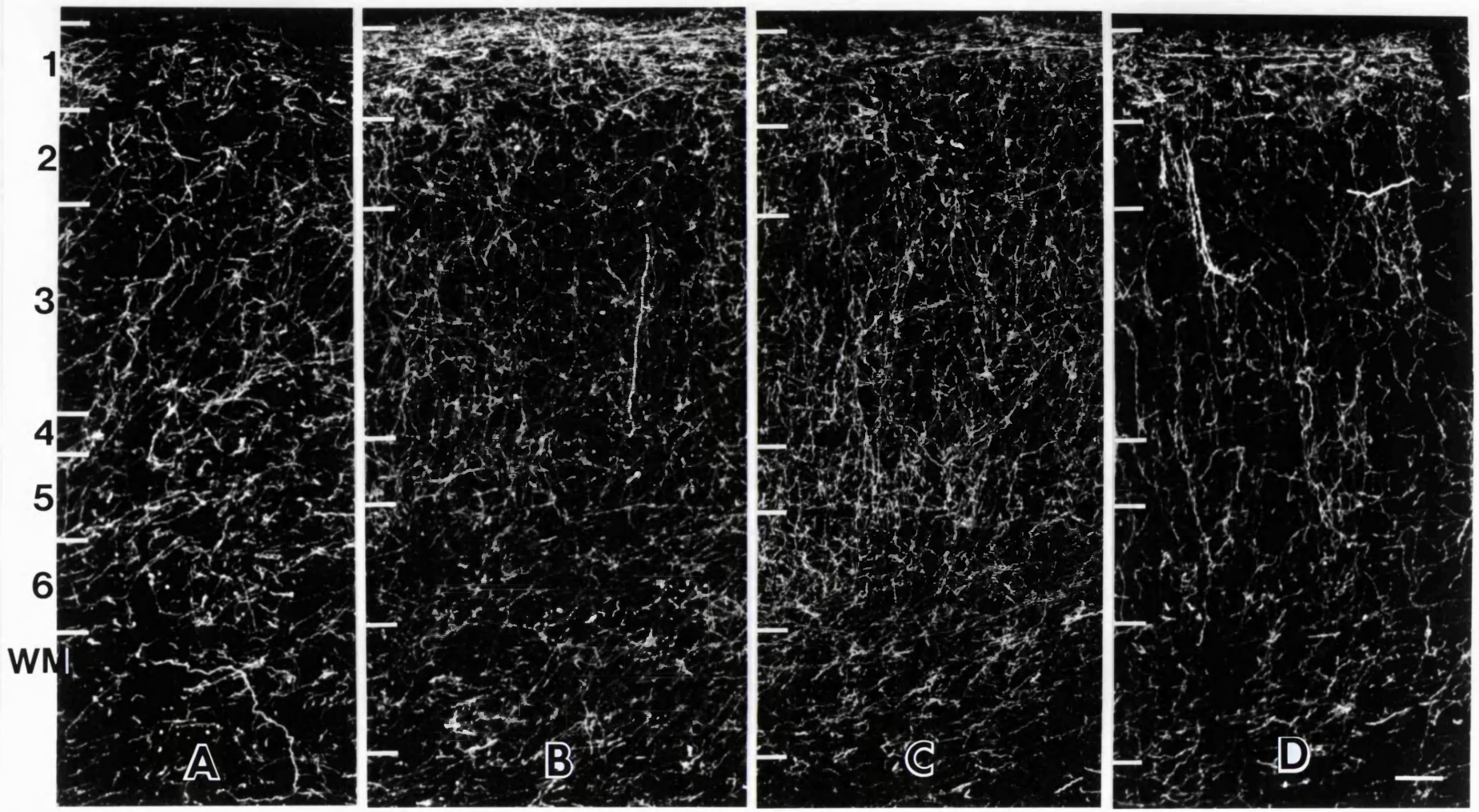

Figure 39 Low-power dark-field photomicrographs showing a pia-to-white matter view of the developing serotonergic (5-HTergic) innervation in the ventral bank of the principal sulcus (area 46), as visualised by an anti-5-HT antibody in the neonatal, infant, juvenile and peripubertal macaque monkey DLPFC, respectively at ages: **A.** 8 days, **B.** 67 days, **C.** 7 months and **D.** 3.0 years. Scale bar represents 100 μm.

(iii) A patchiness or unevenness was evident in the distribution of the 5-HTergic axons, so that a given region of layer 3 in a single animal could be quite denselyinnervated, while less than a few hundred micrometers away there might be a very sparsely innervated expanse of neuropil.

(iv) There was a tendency for complex networks, comprising radial, oblique and tangentially-oriented axons, found at certain ages, to be more densely arranged near the lip of the sulcus in the ventral bank, than within the central portion of the sulcus or near the fundus, particularly seen in the animals of 8 days, 72 days, 78 days, 7 months, 1 year, 1.5 years, 2.3 years and 2.5 years of age.

(v) Clusters of thick varicose axons were first observed in the 2.8-year-old animal and formed noticeably "basket-like" or "pericellular-like" arrangements in layer 3 and elsewhere particularly layers 1, 2 and 4; they were observed with varying levels of prominence in all other animals aged over 2.8 years. These structures have been described previously in the cerebral cortex and hippocampus of the developing (Vu and Törk, 1992) and adult cat (Mulligan and Törk, 1987, 1988, 1993), adult macaque monkey (Wilson and Molliver, 1991a) and the developing (Hornung, 1992a) and adult marmoset (Hornung et al, 1990; Hornung and Celio, 1992) - predominantly in the PFC and hippocampus; but have not been found in the developing or adult rat (reviewed in Kosofsky and Molliver, 1987). The age at which these "basket-like" 5-HT axon arrangements first appear and the maturational time course for their presence, has not to our knowledge been described in the cerebral cortex of the developing macaque monkey.

In a qualitative low power (50x and 100x total magnification) light microscope examination of the material from each animal, **(see Figures 38 and 39)** the time points between which the most dramatic changes in the density of the 5-HTergic axon innervation in layer 3 could be seen were for the animals of ages: 4 and 8 days (decrease), 1.0 and 1.5 years (decrease), 1.5 and 2.3 years (increase), 2.3 and 2.5 years (increase), 2.5 and 2.8 years (decrease), 4.5 and 5.7 years (increase) and 5.7 and 16.7 years (increase).

However, variations in 5-HTergic axon density observed at low magnification in layer 3 between animals of different ages were occasionally found to be unrepresentative of the variability in density within the layer when the same sections were observed in greater detail at a higher magnification. Many of the axons faintly stained with the 5-HT antibody could not be clearly seen at low power whereas axons which were intensely stained and thick in calibre would stand out and tend to give an inaccurate impression of the actual density of the 5-HTergic axons overall. For this reason and others outlined at the beginning of this section, we

undertook a quantitative analysis of the changes in the 5-HTergic axon innervation in layer 3 of area 46 during postnatal development.

13.1(C): Quantitative observations of 5-HTergic axons in mid-layer 3.

N.B. All significance values in this section were derived from the absolute values rounded up conservatively, e.g. $P = 0.003$ would fall between the $P < 0.001$ and $P < 0.005$ bands and so was placed within the $P < 0.005$ band.

The quantitative analyses of the maturational time course of 5-HTergic axons in 3 sampling frames located within mid-layer 3 of the ventral bank of area 46 in the macaque monkey DLPFC (**see Figure 38**) are presented in 3 sections :

(i) Total axon length for all 5-HTergic axons (per 5000 μm^2)

(ii) Total axon length for thick and thin 5-HTergic axons (per 5000 μm^2).

(iii) Varicosity density for all 5-HTergic axons (per 5000 μm^2).

(iv) Varicosity density for thick and thin 5-HTergic axons (per 5000 μm^2).

(v) Varicosities per μm of axon length for all 5-HTergic axons.

(vi) Varicosities per μm of axon length for thick and thin 5-HTergic axons.

The statistical significance of these developmental changes in 5-HTergic axons in mid-layer 3 of area 46 was evaluated for age groups constructed from the results of the individual animals whilst maintaining their correct chronological age sequence. Two groupings were chosen: A and B. Grouping A will be used in the results section, whilst grouping B will be compared to grouping A in the **Discussion section 13.0**.

The groups tested for significance were as follows:

Grouping A.

Age sets in grouping A were chosen on the basis of comparing the most pronounced differences between animals in terms of the total axon length for 5-HTergic axons and both the density per 5000 μm^2 and per μm of axon length of their varicosities with increasing postnatal age. There are 5 age groups in grouping A: 4-22 days (<1 month), 37 days-5 months, 7 months-2.5 years, 2.8-4.5 years and 5.7-16.7 years (>4.5 years).

Grouping B.

Age sets in grouping B were derived from those used to present the data for the postnatal development of the DAergic axon innervation in layer 3 of area 46 (Rosenberg and Lewis, 1995). This was done to enable a comparison to be made of the time courses of maturation for the present 5-HTergic and the previously reported (Rosenberg and

Table 4A. Total axon length (in μm) for 3 boxes per animal.

Age	A	B	C	SEM
4d	711.7	610.3	586.4	± 38.4
8d	491.5	819.2	795.8	±105.6
22d	697.8	520.0	703.9	± 60.3
37d	620.5	198.3	530.4	±128.4
67d	791.5	646.0	509.3	± 81.5
72d	573.9	855.4	738.3	± 81.6
78d	714.1	582.5	607.1	± 40.4
5m	849.0	832.6	618.0	± 74.4
7m	921.8	382.4	990.3	±192.2
1.0yr	821.7	714.8	943.6	± 66.1
1.5yr	692.3	588.4	911.5	± 95.2
2.3yr	393.2	392.5	927.0	±178.1
2.5yr	875.3	1109.0	1067.5	± 72.0
2.8yr	860.5	314.2	184.1	±207.2
3.0yr	544.2	431.4	227.9	± 92.6
4.5yr	683.5	188.0	336.6	±146.8
5.7yr	893.7	1013.9	787.9	± 65.3
16.7yr	1001.2	711.2	1483.9	±225.4

Lewis, 1995) DAergic axon innervations in area 46. There were 5 age groups in grouping B: 4-22 days (< 1 month), 37-78 days (1-3 months), 5-7 months, 1.0-1.5 years, 2.3-3.0 years (2-3 years) and 4.5-16.7 years (> 4.5 years). **See Discussion, 13.3(C):(ii).**

13.1(C).(i): Total axon length for all 5-HTergic axons.

The total axon length of all 5-HTergic axons within 3 sampling areas of 5000 μm^2 each in the ventral bank of the PS was measured for each animal; the mean of these 3 samples was then calculated as a measure of mean total axon length (per 5000 μm^2) at each age across postnatal development (**see Figures 40A and 41A, also see Table 4A for raw data**).

The total axon length for all 5-HTergic axons in early neonatal animals (4 to 22 days of age) remained constant at a moderate level until about the beginning of the first postnatal month (37 days), where it exhibited a much lower value. From 67 days to 1.0 year of age, the total axon length of all 5-HTergic axons showed a gradual but consistent rise. For those animals aged from 1.0 year through to 3.0 years of age there was a marked overall decline in total axon length with age.

One exception to this general trend was a high value for total length of 5-HTergic axons observed in the 2.5-year-old animal during the course of an otherwise uninterrupted decrease in total axon length for the animals aged between 1.0 and 3.0 years of age. The level of 5-HTergic axon innervation in the 2.5-year-old is almost double the value found in the 2.3-year-old animal and over twice the value for the 2.8-year-old animal - its immediate neighbours by age.

The low value of total axon length in the 3.0-year-old animal was maintained in the 4.5-year-old animal. The low levels of total axon length in young adults did not however, appear to remain stable in older adult animals, since those of 5.7 years and 16.7 years of age demonstrated much higher values than those seen for the 3.0- and 4.5-year-olds. A dramatic upward trend in total axon length was observed for the 5.7-year-old and a small further rise was evident for the 16.7-year-old.

Using the Kruskal-Wallis test, for grouping A (**see Figure 42A**), statistically significant changes were observed for total axon length (per 5000 μm^2) with age ($P < 0.05$). Specifically, there was a marked difference between the 7 m-2.5 yrs and 2.8 yrs-4.5 yrs age groups ($P < 0.10$) and between the 2.8 yrs-4.5 yrs and > 4.5 yrs age groups ($P < 0.10$).

A modification of the groupings, i.e. the merging of age groups 1 and 2 (overall: 4 days-5 months) with the Kruskal-Wallis test, produced an increase in the overall significance of changes occurring between age groups (asymptotic, $P < 0.01$). The use of the Bonferroni

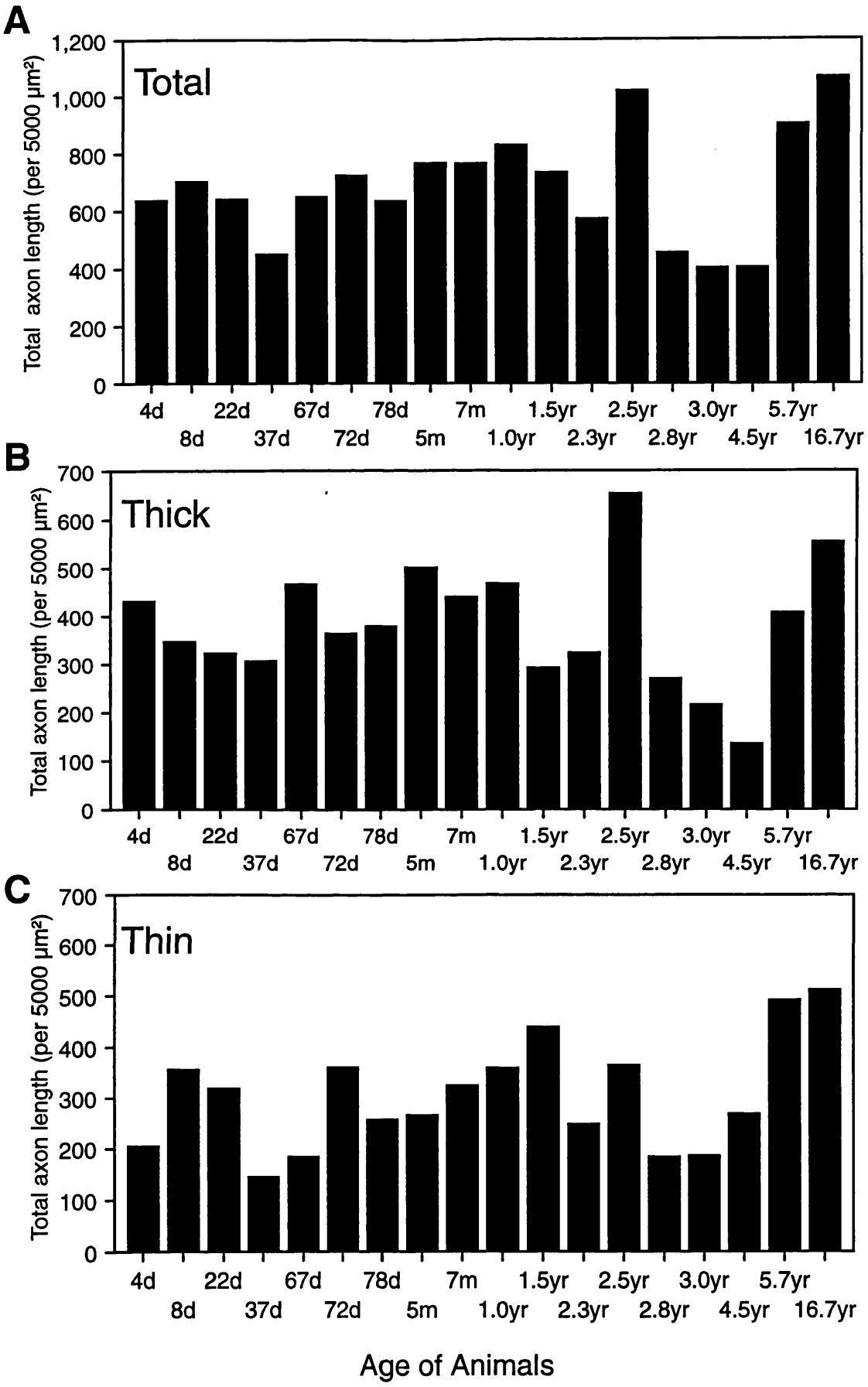

Figure 40. Results for individual animals on a linear scale: Total axon length (per 5000µm²) is shown for (**A**) all 5-HTergic axons; (**B**) thick 5-HTergic axons and (**C**) thin 5-HTergic axons.

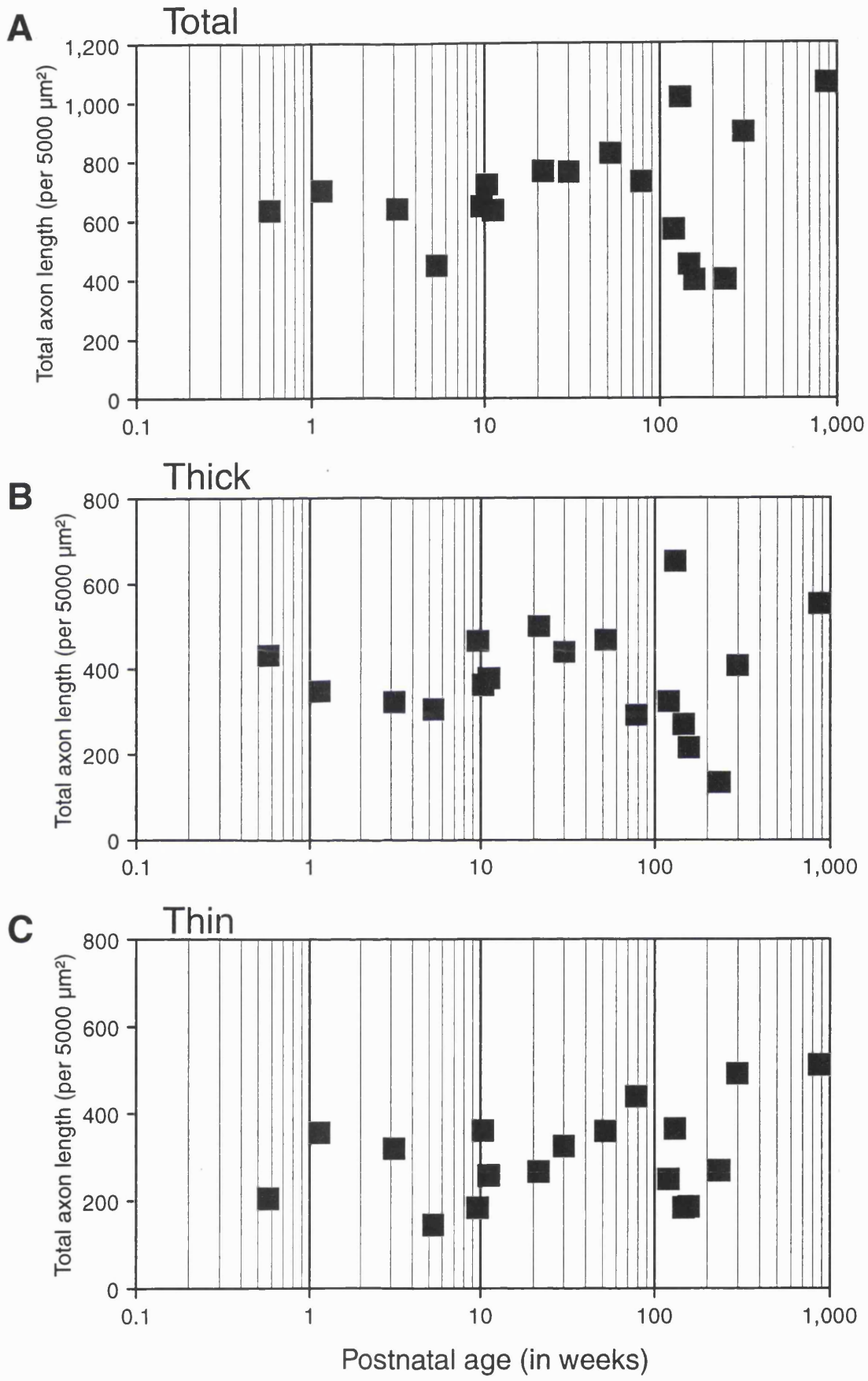

Figure 41. Results for individual animals on a logarithmic scale, illustrating proportional age intervals between animals:Total axon length (per 5000µm²) is shown for (**A**) all 5-HTergic axons; (**B**) thick 5-HTergic axons and (**C**) thin 5-HTergic axons.

Table 4B. Axon length (in μm) for thick and thin axons for 3 boxes per animal.

Age	Thick	Thin	Thick	Thin	Thick	Thin	SEM Thick	Thin
4d	515.1	196.6	353.2	257.1	424.5	161.9	± 46.9	± 27.8
8d	341.5	150.0	395.3	423.9	302.5	493.3	± 26.9	±104.8
22d	381.4	316.4	244.4	275.6	339.0	364.9	± 40.5	± 25.8
37d	489.6	130.9	154.2	44.1	271.6	258.8	± 98.3	± 62.4
67d	489.8	301.7	530.4	115.6	374.9	134.4	± 46.6	± 59.1
72d	368.6	205.3	511.8	343.6	205.5	532.8	± 88.5	± 94.9
78d	629.2	84.9	335.1	247.4	167.6	439.5	±134.9	±102.5
5m	673.7	175.3	512.7	319.9	314.6	303.4	±103.9	± 45.7
7m	397.2	524.6	168.6	213.8	751.9	238.4	±169.7	± 99.8
1.0yr	341.3	480.4	419.0	295.8	641.7	301.9	± 90.0	± 60.5
1.5yr	439.3	253.0	323.2	265.2	111.6	799.9	± 95.9	±180.3
2.3yr	261.4	131.8	264.9	127.6	441.2	485.8	± 59.4	±118.7
2.5yr	683.3	192.0	607.9	501.1	667.7	399.8	± 23.0	± 91.0
2.8yr	422.4	438.1	262.1	52.1	123.6	60.5	± 86.3	±127.3
3.0yr	328.5	215.7	205.9	225.5	110.2	117.7	± 63.2	± 34.4
4.5yr	321.3	362.2	33.4	154.6	48.1	288.5	± 93.6	± 60.8
5.7yr	583.7	310.0	442.0	571.9	194.4	593.5	±113.8	± 91.1
16.7yr	638.9	362.3	382.1	329.1	639.4	844.5	± 85.7	±166.5

correction following an ANOVA, further increased the levels of significant difference ($P < 0.0005$). Specifically, these changes occurred between the new age group and the > 4.5 yrs group ($P < 0.02$), as well as increased levels of significance for the differences in values between the 7 m-2.5 yrs and 2.8 yrs-4.5 yrs groups ($P < 0.005$) and between 2.8 yrs-4.5 yrs and the > 4.5 yrs groups ($P < 0.001$).

13.1(C).(ii): Total axon length for thick and thin 5-HTergic axons.

The total axon lengths for thick (**see Figures 40B and 41B**) and thin (**see Figures 40C and 41C and Table 4B for raw data**) types of 5-HTergic axons, which together comprise the total axon length (per 5000 μm^2) of all 5-HTergic axons, were measured separately in order to examine their relative contribution to changes in overall 5-HTergic axon density that might be taking place during the course of postnatal development.

Total axon length for thick 5-HTergic axons.

The thick variety of 5-HTergic axons (**see Figures 40B and 41B and also Table 4B for raw data**) appeared to show a moderate-to-low level of innervation in the early neonatal period (4- to 37-day-old animals), with a moderate value for the 4-day-old and lower levels in successive ages, reaching a low point in the 37-day-old animal. There appeared to be a general trend of increasing total axon length between the animals ages 37 days and 5 months; only the 67-day-old animal showed a deviation from the general trend, with a much higher level of axon length than animals of a similar age (i.e. 72 and 78 day animals). There was very little variation in the levels of total axon length for the animals aged between 5 months and 1.0 year of age, but there was observed to be a large drop for the animals aged between 1.0 and 1.5 years of age; this lower level was sustained in the 2.3-year-old animal.

As seen for the measures of all 5-HTergic axons there was very high total axon length of thick 5-HTergic axons in the 2.5-year-old animal. Otherwise for the animals aged between 1.0 year and 4.5 years, there total axon length measures seemed to progressively decline for. There was observed to be a triple-fold higher level of axon length in the 5.7-year-old animal compared to the 4.5-year-old animal. In older adult animals, represented by the 16.7-year-old animal the total axon length was only slightly greater than that in the 5.7-year-old.

Non-significant (at the $\alpha = 0.05$ level) but sizeable changes (asymptotic, $P < 0.10$) were observed in total axon length for the thick type of 5-HTergic axons (per 5000 μm^2) during postnatal development, using grouping A (**see Figure 42B**). Specifically, there was a

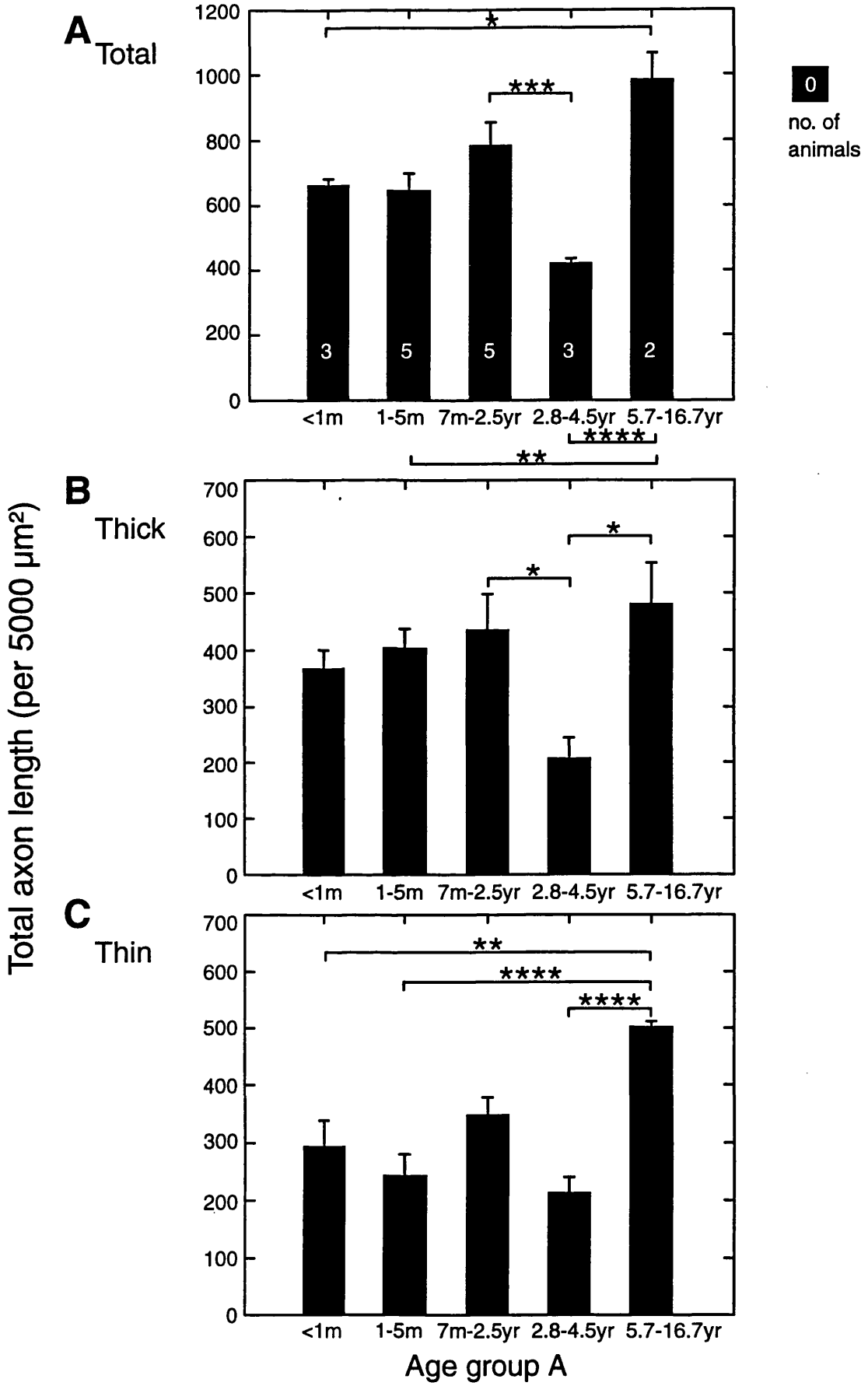

Figure 42. Results for age groups arranged in **grouping A** (the number of animals in each group is indicated): Total axon length (per 5000µm²) is shown for (**A**) all 5-HTergic axons; (**B**) thick 5-HTergic axons and (**C**) thin 5-HTergic axons. The levels of significance for each difference between age groups is shown above the appropriate bars.

large difference between the values for the 7 m-2.5 yrs and the 2.8 yrs-4.5 yrs age groups ($P < 0.10$) and between those of the 2.8 yrs-4.5 yrs and > 4.5 yrs age groups (both $P < 0.10$).

A modification of the groupings, (i.e. groups 1 and 2 combined), did not produce any significant differences between the new age group (4 d-5 m) and the other age groups, although the overall significance for difference across all groups increased (asymptotic, $P < 0.05$). The ANOVA with the Bonferroni correction also appeared to raise the significance of the differences ($P < 0.02$), specifically between the 7 m-2.5 yrs and the 2.8 yrs-4.5 yrs age groups ($P < 0.05$) and of the latter and the > 4.5 yrs groups ($P < 0.06$).

Total axon length for thin 5-HTergic axons.

The thin class of 5-HTergic axons (**see Figures 40C and 41C and also Table 4B for raw data**) in the 4 day animal exhibited a low value for total axon length, whilst the level for the animals of 8 and 22 days of age was nearly twice this value. The lowest overall total axon length was observed for the 37-day old, which represented the beginning of a consistent rise in values from the animal aged 37 days through to the 1.5 year-old. The only exception to this smooth pattern was the high level for axon length found in the 72 day-old animal.

The levels of total axon length in the 2.3-year-old were about half those for the peak in the 1.5-year-old and apart from the consistently higher levels in the 2.5-year-old animal, a downward trend was followed which reached a low point in the 2.8- and 3.0-year-olds. A slightly higher total axon length was evident for the 4.5-year-old and a much higher level was present in the 5.7- and 16.7-year-olds. Thus very high levels of innervation appeared to be the norm for the older adult animals within the age limit of the series (i.e. 16.7 years of age).

Statistically significant changes (asymptotic, $P < 0.05$) were found in the total axon length for the thin 5-HTergic axons (per 5000 μm^2) during postnatal development, as classified by grouping A. Specifically, (**see Figure 42C**) these differences were found between the < 1 m and > 4.5 yrs age groups ($P < 0.10$), between the 1 m-5 m and > 4.5 yrs age groups ($P < 0.01$) and between the 2.8 yrs-4.5 yrs and > 4..5 yrs age groups ($P < 0.01$).

A modification of the groupings (i.e. merging of age groups 1 and 2), with the Kruskal-Wallis test resulted in an increased overall level of significance for differences between age groups (asymptotic, $P < 0.03$). The use of an ANOVA with the Bonferroni correction, produced an increase in the overall level of significance for the changes evident between all age groups ($P < 0.002$). The strongest significant differences were observed to be between the new age group (4 d-5 m) and the 2.8 yrs-4.5 yrs age group ($P < 0.005$), as well between the 7 m-2.5 yrs and 2.8 yrs-4.5 yrs age groups ($P < 0.005$).

Table 5A. Total varicosity density for 3 boxes per animal.

Age	A	B	C	SEM
4d	492	424	393	± 29.2
8d	394	638	624	± 79.1
22d	445	380	512	± 38.1
37d	476	153	476	±107.7
67d	290	244	216	± 21.6
72d	313	414	402	± 31.9
78d	271	323	358	± 25.3
5m	269	436	321	± 49.3
7m	572	261	658	±120.6
1.0yr	486	378	593	± 62.1
1.5yr	410	339	597	± 77.0
2.3yr	111	190	461	±106.0
2.5yr	572	703	704	± 43.8
2.8yr	182	217	123	± 27.4
3.0yr	152	286	166	± 42.5
4.5yr	416	114	174	± 92.3
5.7yr	424	521	445	± 29.5
16.7yr	731	539	1085	±159.9

13.1(C).(iii): Varicosity density per 5000 μm^2 for all 5-HTergic axons.

The postnatal development of varicosity density for all 5-HTergic axons (**see Figures 43A and 44A and also Table 5A for raw data**) in mid-layer 3 of area 46 showed a broadly similar time course to that of the total axon length for all 5-HTergic axons and indeed is a product of total axon length and varicosities per μm of axon. The basically cyclical pattern of the density of innervation for developing 5-HTergic axons observed in mid-layer 3 of area 46 was even more pronounced in the case of the 5-HTergic varicosities.

The density of varicosities for all 5-HTergic axons during the early neonatal period was at moderate levels in the youngest animal of 4 days of age, whilst they were slightly higher in the 8 day animal. Then in the animals between 8 and 67 days of age varicosity density values appeared to decline at an even rate. These observations showed a generally parallel relationship with those for total axon length as described in **section (i)**, although the lowest levels were found in the 37 day animal for the latter parameter, rather than in the 67-day-old.

The downward trend in varicosity density appeared to be reversed from 72 days onwards, to rise in value to the 7-month-old animal. The animals aged between 7 months and 1.5 years illustrated a plateau in their values for varicosity density, which began to fall as shown by the much lower levels seen for the 2.8-year-old. The 2.5-year-old demonstrated a level of varicosity density around three times that of the 2.8-year-old, appearing to be out of the range of all the other animals - apart from the oldest 2 adults - as observed before in the measurement of total axon length in **section (i)**. The 2.8-year-old animal contained the lowest varicosity density of any age examined, but this low density was not maintained into the adult stage of development. A gradual increase was evident at first between the animals of 2.8 and 4.5 years of age, then an acceleration in the density of varicosities seemed to have occurred with a doubling of values between the animals of 4.5 and 5.7 years of age; the highest value of varicosity density at any age examined was seen in the 16.7-year-old, representing a doubling of values from that of the 5.7-year-old animal.

Statistically significant changes (asymptotic, $P < 0.02$) were found in varicosity density (per 5000 μm^2) for the total 5-HTergic axon population across the postnatal period, using grouping A. Specifically, (**see Figure 45A**) there was a sizeable difference between the < 1 m and 2.8 yrs-4.5 yrs age groups ($P < 0.10$) and significant differences between the 1 m-5 m and > 4..5 yrs age groups ($P < 0.10$), between the 7 m-2.5 ys and 2.8 yrs-4.5 yrs age groups ($P < 0.10$) and between the 2.8 yrs-4.5 yrs and > 4.5 yrs age groups ($P < 0.01$).

The modification of age groups (i.e. combining 1 and 2), with the Kruskal-Wallis

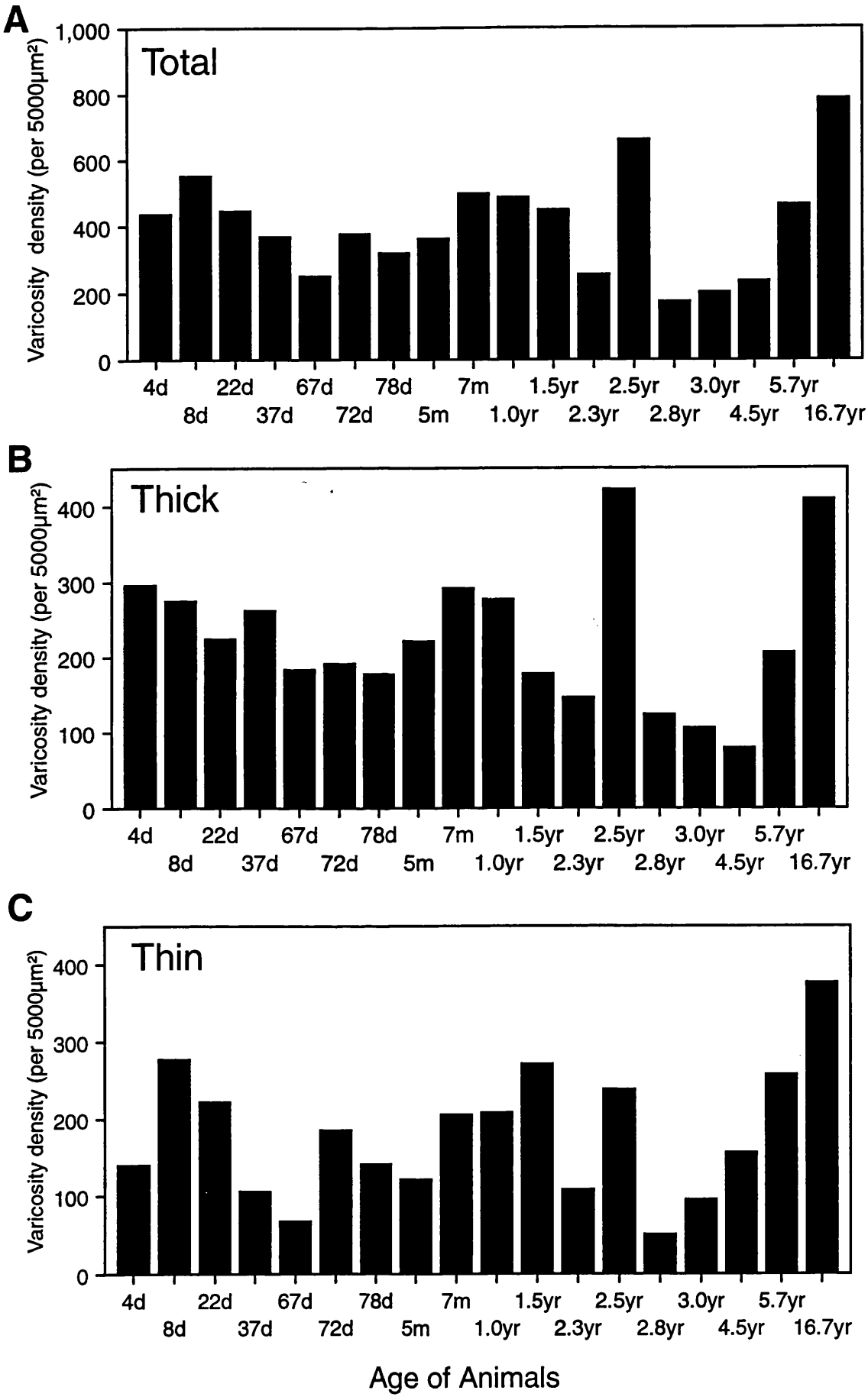

Figure 43. Results for individual animals on a linear scale: Varicosity density (per 5000µm²) is shown for (**A**) all 5-HTergic axons; (**B**) thick 5-HTergic axons and (**C**) thin 5-HTergic axons.

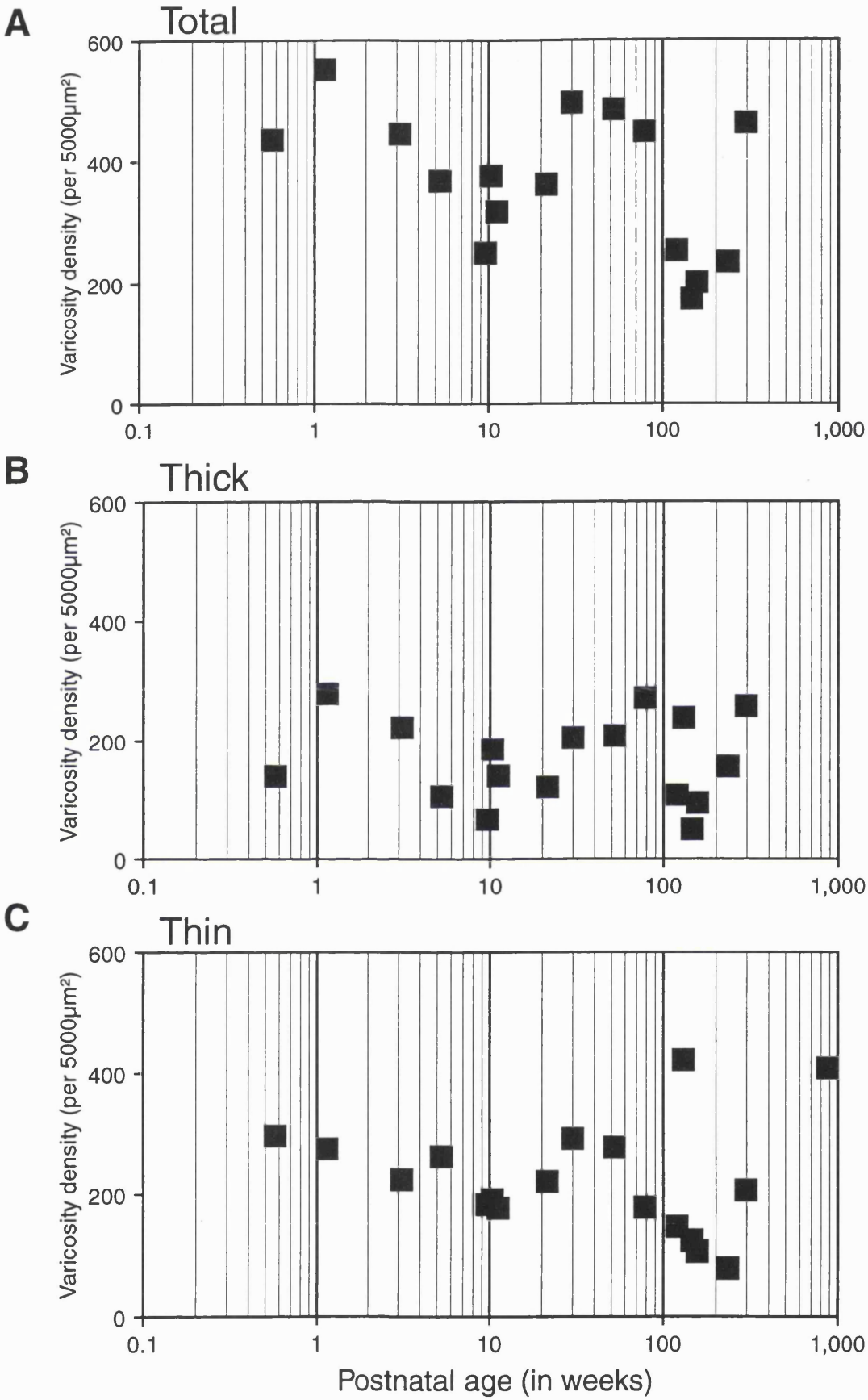

Figure 44 . Results for individual animals on a logarithmic scale, illustrating proportional age intervals between animals: Varicosity density (per 5000µm²) is shown for (**A**) all 5-HTergic axons; (**B**) thick 5-HTergic axons and (**C**) thin 5-HTergic axons.

Table 5B. Varicosity density for thick and thin axons for 3 boxes per animal.

Age	Thick	Thin	Thick	Thin	Thick	Thin	SEM Thick	SEM Thin
4d	356	136	242	182	291	102	± 33.0	± 23.2
8d	282	112	298	340	244	380	± 16.0	± 83.5
22d	238	207	174	206	259	253	± 25.6	± 15.5
37d	382	94	119	34	286	190	± 76.8	± 45.4
67d	188	102	196	48	164	52	± 9.6	± 17.4
72d	207	106	258	156	108	294	± 44.0	± 56.2
78d	238	33	186	137	106	252	± 38.4	± 63.2
5m	230	39	257	179	175	146	± 24.1	± 42.3
7m	264	308	118	143	494	164	±109.4	± 51.9
1.0yr	212	274	218	160	402	191	± 62.4	± 34.0
1.5yr	261	149	196	143	77	520	± 53.9	±124.7
2.3yr	79	32	130	60	230	231	± 44.3	± 62.2
2.5yr	453	119	369	334	444	260	± 26.6	± 63.1
2.8yr	101	81	181	36	89	34	± 28.9	± 15.3
3.0yr	104	48	139	147	76	90	± 18.2	± 28.7
4.5yr	184	232	23	91	29	145	± 52.7	± 41.1
5.7yr	283	141	218	303	117	328	± 48.3	± 58.6
16.7yr	455	276	301	238	741	614	±128.9	±119.5

test revealed no alteration in the overall level of significance for changes in varicosity density during postnatal development ($P < 0.02$). The use of an ANOVA with the Bonferroni correction applied, did raise the overall level of significance for the difference between age groups ($P < 0.01$), but no rise in the case of the new age group (4 d-5 m) and the others, although there was a rise in the significant difference between the 7 m-2.5 yrs and 2.8 yrs-4.5 yrs age groups ($P < 0.05$).

13.1(C).(iv): Varicosity density per 5000 μm^2 for thick and thin 5-HTergic axons.

Varicosity density for thick 5-HTergic axons.

The density of varicosities counted for the thick variety of 5-HTergic axons (**see Figures 43B and 44B and also Table 5B for raw data**) was at moderate levels in the 4 day-old animal, but then exhibited a general decrease in values for most animals until 67 days of age. The animals of ages 67-78 days remained stable in their values, whilst those aged between 78 days and 5 months appeared to demonstrate a steady increase in varicosity density which continued until a peak was reached in the levels for the 7-month-old animal.

Following stable values for the 7-month and 1.0-year-olds, a major decline in varicosities was apparent for animals aged between 1.0 and 4.5 years of age; as before the 2.5-year-old animal was the exception in this trend. The levels for the 4.5-year-old were the lowest of any animal in the present study. A clear up-turn in varicosity density seemed to have taken place between the values for the animals of 4.5 and 5.7 years of age; whilst another large increase was observed to have occurred in the 16.7-year-old animal.

Statistically significant changes (asymptotic, $P < 0.05$) were found in terms of varicosity density (per 5000 μm^2) for the thick 5-HTergic axons in grouping A (**see Figure 45B**), but no significant pair-wise differences between individual groups of animals could be differentiated.

Modification of the groupings (i.e. merging groups 1 and 2), with the Kruskal-Wallis test, did not produce any increase in the significance level of changes occurring for thick 5-HTergic axons, but in fact lowered the significance level (asymptotic, $P < 0.10$). The same result was found, even more prominently, when an ANOVA was employed with the Bonferroni correction ($P = NS$).

Varicosity density for thin 5-HTergic axons.

The thin type of 5-HTergic axons (**see Figures 43C and 44C and also Table 5B for raw data**) showed clear similarities with the overall population of 5-HTergic axons in the

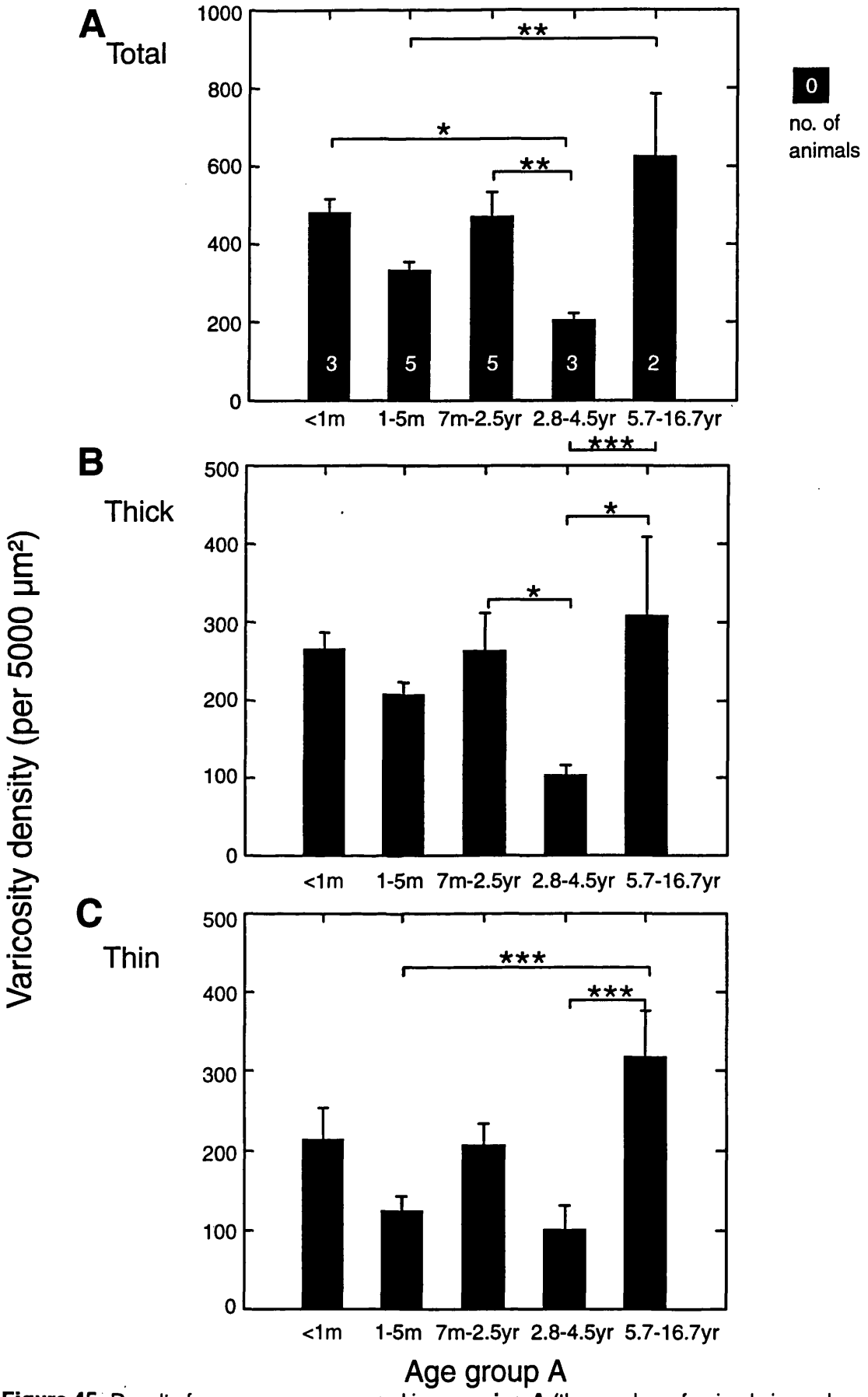

Figure 45. Results for age groups arranged in **grouping A** (the number of animals in each group is indicated): Varicosity density (per 5000µm²) is shown for (**A**) all 5-HTergic axons; (**B**) thick 5-HTergic axons and (**C**) thin 5-HTergic axons.The levels of significance for each difference between age groups is shown above the appropriate bars.

Table 6A. Total varicosities per μm for 3 boxes per animal.

Age	A	B	C	SEM
4d	0.692	0.695	0.670	±0.0079
8d	0.802	0.779	0.784	±0.0070
22d	0.638	0.731	0.727	±0.0300
37d	0.767	0.772	0.939	±0.0570
67d	0.366	0.378	0.424	±0.0180
72d	0.545	0.484	0.544	±0.0200
78d	0.380	0.555	0.590	±0.0650
5m	0.317	0.524	0.519	±0.0680
7m	0.621	0.683	0.664	±0.0180
1.0yr	0.591	0.529	0.628	±0.0290
1.5yr	0.592	0.576	0.655	±0.0240
2.3yr	0.282	0.484	0.497	±0.0700
2.5yr	0.653	0.634	0.659	±0.0075
2.8yr	0.212	0.691	0.668	±0.1560
3.0yr	0.279	0.663	0.728	±0.1401
4.5yr	0.609	0.606	0.517	±0.0030
5.7yr	0.474	0.514	0.565	±0.0260
16.7yr	0.730	0.758	0.731	±0.0092

time course and relative amplitude of postnatal development for their varicosity density. The density of varicosities in the early neonatal animals was quite low in the 4 day animal, whilst the 8-day-old had double this level. From the 8 day animal onwards there appeared to be a trend of decreasing varicosity density until the 67 day animal. Then for the animals aged between 67 days and 1.5 years of age there was much variability in the levels of varicosity density, but overall there was a general upward trend in values, reaching a peak in the 1.5-year-old. A sharp drop in varicosity density was evident in the 2.3-year-old animal, a pattern of declining numbers which continued for the 2.8-year-old, with the 2.5-year-old animal at a much higher value. The 2.8-year-old animal formed a low-point for a steady and consistent rise in the varicosity density for the thin class of 5-HTergic axons over the next 14 year period of adult life, as represented by the age range 2.8-16.7 years of age.

Statistically significant changes (asymptotic, $P < 0.05$) were seen in varicosity density (per 5000 μm^2) for the thin 5-HTergic axon subclass, using grouping A. Specifically, (**see Figure 45C**) significant differences were seen between the 1 m-5 m and > 4.5 yrs age groups ($P < 0.02$) and between the 2.8 yrs-4.5 yrs and > 4.5 yrs age groups ($P < 0.02$).

Modification of the groupings (i.e. combining 1 and 2), with the Kruskal-Wallis test, did not appear to raise the significance level of changes occurring across development for thin 5-HTergic axons, but in fact lowered it (asymptotic, $P < 0.1$). Although, the use of ANOVA with a Bonferroni correction did appear to increase the overall significance level of changes occurring over postnatal development for the varicosity density of thin 5-HTergic axons ($P < 0.02$). The new age group (4 days-5 months) and the 2.8 yrs-4.5 yrs age group demonstrated a moderately significant level of difference ($P < 0.05$) and the 2.8 yrs-4.5 yrs and the > 4.5 yrs age groups illustrating no change in their level of significant difference ($P < 0.02$).

13.1(C).(v): Varicosities per μm of axon length for all 5-HTergic axons.

The postnatal maturation of all 5-HTergic axons (**see Figure 46A and 47A and see Table 6A for raw data**) in terms of the varicosities per μm of axon length did not vary greatly over development, but there did seem to be a broad difference between the neonatal animals and the rest in that the youngest animals (4-37 days of age) exhibited higher values than most of the other ages for varicosities per μm of axon length in mid-layer 3 of area 46.

No statistically significant differences were observed between any of the age groups in either grouping A (**see Figure 48A**; P = NS) for varicosities per μm of axon for the total 5-HTergic axon population. However when varicosities per μm of axon length for all 5-HTergic axons for the neonatal animals (4 d-37 d of age; 0.741 ± 0.050) was compared with

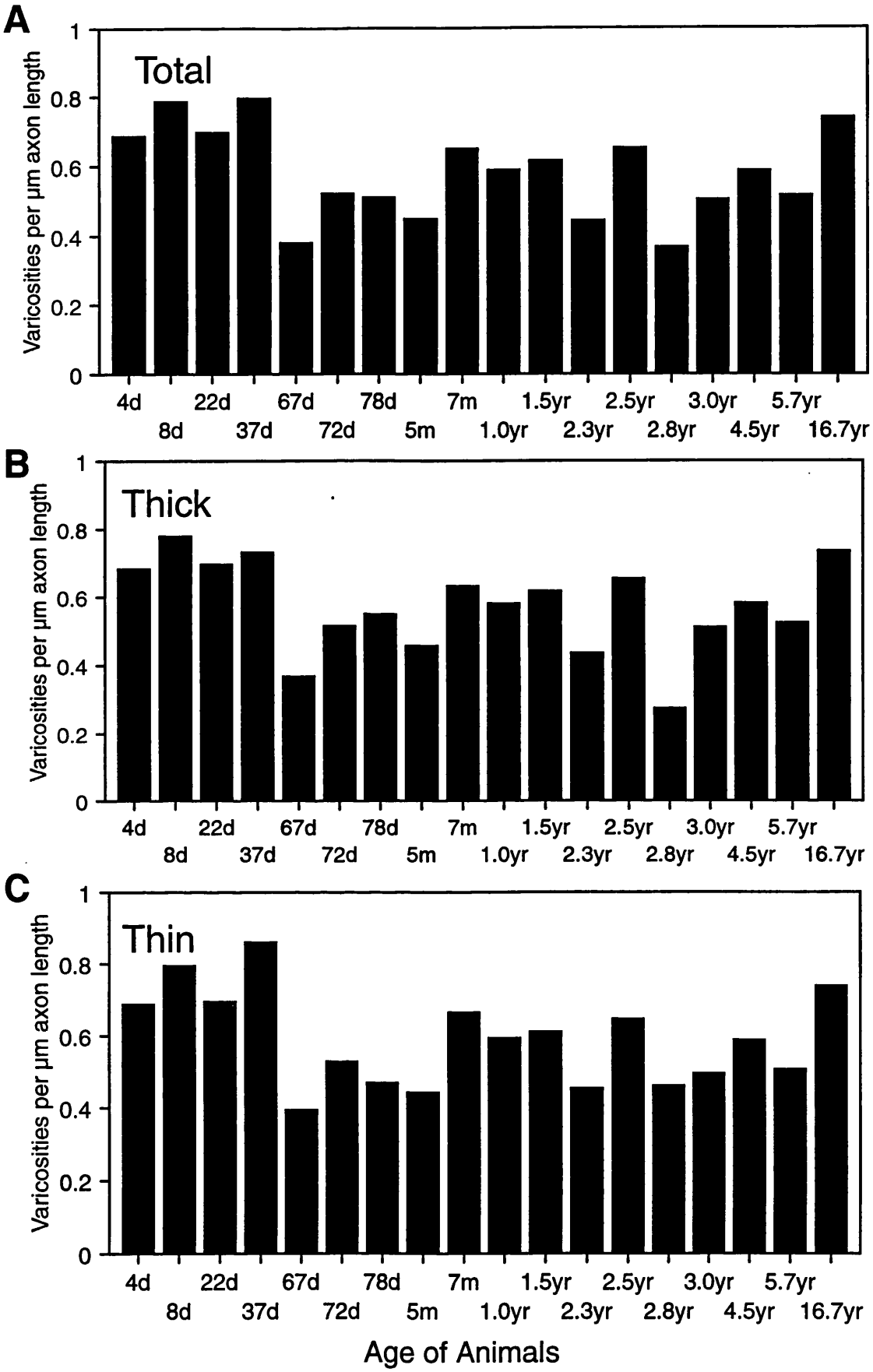

Figure 46 . Results for individual animals on a linear scale: Varicosites per µm of axon length is shown for (**A**) all 5-HTergic axons; (**B**) thick 5-HTergic axons and (**C**) thin 5-HTergic axons.

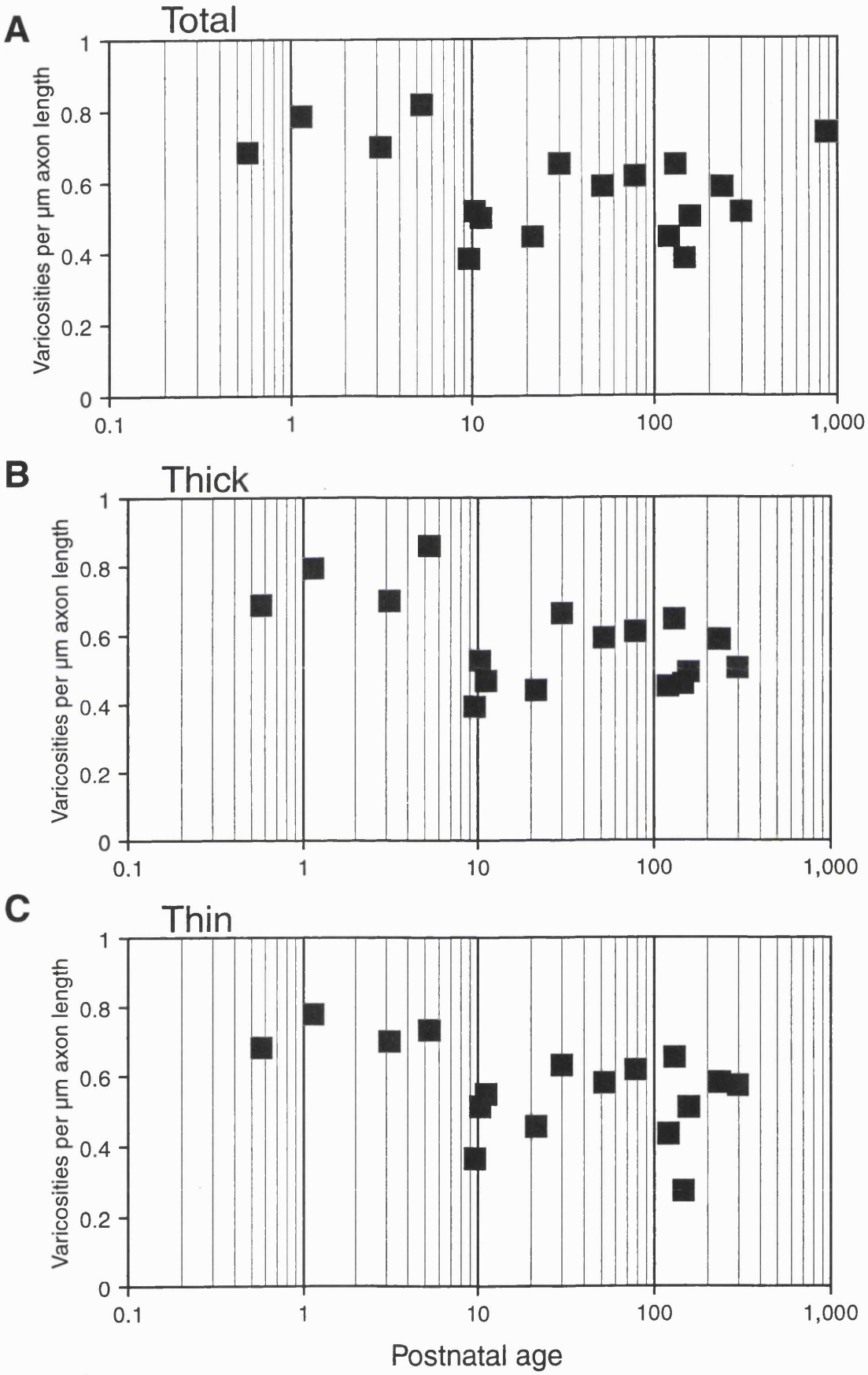

Figure 47. Results for individual animals on a logarithmic scale, illustrating proportional age intervals between animals: Varicosities per µm of axon length is shown for (**A**) all 5-HTergic axons; (**B**) thick 5-HTergic axons and (**C**) thin 5-HTergic axons.

Table 6B. Varicosities per μm for 3 boxes per animal.

Age	Thick	Thin	Thick	Thin	Thick	Thin	SEM Thick	SEM Thin
4d	0.691	0.692	0.685	0.708	0.686	0.630	±0.0019	±0.024
8d	0.826	0.747	0.754	0.802	0.807	0.770	±0.022	±0.016
22d	0.624	0.654	0.712	0.748	0.764	0.693	±0.041	±0.027
37d	0.780	0.718	0.772	0.771	0.807	1.250	±0.011	±0.016
67d	0.384	0.338	0.370	0.415	0.437	0.387	±0.020	±0.023
72d	0.562	0.516	0.504	0.454	0.526	0.552	±0.017	±0.011
78d	0.378	0.389	0.555	0.554	0.632	0.573	±0.075	±0.058
5m	0.341	0.222	0.501	0.560	0.556	0.481	±0.064	±0.102
7m	0.665	0.587	0.700	0.669	0.657	0.688	±0.013	±0.031
1.0yr	0.621	0.570	0.520	0.541	0.627	0.633	±0.035	±0.027
1.5yr	0.594	0.589	0.606	0.539	0.690	0.650	±0.030	±0.032
2.3yr	0.302	0.243	0.491	0.470	0.521	0.476	±0.069	±0.077
2.5yr	0.663	0.620	0.607	0.667	0.665	0.650	±0.019	±0.014
2.8yr	0.239	0.185	0.691	0.691	0.720	0.562	±0.156	±0.152
3.0yr	0.317	0.223	0.675	0.652	0.690	0.765	±0.122	±0.165
4.5yr	0.573	0.641	0.689	0.603	0.503	0.503	±0.054	±0.041
5.7yr	0.485	0.455	0.493	0.530	0.602	0.553	±0.038	±0.030
16.7yr	0.712	0.762	0.788	0.723	0.737	0.727	±0.022	±0.012

that for all other animals (67 d-16.7 yrs of age; 0.536 ± 0.010), (**see Figure 49A**) a statistically significant difference was found ($P < 0.005$). This difference represented a significant drop of 28% in varicosities per μm of axon between the youngest animals and the rest of the animals which occurred between 37 and 67 days of age.

13.1(C).(vi): Varicosities per μm of axon length for thick and thin 5-HTergic axons.

The maturational time course and levels of varicosities per μm of axon length were very similar for both thick (**see Figures 46B and 47B and see Table 6B for raw data**) and thin (**see Figures 46C and 47C and see Table 6B for raw data**) 5-HTergic axons and so exhibited very similar temporal changes to those seen for the overall 5-HTergic axon population in mid-layer 3 of area 46.

Again no statistically significant differences between age groups were seen for grouping A (**see Figures 48B and 48C**; thick: P = NS and thin: P = 0.093). However when varicosities per μm of axon length for the two 5-HTergic axon sub-populations in the neonatal animals (4 d-37 d of age; thick: 0.759 ± 0.048; thin: 0.722 ± 0.055) were compared separately (**see Figures 49B and 49C**) to that for all other animals (67 d-16.7 yrs of age; thick: 0.542 ± 0.026; thin: 0.530 ± 0.029), statistically significant differences were found for both thick ($P < 0.01$) and thin ($P < 0.01$) 5-HTergic axons. These differences represented significant drops of 29% and 27%, in varicosities per μm of axon, respectively for the thick and thin 5-HTergic axon populations.

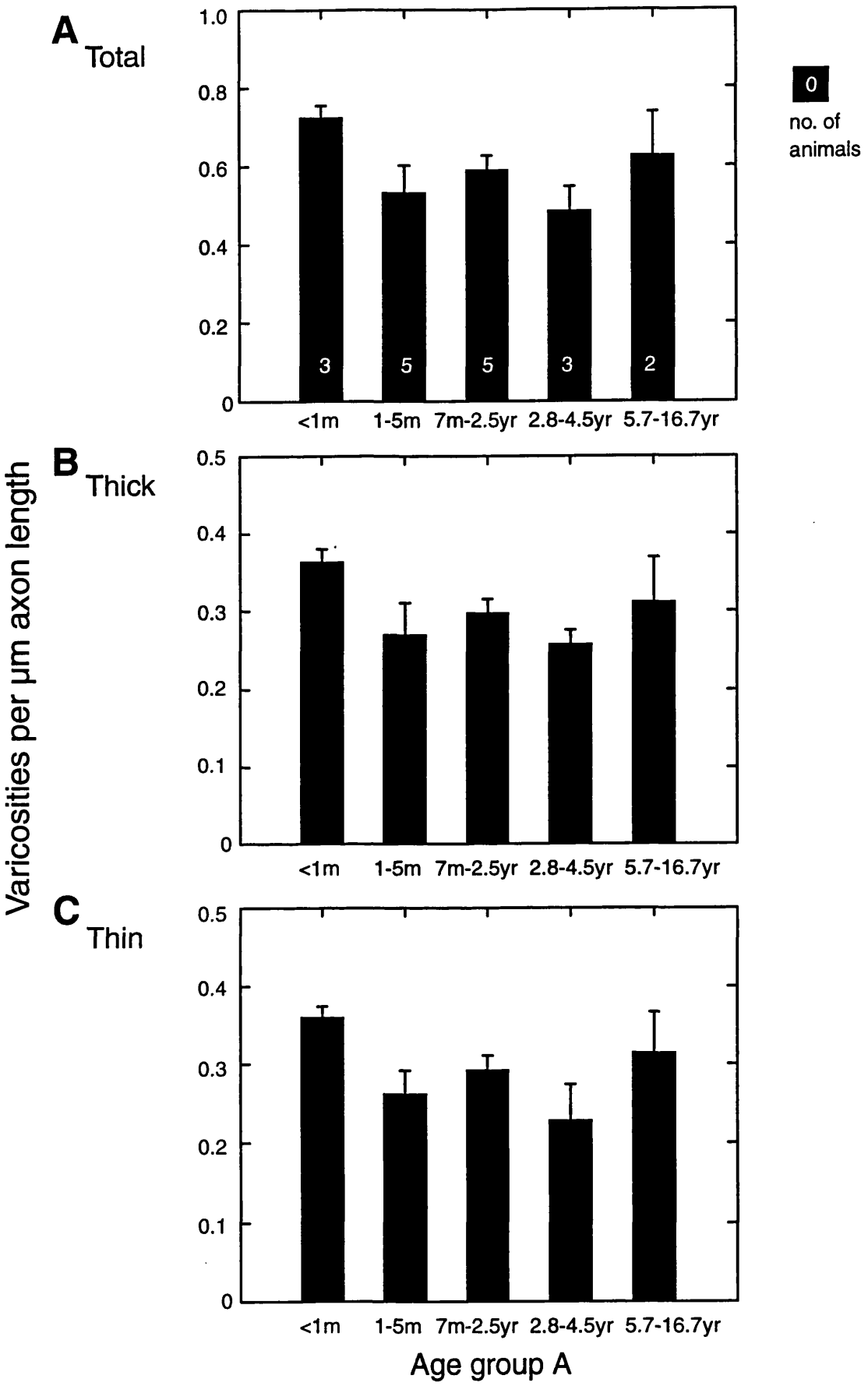

Figure 48. Results for age groups arranged in **grouping A** (the number of animals in each group is indicated): Varicosities per µm of axon length is shown for (**A**) all 5-HTergic axons; (**B**) thick 5-HTergic axons and (**C**) thin 5-HTergic axons.There were no significant differences between age groups for varocosities per µm of axon length during postnatal development.

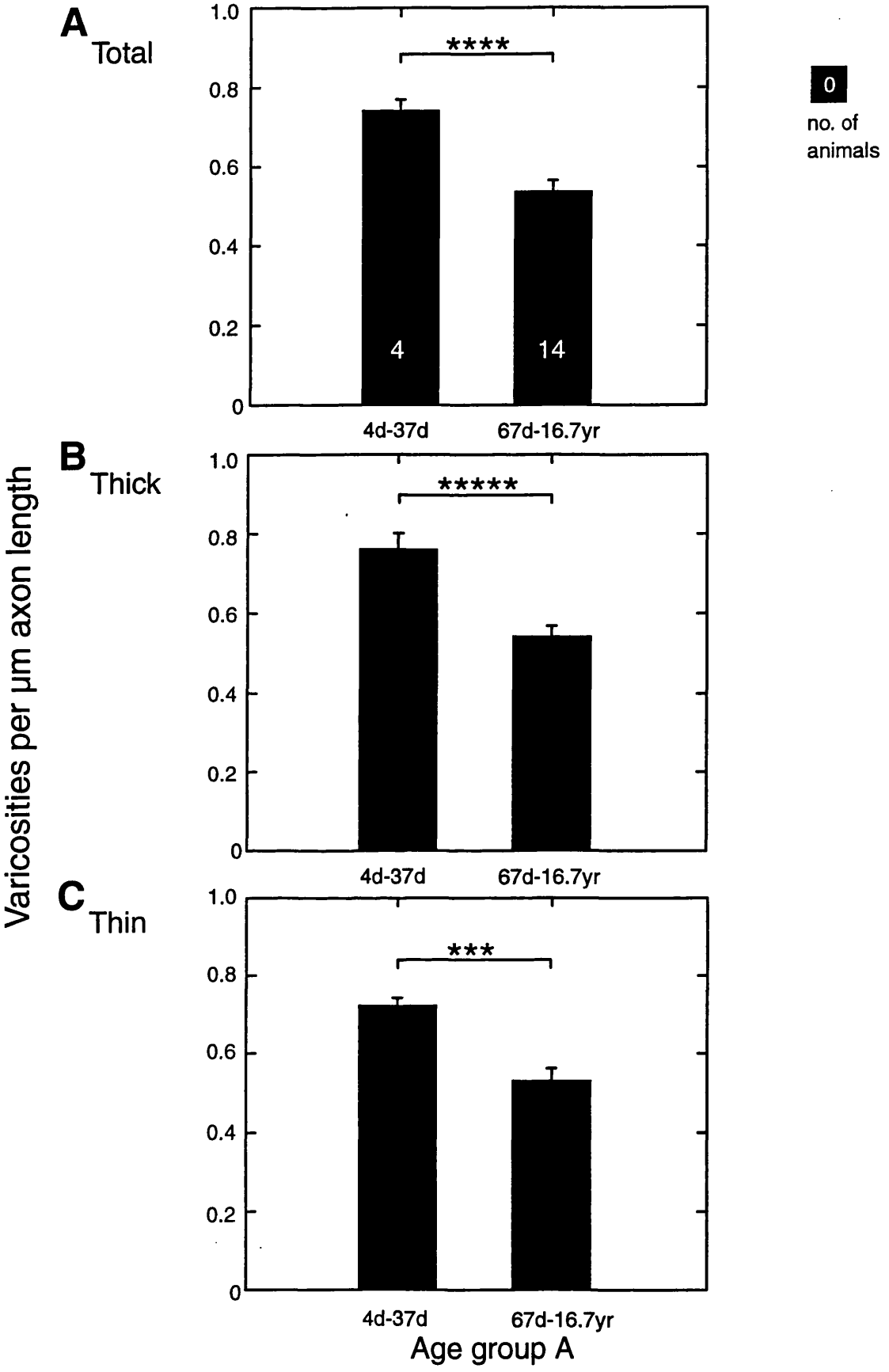

Figure 49 . Results for age groups comparing animals aged between 4-37 days with the rest of the animals (>37days) in the set (the number of animals in each group is indicated): Varicosities per µm of axon length is shown for (**A**) all 5-HTergic axons; (**B**) thick 5-HTergic axons and (**C**) thin 5-HTergic axons.The levels of significance for each difference between age groups is shown above the appropriate bars.

14.0: Discussion

Study 2: A quantitative immunohistochemical study of the postnatal development of 5-HTergic axons in mid-layer 3 of the ventral bank of area 46 in the monkey DLPFC.

14.1: Reliability of the immunohistochemical technique in animals of different ages as a sensitive indicator of the changing levels of serotonergic axons during postnatal development.

As evident from the results above, we saw statistically significant differences between age groups across postnatal development for the 5-HTergic innervation in mid-layer 3 of area 46. There is however a concern regarding the validity of using results obtained from animals of different ages to attempt to reconstruct or recreate the time-course that might be expected to occur within the postnatal life of any one individual animal.

There are several pieces of technical evidence which we can offer in support of the contention that the majority of the changes which we see over age in this study represent a realistic temporal reconstruction of the changes in the density of the 5-HTergic innervation that are usually encountered within the lifetime of an individual animal and not the result of artifactual interference produced during the immunohistochemical tissue processing.

These points are:

1. The anti-rabbit 5-HT-specific antibody employed in this study has been used in previous studies by other investigators in animals of both different species and ages, including monkeys (Fischer et al, 1995; Smiley and Goldman-Rakic, 1996), cats (Gu et al, 1990; Mower, 1991) and rats (MacClean and Shipley, 1987a,b; Rhoades et al, 1990; Bennett-Clarke et al, 1991; Blue et al, 1991; Bennett-Clarke et al, 1994b; Osterheld-Haas et al, 1994). Control experiments show no detectable immunoreaction product when either the primary or secondary antibodies are omitted from the processing (replaced with normal rabbit serum) or the primary is reacted with an excess of 5-HT-bovine serum albumin conjugate (the molecule to which the antibody is directed) for the immunohistochemical reaction (e.g. Bennett-Clarke et al, 1991; Blue et al, 1991; Mower, 1991; Smiley and Goldman-Rakic, 1996). This demonstrates conclusively that the anti-5-HT antibody is specific for the 5-HT molecule only.

2. Two separate experimental 5-HT immunohistochemical reactions were carried out on different occasions, in each case sections from all 21 animals were included. Both sets of sections were qualitatively examined on separate occasions, by 2 investigators (D. Lewis and C. Kye for series 1 and D. Lewis and J. Classey for series 2: the one used in the quantitative analysis) with no knowledge of the tissue's origin or animal age, so that each set was ranked

in order of the increasing density of 5-HT immunoreactive axons in area 46. In both cases the rank-order of sections for 5-HTergic axons tallied almost exactly - a few exceptions occurred when the densities of the innervation were very similar at some ages - with the order of ages derived from the quantitative analysis (also performed without knowledge of the age or number of the animal) as described in this thesis.

3. In both separate immunohistochemical experiments all sections were run together at the same time although not all in the same reaction receptacle, but sections from animals of diverse ages, chosen randomly, e.g. 4 days, 1.0 year and 16.7 years were reacted in the same wells and hence were exposed to the same experimental reaction conditions. Thus there was no opportunity for artificially-induced age differences to occur, which might have resulted from differences in the quality of the exposure to the immunoreaction if animals of all young ages or all old ages had been reacted together in separate groups.

4. Immunohistochemical experiments for different antibodies have previously been conducted in closely adjacent sections from the same age series of animals in areas 9 or 46 of the DLPFC, for dopaminergic axons and varicosities (Rosenberg and Lewis, 1995), CCK neurons (Oeth and Lewis, 1993) and for axons and varicosities immunoreactive for the 5-HT transporter or for the 5-HT-synthetic enzyme tryptophan hydroxylase (Kye and Lewis unpublished observations). In all of these studies, quite distinct sequences of changing levels of immunoreactivity could be visualised by employing antibodies specific to the particular molecules, e.g. CCK versus 5-HT. These previous observations suggest that there is no reason to suppose that any particular experimental parameters or idiosyncrasies (e.g. variable fixation time, use of different fixatives, i.e. paraformaldehyde or glutaraldehyde; thickness of sections; differences in antibody penetration due to increasing myelination with age) could be expected to have adversely affected the levels of immunostaining found for any of the animal tissue.

We have made the assumption on the basis of these 4 different lines of evidence, that the observed changes in levels of 5-HTergic axons and varicosities during the course of postnatal development are real and represent the closest possible indication of the actual levels that were present in each individual animal. We suggest that these levels would be found at these ages over the course of the lifetime for single animals. However, behavioural studies in adult male monkeys (Fontenot et al, 1995) show that 5-HT and 5-HIAA tissue levels measured in the frontal pole (area 10 and rostral area 46) of the PFC are significantly lower in animals who experienced past-stress (15-28 months ago) compared to those who have lived under no-stress social conditions prior to sacrifice, whilst animals experiencing

recent-stress (1-14 months ago) were intermediate in their 5-HT and 5-HIAA levels.

This kind of observation may be relevant to the 2.5-year-old animal, which consistently demonstrated seemingly abnormally high values for total axon length, varicosity density or varicosities per μm of axon, compared to its peers on either side of the time scale. However this animal was not alone in illustrating high values as some of the older animals (15.9-18.0 years of age) also exhibited levels of a very similar magnitude; the question thus arises as to whether all 4 of these animals may have been subject to social conditions which distinguished them from the rest of the age series or if just the 2.5 year old is genuinely exceptional in its 5-HT system compared to the other animals of a similar age.

14.2: Summary of Results.

The time course of development for the 5-HTergic innervation of layer 3 in the monkey DLPFC was found to represent a complex set of changes over time - expressed as a schematic curve; **see Figure 50A,** derived from the values plotted in **Figure 41A** - e.g. it did not show a simple linear or exponential relationship with increasing age. The key finding in terms of a steady set of progressive changes in the 5-HTergic innervation across development was in the levels of mean total varicosity density (per 5000 μm^2), i.e. derived from the multiple of mean varicosities per μm of axon length and the mean total axon length (in μm) for 3 sampling frames for each animal. The changes in the number of varicosities (potential release sites of 5-HT) present on the sampled population of 5-HTergic axons, were of a cyclic nature, with peaks and troughs in the population distribution across time, which were representative of the values for groups of animals at particular stages of postnatal development (**see Figure 50A**).

The most significant differences observed during development for total varicosity density (per 5000 μm^2) of 5-HTergic axons were exhibited by the large increases in values from the low values of the peri-/post-pubertal animals (2.8 yrs-4.5 yrs) and the infants (1 m-5 m) to the high values seen in the adults (5.7 yrs-16.7yrs). Also significant was the change from the low values of the peri-/post-pubertal (2.8 yrs-4.5 yrs) animals to the high values of the juvenile/adolescent (7 m-2.5 yrs) animals.

We concluded - using the Spearman rank correlation coefficient - that the two 5-HTergic axon types - previously observed in other studies in monkeys and other species (**see Serotonin review section 7.4**) - were justified in being described as separate sub-populations. We show that each population possibly contributes somewhat differently to

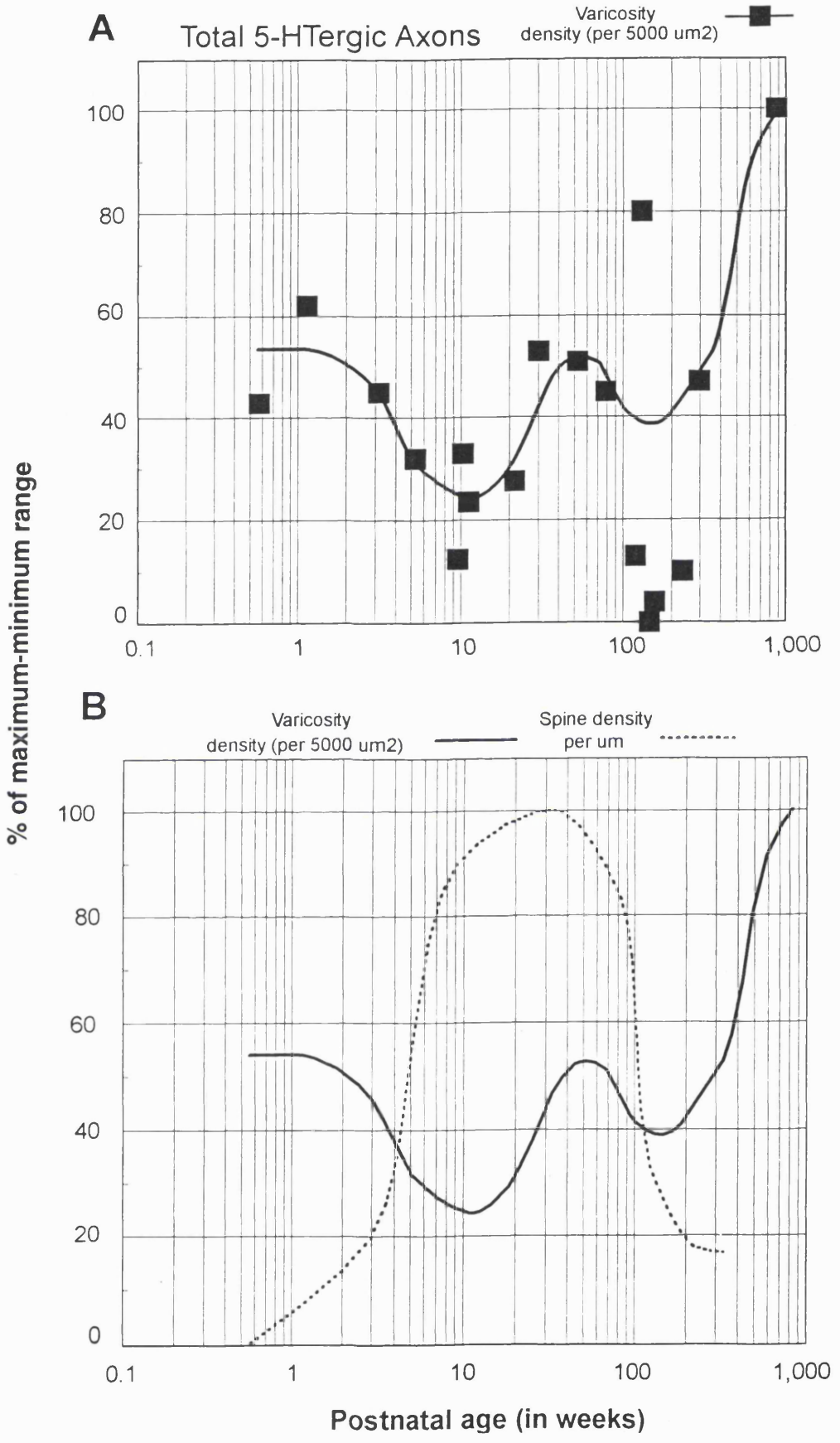

Figure 50. Schematic summary curves illustrating the percentage of maximum and minimum values for varicosity density of all 5-HTergic axons in mid-layer 3 during postnatal development, with a comparison to the spine density on mid-layer 3 pyramidal neurons. **(A)** Varicosity density for all 5-HTergic axons (per 5000 μm^2), **(B)** Varicosity density (per 5000μm^2) and spine density (per μm).

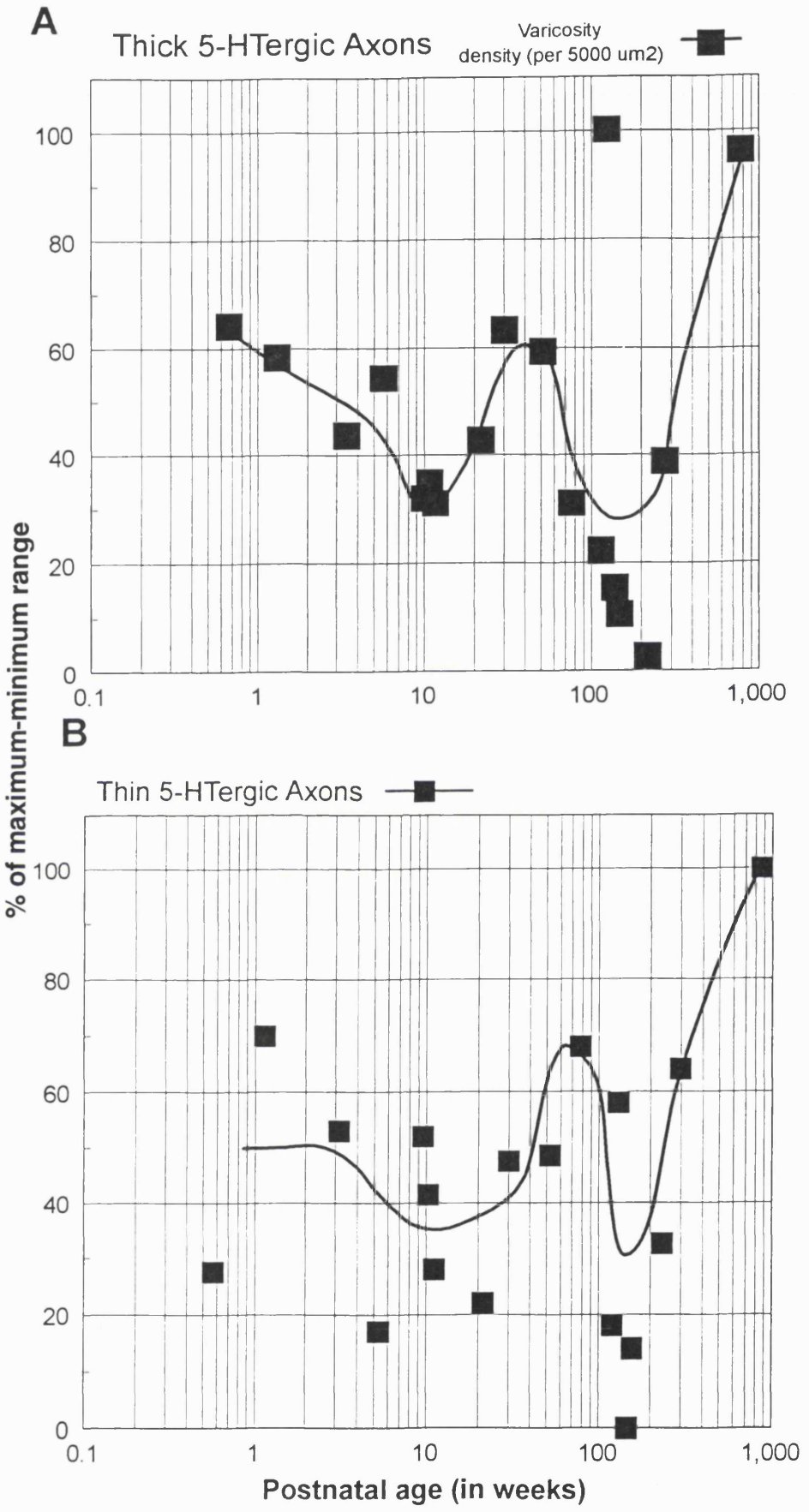

Figure 51. Schematic summary curves illustrating the percentage of maximum and minimum values for varicosity density of thick and thin classes of 5-HTergic axons in mid- layer 3 during postnatal development. Varicosity density (per 5000 μm²) for **(A)** thick and **(B)** thin 5-HTergic axons.

the overall changes observed for the maturation of the serotonergic axon innervation during postnatal development, as compared to their summed total for the 5-HTergic axon system over the same period. The possibly differential contribution of the individual axon sub-populations to the time course and pattern of maturation for the overall 5-HTergic axon innervation, could be indicative of diverse functional effects on cells postsynaptic to 5-HTergic axons. This would presumably be supported by virtue of the existence of multiple subtypes of 5-HT receptors, but also the presence of 5-HTergic axons exhibiting variably-sized 5-HT-filled varicosities would conceivably provide a differential mechanism by which to regulate the rate and magnitude of 5-HT release at various times both tonically, i.e. over a matter of seconds or minutes, as well as phasically, i.e. over a longer time period of hours or even days.

Of the significant differences in varicosity density exhibited by the total 5-HTergic axon population during postnatal development, two in particular coincided with significant changes in the varicosity density of the thin varicose 5-HTergic axons. These were observed for the low values of the infant animals and high values of the adults and between the low values of the peri-/post-pubertal (2.8-4.5yrs) and the high values of the adult animals (5.7-16.7yrs) expressed as an extrapolated curve (**see Figure 51B**). No statistically significant changes were observed for the varicosities of thick 5-HTergic axons during postnatal development (**see Figure 51A**), however, there were observed to be marked differences between the levels of varicosity density in the high values of the juvenile/adolescent animals (7m-2.5yrs) and the low values of the peri-/post-pubertal animals (2.8-4.5yrs) and also between the latter and the high values of the adults (5.7-16.7yrs).

Slight lags in the rate of change for varicosity density (per 5000 μm^2) discerned between the two 5-HTergic axon sub-populations during postnatal development, hint that perhaps the form and magnitude of 5-HT release by the two 5-HTergic axon populations, defined in this thesis study, may vary at different times, with shifts between one or other population having the dominant modulatory influence over circuitry during particular stages of development. This hypothesis would also have to take into account the existence of the many 5-HT receptor subtypes some of which are known to be localised to different sub-cellular sites on the same class of neurons and/or in the same sub-cellular location for a variety of neuron populations and that the properties of these receptors may vary at different stages of postnatal development in both their levels of density and also in their degree of functionally active state.

Serotonergic$_{2A}$r's have been shown to be located both on 5-HTergic axon terminals (as autoreceptors) and glutamatergic afferent terminals (as heteroreceptors), on the cell bodies of GABAergic interneurons and also on the distal dendrites and cell bodies of pyramidal neurons in adult rats, monkeys and humans - **see Serotonin review section 7.9(A).(ii)** - while 5-HT$_{2C}$r's have been localised to pyramidal neurons and unidentified axon terminals in adult rats and humans - **see Serotonin review section 7.9(G).(ii)**.

The functionally active state of 5-HT receptors has been observed to vary in the developing rat hippocampus (Ike et al, 1995), as investigated with pharmacological techniques. Specifically, between the first and third week of postnatal development the identity of the functionally active 5-HT receptor (r) subtype linked to the 5-HT-induced phosphoinositide (PI) hydrolysis effector pathway was observed to switch from 5-HT$_{2A}$r's to 5-HT$_{2C}$r's.

It is possible that 5-HT$_{2A}$ and 5-HT$_{2C}$ receptors in the primate DLPFC may vary in their functionally active states during the course of various stages of development, such that the variations in the levels of 5-HT release or storage occurring at different ages, as indicated by the changes in varicosity density and axon length observed in this study may have relatively distinct effects at different stages of the postnatal period directly at 5-HT$_{2A}$r's on pyramidal neurons or indirectly on pyramidal neurons via action at 5-HT$_{2C}$r's localised to GABAergic interneurons (**see Concluding Discussion section 15.0,** for implications in schizophrenia).

The 5-HT system in the DLPFC has the potential for achieving a variety of modulatory effects on pyramidal neuron and interneuron activity, via different 5-HT receptor subtypes expressed specifically on the surfaces of different classes of neurons and on incoming thalamocortical and corticocortical afferents and those of other neurotransmitter systems (DAergic, NAergic and AChergic). The existence of indirect or direct actions of 5-HT on mid-layer 3 pyramidal neurons in the DLPFC, by way of diverse and perhaps temporally expressed receptor subtypes, may be integral to the prolonged maturational time course for pyramidal neuron spine acquisition and attrition seen in this cortical region during postnatal development in both monkeys and humans.

14.3: Comparison of the time courses of maturation for 5-HTergic axons and those for other neurotransmitter and neural components in layer 3.

Another rationale for testing the validity of the data for the 5-HTergic axon study was to directly compare the results with those of the other studies mentioned previously, which were carried out using material from all or part of the same age series of animals in area

46 of the monkey DLPFC. The premise being that if there are temporal correlation's between the time courses of some but not every cellular or axonal chemical marker in layer 3 during postnatal development, it is very probable that the differences observed between animals of different ages actually do exist *in vivo* and are in such a temporal alignment due to their intimate relationship with or participation in common events occurring at certain developmental stages. Comparing the timing of the changes in the levels of 5-HT varicosity and pyramidal neuron spine density across postnatal development, we concluded that there is a clear relationship between the 2 time courses, such that a close functional interaction is likely to exist between them, with 5-HT released from 5-HTergic varicosities acting via the specific 5-HT receptor subclass located on dendritic spines.

14.3(A).(i): Comparison of the postnatal time courses for 5-HTergic varicosity density (per 5000 μm^2) and pyramidal neuron spine density.

We find that there is some correlation between the timing of changes in total 5-HTergic varicosity density (per 5000 μm^2) for all 5-HTergic axons and those for mean spine density in layer 3, with a fall in total 5-HTergic axon varicosity density occurring during the climbing phase of spine density, recovery of the levels of 5-HTergic varicosity density as spine density values plateau and both measures decline concurrently at around puberty.

As well as similarities during the time courses (**see Figure 52A**) there was a disparity in the development of thick and thin 5-HTergic axons compared to that of spine density, as the varicosity density of thin 5-HTergic axons climbed immediately after birth to match that of the already higher thick 5-HTergic varicosity density.

14.3(A).(ii): Significance of the postnatal time courses for 5-HTergic varicosities per μm of axon and pyramidal neuron mean dendritic spine density.

This inverse temporal correlation in the first 10 weeks of postnatal development is hard to account for on the basis of direct interactions, since the majority of 5-HTergic varicosities in layer 3 of area in the adult monkey do not seem to form conventional synapses and those that do - on average about 23% of 5-HTergic varicosities at EM level - contact the relatively spine-free dendrites of GABAergic interneurons (Smiley and Goldman-Rakic, 1996). Since EM studies of 5-HTergic axons have not so far been conducted in younger animals, it is not known how the microanatomy of the 5-HTergic innervation may be organised in the developing monkey between birth and adulthood. If the majority of the small numbers of synapses formed by 5-HTergic axon varicosities are in fact primarily

associated with GABAergic interneurons even during early postnatal development, they may be in a position to indirectly regulate the acquisition of pyramidal neuron dendritic spines via disinhibitory effects on those interneurons (chandelier and basket neurons) which have inhibitory action on pyramidal neuron activity levels.

Different 5-HT receptor subtypes have been localised to various sites on cortical pyramidal neurons in a variety of adult mammalian species, which would certainly provide 5-HT with the means to play an intimate role in the maturational development of these ubiquitously found cells. Despite the evidence for very little direct synaptic interaction between 5-HTergic axon varicosities and pyramidal neurons in the monkey DLPFC the expression of these 3 distinct 5-HTr subtypes on different and in some cases the same portions of pyramidal neurons in the adult - and presumably during postnatal development of the - DLPFC provides an indirect means for 5-HT to significantly influence particular aspects of pyramidal neuron activity for large number of cells over a large area of cortex in quick succession. It is presumed that each receptor subtype has its own unique functional role (via effector or signal transduction pathways) in modulating the activity of pyramidal neuron output (excitatory postsynaptic action potentials) and input (afferent "drive" or inhibitory or excitatory presynaptic potentials).

Several 5-HTr subtypes have been localised to inhibitory interneurons in the same regions and species as those 5-HTr's expressed by pyramidal neurons. Specifically, 5-HT_{1A}r's have been found on the cell bodies of various kinds of non-pyramidal cells in rat cerebral cortex, 5-HT_{2A}r's are located on the cell bodies of GABAergic interneurons in the rat neocortex and in the monkey DLPFC, 5-HT_3r's are present on the cell bodies of GABAergic basket interneurons in the rat neocortex (mainly PV-IR), 5-HT_{4S}r's can be observed on the cell bodies and dendrites of non-pyramidal cells in the hippocampus and have been detected in the monkey (substantia nigra, striatum) and human (frontal cortex) brain and thus may at least be present in human cortical interneurons. This distribution of 5-HTr subtypes on GABAergic interneurons which are known to form extensive synaptic contacts with the cell bodies, AIS's and dendritic spines and shafts of pyramidal neurons in the adult monkey DLPFC and to have a strong inhibitory modulatory influence on their activity, provides another means by which the 5-HTergic axons in the DLPFC can potentially indirectly modulate pyramidal neuron activity in the DLPFC, i.e. by disinhibitive effects on GABAergic interneuron output to pyramidal neurons.

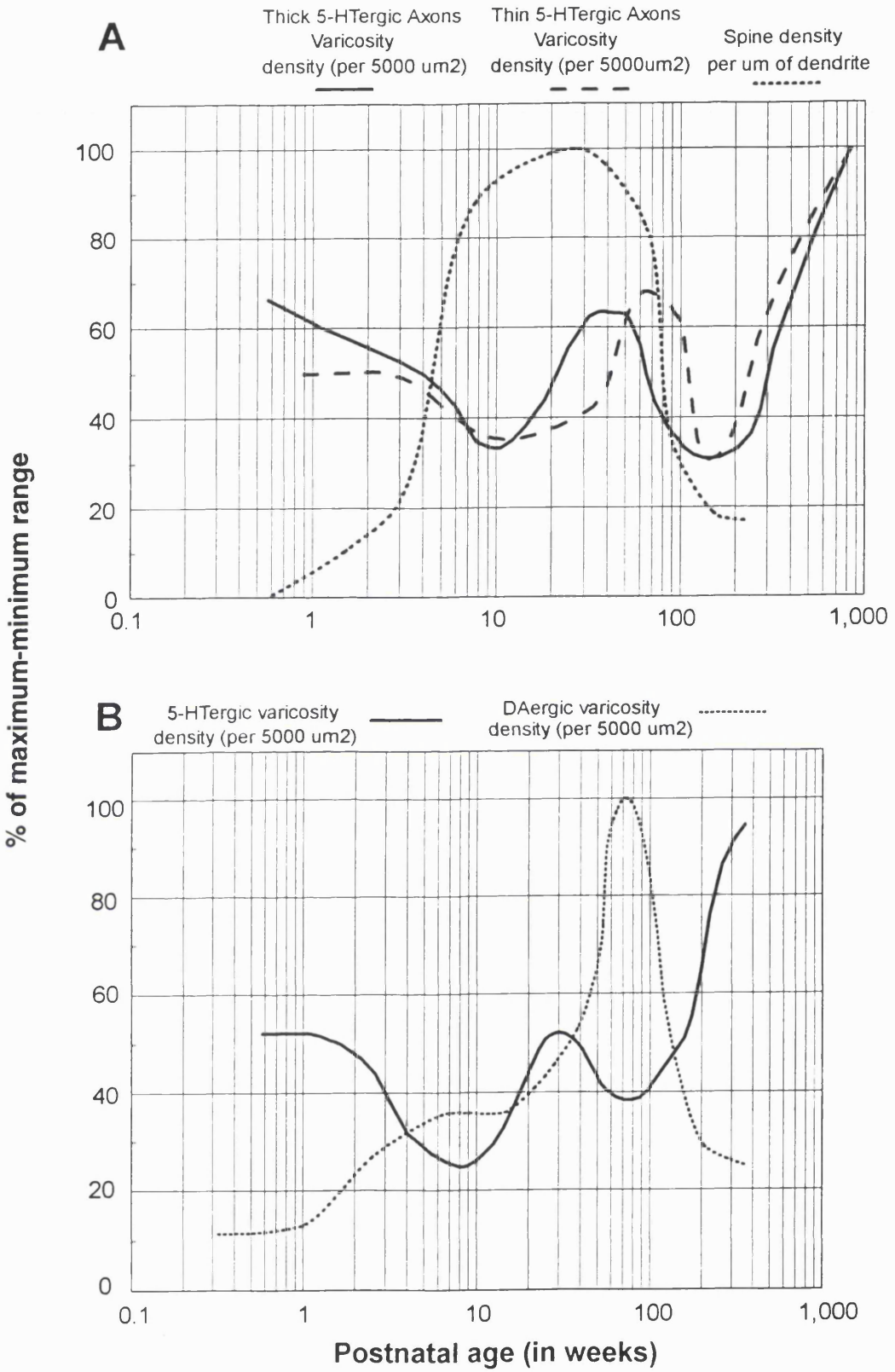

Figure 52. Schematic summary curves illustrating the percentage of maximum and minimum values for varicosity density of thick and thin 5-HTergic axons with a comparison to the spine density on mid-layer 3 pyramidal neurons and with the varicosity density for DAergic axons in deep layer 3. (data from Rosenberg and Lewis, 1995). **(A)** Varicosity density (per 5000 μm^2) for thick and thin 5- HTergic axons compared to spine density (per μm), **(B)** Varicosity density (per 5000 μm^2) compared for all 5-HTergic and DAergic axons.

14.3(B): Comparison of the postnatal maturation of the 5-HTergic axon innervation in mid-layer 3 and PV-IR neurons and PV-IR axon cartridges.

Two classes of local circuit neuron, i.e. chandelier and basket neurons, have been shown to express the calcium-binding protein parvalbumin (PV) in comparative Golgi and immunocytochemical studies in the monkey prefrontal cortex (Lewis and Lund, 1990; Lund and Lewis, 1993; Condé et al, 1994). The axons of chandelier neurons in Golgi preparations are seen to form characteristic termination's, i.e. "cartridges" composed of many varicosities targeting the axon initial segments (AIS) of un-impregnated pyramidal neurons in DLPFC (Lewis and Lund, 1990; Lund and Lewis, 1993, **see Neurotransmitters review section 6.5(B)**, for details on earlier studies in other cortical areas). Golgi-impregnated and PV-IR wide arbour or "basket" neurons have been described in the monkey DLPFC, but were only visualised in infant animals (Lund and Lewis, 1993).

Another immunocytochemical study at both light microscope and EM level in area 46 of adult monkey PFC (Williams et al, 1992) has demonstrated the presence of PV-IR basket neurons and also the characteristic pericellular cluster arrangements of their axon terminals which surround and form symmetric synaptic contacts with the cell body and the proximal dendrites of pyramidal neurons in layers 2 and 3, as previously only seen at light microscope level in visual (layers 5 and 6) and motor (layers 3 and 5) regions of the cerebral cortex (Hendry et al, 1989; Akil and Lewis, 1992a,b).

A third subtype of PV-IR interneuron has also been hypothesised to play a role in the local inhibitory circuitry of the DLPFC, namely the short axon multipolar cell, which is likely to be the source of many of the symmetric synapses formed between PV-IR varicosities and the dendritic shafts and spines of presumed pyramidal cells seen at EM level in layers 2 and 3 of area 46 (Williams et al, 1992).

Recently, it has been shown that varicosities of 5-HTergic axons form synaptic contacts with the somata of PV-IR neurons at EM level in area 46 of the adult monkey DLPFC (Jakab and Goldman-Rakic, 1996). From the evidence of 5-HTergic axon interactions with PV-IR interneurons, it might be expected that the time course of maturation for a sub-population (perhaps thick or thin classes) of 5-HTergic axons in mid-layer 3 would show a partial similarity to the postnatal time course for the overall numbers of PV-IR neurons in layers 2 and 3 of area 46, the limitation being that it is not known yet which of the 3 subclasses of PV-IR neuron might be contacted by 5-HTergic axons.

14.3(C): Comparison of the postnatal time courses for the maturation of 5-HTergic and DAergic axons in mid-layer 3.

The time course of maturation for DAergic axons during postnatal development (from the data of Rosenberg and Lewis, 1995) has been described already in the **Spine study discussion section 11.2(C)**. Here we will confine ourselves to a comparison of the changes in the levels of DAergic axons and varicosities during development relative to that for 5-HTergic axons and varicosities.

14.3(C).(i): Comparison of the varicosity density (per 5000 μm^2) for 5-HTergic and DAergic axons.

The time course of postnatal maturation of 5-HTergic axon varicosity density (per 5000 μm^2) appears to bear a reciprocal relationship to that of DAergic axon varicosities in layer 3 of area 46 (from Rosenberg and Lewis, 1995; **see Figure 52B**).

In order to test the degree of significance of the reciprocal pattern shown by the time courses for the varicosity density (per 5000 μm^2) of 5-HTergic and DAergic axons (**see Figure 52B**), it was decided to compare the data from the 5-HT study in both the age groups used in the DA study (Rosenberg and Lewis, 1995; i.e. **grouping B mentioned in the Results section 13.1(C),** as well as in age **grouping A** used for the 5-HT results in this thesis. The results for 5-HTergic axons in the above modified DA age **grouping B** can be summarised as follows (**see Figure 53A**): No statistically significant changes (F-ratio = 0.702, P = NS) were observed in the varicosity density (per 5000 μm^2) of the total 5-HTergic axon population during postnatal development. Neither were there any significant differences between age groups for the thick (F-ratio = 0.199, P = NS) or thin (F-ratio = 2.058, P = NS) 5-HTergic axon subclasses during the postnatal period (not shown).

The data for the complete set of animals used in the Rosenberg and Lewis (1995) study were modified by removing the measures for the 4 animals not used in the 5-HT study **(mentioned in the Results section, 12.1(C)**. The consequences of this reduced number of subjects on the DAergic axon varicosity density (per 5000 μm^2) measures during development can be summarised as follows (**see Figure 53B**): There was a significantly higher ($P < 0.05$) varicosity density (per 5000 μm^2) for the 2-3yrs age group than the < 1m age group. Also there was a markedly ($P < 0.10$) higher level of varicosity density (per 5000 μm_2) between 2-3yrs than for the 1-3m age group, which was just outside the $\alpha = 0.05$ significance level used in this thesis. The use of only those 18 animals used in both the DA and 5-HT studies has lowered the significance levels of those differences between the high

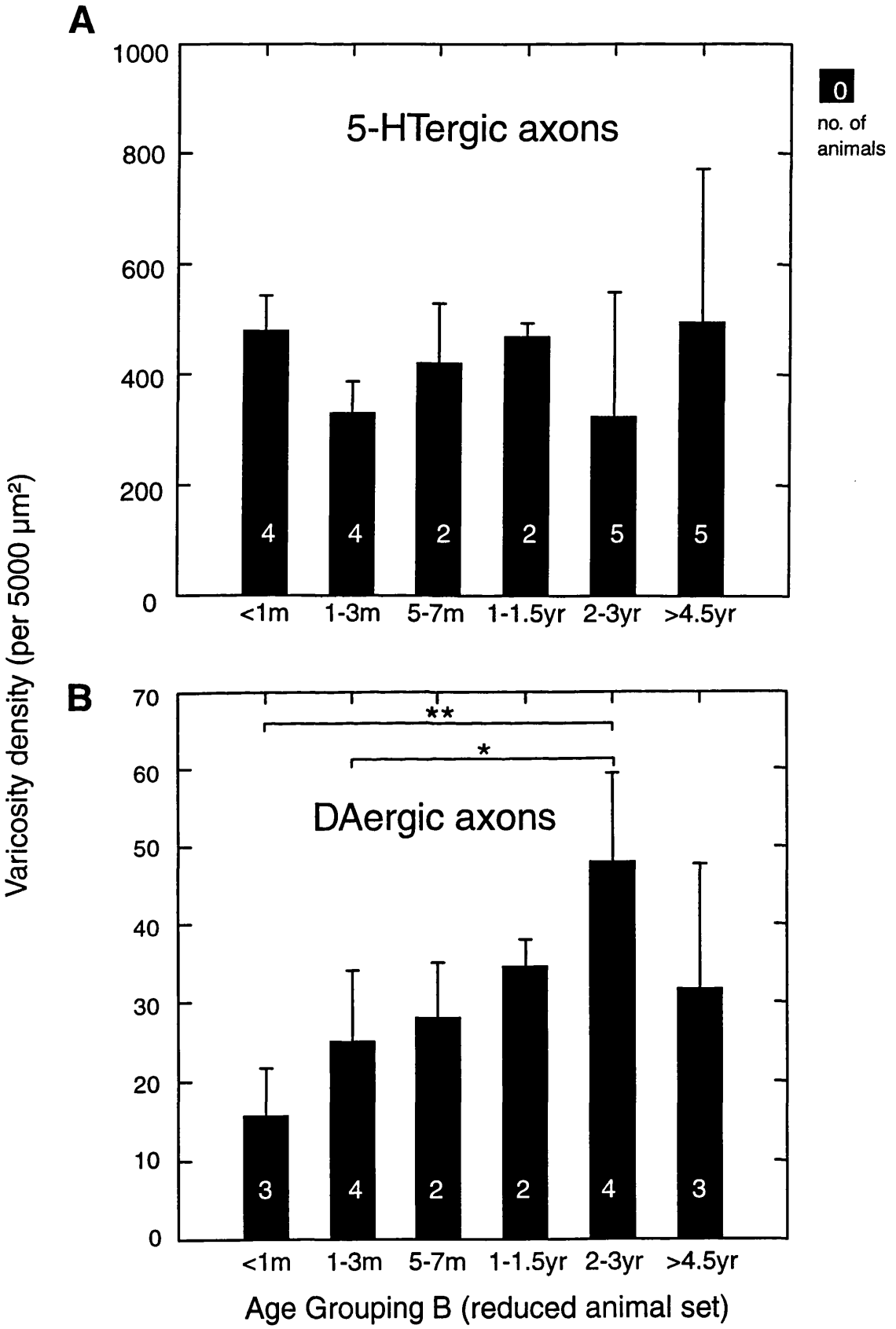

Figure 53. (A). The results for varicosity density (per 5000 μm^2) of all 5-HTergic axons in mid-layer 3 from the present study, re-plotted in the age groups used in the original DA study (Rosenberg and Lewis, 1995). No statistically significant changes over age were apparent for the 5-HTergic axons using age grouping B. **(B).** The results for DAergic axon varicosity density (per 5000 μm^2) from the original DA study (Rosenberg and Lewis, 1995), re-plotted for this present study using the age groups from that study, using only the 18 animals used in both DA and the 5-HT studies.

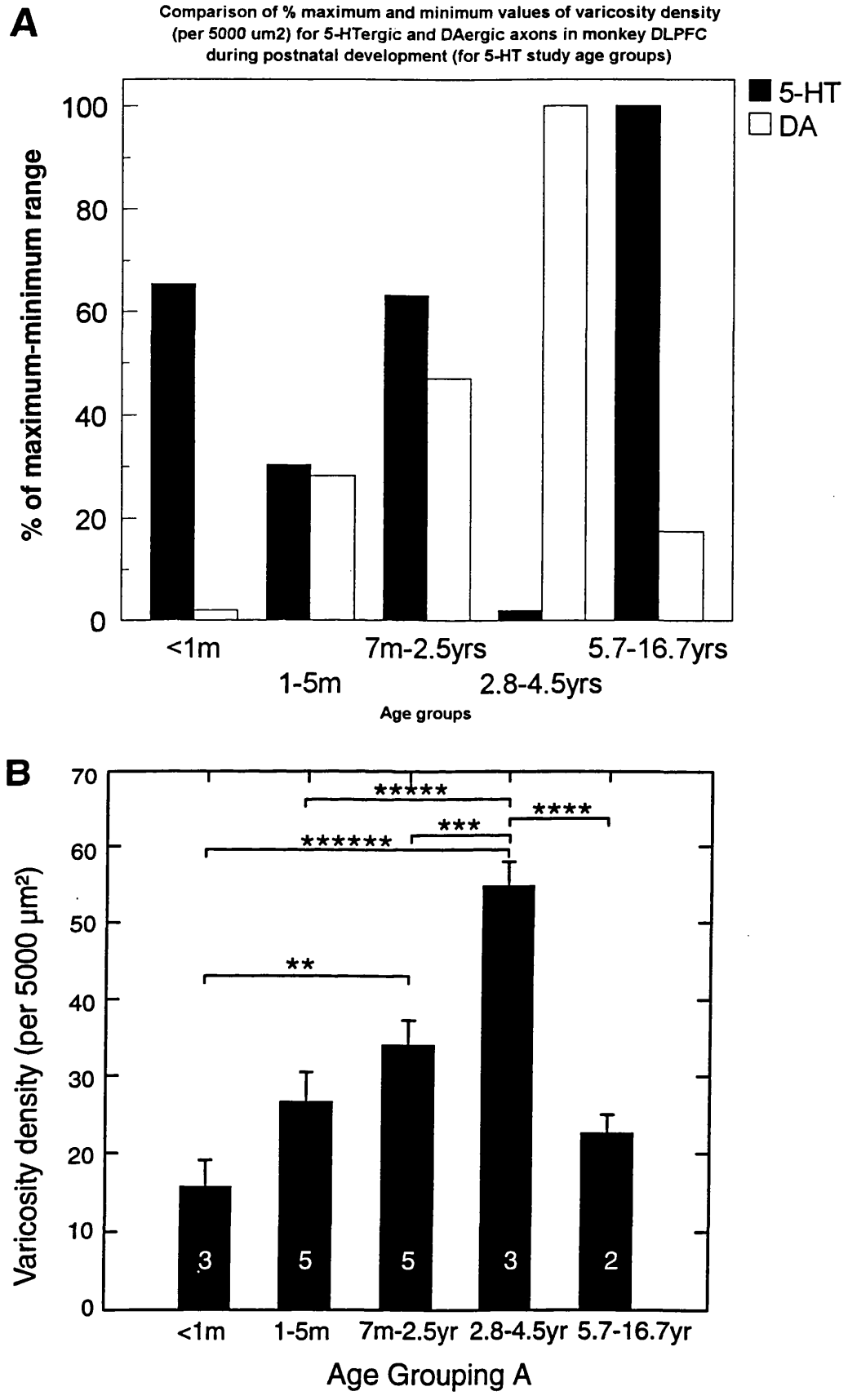

Figure 54. (A). A comparison of the percentage maximum-minimum range of values for varicosity density of all 5-HTergic axons (present study) and the re-plotted data from the original DA study (Rosenberg and Lewis, 1995). **(B).** The results for DAergic axon varicosity density (per 5000 μm^2)in their re-plotted format (from Rosenberg and Lewis, 1995) arranged in the age groups used in the present 5-HT study, for only the 18 animals used in both studies.

varicosity density (per 5000 μm^2) of the 2-3yrs age group and the < 1m age group. Also the highly significant levels in the differences for the other age groups and the 2-3yrs age group have been rendered non-significant. This transformation illustrates the limitations of attempting to compare the data from the 5-HT and DA studies in the age **grouping B** used in the DA study (Rosenberg and Lewis, 1995).

The transfer of the data for DAergic axon measures of varicosity density during development (retaining all animal ages) to the age groupings used in the present study of 5-HTergic axon varicosity density, has in fact retains the high levels of significance for the differences in DAergic varicosity density between age groups observed at various stages of development in the original study (Rosenberg and Lewis, 1995). This evidence suggests that as well as being an ideal grouping for changes in 5-HTergic axons across development, age **grouping A** may permit a more representative assessment of the changes occurring for DAergic axons during the same time period than for age **grouping B** from the original DA study (Rosenberg and Lewis, 1995).

For instance, the differences between the high levels of varicosity density in the 2.8-4.5 years age group compared to the lower values of the < 1m, 1-5m and 7m-2.5yrs age groups are of greater significance than the nearest equivalent groupings in the original study - although in the latter the 2-3yrs age group was significantly higher ($P < 0.05$) than all the other age groups across development, these were of lower significance levels than for the reorganised groupings here. In addition, this regrouping has brought 2 other differences between age groups to significance levels, that were evident but not significant in the original study, namely the higher levels at 7m-2.5yrs than < 1m and also the higher value for the 2.8-4.5yrs age group compared to that between 5.7-18.0 yrs.

Removal from this analysis of the 4 animals not utilised in the 5-HT study (**see Figure 54A**), in order to directly compare the 2 sets of data for the 5-HT and DA studies results in a slight drop in the significance levels (F-ratio = 13.018, $P < 0.0001$) of the above age group differences for the varicosity density of DAergic axons during development. There are slight reductions in the significance levels for the higher value of varicosity density (per 5000 μm^2) in the 7m-2.5yrs ($P < 0.05$) age group than in the < 1m age group and for the higher values at 2.8-4.5yrs compared to the 1-5m ($P < 0.05$) and 5.7-16.7yrs ($P < 0.005$) age groups. There is no change in the level of significantly higher varicosity density (per 5000 μm^2) between the 2.8-4.5 and < 1m age groups ($P < 0.0001$). Overall the differences observed above for all ages used in the DA study between the values of varicosity density for DAergic axons are reasonably robustly conserved, even when the 4

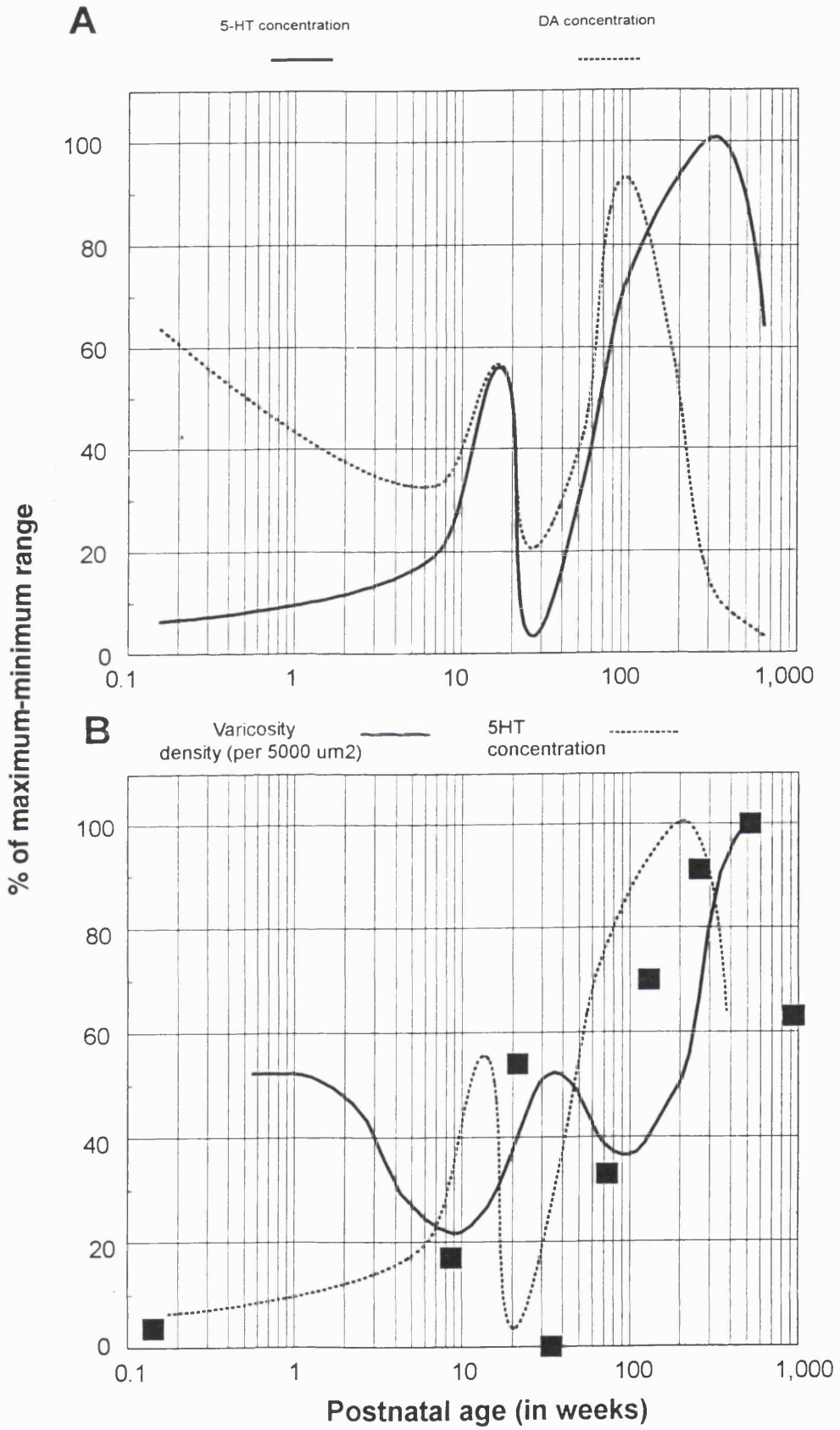

Figure 55. Schematic summary curves illustrating the percentage of maximum and minimum values for tissue concentrations of 5-HT and DA in the PFC (data plotted for thesis from Goldman-Rakic and Brown. 1981, 1982) compared and the varicosity density of all 5-HTergic axons in mid-layer 3 compared to the tissue concentration of 5-HT in the PFC. (data from Goldman-Rakic and Brown. 1981, 1982) **(A)** 5-HT and DA tissue concentrations (nmol/g), **(B)** Varicosity density (per 5000 μm^2) and 5-HT tissue concentration (nmol/g).

animals not used in the 5-HT study are omitted.

These observations provided a strong basis on which to directly compare the data for the 5-HT and DA studies in identical age groups with varicosity density values derived from analysis of tissue obtained from exactly the same animals. Comparing **Figures 52B** and **54B**, it is possible in both to see a basically inverse relationship between the percentage of maximum and minimum values for the levels of varicosity density (per 5000 μm^2) for 5-HTergic and DAergic axons during development. Thus at < 1m, 5-HT value is high and DA is low, at 1-5m the DA value is high, whilst the 5-HT one is low, for 7m-2.5yrs the 5-HT level is high again and DA is about the same

The above rearrangements of the DA study data (from Rosenberg and Lewis, 1995) into age groupings appropriate for a comparison with the 5-HT results have shown that a strong degree of reciprocity exists between the relationship of the time courses of development for the DAergic and 5-HTergic axon populations in the monkey DLPFC. In this new format this relationship is more obvious than could be observed for the original DA data and the 5-HT study data separately. In addition the replotting of the DA study for both all its original animal ages and without those omitted in the 5-HT study, reveals a greater level of significance for the differences in DAergic axon varicosity density at various stages across development in the monkey DLPFC.

We also examined the degree of reciprocity between the time courses of development for the 5-HTergic and DAergic axon populations in **Figure 52B**. As we used in the comparison of thick and thin 5-HTergic axons in **section 14.2 (see for rationale behind test),** the Spearman rank correlation coefficient was employed to examine the relative strength of the temporal relationship between the 2 axon populations. In terms of total varicosity density (per 5000 μm^2), for the 5-HTergic and DAergic axon populations, r_s = - 0.362 (- 36%; P = NS), i.e. there was greater evidence for a reciprocal relationship than one of concurrence, between 5-HTergic and DAergic axons during development. There was a much greater degree of reciprocity between the 2 neurotransmitter axon populations for total varicosity density compared to total axon length. The difference in rankings for the two axon populations, in terms of total axon length (in μm; per 5000 μm^2), was r_s = - 0.117 (P = NS). Since r_s = -1.0, represents absolute reciprocity between 2 related populations, it can be only be tentatively concluded, that there is a greater degree of reciprocity (-12%), than of concurrence between the time courses of 5-HTergic and DAergic axons during postnatal development.

A comparison of the tissue concentration of 5-HT (Goldman-Rakic and Brown, 1981, 1982) and the varicosity density for 5-HTergic axons in the DLPFC (from this thesis; **see Figure 55B**) would suggest that the changes in density of 5-HT varicosities is the converse of the changes in the tissue levels of the neurotransmitter 5-HT itself. This suggests that high levels of 5-HTergic immunoreactivity in varicosities might reflect a local sequestering of 5-HT; as the levels of 5-HTergic varicosities decline, the tissue levels of 5-HT increase and vice versa, throughout the course of development and during normal adulthood.

A comparison of the developmental time courses for thick 5-HTergic axons and DAergic axons in terms of varicosity density (per 5000 μm^2) using the Spearman rank correlation coefficient test, resulted in $r_s = -0.441$ (- 44%; $P < 0.05$,1-tailed; P = NS, 2-tailed). The same comparison made between thin 5-HTergic and DAergic axons yielded a value of $r_s = -0.406$ (- 41%; $P < 0.05$, 1-tailed; P = NS, 2-tailed). In terms of axon length (in μm, per 5000 μm^2), the value for thick 5-HTergic and DAergic axons was $r_s = -0.313$ (- 31.0 %; P < NS, 1-tailed; P < NS, 2-tailed), whilst the value for thin 5-HTergic and DAergic axons was $r_s = 0.081$ (+ 8%; P = NS, 1-tailed; P = NS, 2-tailed).

A similar finding of a reciprocal relationship between the time courses of 5-HT and DA system development seen in this thesis, was observed by Goldman-Rakic and Brown (1982) in their study of the postnatal maturation of monoamine tissue concentration levels in the monkey cerebral cortex (including the PFC). However, Goldman-Rakic and Brown (1982) found that the concentrations of 5-HT and DA tissue concentration were only inversely related in the youngest and oldest age groups (i.e. new-borns and 2.0-3.0 years of age) while there was a synchrony in the levels for the intervening age groups (**see Figure 55A**).

Goldman-Rakic and Brown (1982) found there to be a striking reciprocity in the rates of production of serotonin (as measured by 5-HTP production) and dopamine (as measured by DOPA production). They stated that "a consistent finding at all ages is that the distribution of catecholaminergic (i.e. DA and noradrenaline) synthesis varies inversely with that of serotonergic synthesis, indicating substantial interaction in the regulation of the two cortical systems."

In a study of the tissue concentrations of monoamines in adult and ageing monkeys Goldman-Rakic and Brown (1981) found that as for the developing animals, there was some evidence of reciprocity in the levels of 5-HT and DA over senescence, mostly due to relatively stable high levels of 5-HT and a significant decrease in the levels of DA in the 2

oldest groups of animals (**see Figure 55A**). Goldman-Rakic and Brown (1981) stated that there appeared to be no evident change in 5-HT levels throughout adulthood and neither did the levels of 5-HTP change significantly between 2.0-3.0 years and > 18.0 years of age.

In the present thesis study, however the levels of background neuropil 5-HT immunoreactivity (presumably representing tissue or extracellular levels of 5-HT released prior to the animals' perfusion) were proportionally related to the levels of 5-HT present within the axon innervation of layer 3. Thus, high neuropil levels of 5-HT were more often than not accompanied by high levels of 5-HT stored in axons and varicosities. These observations are the converse of that expected from the Goldman-Rakic and Brown studies, above.

Much more needs to be known regarding the mechanisms *in vivo*, which regulate and control the rates and absolute levels of turnover for 5-HT, i.e. its release, synthesis and re-uptake and what relative rates are expressed in the mid-brain cell synthesis, compared to levels in their cortical axon varicosities and release into cortical tissue. Many questions still remain unanswered as to what immunohistochemical findings in adults, as well as in developing animals may mean in terms of functional activity and modulatory influence. For now, in the absence of convincing evidence to the contrary, we shall presume that the high levels of 5-HT present in axons and varicosities at different ages in the DLPFC is representative of potentially high levels of release and availability of the neurotransmitter at that stage of development. These are believed to change dynamically over time, with regard to many variables in the short-term such as stress and physiological demands, as well as more long-term influences such as genetic predisposition, rearing conditions (again stress has an influence here) and any other effects such as the animal's diet, sexual development, other endocrine influences and history of disease.

Despite the apparent observation of concurrent tissue levels of 5-HT and DA during most of the pre-adult postnatal period (concerning relations to the development of other cortical components; i.e. 10 weeks to 4 years of age) by Goldman-Rakic and Brown (1981, 1982), there is compelling evidence from other studies in the adult monkey to suggest that 5-HT and DA exhibit a reciprocal relationship in both the relative distribution of their tissue levels (Brown et al, 1979) and axons (Lewis et al, 1985; Berger et al, 1986, 1988; Lewis, 1990; Schwartz and Mrzljak, 1992) in cortical and subcortical areas. This suggests that 5-HT and DA may play complementary roles in various aspects of behaviour which are likely to involve multiple brain regions.

The innervation of cortical regions by DAergic and 5-HTergic axons may show

a complementary laminar organisation, most notably in the DLPFC - Berger et al (1988); Lewis (1990); compare Lewis (1988) or Williams and Goldman-Rakic (1993) with Wilson and Molliver (1991a). This implies that the most dense portions of these innervations are likely exhibit their most potent modulatory influences over classes of neurons located in different layers, each with specific patterns of afferent projection targets and reciprocal incoming afferents. Also both DA and 5-HT demonstrate mutually inhibitory and excitatory modulation of each other's release via presynaptic or non-synaptic release-site heteroreceptors (e.g. 5-HT receptors sited on DAergic axon terminals and vice versa) and also via neuronal, i.e. somato-dendritically-located receptors - **see Neurotransmitter review sections 6.1(E) and 6.2(E).**

The significance of the variations in the tissue levels of 5-HT and DA in the early part of postnatal development and throughout adulthood (Goldman-Rakic and Brown, 1981, 1982) can be examined in the light of pharmacological studies conducted with 5-HT and DA receptor antagonists and agonists in the medial PFC of adult rats (Pehek, 1996) and the neostriatum in baboons (Dewey et al, 1995) and humans (Tiihonen et al, 1996; Smith et al, 1997). These studies have concluded that complex interactions exist between the levels of 5-HT and DA in both the DLPFC and the neostriatum, which are presumed to be mediated via the binding of each neurotransmitter to its variously located receptor subtypes. There thus exists indirect pharmacological evidence (**see above studies**) that 5-HT and DA can reciprocally modulate each others release, by way of the heteroreceptors located on the others axon varicosities.

The evidence from 5-HTr antagonist studies in the rat medial PFC (Nomikos et al, 1994; Pehek et al, 1996) is that 5-HT may inhibit intrinsic cortical DA release by its action at 5-HT_{2A}r's located on DAergic axons. Other studies comparing the effects of direct administration of 5-HT and 5-HTr agonists on DA release, usually demonstrate increased extracellular levels of DA, via the activation of 5-HT_{1B}r's or 5-HT_{3}r's located on DAergic axon varicosities in the anterior neostriatum (Benloucif and Galloway, 1991; Benloucif et al, 1993).

The PET receptor-binding studies of 5-HT and DA interactions in humans have been restricted to an examination of the neostriatum only. Tiihonen et al (1996) have found that the administration of a 5-HT transporter (or re-uptake site) inhibitor, citalopram, incurred a slight decrease in the binding of a DA antagonist ($[^{11}C]$-raclopride) at D_2r's, thought to indicate increased levels of DA release, modulated by 5-HT. Another recent study (Smith et al, 1997) has used the same D_2r antagonist to investigate the effects of another potent 5-

HT re-uptake inhibitor, fenfluramine on levels of DA release, again a significant increase in specific D_2r binding was observed, reflecting raised levels of extracellular DA in the striatum, modulated by 5-HT.

The results of these studies demonstrate that due to the different weightings of 5-HT and DA receptor subtypes in the cortex and neostriatum, care should be taken in trying to extrapolate the findings of 5-HT and DA interactions in the rat and human neostriatum, to those seen in the rat medial PFC. Despite the observation of similar 5-HT and DA receptor interactions in the baboon neostriatum (Dewey et al, 1995), it is not possible to say for certain, what interactions may be taking place between 5-HT and DA, via their different receptor subtypes in the adult (less still the developing) monkey DLPFC.

14.4: Final Conclusions.

The changes in the levels of 5-HT and its receptors in the monkey DLPFC during development are likely to be inextricably linked to the formation and refinement of intrinsic lattice circuitry by layer 2/3 pyramidal neurons and therefore associated with, perhaps the nearest equivalent measure of a critical period for the DLPFC to that found for example for ocular dominance columns in the visual cortex. It may be that 5-HT receptor subtypes, e.g. 5-HT_{1D}r's or 5-HT_{2A}r's are localised on the axon terminals of the recurrent collateral's arising from intrinsic pyramidal neurons which form the lattice structure through layers 1-3 in the DLPFC. Additionally, other 5-HT receptor subtypes present on pyramidal neurons participating in the intrinsic lattice (either furnishing these projections and/or the target of them) could express 5-HT_{1A}r's on their axon initial segments and 5-HT_{2C}r's on their cell bodies and dendrites.

The inhibitory GABAergic "basket" neurons proposed to reciprocally interact with this pyramidal neuron lattice (Lund et al, 1993; Goldman-Rakic, 1995b, 1996) may express 5-HT_{2A}r's or 5-HT_3r's on their cell bodies or 5-HT_{1D}r's on their axon terminals in contact with pyramidal neurons. These various 5-HT receptor subtypes are known to be expressed on different portions of pyramidal neurons, GABAergic interneurons and axon terminals in various species and regions. Immunohistochemical studies of the adult monkey DLPFC with specific antibodies are required to show whether these various 5-HT receptor subtypes are in fact localised to the same or similar portions of the cellular components of the excitatory intrinsic lattice circuitry and its modulatory local circuit interneurons as have been found in previous studies in other regions and species. Secondly, the developmental time courses of the expression of these 5-HT receptor subtypes is needed to establish which of

them may exist at transiently high levels at different stages of development. In combination with the modulatory effects of other neurotransmitters, such as DA, and the expression of their receptor subtypes on the various neuronal portions of this circuitry, 5-HT and certain 5-HT receptors might prove to be important ingredients in the maturational "chemical cocktail" which could ensure the correct formation of axonal arbours, dendritic trees, dendritic spines and synaptic connectivity as a gradual process beginning prior to birth and continuing through development until puberty. This stage of development in primates (monkeys and humans) would seem to be the culmination of many maturational processes (anatomical and functional), seemingly with different time courses in different layers of the DLPFC region (dendritic spines on pyramidal neurons in layers 4 and 6 - unpublished observations from our laboratory; PV-IR axon cartridges, PV-IR neurons, CCK-IR neurons and DAergic axons; discussed in Anderson et al, 1995; Rosenberg and Lewis, 1995 and Condé et al, 1996; **see in Concluding Discussion section 15.0**).

The observations of this thesis **study 2**, regarding the maturation of the 5-HT innervation in layer 3, in relation to the expression of various 5-HT receptors, could have important implications for the normal development of the pyramidal neuron intrinsic excitatory lattice circuitry in the DLPFC of monkeys (as examined in **study 1** of the thesis) and humans. The findings in both **studies 1 and 2** of this thesis, could also be important for the reformulation of the various hypotheses of a neurodevelopmental cause underlying the emergence of an array of devastating symptoms - thought at least to be partly due to significant loss of integrative, cognitive and mnemonic functions in the DLPFC - exhibited in the early-onset (puberty/late adolescence) of schizophrenia (reviewed in Lewis and Anderson, 1995; Weinberger, 1995, 1996).

15.0: Concluding Discussion.

15.1(A): The postnatal maturation of the primate DLPFC: hierarchical or concurrent pattern of developmental time course within DLPFC and between DLPFC and other cortical areas.

In considering the broader implications of our findings from the two studies in this thesis, concerning the maturation of the monkey DLPFC, it should be asked if a similar time course for 5-HTergic axon and pyramidal neuron maturation occurs in all laminar depths in the DLPFC and even across all cortical areas; or if the events we have described for layer 3 are unique to that particular environment in the superficial layers in the DLPFC. We have reviewed evidence - **see sections 2.2(A) and (B)** - for two broad theories of cortical

development. One theory, which is the most recently formulated of the two - **see section 2.2(A)** - proposes that all cerebral cortical areas in the primate (i.e. monkeys and humans) show a synchronous developmental time course, including concurrent maturation of all layers in these areas. The second theory which has been long-standing for nearly a century - **see section 2.2(B)** - proposes that the various cortical regions reach their anatomical and hence functional maturity, in a sequence based on a hierarchy of the relative complexity of their information processing and their level of participation in sensory-, cognitive- and motor-guided behaviours. In this case, the sensory areas, such as primary visual and auditory cornices would reach their adult state earlier than the more cognitively-related association regions such as the DLPFC, with variations in the time of maturation among individual layers, both between and within each region.

15.1(B): The relation of the time courses of postnatal development for pyramidal neurons, 5-HTergic axons and other components in layer 3, to the overall maturation of the monkey DLPFC.

Comparing the results in studies 1 - **see Spine study section 9.1(A) and (B) -** and 2 - **see Serotonin study section 13.1(B) and (C)** - with other studies of anatomical maturation in area 46 of both macaque monkeys and humans - **see Spine and Serotonin study Discussion sections 11.2(A-E) and 14.3(A-D)** - several similarities and differences are apparent.

The general time course for pyramidal neuron dendritic spine development in our study of layer 3 in areas 9 and 46, was very similar to that for the maturational development of asymmetric (excitatory) synaptic density in layer 3 of area 46 (Bourgeois et al, 1994), with a rapid phase of synaptic and spine growth, during the first 10 weeks of life reaching a peak at around 2 months of age, remaining at a plateau level and declining in later life. However, the exact timing of these events in the 2 studies also demonstrated important differences, with the declining phase in our study, characterised by a steady reduction in the numbers of dendritic spines, occurring earlier in development (from 1.5 years of age to 4.6 years) than the markedly protracted plateau phase and later more gradual decline (from 3.0 years of age) in the density of asymmetric synapses throughout adulthood (Bourgeois et al, 1994). The difference in the rate of decline between asymmetric synapses and the majority of their postsynaptic sites, i.e. spines, may be due to the fact that synaptic loss is more protracted than that for spines. This difference may be accounted for by the variation between the time courses of maturation for asymmetric synapses, many associated with the apical

dendrites passing through layer 3, of pyramidal neurons in deeper layers, by inclusion of asymmetric contacts onto non-spiny cells, i.e. smooth interneuron dendrites or changes in neuropil volume during development.

Comparison with other postnatal developmental studies of components of cortical circuitry in various layers of areas 9 and 46 in the monkey DLPFC (Mrzljak et al, 1990, 1992; Rosenberg and Lewis, 1995; Condé et al, 1996) reveals that different cortical layers show different schedules of development for pyramidal neurons, neurotransmitter-specific axons and interneurons, e.g. PV-IR axon cartridges and dopaminergic axons. There is also variation between these components within the confines of a particular laminar environment, e.g. differences between DAergic axons in middle and deep layer 3.

Different time courses of morphological development have been observed for layer 3 and 5 pyramidal neurons in the human DLPFC on the basis of changes in their basal dendritic tree (Mrzljak et al, 1990; Mrzljak et al, 1992; Koenderink et al, 1994; Koenderink and Uylings, 1995). Layer 3 pyramidal neurons appeared to mature earlier than layer 5 pyramidal neurons, since they attained a mature level of dendritic length and branching by the beginning of the first year of postnatal life, while layer 5 pyramidal neurons grew rapidly in the first year and continued to develop in their dendritic extent and branching up until 5.0 years of age.

Although we demonstrate that the developmental time courses for the elements of 2 distinct but synaptically-connected cell populations in layer 3 are virtually identical (pyramidal neuron dendritic spines and parvalbumin-IR changes in chandelier neuron axon cartridges), in the same layer the developmental progression of maturation for dendritic spines and dopaminergic axons shows marked differences in the form of their time course. Nonetheless, coincidence at several points during the developmental time course of dendritic spines and dopamine, suggests that dopamine may play a role in the developmental regulation of the processes of spine acquisition and loss on the dendrites of pyramidal neurons in layer 3 of the monkey DLPFC. The temporal concurrence of the periods of maximal change for both of these components of the cortical circuitry in this layer, implies that there is some functional interrelation and it is known that DAergic synapses occur on pyramidal neuron dendritic spines - **see Neurotransmitters section 6.1(C)**. Additionally, both systems could also be under the influence of a common regulatory substance, e.g. hormones or growth factors.

In summary, our observations in the DLPFC give support to a hierarchical mode of cortical development in the macaque monkey brain, with a later completion of maturation for the DLPFC than for the primary sensory regions, e.g. area 17, as well as differential rates of development even within single layers of a region, for different cellular components.

15.2(A): The relevance of developmental anatomical studies in monkeys to observations made in post-mortem human material and to developmental hypotheses for the aetiology of schizophrenia.

There have been several theories proposed in the last decade or so which have highlighted the possibility of an aberrant process of maturation in cortical regions - including the DLPFC - during postnatal development as a cause for schizophrenia (reviewed in Jones, 1995; Lewis and Anderson, 1995; Weinberger and Berman, 1996). These hypotheses are based on the observation of many and varied anatomical abnormalities found to exist in the post-mortem schizophrenic human brain, which could contribute to the cognitive dysfunction's evident in the performance of tasks requiring high levels of focused attention, mnemonic ability, goal-directed behaviour or planning and also the implied alterations in levels of neuronal activity observed in functional imaging studies.

It is of importance for us to examine the anatomical and functional evidence which supports the above hypotheses and consider how the disruption of developmental events in the normal monkey DLPFC described in this thesis might contribute to behavioural disturbance in later life.

Various cortical components have been implicated in the aetiology of schizophrenia, including abnormal levels of synaptic proteins, e.g. synaptophysin and GAP-43, altered levels of dopamine, serotonin, GABA or glutamate and their receptors, aberrant sets of certain CBP-containing GABAergic interneurons as well as overall alterations in the densities of neurons and changes in the proportions of cells based on their somal size.

Observations indicating that normal neuronal migration may be disrupted for many classes of neurons as part of the aetiology of schizophrenia, are important in that this could result in the malformation of intrinsic lattice circuitry in the superficial layers of the DLPFC, as well as an abnormal balance of excitatory and inhibitory neural elements and their interrelations during development.

15.2(A).(i): Pyramidal neurons and dendritic spines.

As mentioned in the **Pyramidal neuron review section 5.0**, there have been several reports of abnormally low levels of dendritic spines on the pyramidal neurons in the DLPFC of the post-mortem schizophrenic brain (Garey et al, 1995; Glantz and Lewis, 1995, 1996), a finding which has been localised particularly to pyramidal neurons in layer 3 (Glantz and Lewis, 1996). On the basis of the normal process of synaptic "pruning" during puberty in the DLPFC, observed both in monkeys (Rakic et al, 1986) and in humans (reviewed in

Huttenlocher, 1993), it has been hypothesised that the DLPFC, with a more prolonged time course of maturation than other cortical regions, is more vulnerable to long-lasting effects of abnormal developmental events (Feinberg, 1987, 1992; Saugstad, 1994). Aberrant developmental processes might occur prenatally or in the early postnatal period (reviewed in Jones, 1995) and the resultant anatomical and functional ramifications may not become apparent until puberty, the typical time of onset for the symptoms of schizophrenia. With regard specifically to dendritic spines, hypotheses (Feinberg, 1982; Keshavan et al, 1994) have predicted that excessive synaptic "pruning" or the opposite, i.e. ineffectual synaptic "pruning", leading to depleted or excessive levels of synapses, respectively might account for the timing and types of symptoms emerging around the time of puberty in schizophrenic patients.

Our developmental studies in the macaque monkey would suggest that if the same processes do occur in normal humans, then puberty would be a very vulnerable period for the disruption of various cortical components in the DLPFC, which would seem to mature around this time. For the monkey DLPFC, puberty is known to be a time of complex interactions between neurotransmitters, excitatory and inhibitory neurons and the refinement of excitatory synapses. Abnormal patterns of events occurring for any one of these components, e.g. 5-HT, DA or pyramidal neurons themselves, would almost certainly derail the normal sequence of events in the formation of the intricately-organised intrinsic lattice circuitry of the superficial layers. The result of this failure in normal maturational processes in the DLPFC would undoubtedly be manifested in the form of dysfunctional behaviours due to deficits in cognitive and mnemonic information processing, as are observed in most cases of schizophrenia.

15.2 (A).(ii): Glutamate receptors.

As reviewed in the **Pyramidal neuron review section 5.10,** many pyramidal neurons in monkey and human neocortex, express NMDA and non-NMDA receptor subunits, as do many GABAergic interneurons. The presence of these receptors in the DLPFC on various pyramidal neurons in layers 2 and 3, involved in intraareal intrinsic lattice circuitry, as well as sending extrinsic projections to other cortical and subcortical regions and receiving incoming glutamatergic afferents from pyramidal neurons in other cortical regions allows for activity-dependent modulation, which is likely to be most susceptible to aberrant disruption during the late maturational phase, i.e. around puberty.

Changes in the levels of mRNA signal coding for particular NMDAR's have

been reported for the DLPFC of the post-mortem schizophrenic brain. These changes have been hypothesised to be at least partially the result of an abnormal series of developmental errors in the maturation of the reciprocal corticocortical and thalamic-connecting pyramidal neuron circuitry which ultimately may lead to subtle specific alterations in many diverse neurotransmitters, synaptic proteins and receptor classes (Akbarian et al, 1996).

Such potential alterations in the normal complements of both NMDA and non-NMDA receptors in the human DLPFC, each known to play an important role in the normal modulation of information processing via excitatory cortical projections in the monkey neocortex, would almost certainly impinge on the maturation of the intrinsic lattice circuitry of the DLPFC, as well disrupt its numerous interactions with interareal connections during development and in their subsequent refinement. The presence of NMDA and non-NMDA receptor subunits on asymmetric synapses in adult monkeys, implies that they may have been present at these sites associated with pyramidal neuron dendritic spines from the early stages of postnatal development. Increased levels of these receptors might thus be expected to accompany the rising levels of excitatory synapses and dendritic spines seen during the first two months of postnatal life. It might also be expected that the density of glutamate receptors might decrease in line with either the decline in spine numbers (from 1.5 years of age) or synapses (from 3.0 years of age). No studies have yet been conducted of NMDA or non-NMDA receptor development in the monkey DLPFC, although a preliminary study in the visual cortex (area 17) has shown that several subtypes of these receptors, exhibit changes of density that seem to show some temporal coincidences in line with the synaptic development of this sensory cortical region.

15.2(B): γ-aminobutyric acid (GABA)ergic interneurons and GABA receptors.

An increase in the density of the CB-IR class, but not PV-IR or CR-IR classes of GABAergic interneurons has been found within layer 3 of the DLPFC in schizophrenics. Since the axons of CB-IR neurons are known to form synaptic contacts with the dendritic shafts and spines of pyramidal neurons in many cortical areas - **see Neurotransmitters section 6.5(D)** - a rise in the numbers of cells exhibiting CB-IR, might indicate an alteration in the degree of inhibitory regulation of at least some of the excitatory pyramidal neuron intrinsic and corticocortical circuitry as part of the aetiology of this disease. In terms of the symptoms which are manifested by patients, such as the disintegration of cognitive and mnemonic functions; these could clearly be interpreted as a lack of appropriate modulation of pyramidal neurons by GABAergic cells. Since CB-IR neurons may also form synaptic contacts

with other interneurons, abnormally high numbers of neurons demonstrating CB-IR in schizophrenics, may also reflect abnormal inhibitory modulation among subtypes of interneurons, which could also adversely affect their regulation influence over pyramidal neuron excitatory activity.

Lack of appropriate GABAergic modulation could permit the abnormal excitation of intrinsic connectivity in the DLPFC, since a constant flow of information from diverse afferent inputs converges on these pyramidal neurons as well as inputs from other layers. Hence, an unregulated or inappropriate modulation of excitatory neurotransmission might ensue within the pyramidal neuron lattice circuitry, which could cause extensive disruption throughout the PFC as a whole, since the layer 3 intrinsic lattice circuits in DLPFC appear not to be restricted to cytoarchitectonic borders but spread continuously across areas 9 and 46 and probably across other PFC areas.

There is also known to be extensive interaction of callosal and associative corticocortical pathways (**see Anatomical connections review section 3.6**) between different PFC regions (including the DLPFC, cingulate, orbital and ventrolateral areas) primarily mediated by layer 3 pyramidal neurons. In schizophrenia, a lack of inhibitory regulation in just one region e.g. area 46, producing overactivity or inappropriate patterns of activity might invoke disturbance of processing in more distant regions as well as the possible dissociation of limbic functions (in orbital PFC) from those of mnemonic (DLPFC, FEF and ventrolateral areas) and motor-related functions (cingulate areas). A general overactivity or imbalance in the information flow among these projection pathways correlates with some reports of "hyperactivity" of blood-flow observed in the DLPFC region in rCBF studies of schizophrenics, which may in turn be indicative of the phases of florid symptoms (hallucinations and delusions, etc) which have been described for most patients.

Changes have also been noted in the density of GABA receptors in the post-mortem DLPFC of schizophrenic patients, with a selective up-regulation of the $GABA_A$ receptor subtype reported in cingulate and DLPFC (area 10) regions, but no changes in the levels of $GABA_A$ receptor mRNA expression in the DLPFC (area 46). The increase in the presence of $GABA_A$ receptors in the DLPFC and cingulate cortex has been hypothesised to correlate with the findings of "hypoactivity" of blood-flow in the DLFPC region from rCBF studies in schizophrenic patients. These observations might perhaps be indicative of the phase of negative symptoms (loss of affect, blunting of emotion, social isolation) often observed in chronic, so-called untreatable schizophrenics, in between their acute bouts of positive symptoms or manic episodes. The lack of alteration in gene expression for $GABA_A$

receptors, means that the increase in numbers of binding sites would most likely be due to post-translational or post-synthesis changes in the production of these receptors. The extrinsic connections between different areas of the PFC and the cingulate cortex would suggest these GABAergic receptor changes to have widespread disruptive effects even if limited to specific areas.

15.2(C): Serotonergic and dopaminergic neurotransmitter and receptor interactions.

The DAergic axon innervation of the DLPFC in monkeys and humans is present at a moderate density in layer 3 and is known to directly contact the dendritic spines and shafts of pyramidal neurons as well as their PV-IR interneuron modulators - **see Neurotransmitters review section 6.1(B)**. In view of the remedial effects of neuroleptic drugs on DA release and binding at its variously located receptors in primates (Lidow and Goldman-Rakic, 1994; Lundberg et al, 1996) dopamine has been implicated in playing a major role in the biochemical mechanisms of dysfunction in schizophrenia, including its role in the DLPFC (Carlsson, 1988; Weinberger, 1988).

This thesis provides anatomical evidence in the macaque monkey that there are likely to be extensive interactions between 5-HT and DA during the course of postnatal development in layer 3 of the DLPFC and there is considerable pharmacological evidence to support the existence of extensive modulatory interactions between 5-HT and DA. The enormous range of potential locations for 5-HT-DA interaction in the primate brain, including within the DLPFC, at the level of both presynaptic and postsynaptic receptors located on axon terminals and neurons, may account for many of the complex effects of atypical antipsychotic drugs which appear to alleviate both the positive and to some extent the negative symptoms exhibited in schizophrenia (Lundberg et al, 1996; reviewed in Hagan et al, 1993; Kahn and Davidson, 1993; Schmidt et al, 1995; Kapur and Remington, 1996).

This interaction of 5-HT and DA is exhibited also in the demonstration of a reciprocal relationship for the tissue concentrations of 5-HT and DA (Goldman-Rakic and Brown, 1981, 1982) and for the densities of 5-HTergic and DAergic axons and varicosities - Rosenberg and Lewis (1995) and **5-HT study Discussion section 14.3(C).(i) -** during the course of postnatal maturation and senescence. In addition the hourly rates of 5-HT and DA neurotransmitter turnover and synthesis (Brown et al, 1979) within individual adult monkeys have been found to show reciprocity in their values, whilst a complementary laminar distribution for 5-HTergic and DAergic axons has been described using a thin section autoradiographic visualisation technique in the DLPFC of the adult monkey (Berger et

al, 1986, 1988) - **see 5-HT study Discussion section 14.3(C).(i).**

There appears to be a process of structural or biochemical compensation by the 5-HTergic system for reduced levels of DA or DAergic axons implying that the 5-HT and DA systems are interactive or mutually inhibitory. The emergence of high levels of 5-HT and an excessive 5-HTergic axon innervation could be an attempt to correct the imbalance between the 5-HTergic and DAergic innervations by a form of plasticity involving 5-HT in a facilitatory role, e.g. by activating growth factors such as S100ß (Azmitia et al, 1990).

15.3: Summary.

The major findings of the two studies which form the basis for this thesis are:

1. Using quantitative analysis, changes in the numbers of dendritic spines present on Golgi-stained pyramidal neurons in layer 3 of the monkey DLFPC (areas 9 and 46), were used as an indication of the degree of pyramidal neuron synaptic maturation across the course of postnatal development. The time course of spine development consisted of an initially rapid rise in spines in early postnatal life, with a plateau phase characterised by high levels of spines from 10 weeks to 1.5 years of age and a gradual but steady decline in spine numbers thereafter until around 4.5 years of age. This time course parallels that for asymmetric synapses reported previously for all layers in area 46 (Bourgeois et al, 1994). However, there appeared to be an earlier initiation (at 1.5 years of age) to the phase of refinement for dendritic spines, compared to that found for excitatory synapses (3.0 years of age onwards). Since mid-layer 3 pyramidal neurons provide unique intrinsic intraareal and extrinsic interareal connectivity patterns, their developmental time course should thus be indicative of the "critical period" for the anatomical and functional maturation of the DLPFC.

2. The time course of pyramidal neuron spine development shows a striking similarity to the time course of development of a particular class of inhibitory input, the PV-IR axon cartridges of chandelier neurons in area 46 (Anderson et al, 1995), known to terminate synaptically onto the axon initial segments of layer 3 pyramidal neurons in the DLPFC. This close match of developmental time courses of pre- and postsynaptic sites is thought to imply the balance of weight of inhibitory modulation to the weight of excitatory input to the layer 3 pyramidal neurons during the phases of rapid growth and refinement of high numbers of dendritic spine synapses.

3. The schedule of dendritic spine maturation in layer 3 was found to show a temporal relationship to stages of the maturational time course of DAergic axons in the same layer of area 46 (Rosenberg and Lewis, 1995). The varicosity density of DAergic axons rises in

2 stages during postnatal development, the first rise coinciding with the increase in pyramidal neuron spine density and the second rise is in temporal alignment with the reduction of spines. These close temporal relations are taken to indicate a modulatory involvement of DA in spine development. This hypothesis is supported by previous evidence of DAergic axon varicosities forming synaptic contacts with pyramidal neuron dendritic spines and shafts as well as with the smooth dendrites of PV-IR neurons (modulators of pyramidal neurons) in the monkey DLPFC.

The initial rise in DAergic varicosities and dendritic spines may reflect indirect DAergic disinhibitory action on spines, via the suppression of the PV-IR neuron inhibitory influence over pyramidal neurons, while the second rise in DAergic varicosities with concurrent decline in spines, may indicate the direct inhibitory modulation of pyramidal neuron spines.

4. In a quantitative analysis of immunohistochemically-labelled 5-HTergic axons in layer 3 of the monkey DLPFC (area 46), the postnatal time course of development for all 5-HTergic axons (in terms of their varicosity density per 5000 μm^2) exhibits a complex cyclical time course, consisting of 2 distinct stages (infancy and puberty/early adulthood) when low varicosity densities predominate and 3 stages (neonatal period, juvenile phase and later adulthood) when there is a high density of varicosities.

5. Evidence from previous studies has suggested that 2 forms of 5-HTergic axons exist in the adult macaque monkey cerebral cortex. In this thesis, we have attempted to differentiate the individual developmental time courses for these 2 sub-populations of axons in layer 3 of the DLPFC. Despite careful analysis of 5-HTergic axons, clear differentiation of 5-HTergic axons into 2 morphological forms was not clearly evident. Using a criterion of larger versus finer diameter varicosities and intervaricose segments to attempt to analyse separate sub-populations, it was not possible to demonstrate a different pattern of maturational time course for two 5-HTergic axon sub-populations, although the timing of each stage was slightly different for the 2 groups we defined. This led to the conclusion that 5-HTergic axon sub-populations are either not clearly distinguishable in their forms during development or the 2 types of 5-HTergic axons almost certainly follow a common time course of maturation.

6. A comparison of the maturational sequences of 5-HTergic axons and dendritic spines in layer 3, revealed that there may be some correspondence between the timing of rises and falls in the 5-HTergic varicosity density and the rise and fall of dendritic spines during postnatal development. Coincidence between the 5-HT system and pyramidal neurons occurred between the fall in 5-HTergic varicosity density and the rise in dendritic

spines, recovery in 5-HTergic varicosity density with the plateau phase of spine numbers, the fall in the density of 5-HTergic varicosities and the decline in dendritic spines and finally the rise in 5-HTergic varicosity density and achievement of mature levels of spine density. Previous evidence suggests that 5-HTergic axon varicosities in the adult monkey DLPFC form synaptic contacts primarily with GABAergic interneurons (PV-IR and CB-IR types) and only a minority with pyramidal neurons, suggesting a lack of direct synaptic modulation of pyramidal neuron maturation by 5-HT. However, as for DA and its receptor distribution on pyramidal neurons, some 5-HT receptors are known to be localised to pyramidal cells (5-$HT_{1A,\ 2A}$ and others to GABAergic interneurons, providing 5-HT with an alternative extra-synaptic means to modulate these neurons.

7. Comparing the maturational time courses for 5-HTergic axons, as defined in this thesis and DAergic axons (as defined by Rosenberg and Lewis, 1995), in terms of their varicosity density (per 5000 μm^2) in area 46, revealed a remarkable degree of reciprocity in density between these 2 neurotransmitter innervations in layer 3, across the entire age range of animals examined (the same animals were analysed in both studies). This inverse relationship in the numbers of potential 5-HT and DA release sites over postnatal development suggests a complementary modulation of each other's activity, via receptors known to be located on their axon varicosities.

The maturation of dendritic spines may be partially mediated by both these neurotransmitters. with 5-HT mediating GABAergic interneuron (e.g. CB-IR and PV-IR varieties) inhibitory influence over pyramidal neuron excitatory activity, while DA provides direct innervation to postsynaptic sites of excitatory input to pyramidal neurons. Alternatively, other components of the layer 3 circuitry not examined in this study may be modulated by the actions of 5-HT and DA release and these in turn might affect the pyramidal neuron excitatory lattice circuitry.

8. By re-plotting the DAergic axon data of Rosenberg and Lewis (1995) in the age groups that showed significant changes for 5-HTergic axons during development, we were able to show significant reciprocity between the changes in varicosity density for 5-HTergic and DAergic axons across postnatal development. This led to the conclusion that our selection of age groups may provide a more exact representation of the time-scale for interactions across postnatal development, between the different components of the cortical circuitry in layer 3 of the monkey DLPFC.

9. The time courses of development for 5-HTergic axon varicosity density and 5-HT tissue concentration (Goldman-Rakic and Brown, 1981, 1982) in the DLPFC, also

appeared to show a reciprocal relationship during postnatal development. It is not immediately apparent why the mean levels of released 5-HT free in the neuropil should be the inverse of the mean levels of 5-HT stored in varicosities at each age, but it is possible that this reflects variations in rate of synthesis and turnover of 5-HT at each age, although it is significant that previous studies in the DLPFC of developing and adult monkeys suggest that the rate of 5-HT synthesis and breakdown remains at relatively the same mean rates throughout postnatal life.

However, preliminary evidence supporting changes in 5-HT production, release and re-uptake during development is shown by the changes in the density of varicosities positive for an antibody specific to the 5-HT transporter in PFC area 9 (Kye and Lewis, unpublished observations). This transporter molecule mediates the re-uptake of released 5-HT and exhibits a time course synchronous with our analyses of 5-HT varicosity density during development. Also, the varicosity density of axons positive for the 5-HT synthetic enzyme, tryptophan hydroxylase in layer 3 of area 46 have been found to show a reciprocal developmental relationship to the time course for 5-HTergic axon varicosity density in this same location (Kye and Lewis, unpublished observations). Both these additional observations would seem to support our finding of a cyclical time course of progression for 5-HTergic axons in area 46, during postnatal development.

10. All of these temporal relationships for pyramidal neuron dendritic spines and 5-HTergic axons described above in points **1-9**, are relevant to the postnatal development of the uniquely stripe-like terminal fields of pyramidal neuron intrinsic lattice circuitry in layers 1-3 of the DLPFC (area 9 and 46). The dendritic spines of pyramidal neurons in layer 3, studied in this thesis reflect both pre- and postsynaptic sites contributing to this intrinsic lattice structure, which is on of the chief anatomical substrates for DLPFC function in primates. From the above observations, it is apparent that DA and 5-HT are likely to play very important roles in the modulation of this structural development in the superficial layers of the DLPFC; this modulation of most probably includes both synaptic and non-synaptic components, involving the participation of a variety of 5-HT and DA receptor subtypes.

11. In conclusion, the implications of the results from the 2 studies in this thesis and the comparative developmental relationships demonstrated between them has provided an important contribution to the continuing process of establishing the temporal relations of events occurring in the normal postnatal development of the monkey DLPFC.

As described in the detailed introduction: **section 2.3**, the developmental time course for different cortical layers, as well as maybe differing between distinct cortical regions,

may even vary within the same cortical area, or perhaps differs for particular neuronal populations and their various cellular compartments, according to their immediate laminar environment, i.e. the hierarchical hypothesis . In the case of basal dendritic spine density for layer 3 pyramidal neurons, the pattern of changes in levels of spines with time, indicates that anatomical - and by extrapolation - the functional maturation of area 46, is achieved much later (around 2.5-3.0 years) than for the corresponding layer 3 pyramidal neurons in primary visual cortex (1.0 year; area 17; Boothe et al,1979). The alternative pattern of cortical development, i.e. the concurrent hypothesis, as described in **section 2.2**, can be partially discounted on the basis that the developmental study of excitatory synapses in layers 1-6 in area 46 (Bourgeois et al, 1994), did not take into account the fact that different compartments of a given pyramidal neuron are likely to exhibit different rates of developmental time course. The same is true of synaptic development studies conducted in other cortical areas (Rakic et al, 1986), of which careful re-examination may later bring to light that these different regions do indeed show a similar level of concurrent maturation at the gross laminar level, but at the neuronal level, development may be found to be more specifically related to their immediate laminar environment.

In the case of 5-HTergic axons, the evidence for differential rates of development between cortical areas, is less clear since we only have the current quantitative thesis study in area 46 and a qualitative study conducted in area 17 (Foote et al, 1984). It would appear from a comparative examination of the 5-HTergic axon development in the 2 regions, that area 46 achieves its mature level of 5-HTergic axon innervation density at a later age (around 3.0 years) than area 17 (5-7 months). In addition, in area 46, the mature levels of 5-HTergic axon innervation do not appear to remain stable for long, but from 6.0 years onwards they appear to vary throughout the rest of adulthood.

12. The accumulation of information forming the basis of this thesis will potentially provide a firm anatomical basis for modelling human DLFPC maturation and will facilitate further investigation of anatomical, neurophysiological and pharmacological aspects of the superficial layer intrinsic lattice circuitry of the monkey DLFPC. These studies lay a better foundation for the pathological studies of disrupted structure and function in the human DLPFC, disruption which would seem to be integral to the dysfunction of working memory and cognitive processing that is characteristic of schizophrenia. The developmental studies in this thesis may ultimately help to reveal the contribution that the abnormal development of the human DLPFC may make towards symptoms of working memory deficit, as observed in schizophrenic patients.

15.4: Appendix.

15.4(A): Graphs from Spine study results - S. Anderson contribution to Anderson et al (1995).

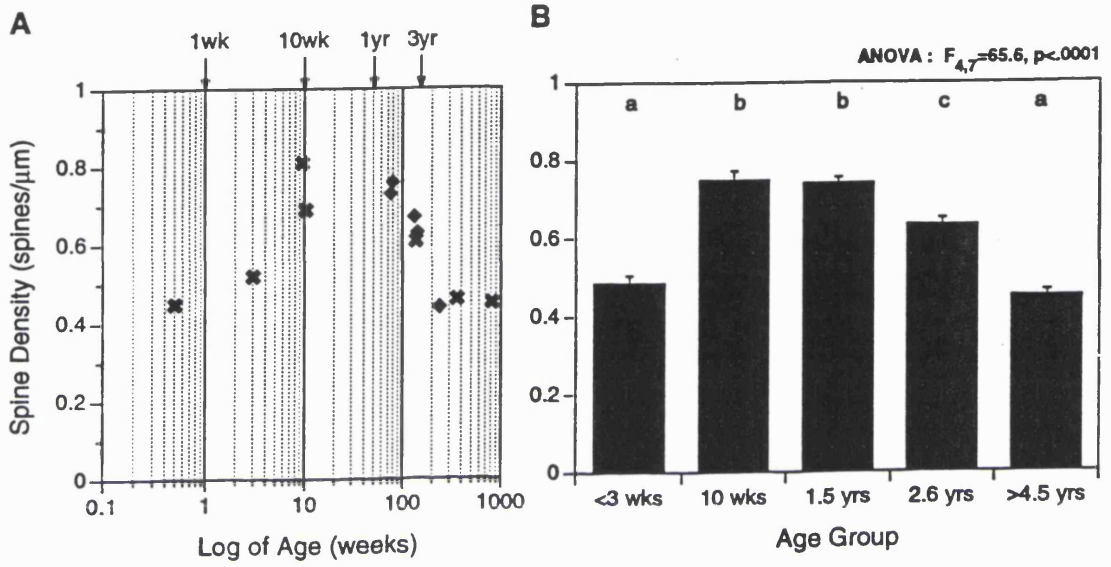

Figure 56. Mean relative spine density (per µm) on apical dendrites of mid-layer 3 pyramidal neurons (Golgi study 1 in Anderson et al , 1995). **(A)** histogram showing the results for individual animals on a proportional logarithmic time scale and **(B)** bar plot showing the results plotted in 5 age groups used for Golgi studies 1 and 2 in Anderson et al, (1995). Standard errors indicated. Figure from Anderson et al, (1995).

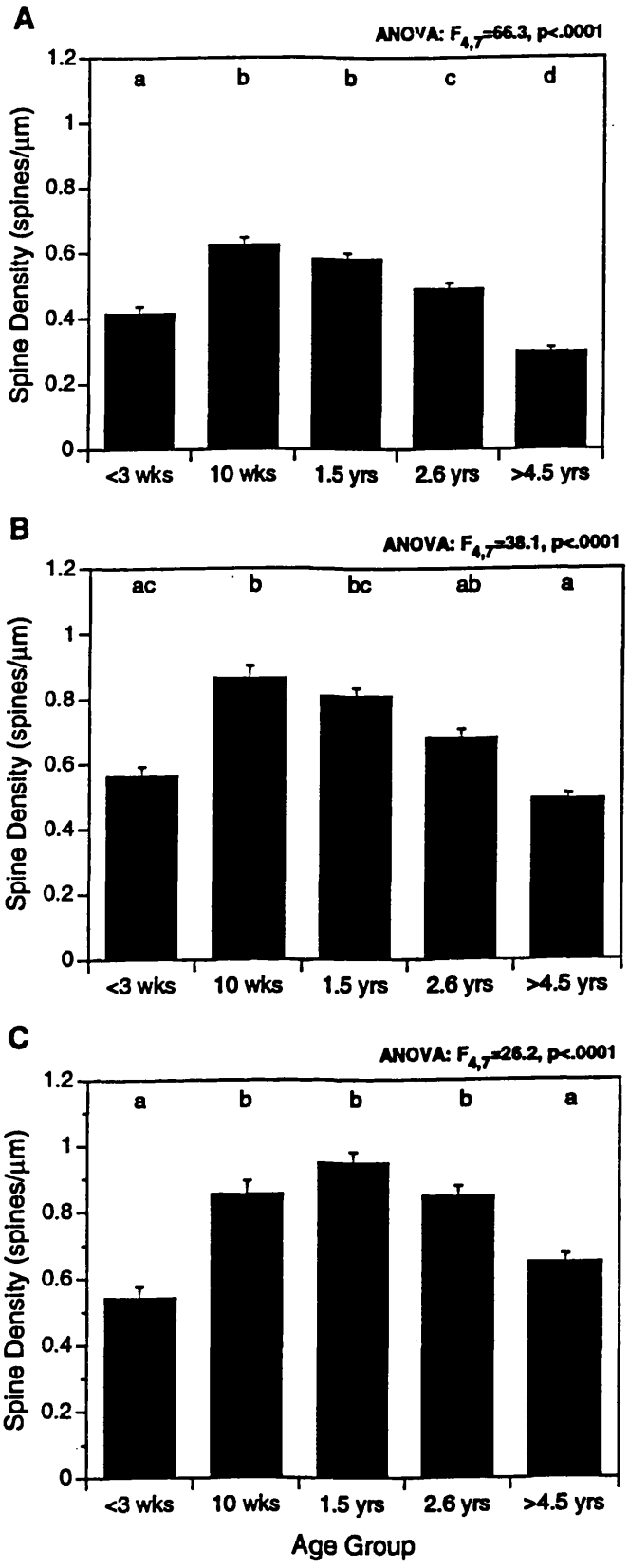

Figure 57. Variability of mean relative spine density (per µm) for different laminar locations on apical dendrites of mid-layer 3 pyramidal neurons (Golgi study 1 in Anderson et al, 1995). (A) shows the spine density (per µm) for proximal portions close to the cell body in mid-layer 3, (B) shows spine density (per µm) for middle portions located in layer 2 and superficial layer 3 and (C) shows spine density (per µm) for distal portions situated in layer 1. Notice a slightly different time course of spine development in the proximal portions compared to the middle and distal portions of apical dendrites, i.e. in mid-layer 3 relative to layers 1 and 2, indicating that there might be a slightly later maturation of spine numbers in mid-layer 3. Standard errors are shown. Figure from Anderson et al , (1995).

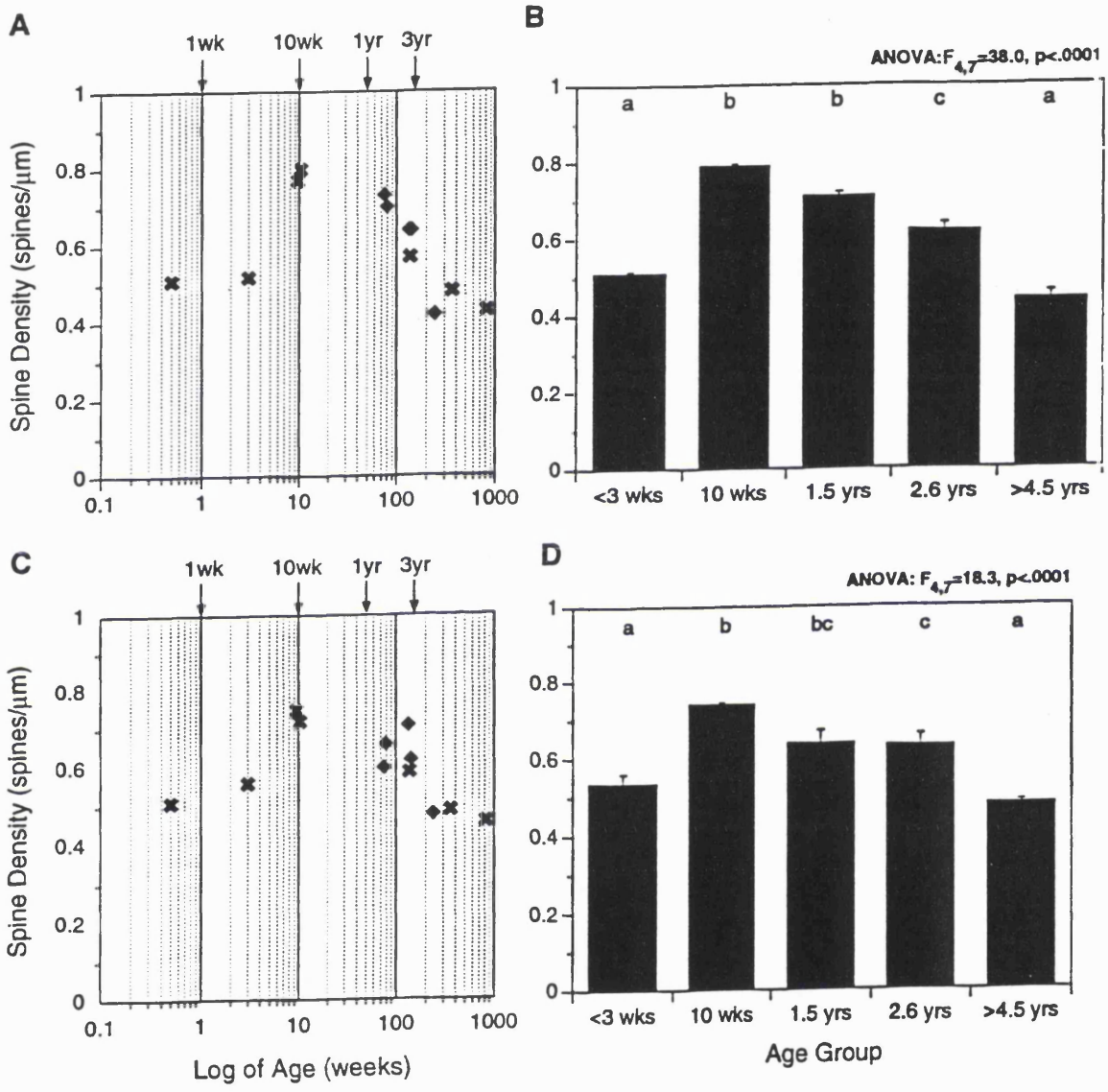

Figure 58. Mean relative spine density (per µm) on apical oblique (**A** and **B**) and basal (**C** and **D**) dendrites of mid-layer 3 pyramidal neurons (Golgi study 1 in Anderson et al, 1995). (**A** and **C**) histogram showing results for individual animals on a proportional logarithmic time scale, (**B** and **D**) bar plot showing the results plotted in 5 age groups used for Golgi studies 1 and 2 in Anderson et al, (1995). Standard errors are shown. Figure from Anderson et al, (1995).

16.0: References.

Akbarian, S., J.J. Kim, S.G. Potkin,W.P. Hetrick, W.E. Bunney Jr and E.G. Jones (1996) Maldistribution of interstitial neurons in prefrontal white matter of the brains of schizophrenic patients. **Arch. Gen. Psychiatry. 53:425-436.**

Akil, M. and D.A. Lewis (1992a) Postnatal development of parvalbumin immunoreactivity in axon terminals of basket and chandelier neurons in monkey neocortex. **Prog. Neuro-psychopharmacol. and Biol. Psychiat. 16:329-337.**

Akil, M. and D.A. Lewis (1992b) Differential distribution of parvalbumin-immunoreactive peri-cellular clusters of terminal boutons in developing and adult monkey neocortex. **Exp. Neurol. 115:239-249.**

Alexander, G.E. (1982) Functional development of frontal association cortex in monkeys: Behavioural and electrophysiological studies. **In Rakic, P. and P.S. Goldman-Rakic (Eds) Development and Modifiability of the Cerebral Cortex. The MIT Press, Cambridge, Massachusetts. USA. pp 492-507.**

Alexander, G.E., M.D. Crutcher and M.R. DeLong (1990) Basal ganglia-thalamocortical circuits: Parallel substrates for motor, oculomotor, "prefrontal" and "limbic" functions. **In Uylings, H.B.M. et al (Eds) Progress in Brain Research, Vol. 85: Elsevier Science Publishers, BV, Amsterdam, pp 119-146.**

Alexander, G.E., M.H. DeLong and P.L. Strick (1986) Parallel organisation of functionally segregated circuits linking basal ganglia and cortex. **In Cowan W.M. et al (Eds) Ann. Rev. Neurosci., Vol. 9: Annual Reviews, Inc., Palo Alto, pp 357-381.**

Alexander, G.E. and P.S. Goldman (1978) Functional development of the dorsolateral prefrontal cortex: An analysis utilising reversible cryogenic depression. **Brain Res. 143:233-249.**

Alvarez-Bolado, G., P. Rodriguez-Sanchez, P. Tejero-Diez, A. Fairen and F.J. Diez-Guerra (1996) Neurogranin in the development of the rat telencephalon. **Neurosci. 73:565-580.**

Amunts, K., V. Istomin, A. Schleicher and K. Zilles (1995) Postnatal development of the human primary motor cortex: A quantitative cytoarchitectonic study. **Anat. Embryol. Berl. 192:557-571.**

Andersen, R.A., C. Asanuma, G. Essick and R.M. Siegel (1990) Corticocortical connections of anatomically and physiologically defined subdivisions within the inferior parietal cortex. **J. Comp. Neurol. 296:65-111.**

Anderson, S.A., J.D. Classey, F. Condé, J.S. Lund and D.A. Lewis (1995) Synchronous development of pyramidal neurons dendritic spines and parvalbumin-immunoreactive chandelier neuron axon terminals in layer III of monkey prefrontal cortex. **Neurosci. 67:7-22.**

Anderson, S.A., J.D. Classey, D.A. Lewis and J.S. Lund (1993) Postnatal developmental changes in dendritic spine density on layer III pyramidal neurons in monkey prefrontal cortex. **Soc. Neurosci. Abstr. 19:1445.**

Armand, J., S.A. Edgley, R.N. Lemon and E. Oliver (1994) Protracted postnatal development of corticospinal projections from the primary motor cortex to hand motoneurones in the macaque monkey. **Exp. Brain Res. 101:178-182.**

Arnsten, A.F.T., J.X. Cai, B.L. Murphy and P.S. Goldman-Rakic (1994) Dopamine D_1 receptor mechanisms in the cognitive performance of young adult and aged monkeys. **Psychopharmacol. 116:143-151.**

Arnsten, A.F.T., J.X. Cai, J.C. Steere and P.S. Goldman-Rakic (1995) Dopamine D_2 receptor mechanisms contribute to age-related cognitive decline: The effects of quinpirole on memory and motor performance in monkeys. **J. Neurosci. 15:3429-3439.**

Arnsten, A.F.T. and P.S. Goldman-Rakic (1984) Selective prefrontal cortical projections to the region of the locus coeruleus and raphe nuclei in the rhesus monkey. **Brain Res. 306:9-18.**

Asanuma, C., R.A. Andersen and W.M. Cowan (1985) The thalamic relations of the caudal inferior parietal lobule and the lateral prefrontal cortex in monkeys: Divergent cortical projections from cell clusters in the medial pulvinar nucleus. **J. Comp Neurol. 241:357-381.**

Azmitia, E.C., K. Dolan and P.M. Azmitia-Whitaker (1990) S100ß but not NGF, EGF, insulin or calmodulin is a serotonergic growth factor. **Brain Res. 516:354-356.**

Azmitia, E.C. and P.J. Gannon (1986) The primate serotoninergic system: A review of human and animal studies and a report on *Macaca fascicularis*. **In Fahn, S. et al (Eds) Advances in Neurobiology. Vol. 43: Myoclonus, Raven Press, New York, N.Y. pp 407-468.**

Bachevalier, J. and M. Mishkin (1984) An early and a late developing system for learning and retention in infant monkeys. **Behav. Neurosci. 98:770-778.**

Baizer, J.S., L.G. Ungerleider and R. Desimone (1991) Organisation of visual inputs to the inferior temporal and posterior parietal cortex in macaques. **J. Neurosci. 11:168-190.**

Barbas, H. (1988) Anatomic organisation of basoventral and mediodorsal visual recipient prefrontal regions in the rhesus monkey. **J. Comp. Neurol. 276:313-342.**

Barbas, H. (1992) Architecture and cortical connections of the prefrontal cortex in the rhesus monkey. **In Chauvel, P. et al (Eds) Advances in Neurology, Vol. 57, Raven Press Ltd, New York, pp 91-115.**

Barbas, H., T.H. Haswell Henion and C.R. Dermon (1991) Diverse thalamic projections to the prefrontal cortex in the rhesus monkey. **J. Comp. Neurol. 313:65-94.**

Barbas, H. and M-M. Mesulam (1981) Organisation of afferent input to subdivisions of area 8 in the rhesus monkey. **J. Comp. Neurol. 200:407-431.**

Barbas, H. and D.N. Pandya (1989) Architecture and intrinsic connections of the prefrontal cortex in the rhesus monkey. **J. Comp. Neurol. 286:353-375.**

Barbas, H. and D.N. Pandya (1991) Patterns of connections of the prefrontal cortex in the rhesus monkey associated with cortical architecture. **In Levin, H.S. et al (Eds) Frontal Lobe Function and Dysfunction. Oxford University Press, Oxford, pp 35-58.**

Barr, G.A., T.C. Eckenrode and M. Murray (1987) Normal development and effects of early deafferentation on choline acetyltransferase, substance P and serotonin-like immunoreactivity in the interpeduncular nucleus. **Brain Res. 418:301-313.**

Benloucif, S. and M.P. Galloway (1991) Facilitation of dopamine release *in vivo* by serotonergic agonists: Studies with microdialysis. **Eur. J. Pharmacol. 200:1-8.**

Benloucif, S., M.J. Keegan and M.P. Galloway (1993) Serotonin-facilitated dopamine release *in vivo*: Pharmacological characterisation. **J. Pharmacol. Exp. Ther. 265:373-377.**

Bennett-Clarke, C.A., N.L. Chiaia, R.S. Crissman and R.W. Rhoades (1991) The source of the transient serotoninergic input to the developing visual and somatosensory cortices in rat. **Neurosci. 43:163-183.**

Bennett-Clarke, C.A., R.D. Lane and R.W. Rhoades (1995) Fenfluramine depletes serotonin from the developing cortex and alters thalamocortical organisation. **Brain Res. 702:255-260.**

Bennett-Clarke, C.A., M.J. Leslie, N.L. Chiaia and R.W. Rhoades (1993) Serotonin$_{1B}$ receptors in the developing somatosensory and visual cortices are located on thalamocortical axons. **Proc. Natl. Acad. Sci. USA 90:153-157.**

Bennett-Clarke, C.A., M.H. Hankin, M.J. Leslie, N.L. Chiaia and R.W. Rhodes (1994a) Patterning of neocortical projections from the raphe nuclei in perinatal rats - Investigation of potential organisational mechanisms. **J. Comp. Neurol. 348:277-290.**

Bennett-Clarke, C.A., M.J. Leslie, R.D. Lane and R.W. Rhoades (1994b) Effect of serotonin depletion on vibrissa-related patterns of thalamic afferents in the rat's somatosensory cortex. **J. Neurosci. 14:7594-7607.**

Berger, B., S. Trottier, P. Gaspar, C. Verney and C. Alvarez (1986) Major dopamine innervation of the cortical motor areas in the cynomolgus monkey. A radioautographic study with comparative assessment of

serotonergic afferents. **Neurosci. Letts. 72:121-127.**

Berger, B., S. Trottier, C. Verney, P. Gaspar and C. Alvarez (1988) Regional and laminar distribution of the dopamine and serotonin innervation in the macaque cerebral cortex: A radioautographic study. **J. Comp. Neurol. 273:99-119.**

Blue, M.E., R.S. Erzurumlu and S. Jhaveri (1991) A comparison of pattern formation by thalamocortical and serotonergic afferents in the rat barrel field cortex. **Cerebral Cortex 1:380-389.**

Blue, M.E., K.A. Yagaoff, L.A. Mamounas, P.R. Hartig and M.E. Molliver (1988) Correspondence between 5-HT_2 receptors and serotonergic axons in rat neocortex. **Brain Res. 453:315-328.**

Bonin, G. von and P. Bailey (1947) The Neocortex of *Macaca mulatta*. **The University of Illinois Press, Urbana, Illinois.**

Boothe, R.G., V. Dobson and D.Y. Teller (1985) Postnatal development of vision in human and non-human primates. **Ann. Rev. Neurosci. 8:495-545.**

Boothe, R.G., W.T. Greenough, J.S. Lund and K. Wrege (1979) A quantitative investigation of spine and dendrite development of neurons in visual cortex (Area 17) of *Macaca nemestrina* monkeys. **J. Comp. Neurol. 186:473-490.**

Bourgeois, J-P., P.S. Goldman-Rakic and P. Rakic (1994) Synaptogenesis in the prefrontal cortex of rhesus monkeys. **Cerebral Cortex 4:78-96.**

Bourgeois, J-P. and P. Rakic (1993) Changes of synaptic density in the primary visual cortex of the macaque monkey from foetal to adult stage. **J. Neurosci. 13:2801-2820.**

Brammer, G.L., M.T. McGuire and M.J. Raleigh (1987) Similarity of 5-HT_2 receptor sites in dominant and subordinate vervet monkeys. **Pharm. Biochem. Behav. 27:701-705.**

Brodmann, K. (1905) Beitraege zur histologischen lokalisation der grosshirnrinde. Dritte mitelleilung: Die rindenfelder niederen affen. **J. Psychol. Neurol. Leipzig 9:177-226.**

Brodmann, K. (1909) Vergleichende lokalisationslehre der grosshirnrinde in ihren prinzipien dargestellt auf grund des zellenbaues. **Barth, Leipzig.**

Brodmann, K. (1912) Neue ergebnisse uber die vergleichende histologische lokalisation der grosshirnrinde mit besonderer berucksichtigung des strinhirns. **Anat. Anz [Suppl] 41:157-216.**

Brown, R.M., A.M. Crane and P.S. Goldman (1979) Regional distribution of monoamines in the cerebral cortex and sub-cortical structures of the rhesus monkey: Concentrations and *in vivo* synthesis rates. **Brain Res. 168:133-150.**

Brown, R.M. and P.S. Goldman (1977) Catecholamines in neocortex of rhesus monkeys: Regional distribution and ontogenetic development. **Brain Res. 124:576-580.**

Brozoski, T., R.M. Brown, H.E. Rosvold and P.S. Goldman (1979) Cognitive deficit caused by depletion of dopamine in prefrontal cortex of rhesus monkey. **Science 205:929-931.**

Buhot, M.-C. (1997) Serotonin receptors in cognitive behaviours. **Curr. Opin. Neurobiol. 7:243-254.**

Buhot, M.-C., S.K. Patra and S. Naili (1995) Spatial memory deficits following stimulation of hippocampal 5-HT_{1B} receptors in the rat. **Eur. J. Pharmacol. 285:221-228.**

Butters, N., D. Pandya, K. Sanders and P. Dye (1971) Behavioural deficits in monkeys after selective lesions within the middle third of sulcus principalis. **J. Comp. Physiol. 76:8-14.**

Butters, N., D. Pandya, D. Stein and J. Rosen (1972) A search for the spatial engram within the frontal lobes of monkeys. **Acta. Neurobiol. Exp. 32:305-329.**

Cai, J.X., Y-Y. Ma, L. Xu and X-T, Hu (1993) Reserpine impairs spatial working memory performance in monkeys: Reversal by the α_2-adrenergic agonist clonidine. **Brain Res. 614:191-196.**

Carey, G.J., B. Costall, A.M. Domeney, P.A. Gerrard, D.N. Jones, R.J. Naylor and M.B. Tyers (1992) Ondansetron and arecoline prevent scopolamine-induced cognitive deficits in the marmoset. **Pharmacol. Biochem. Behav. 42:75-83.**

Carlson, M. (1984) Development of tactile discrimination capacity in *Macaca mulatta*. I. Normal infants. **Brain Res. 318:69-82.**

Carlsson, A. (1988) The current status of the dopamine hypothesis of schizophenia. **Neuropsychopharmacol. 1:179-186.**

Carmichael, S.T. and J.L. Price (1994) Architectonic subdivision of the orbital and medial prefrontal cortex in the macaque monkey. **J. Comp. Neurol. 346:366-402.**

Casey, B.J., J.D. Cohen, P. Jezzard, R. Turner, D.C. Noll, R.J. Trainor, J. Giedd, D. Kaysen, L. Hertz-Pannier and J.L. Rapoport (1995) Activation of prefrontal cortex in children during a non-spatial working memory task with functional MRI. **Neuroimage 2:221-229.**

Cassel, J.-L. and H. Jeltsch (1995) Serotonergic modulation of cholinergic function in the cerebral nervous system: Cognitive implications. **Neurosci. 69:1-41.**

Cavada, C. and P.S. Goldman-Rakic (1989) Posterior parietal cortex in rhesus monkey: II. Evidence for segregated corticocortical networks linking sensory and limbic areas with the frontal lobe. **J. Comp. Neurol. 287:422-445.**

Celio, M.R. (1986) Parvalbumin in most γ-aminobutyric acid-containing neurons of the rat cerebral cortex. **Science 231:995-997.**

Celio, M.R. (1990) Calbindin D-28k and parvalbumin in the rat nervous system. **Neurosci. 35:375-475.**

Chavis, D.A. and D.N. Pandya (1976) Further observations on corticofrontal connections in the rhesus monkey. **Brain Res. 117:369-386.**

Chiron, C., Raynaud, B. Maziere, M. Zilbovicius, L. Laflamme, M.C. Masure, O. Dulac, M. Bourguignon and A. Syrota (1992) Changes in regional cerebral blood flow during brain maturation in children and adolescents. **J. Nucl. Med. 33:696-703.**

Chugani, H.T. and M.E. Phelps (1986) Maturational changes in cerebral function in infants determined by ^{18}FDG positron emission tomography. **Science 231:840-843.**

Chugani, H.T., M.E. Phelps and J.C. Mazziotta (1987) Positron emission tomography study of human brain functional development. **Ann. Neurol. 22:487-497.**

Classey, J.D., S.A. Andersen, D.A. Lewis (1994) Postnatal developmental changes in dendritic spine density on layer III pyramidal neurons in monkey prefrontal cortex. **Brain Res. Assoc. Abstr. 11:28.4.**

Condé, F, J.S. Lund, D.M. Jacobowitz, K.G. Baimbridge and D.A. Lewis (1994) Local circuit neurons immunoreactive for calretinin, calbindin D-28k or parvalbumin in monkey prefrontal cortex: distribution and morphology. **J. Comp. Neurol. 341:95-116.**

Condé, F, J.S. Lund and D.A. Lewis (1996) The hierarchical development of monkey visual cortical regions as revealed by the maturation of parvalbumin-immunoreactive neurons. **Dev. Brain Res. 96:261-276.**

D'Amato, R.J., M.E. Blue, B.L. Largent, D.R. Lynch, D.J. Ledbetter, M.E. Molliver and S.H. Snyder (1987) Ontogeny of the serotonergic projection to rat neocortex: Transient expression of a dense innervation to primary sensory areas. **Proc. Natl. Acad. Sci. USA 84:4322-4326.**

De Lima, A.D., F.E. Bloom and J.H. Morrison (1988) Synaptic organisation of serotonin-immunoreactive fibres in primary visual cortex of the macaque monkey. **J. Comp. Neurol. 274:280-294.**

DeFelipe, J. (1993) Neocortical neuronal diversity: Chemical heterogeneity revealed by colocalisation studies of classic neurotransmitters, neuropeptides, calcium-binding proteins, and cell surface molecules. **Cerebral Cortex 3:273-289.**

DeFelipe, J. and I. Farinas (1992) The pyramidal neuron of the cerebral cortex - morphological and chemical characteristics of the synaptic inputs. **Progr. Neurobiol. 39:563-607.**

DeFelipe, J., S.H.C. Hendry, T. Hashikawa, M. Molinari and E.G. Jones (1990) A microcolumnar structure of monkey cerebral cortex revealed by immunocytochemical studies of double bouquet cell axons. **Neurosci. 37:655-673.**

DeFelipe, J., S.H.C. Hendry and E.G. Jones (1989a) Visualisation of chandelier cell axons by parvalbumin immunoreactivity in monkey cerebral cortex. **Proc. Natl. Acad. Sci. USA 86:2093-2097.**

DeFelipe, J., S.H.C. Hendry and E.G. Jones (1989b) Synapses of double bouquet cells in monkey cerebral cortex visualised by calbindin immunoreactivity. **Brain Res. 503:49-54.**

DeFelipe, J., S.H.C. Hendry, E.G. Jones and D. Schemechel (1985) Variability in the termination's of GABAergic chandelier cell axons on initial segments of pyramidal cell axons in the monkey sensory-motor cortex. **J. Comp. Neurol. 231:364-384.**

DeFelipe, J., and E.G. Jones (1985) Vertical organisation of γ-aminobutyric acid-accumulating intrinsic neuronal systems in monkey cerebral cortex. **J. Neurosci. 5:3246-3260.**

Denoble, V.J., L.M. Schrack, A.L. Reigel and K.F. Denoble (1991) Visual recognition memory in squirrel monkeys: Effects of serotonin antagonists on baseline and hypoxia-induced performance deficits. **Pharmacol. Biochem. Behav. 39:991-996.**

Descarries, L., P. Séguéla and K.C. Watkins (1991) Nonjunctional relationships of monoamine axon terminals in the cerebral cortex of adult rat. **In Fuxe, K. and L.F. Agnati (Eds) Advances in Neuroscience, Vol. 1: "Volume transmission in the brain: Novel mechanisms for neural transmission. pp 53-62, Raven, New York.**

Dewey, S.L., G.S. Smith, J. Logan, D. Alexoff, Y.S Ding, P. King, N. Pappas, J.D. Brodie and C.R. Ashby (1995) Serotonergic modulation of striatal dopamine measured with positron emission tomography (PET) and *in vivo* micodialysis. **J. Neurosci. 15:821-829.**

Diamond, A. (1995) Evidence of robust recognition memory early in life even when assessed by reaching behaviour. **J. Exp. Child Psychol. 59:419-456.**

Diamond, A. and B. Doar (1989) The performance of human infants on a measure of frontal cortex function, the delayed response task. **Dev. Psychobiol. 22:271-294.**

Diamond, A. and P.S. Goldman-Rakic (1986) Comparative development in human infant rhesus monkeys of cognitive functions that depend on prefrontal cortex. **Soc. Neurosci. Abstr. 12:742.**

Diamond, A. and P.S. Goldman-Rakic (1989) Comparison of human infants and rhesus monkeys on Piaget's AB task: Evidence for dependence on dorsolateral prefrontal cortex. **Exp. Brain Res. 74:24-40.**

Diamond, A., C. Towle and K. Boyer (1994) Young children's performance on a task sensitive to the memory functions of the medial temporal lobe in adults - the delayed non-matching-to-sample task reveals problems that are due to non-memory task demands. **Behav. Neurosci. 108:659-680.**

Distler, C., J. Bachevalier, C. Kennedy, M. Mishkin and L.G. Ungerleider (1996) Functional development of the corticocortical pathway for motion analysis in the macaque monkey: A ^{14}C-2-Deoxyglucose study. **Cerebral Cortex 6:184-195.**

Edagawa, Y., H. Saito and K. Abe (1996) Serotonin inhibits the induction of long-term potentiation in rat primary visual cortex. **Soc. Neurosci. Abstr. 22:331.**

Farkas-Bargeton, and M.F. Diebler (1978) A topographical study of enzyme maturation in human cerebral

neocortex: A histochemical and biochemical study. **In Brazier, M.A.B. and H. Petsche (Eds.) Architectonics of the Cerebral Cortex, Raven Press, New York, NY pp 175-190.**

Feinberg, I. (1982) Schizophrenia: Caused by a fault in programmed synaptic elimination during adolescence? **J. Psychiat. Res. 17:319-334.**

Feinberg, I. (1987) Adolescence and mental illness. (Letter) **Science 236:507.**

Feinberg, I. (1992) Neurodevelopmental model of schizophrenia. **Biol. Psychiatry. 32:212-213.**

Feinberg, I., H.C. Thode, H.T. Chungani and J.D. March (1990) Gamma distribution model describes maturational curves for delta wave amplitude, cortical metabolic rate and synaptic density. **J. Theor. Biol. 142:142-161.**

Feldman, M.L. (1984) Morphology of the neocortical pyramidal neuron. **In Peters, A. and E.G. Jones (Eds.) Cerebral Cortex , Vol. 1:Cellular Components of the Cerebral Cortex, Plenum Press, New York, NY. pp 89-102.**

Feldman, M.L. and A. Peters (1979) A technique for estimating total spine numbers on Golgi-impregnated dendrites. **J. Comp. Neurol. 188:527-542.**

Fischer, C., G. Hatzidimitriou, J. Wlos, J. Katz and G. Ricaurte (1995) Reorganisation of ascending 5-HT axon projections in animals previously exposed to the recreational drug (+/)-3,4-dimethylenedioxymethamphetamine (MDMA, Ecstasy). **J. Neurosci. 15:5476-5485.**

Flechsig, P. (1920) Anatomie des menschlichen gehirns und ruckenmarks auf myelogenetischer grundlage. **Thieme, Leipzig.**

Fontenot, M.B., J.R. Kaplan, S.B. Manuck, V. Arango and J.J. Mann (1995) Long-term effects of chronic social stress on serotonergic indices in the prefrontal cortex of adult male cynomolgus macaques. **Brain Res. 705:105-108.**

Foote, S.L. and J.H. Morrison (1984) Postnatal development of laminar innervation patterns by monoaminergic fibres in monkey (*Macaca fascicularis*) primary visual cortex. **J. Neurosci. 4:2667-2680.**

Foote, S.L. and J.H. Morrison (1987a) Extrathalamic modulation of cortical function. **In Cowen, W.M. et al (Eds), Ann. Rev. Neurosci., Vol . 10, Annual Reviews, Inc, Palo Alto, pp 67-95.**

Foote, S.L. and J.H. Morrison (1987b) Development of the noradrenergic, serotonergic and dopaminergic innervation of neocortex. **Curr. Top. Dev. Biol. 21:391-423.**

Friedman, H.R., C.J. Bruce and P.S. Goldman-Rakic (1987) A sequential double-label [^{14}C]- and [^{3}H]-2DG technique: Validation by double-dissociation of functional states. **Exp. Brain Res. 66:543-554.**

Friedman, H.R., C.J. Bruce and P.S. Goldman-Rakic (1989) Resolution of metabolic columns by a double-label 2-DG technique: Interdigitation and coincidence in visual cortical areas of the same monkey. **J. Neurosci. 9:4111-4121.**

Friedman, H.R. and P.S. Goldman-Rakic (1994) Co-activation of prefrontal cortex and inferior parietal cortex in working memory tasks revealed by 2DG functional mapping in the rhesus monkey. **J. Neurosci. 14:2775-2788.**

Funahashi, S., C.J. Bruce and P.S. Goldman-Rakic (1989) Mnemonic coding of visual space in the monkey's dorsolateral prefrontal cortex. **J. Neurophysiol. 61:331-349.**

Funahashi, S., C.J. Bruce and P.S. Goldman-Rakic (1990) Visuospatial coding in primate prefrontal neurons revealed by oculomotor paradigms. **J. Neurophysiol. 63:814-831.**

Funahashi, S., C.J. Bruce and P.S. Goldman-Rakic (1991) Neuronal activity related to saccadic eye movements in the monkey's dorsolateral prefrontal cortex. **J. Neurophysiol. 65:1464-1483.**

Funahashi, S. and K. Kubota (1994) Working memory and prefrontal cortex. **Neurosci. Res. 21:1-11.**

Fuster, J.M. (1973) Unit activity in the prefrontal cortex during delayed-response performance: Neuronal correlates of transient memory. **J. Neurophysiol. 36:61-78.**

Fuster, J.M. (1985a) The Prefrontal Cortex and temporal integration. **In Peters, A. and E.G. Jones (Eds) Cerebral Cortex. Vol. 4: Association and Auditory cortices. New York, NY: Plenum Press, pp 151-177.**

Fuster, J.M. (1985b) The prefrontal cortex, mediator of cross-temporal contingencies. **Hum. Neurobiol. 4:169-179.**

Fuster, J.M. (1989) **The Prefrontal Cortex: Anatomy, physiology and neuropsychology of the frontal lobe. Raven Press, New York.**

Fuster, J.M. (1990a) Behavioural electrophysiology of the prefrontal cortex of the primate. **Progress in Brain Res. 85:313-324.**

Fuster, J.M. (1990b) Prefrontal cortex and the bridging of temporal gaps in the perception-action cycle. **In Diamond, A. (Ed) The Development and Neural Bases of Higher Cognitive Functions. Annals of the New York Academy of Sciences. New York, N.Y. 608:318-336.**

Fuster, J.M. and G.E. Alexander (1971) Neuron activity related to short-term memory. **Science 173:652-654.**

Fuster, J.M. and G.E. Alexander (1973) Firing changes in cells of the nucleus medialis dorsalis associated with delayed response behaviour. **Brain Res. 61:79-91.**

Gabbott, P.L.A. and S.J. Bacon (1996a) Local circuit neurons in the medial prefrontal cortex (areas 24a,b,c, 25 and 32) in the monkey: I. cell morphology and morphometrics. **J. Comp. Neurol. 364:567-608.**

Gabbott, P.L.A. and S.J. Bacon (1996b) Local circuit neurons in the medial prefrontal cortex (areas 24a,b,c, 25 and 32) in the monkey: II. quantitative areal and laminar distributions. **J. Comp. Neurol. 364:609-636.**

Galea, M.P. and I. Darian-Smith (1995) Postnatal maturation of the direct corticospinal projections in the macaque monkey. **Cerebral. Cortex. 5:518-540.**

Garey, L.J. (1984) Structural development of the visual system of man. **Human Neurobiol. 3:75-80.**

Garey, L.J. (1995) Reduction in dendritic spine number on cortical pyramidal neurons in schizophrenia. **Soc. Neurosci. Abstr. 21:237.**

Gay, V.L. and T.M. Plant (1987) L-aspartate elicits hypothalamic gonadotropin-releasing hormone release in pre-pubertal male rhesus monkeys (*Macaca mulatta*). **Endocrinol. 120:2281-2296.**

Gay, V.L. and T.M. Plant (1988) Sustained intermittent release of gonadotropin-releasing hormone in the pre-pubertal male rhesus monkey induced by N-methyl-DL-aspartic acid. **Neuroendocrinol. 48:147-152.**

Gibson, K.R. (1970) Sequence of myelinisation in the brain of *Macaca mulatta.* **Ph.D. dissertation, University of California, Berkeley.**

Giguere, M. and P.S. Goldman-Rakic (1988) Mediodorsal nucleus: Areal, laminar and tangential distribution of afferents and efferents in the frontal lobe of rhesus monkeys. **J. Comp. Neurol. 277:195-213.**

Girard, N., C. Raybaud and P. du-Lac (1991) MRI study of brain myelination. **J. Neuroradiol. 18:291-307.**

Glantz, L.A. and D.A. Lewis (1995) Assessment of spine density on layer III pyramidal cells in the prefrontal cortex of schizophrenic subjects. **Soc. Neurosci. Abstr. 21:239.**

Glantz, L.A. and D.A. Lewis (1996) Specificity of decreased spine density on layer III pyramidal cells in schizophrenia. **Soc. Neurosci. Abstr. 22:658.**

Goldman, P.S. (1971) Functional development of the prefrontal cortex in early life and the problem of

neuronal plasticity. **Exp. Neurol. 32:366-387.**

Goldman, P.S. (1972) Developmental determinants of cortical plasticity. **Acta. Neurobiol. Exp. 32:495-511.**

Goldman, P.S. and G.E. Alexander (1977) Maturation of prefrontal cortex in the monkey revealed by local reversible cryogenic depression. **Nature 267:613-615.**

Goldman, P.S. and R.M. Brown (1975) The influence of neonatal androgen on the development of cortical function in the rhesus monkey. **Soc. Neurosci. Abstr. 1:494.**

Goldman, P.S., H.T. Crawford, L.P. Stokes, T.W. Galkin and H.E. Rosvold (1974) Sex-dependent behavioural effects of cerebral cortical lesions in the developing rhesus monkey. **Science 186:540-542.**

Goldman, P.S. and Galkin, T.W. (1978) Prenatal removal of frontal association cortex in the foetal rhesus monkey: Anatomical and functional consequences in postnatal life. **Brain Res. 152:451-485.**

Goldman, P.S. and W.J.H. Nauta (1977) Columnar distribution of corticocortical fibres in the frontal association, limbic and motor cortex of the developing rhesus monkey. **Brain Res. 122:393-413.**

Goldman, P.S. and H.E. Rosvold (1970) Localisation of function within the dorsolateral prefrontal cortex of the rhesus monkey. **Exp. Neurol. 27:291-304.**

Goldman, P.S., H.E. Rosvold, B. Vest and T.W. Galkin (1971) Analysis of the delayed-alternation deficit produced by dorsolateral prefrontal lesions in the rhesus monkey. **J. Comp. Physiol. Psychol. 77:212-220.**

Goldman-Rakic, P.S. (1981) Development and plasticity of primate frontal association cortex. **In Francis, O. et al (Eds.) The Organisation of the Cerebral Cortex, The MIT Press, Cambridge, Mass. USA. pp 69-97.**

Goldman-Rakic, P.S. (1982) Neuronal development and plasticity of association cortex in primates. **In Rakic, P. and P.S. Goldman-Rakic (Eds.) Development and Modifiability of the Cerebral Cortex, The MIT Press, Cambridge, Mass. USA.** pp 520-532.

Goldman-Rakic, P.S. (1987a) Circuitry of primate prefrontal cortex and regulation of behaviour by representational memory. **In Plum, F. and V. Mountcastle (Eds) Handbook of Physiology, Vol. 5, American Physiological Society, Bethesda, Maryland, pp 373-417.**

Goldman-Rakic, P.S. (1987b) Development of cortical circuitry and cognitive function. **Child Dev. 58:601-622.**

Goldman-Rakic, P.S. (1988) Topography of cognition: Parallel distributed networks in primate association cortex. **Ann. Rev. Neurosci. 11:137-56.**

Goldman-Rakic, P.S. (1995) Cellular basis of working memory. **Neuron 14:477-485.**

Goldman-Rakic, P.S. (1996) Regional and cellular fractionation of working memory. **Proc. Natl. Acad. Sci. USA. 93:13473-13480.**

Goldman-Rakic, P.S. and R.M. Brown (1981) Regional changes of monoamines in cerebral cortex and sub-cortical structures of ageing rhesus monkeys. **Neurosci. 6:177-187.**

Goldman-Rakic, P.S. and R.M. Brown (1982) Postnatal development of monoamine content and synthesis in the cerebral cortex of rhesus monkeys. **Dev. Brain Res. 4:339-349.**

Goldman-Rakic, P.S. and H.R. Friedman (1991) The circuitry of working memory revealed by anatomy and metabolic imaging. **In Levin, H.S. et al (Eds) Frontal Lobe Function and Dysfunction, Oxford University Press, New York, pp 72-91.**

Goldman-Rakic, P.S., S. Funahashi and C.J. Bruce (1990) Neocortical memory circuits. **Cold Spr. Harb. Sym. Quant. Biol., Vol. 55, Cold Spring Harbour Laboratory Press, pp 1025-1038.**

Goldman-Rakic, P.S., C. Leranth, S.M. Williams, N. Mons and M. Geffard (1989) Dopamine synaptic complex with pyramidal neurons in primate cerebral cortex. **Proc. Natl. Acad. Sci. USA. 86:9015-9019.**

Goldman-Rakic, P.S. and L.J. Porrino (1985) The primate mediodorsal (MD) nucleus and its projection to the frontal lobe. **J. Comp. Neurol. 242:535-560.**

Goldman-Rakic, P.S. and S.M. Williams (1995) Diverse mesencephalic dopaminergic cell groups project to the macaque frontal cortex. **Soc. Neurosci. Abstr. 21:371.**

Granger, B., F. Tekaia, A.M. Le Sourd, P. Rakic and J-P. Bourgeois (1995) Tempo of neurogenesis and synaptogenesis in the primate cingulate mesocortex: Comparison with the neocortex. **J. Comp. Neurol. 360:363-376.**

Grasby, P.M., K.J. Friston, C.J. Bench, C.D. Frith, E. Paulesu, P.J. Cowen, P.F. Liddle, R.S.J. Frackowiak and R.J. Dolan. (1992). The effect of apomorphine and buspirone on regional cerebral blood flow during the performance of a cognitive task - measuring neuromodulatory effects of psychotropic drugs in man. **Eur. J. Neurosci. 4:1203-1212.**

Grasby, P.M., C.D. Frith, E. Paulesu, K.J. Friston, R.S.J. Frackowiak and R.J. Dolan (1995) The effect of the muscarinic antagonist scopolamine on regional cerebral blood flow during the performance of a memory task. **Exp. Brain. Res. 104:337-348.**

Gray, E.G. (1959) Axo-somatic and axo-dendritic synapses of the cerebral cortex: An electron microscope study. **J. Anat. 93:420-433.**

Greenfield (1991) Language, tools and brain: The ontogeny and phylogeny of hierarchically organised sequential behaviour. **Behav. Brain Sci. 14:531-595.**

Gu, Q., L. Kojic, R.M. Douglas and M.S. Cynader (1995) Serotonin facilitates synaptic plasticity in kitten visual cortex - an *in vitro* study. **Soc. Neurosci. Abstr. 21:1655.**

Gu, Q., B. Patel and W. Singer (1990) Laminar distribution and postnatal development of serotonin-immunoreactive axons in the cat primary visual cortex. **Exp. Brain Res. 81:257-266.**

Gu, Q. and W. Singer (1995) Involvement of serotonin in developmental plasticity of kitten visual cortex. **Eur. J. Neurosci. 7:1146-1153.**

Hagan, R.M., G.J. Kilpatrick and M.B.Tyers (1993) Interactions between 5-HT_3 receptors and cerebral dopamine function: Implications for the treatment of schizophrenia and psychoactive substance abuse. **Psychopharmacol. 112:568-575.**

Hagger, C., J. Bachevalier and B.B. Bercu (1986) The effects of perinatal testosterone on the development of habit formation in infant rhesus monkeys. **Soc. Neurosci. Abstr. 12:23.**

Harder, J.A., C.J. Maclean, J.T. Alder, P.T. Francis and R.M. Ridley (1996) The 5-HT_{1A} antagonist, WAY-100635, ameliorates the cognitive impairment induced by fornix transection in the marmoset. **Psychopharmacol. 127:245-254.**

Haring, J.H., W. Yan and C.C. Wilson (1995) 5-HT_{1A} receptors mediate the effects of 5-HT on developing dentate granule cells. **Soc. Neurosci. Abstr. 21:862.**

Harlow, H.F., K. Akert and K.A. Schiltz. (1964) The effects of bilateral prefrontal lesions on learned behaviour of neonatal, infant and preadolescent monkeys. **In Warren, J.M. and K. Akert (Eds) The Frontal Granular Cortex and Behaviour. McGraw-Hill Book Company, New York, pp 126-148.**

Hays, W.L. (1981) **Statistics. 3rd Edition, Holt, Rinehart and Winston, Inc, pp 596-598.**

Hayes, T.L. and D.A. Lewis (1992) Non-phosphorylated neurofilament protein and calbindin immunoreactivity in layer III pyramidal neurons of human neocortex. **Cerebral Cortex 2:56-67.**

Hendry, S.H.C., C.R. Houser, E.G. Jones and J.E. Vaughan (1983) Synaptic organisation of

immunocytochemically identified GABA neurons in the monkey sensory-motor cortex. **J. Neurocytol. 12:639-660.**

Hendry, S.H.C., E.G. Jones, J. DeFelipe, D. Schmechel, C. Brandon and P.C. Emson (1984) Neuropeptide-containing neurons of the cerebral cortex are also GABAergic. **Proc. Natl. Acad. Sci. USA 81:6526-6530.**

Hendry, S.H.C., E.G. Jones, P.C. Emson, D.E.M. Lawson, C.W. Heizmann and P. Streit (1989) Two classes of cortical GABA neurons defined by differential calcium binding protein immunoreactivities. **Exp. Brain Res. 76:467-472.**

Herremans, A.H.J., T.H. Hijzen, B. Oliver and J.L. Slangen (1995) Serotonergic drug effects on a delayed conditional discrimination task in the rat: Involvement of the 5-HT_{1A} receptor in working memory. **J. Psychopharmacol. 9:242-250.**

Hofsen, C. von-. and S. Fazel-Zandy (1984) Development of visually-guided hand orientation in reaching. **J. Exp. Child. Psychol. 38:208-219.**

Hofsen, C. von-. and J. Ronnqvist (1988) Preparation for grasping an object: A developmental study. **J. Exp. Psychol. Hum. Percept. Perform. 14:610-621.**

Horner, C.H. and E. Arbuthnott (1991) Methods of estimation of spine density - are spines evenly distributed throughout the dendritic field? **J. Anat. 177:179-184.**

Hornung, J-P. (1992) Postnatal development of the dual serotonergic innervation of the marmoset cerebral cortex. **Eur. Neurosci. Assoc. Abstr. 15:181.**

Hornung, J-P. and M.R. Celio (1992) The selective innervation by serotoninergic axons of calbindin-containing interneurons in the neocortex and hippocampus of the marmoset. **J. Comp. Neurol. 320:457-467.**

Hornung, J-P., J-M. Fritschy and I. Tork (1990) Distribution of two morphologically distinct subsets of serotonergic axons in the cerebral cortex of the marmoset. **J. Comp. Neurol. 297:165-181.**

Hsu, S.-M., L. Raine and H. Fanger (1981) Use of avidin-biotin-peroxidase complex (ABC) in immunoperoxidase techniques: A comparison between ABC and unlabelled antibody (PAP) procedures. **J. Histochem. Cytochem. 29:577-580.**

Hudspeth, W.J. and K.H. Pribram (1992) Psychophysiological indices of cerebral maturation. **Int. J. Psychophysiol. 12:19-29.**

Huttenlocher, P.R. (1979) Synaptic density in human frontal cortex - developmental changes and effects of ageing. **Brain Res. 163:195-205.**

Huttenlocher, P.R. (1984) Synapse elimination and plasticity in developing human cerebral cortex. **Am. J. Ment. Defic. 88:488-496.**

Huttenlocher, P.R. (1993) Morphometric study of human cerebral cortex development. **In Johnson, M.H. (Ed) Brain Development and Cognition: A Reader. Blackwell Publications, Cambridge, Massachusetts, pp 113-124.**

Huttenlocher, P.R. and A.S. Dabholkar (1997) Regional differences in synaptogenesis in human cerebral cortex. **J. Comp. Neurol. 387:167-178.**

Huttenlocher, P.R., C. de Courten, L.J. Garey and H. Van Der Loos (1982) Synaptogenesis in human visual cortex - evidence for synapse elimination during normal development. **Neurosci. Lett. 33:247-252.**

Jacobs, B., H.T. Chugani, V. Allada, S. Chen, M.E. Phelps, D.B. Pollack and M.J. Raleigh (1995) Developmental changes in brain metabolism in sedated rhesus macaques and vervet monkeys revealed by positron emission tomography. **Cerebral Cortex 3:222-233.**

Jacobs, B.L. and E.C. Azmitia (1992) Structure and function of the brain serotonin system. **Physiolog. Revs. 72:165-229.**

Jacobson (1975) The cortical afferents to the arcuate cortex of the rhesus monkey. **Anat. Rec. 181:383.**

Jakab, R.L. and P.S. Goldman-Rakic (1996) Serotonin innervation of neurochemically identified interneuron subtypes in the monkey prefrontal cortex. **Soc. Neurosci. Abstr. 22:905.**

Jernigan, T.L., D.A. Trauner, J.R. Hesselink and P.A. Tallal (1991) Maturation of human cerebrum observed *in vivo* during adolescence. **Brain 114:2037-2049.**

Jones, E.G. (1995) Cortical development and neuropathology in schizophrenic. **In Development of the Cerebral Cortex. Ciba Foundation Symposium 193. John Whiley and Sons. pp 277-295.**

Jones, E.G. and S.H.C. Hendry (1984) Basket cells. **In Peters, A. and E.G. Jones (Eds) Cerebral Cortex. Vol. 1: Cellular components of the cerebral cortex. New York, NY: Plenum Press, pp 309-336.**

Jones, E.G., S.H.C. Hendry, J. DeFelipe and D.L. Benson (1994) GABA neurons and their role in activity-dependent plasticity of adult primate visual cortex. **In Peters, A. and K.S. Rockland (Eds.) Cerebral Cortex. Vol. 10: Primary Visual Cortex in Primate, Plenum Press, New York, NY. pp 61-140.**

Jones, E.G. and T.P.S. Powell (1970) An anatomical study of converging sensory pathways within the cerebral cortex of the monkey. **Brain 93:793-820.**

Kahn, R.S. and M. Davidson (1993) Serotonin, dopamine and their interactions in schizophrenia: An editorial. **Psychopharmacol. 112:S1-S4.**

Kapur, S. And G. Remington (1996) Serotonin-dopamine interaction and its relevance to schizophrenia. **Am. J. Psych. 153:466-476.**

Kawamura, K. and J. Naito (1984) Corticocortical projections to the prefrontal cortex in the rhesus monkey investigated with horseradish peroxidase techniques. **Neurosci. Res. 1:89-103.**

Kennedy, C., O. Sakurada, M. Shinohara, J. Jehle and L. Sokoloff (1978) Local cerebral glucose utilisation in the normal conscious macaque monkey. **Ann. Neurol. 4:293-301.**

Kennedy, C., O. Sakurada, M. Shinohara and M. Miyaoka (1982) Local cerebral glucose utilisation in the new-born macaque monkey. **Ann. Neurol. 12:333-340.**

Keshaven, M.S., S. Anderson and J.W. Pettegrew (1994) Is schizophenia due to excessive synaptic pruning in the prefrontal cortex? The Feinberg hypothesis revisited. **J. Psychiatry Res. 28:239-265.**

Killackey, H.P., R.W. Rhoades and C.A. Bennett-Clarke (1995) The formation of a cortical somatotopic map. **Trends Neurosci. 18:402-407.**

Kirkwood, A., M.C. Riolt and M.F. Bear (1996) Experience-dependent modification of synaptic plasticity in visual cortex. **Nature 381:526-528.**

Kisvarday, Z.F., K.A.C. Martin, T.F. Freund, Z. Magloczky, D. Whitteridge and P. Somogyi (1986) Synaptic targets of HRP-filled layer 3 pyramidal cells in the cat striate cortex. **Exp. Brain Res. 64:541-552.**

Koenderink, M.J.Th. and H.B.M. Uylings (1995) Postnatal maturation of layer V pyramidal neurons in the human prefrontal cortex. A quantitative Golgi analysis. **Brain Res. 678:233-243.**

Koenderink, M.J.Th., H.B.M. Uylings and L. Mrzljak (1994) Postnatal maturation of the layer III pyramidal neurons in the human prefrontal cortex: A quantitative Golgi analysis. **Brain Res. 653:173-182.**

Kojic, L., Q. Gu, R.M. Douglas, J. Matsubara and M.S. Cynader (1996) Serotonin-induced plasticity in the kitten visual cortex is associated with an activation of NMDA receptors and voltage-gated calcium channels. **Soc. Neurosci. Abstr. 22:331.**

Kojima, S., M. Kojima and P.S. Goldman-Rakic (1982) Operant behavioral analysis of memeory loss in monkeys with prefrontal lesions. **Brain Res. 248:51-59.**

Kosofsky, B.E. and N.W. Kowall (1989) Demonstration of two morphologic classes of serotonergic fibres in human cortex. **Soc. Neurosci. Abstr. 15:5.**

Kosofsky, B.E. and M.E. Molliver (1987) The serotonergic innervation of cerebral cortex: different classes of axon terminals arise from dorsal and median raphe nuclei. **Synapse 1:153-168.**

Kosofsky, B.E., M.E. Molliver, J.H. Morrison and S.L. Foote (1984) The serotonin and norepinephrine innervation of primary visual cortex in the cynomolgus monkey (*Macaca fascicularis*). **J. Comp. Neurol. 230:168-178.**

Köstner, E. and J.-P. Hornung (1995) Maturation of cerebral cortical neurons *in vitro* is modulated by serotonin receptor subtypes. **Soc. Neurosci. Abstr. 21:862.**

Kostovic, I. (1990) Structural and histochemical reorganisation of the human prefrontal cortex during perinatal and postnatal life. **In Uylings, H.B.M. et al (Eds) Prog. Brain Res. Vol. 85, Elsevier Science Publishers BV, pp 223-238.**

Kostovic, I. and P.S. Goldman-Rakic (1983) Transient cholinesterase staining in the mediodorsal nucleus of the thalamus and its connections in the developing human and monkey brain. **J. Comp. Neurol. 219:431-447.**

Kostovic, I., M. Judas, Z. Petanjek and G. Simic (1995) Ontogenesis of goal-directed behaviour: Anatomo-functional considerations. **Int. J. Psychophysiol. 19:85-102.**

Kostovic, I., J. Skavic and D. Strinovic (1988) Acetylcholinesterase in the human frontal associative cortex during the period of cognitive development: Early laminar shifts and late innervation of pyramidal neurons. **Neurosci. Letts. 90:107-112.**

Kritzer, M.F. (1994) Intrinsic circuits of functionally specialised subdivisions of human cerebral cortex. **Soc. Neurosci. Abstr. 20:578.**

Kritzer, M.F. and P.S. Goldman-Rakic (1993) Intrinsic circuits of human prefrontal cortex. **Soc. Neurosci. Abstr. 19:590.**

Kritzer, M.F. and P.S. Goldman-Rakic (1995) Intrinsic circuit organisation of the major layers and sub-layers of the dorsolateral prefrontal cortex in the rhesus monkey. **J. Comp. Neurol. 359:131-143.**

Kubota, K. (1978) Neuronal activity in the dorsolateral prefrontal cortex of the monkey and initiation of behaviour. **In Ito, M. et al (Eds.) Integrative Control Functions of the Brain, Vol. 1, Kohdansha - Elsevier, Tokyo. pp 407-417.**

Kubota (1993) Delayed response and perseverative errors in newborn infant rhesus monkeys. **In Ono, T. et al (Eds.) Brain mechanisms of perception and memory. From neuron to behaviour, Oxford University Press, New York, pp 457-463.**

Kubota, K. (1994) Learning of a hiding task and a delayed response task in infant rhesus monkeys. **Neurosci. Res. 18:301-313.**

Kubota, K. and H. Niki (1971) Prefrontal cortical unit activity and delayed alternation performance in monkeys. **J. Neurophysiol. 34:337-347.**

Kubota, K., T. Iwamoto and H. Suzuki (1974) Visuokinetic activities of primate prefrontal neurons during delayed-response performance. **J. Neurophysiol 37:1197-1211.**

Kuypers H.G.J.M., M.K. Szwarcbart, M. Mishkin and H.E. Rosvold (1965) Occipitotemporal cortical connections in the rhesus monkey. **Exp. Neurol. 11:245-262.**

LaMantia, A.-S. and P. Rakic (1990) Axon overproduction and elimination in the corpus callosum of the developing rhesus monkey. **J. Neurosci. 10:2156-2175.**

LaMantia, A.-S. and P. Rakic (1994) Axon overproduction and elimination in the anterior commissure of the

developing rhesus monkey. **J. Comp. Neurol. 340:328-336.**

Lauder, J.M. (1993) Neurotransmitters as growth regulatory signals: Role of receptors and second messengers. **Trends Neurosci. 16:233-239.**

Lauder, J.M. and H. Krebs (1978) Serotonin as a differentiation signal during development. **Dev. Neurosci. 1:15-30.**

Lawrence, D.G. and D.A. Hopkins (1976) The development of motor control in the rhesus monkey: Evidence concerning the role of corticomotoneuronal connections. **Brain 99:235-254.**

LeVay, S., T.N. Wiesel and D.H. Hubel (1980) The development of ocular dominance columns in normal and visually-deprived monkeys. **J. Comp. Neurol. 191:1-51.**

Levitt, J.B., D.A. Lewis, T. Yoshioka and J.S. Lund (1993) Topography of pyramidal neuron intrinsic connections in macaque monkey prefrontal cortex (areas 9 and 46). **J. Comp. Neurol. 338:360-376.**

Lewis, D.A. (1990) The organisation of chemically-identified neural systems in monkey prefrontal cortex: Afferent systems. **Prog. Neuropsychopharmacol. & Biol. Psychiat. 14:371-377.**

Lewis, D.A. and S.A. Anderson (1995) The functional architecture of the prefrontal cortex and schizophrenia. **Psychol. Med. 25:887-894.**

Lewis, D.A., M.J. Campbell, S.L. Foote, M. Goldstein and J.H. Morrison (1985) An immunohistochemical characterisation of the dopaminergic (DA), noradrenergic (NA), and serotonergic (5HT) innervation of primate prefrontal and temporal cortical regions. **Soc. Neurosci. Abstr. 13:154.**

Lewis, D.A., M.J. Campbell, S.L. Foote, M. Goldstein and J.H. Morrison (1987) The distribution of tyrosine hydroxylase-immunoreactive fibres in primate neocortex is widespread but regionally specific. **J. Neurosci. 7(1):279-290.**

Lewis, D.A., S.L. Foote, M. Goldstein and J.H. Morrison (1988) The dopaminergic innervation of monkey prefrontal cortex: a tyrosine hydroxylase immunohistochemical study. **Brain Res. 449:225-243.**

Lewis, D.A., V.A. Hawrylak, D.S. Melchitzky and S.R. Sesack (1996) Dopamine terminals in the monkey prefrontal cortex selectively innervate parvalbumin-containing local circuit neurons. **Soc. Neurosci. Abstr. 22:1321.**

Lewis D.A. and J.S. Lund (1990) Heterogeneity of chandelier neurons in monkey neocortex: Corticotropin-releasing factor- and parvalbumin-immunoreactive populations. **J. Comp. Neurol. 293:599-615.**

Li, B-M. and Z-T. Mei (1994) Delayed-response deficit induced by local injection of the α_2-adrenergic antagonist yohimbine into the dorsolateral prefrontal cortex in young adult monkeys. **Behav. Neural. Biol. 62:134-139.**

Lidov, H.G.W., R. Grzanna and M.E. Molliver (1980) The serotonergic innervation of the rat cerebral cortex -an immunohistochemical analysis. **Neurosci. 5:207-227.**

Lidov, H.G.W. and M.E. Molliver (1982) An immunohistochemical study of serotonin neuron development in the rat: Ascending pathways and terminals fields. **Brain Res. Bull. 8:389-430.**

Lidow, M.S. and P.S. Goldman-Rakic (1994) A common action of clozapine, haloperidol and remoxipride on D_1 and D_2-dopaminergic receptors in the primate cerebral cortex. **Proc. Natl. Acad. Sci. USA 91:4353-4356.**

Luciana, M. and C.A. Nelson (1996) Evidence for sequential development of temporal then frontal lobe functions in 4-to-8 year old children. **Soc. Neurosci. Abstr. 22:1107.**

Lund, J.S. (1973) Organisation of neurons in the visual cortex, area 17, of the monkey (*Macaca mulatta*). **J. Comp. Neurol. 147:147-496.**

Lund, J.S. and S.M. Holbach (1991) Postnatal development of thalamic recipient neurons in the monkey striate cortex: I. Comparison of spine acquisition and dendritic growth of layer 4C alpha and beta spiny stellate neurons. **J. Comp. Neurol. 309:115-128.**

Lund, J.S., S.M. Holbach and W.W. Chung (1991) Postnatal development of thalamic recipient neurons in the monkey striate cortex: II. Influence of afferent driving on spine acquisition and dendritic growth of layer IVCα and β spiny stellate neurons. **J. Comp. Neurol. 309:115-128.**

Lund, J.S., D.A. Lewis (1993) Local circuit neurons of developing and mature macaque prefrontal cortex: Golgi and immunocytochemical characteristics. **J. Comp. Neurol. 328:282-312.**

Lundberg, T., L. Lindström, P. Hartvig, L. Reibring, H. Ågren, H. Lundqvist, K.J. Fasth, G. Antoni and B. Långström. (1996) Serotonin-2 and dopamin-1 binding components of clozapine in frontal cortex and striatum in the human brain visualised by positron emission tomography. **Psychiat. Res. Neuroimaging 67:1-10.**

MacBrown, R. and P.S. Goldman (1977) Catecholamines in neocortex of rhesus monkeys: regional distribution and ontogenetic development. **Brain Res. 124:576-580.**

MacLuskey, N.J., F. Naptolin and P.S. Goldman-Rakic (1986) Oestrogen formation and binding in the cerebral cortex of the developing rhesus monkey. **Proc. Natl. Acad. Sci. USA. 83:531-516.**

McClean, J.H. and M.T. Shipley (1987a) Serotonergic afferents to the rat olfactory bulb: I. Origins and laminar specificity of serotonergic inputs in the adult rat. **J. Neurosci. 7:3016-3028.**

McClean, J.H. and M.T. Shipley (1987b) Serotonergic afferents to the rat olfactory bulb: II. Changes in fibre distribution during development. **J. Neurosci. 7:3029-3039.**

McGuire, B.A., C.D. Gilbert, P.K. Rivlin and T.N. Wiesel (1991) Targets of horizontal connections in macaque primary visual cortex. **J. Comp. Neurol. 305:370-392.**

Mamounas, L.A and M.E. Molliver (1988) Evidence for dual serotonergic projections to neocortex: Axons from the dorsal and median raphe nuclei are differentially vulnerable to the neurotoxin p-chloroamphetamine (PCA). **Expl. Neurol. 102:23-36.**

Mamounas, L.A., C.A. Mullen, E. O'Hearn and M.E. Molliver (1991) Dual serotoninergic projections to forebrain in the rat: Morphologically distinct 5-HT axon terminals exhibit differential vulnerability to neurotoxic amphetamine derivatives. **J. Comp. Neurol. 314:558-586.**

Mates, S.L. and J.S. Lund (1983a) Spine formation and maturation of type 1 synapses on spiny stellate neurons in primate visual cortex. **J. Comp. Neurol. 221:91-97.**

Mates, S.L. and J.S. Lund (1983b) Developmental changes in the relationship between type 2 synapses on spiny neurons in the monkey visual cortex. **J. Comp. Neurol. 221:98-105.**

Matsukawa, M., K. Nakadate and N. Okado (1995) Synaptic loss following removal of serotonergic and/or noradrenergic fibres in the visual cortex of the developing and adult rat. **Soc. Neurosci. Abstr. 21:445.**

Mattay, V.S., K.F. Berman, J.L. Ostrem, G. Esposito, J.D. Van Horn, L.B. Bigelow and D.R. Weinberger (1996). Dextroamphetamine enhances "neural network-specific" physiological signals: A positron-emission tomography rCBF study. **J. Neurosci. 16:4816-4822.**

Melchitzky, D.S., S.R. Sesack and D.A. Lewis (1996) Synaptic targets of intrinsic and associational cortical projections of pyramidal neurons in monkey prefrontal cortex. **Soc. Neurosci. Abstr. 22:905.**

Melchitzky, D.S., S.R. Sesack, M.L. Pucak and D.A. Lewis (1995) Synaptic targets of pyramidal neuron axon collateral's providing horizontal connections in monkey prefrontal cortex. **Soc. Neurosci. Abstr. 21:409.**

Mendelson, M.J., M.M. Haith and P.S. Goldman-Rakic (1983) Scanning of compound geometric forms in infant rhesus monkeys. **Dev. Psychol. 19:387-397.**

Meneses, A. and E. Hong (1997) Effects of 5-HT_4 receptor agonists and antagonists in learning. **Pharmacol. Biochem. Behav. 56:347-351.**

Mesulam, M-M and E.J. Mufson (1982) Insula of the old world monkey. II: Efferent cortical input and comments on function. **J. Comp. Neurol. 212:38-52.**

Mishkin, M. (1964) Perseveration of central sets after frontal lesions in monkeys. **In Warren, J.M. and K. Akert (Eds) The Frontal Granular Cortex and Behaviour. McGraw-Hill Book Company, New York, pp 219-241.**

Morel, A. and J. Bullier (1990) Anatomical segregation of two cortical visual pathways in the macaque monkey. **Visual Neurosci. 4:555-578.**

Morrison, J.H. and S.L. Foote (1986) Noradrenergic and serotonergic innervation of cortical, thalamic and tectal structures in old and new world monkeys. **J. Comp. Neurol. 243:117-138.**

Morrison, J.H., S.L. Foote and F.E. Bloom (1984) Regional, laminar, developmental and functional characteristics of noradrenaline and serotonin innervation patterns in monkey cortex. **In. Palay, S.L and V. Chan-Palay (Eds) Monoamine Innervation of Cerebral Cortex. Alan R. Liss, Inc, New York, pp 61-75.**

Morrison, J.H., S.L. Foote, M.E. Molliver, F.E. Bloom and H.G.W. Lidov (1982) Noradrenergic and serotonergic fibres innervate complementary layers in monkey visual cortex: An immunohistochemical study. **Proc. Natl. Acad. Sci. USA. 79:2401-2405.**

Mower, G.D. (1991) Comparison of serotonin 5-HT_1 receptors and innervation in the visual cortex of normal and dark reared cats. **J. Comp. Neurol. 312:223-230.**

Mrzljak, L. and P.S. Goldman-Rakic (1992) Acetylcholinesterase reactivity in the frontal cortex of human and monkey: Contribution of AChE-rich pyramidal neurons. **J. Comp. Neurol. 324:261-281.**

Mrzljak L., M. Pappy, C. Leranth and P.S. Goldman-Rakic (1995) Cholinergic synaptic circuitry in the macaque prefrontal cortex. **J. Comp. Neurol. 357:603-617.**

Mrzljak, L., H.B.M. Uylings, C.G. Van Eden and M. Judás (1990) Neuronal development in human prefrontal cortex in prenatal and postnatal states. **In Uylings, H.B.M. et al (Eds.) The Prefrontal Cortex, its Structure, Function and Pathology, Progress in Brain Research, Vol. 85, Amsterdam, Elsevier, pp 185-222.**

Muck-Seler, D. and M. Diksic (1996) DL-fenfluramine increases the 5-HT synthesis rate in the terminals while decreasing it in the cell bodies of the rat brain. **Brain Res. 737:45-50.**

Mufson, E.J. and M.M. Mesulam (1982) Insula of the old world monkey. II: Afferent cortical output and comments on the claustrum. **J. Comp. Neurol. 212:23-37.**

Muller, K., B. Ebner and V. Homberg (1994) Maturation of fastest afferent and efferent central and peripheral pathways: No evidence for a constancy of central conduction delays. **Neurosci. Letts. 166:9-12.**

Mulligan, K.A. and I. Törk (1987) Serotonergic axons form basket-like terminals in cerebral cortex. **Neurosci. Letts. 81:7-12.**

Mulligan, K.A. and I. Törk (1988) Serotoninergic innervation of the cat cerebral cortex. **J. Comp. Neurol. 270:86-110.**

Mulligan, K.A. and I. Törk (1993) Serotoninergic innervation of area 17 in the cat. **Cerebral Cortex 3:108-121.**

Neal, J.W., R.C.A. Pearson and T.P.S. Powell (1990) The connections of area PG, 7a, with cortex in the parietal, occipital and temporal lobes of the monkey. **Brain Res. 532:249-264.**

Niki, H. (1974a) Prefrontal unit activity during delayed alternation in the monkey. I. Relation to direction of response. **Brain Res. 68:185-196.**

Niki, H. (1974b) Prefrontal unit activity during delayed alternation in the monkey. II. Relation to absolute versus relative direction of response. **Brain Res. 68:185-196.**

Niki, H. (1974c) Differential activity of prefrontal units during right and left delayed response trials. **Brain Res. 70:346-349.**

Niki, H. and M. Watanabe (1979) Prefrontal and cingulate unit activity during timing behaviour in the monkey. **Brain Res. 171:213-224.**

Nishi, M., P.M. Whitaker-Azmitia, E.C. Azmitia (1996) Enhanced synaptophysin immunoreactivity in rat hippocampal culture by 5-HT_{1A} agonist, S100ß and corticosteroid receptor agonists. **Synapse 23:1-9.**

Noack, H.J. and D.A. Lewis (1989) Antibodies directed against tyrosine hydroxylase differentially recognise noradrenergic axons in monkey neocortex. **Brain Res. 500:313-324.**

Nomikos, G.G., M. Iurlo, J.L. Andersson, K. Kimura and T.H. Svensson (1994) Systemic administration of amperozide: A new atypical antipsychotic drug, preferentially increases dopamine release in the rat prefrontal cortex.. **Psychopharmacol. 115:147-156.**

Nomura, Y., H. Sakuma, K. Takeda, T. Tagami, Y. Okuda and T. Nakagawa (1994) Diffusional anisotropy of the human brain assessed with diffusion-weighted MR: Relation with normal brain development and ageing. **Am. J. Neuroradiol. 15:231-238.**

Oeth, K.M. and D.A. Lewis (1993) Postnatal development of the cholecystokinin innervation of monkey prefrontal cortex. **J. Comp. Neurol. 336:400-418.**

Ogawa, M., M. Matsukawa and N. Okado (1995) Synaptic loss following removal of serotonergic and/or cholinergic fibres in the hippocampus **Soc. Neurosci. Abstr. 21:1217.**

Oliver, E., S.A. Edgley, J. Armand and R.N. Lemon (1997) An electrophysiological study of the postnatal development of the corticospinal system in the macaque monkey. **J. Neurosci. 17:267-276.**

Osterheld-Haas, M.C., H. Van der Loos and J.P. Hornung (1994) Monoaminergic afferents to cortex modulate structural plasticity in the barrelfield of the mouse. **Dev. Brain Res. 77:189-202.**

Overman, W.H., J. Bachevalier, F. Sewell and J. Drew (1993) A comparison of children's performance on two recognition memory tasks: Delayed nonmatch-to-sample versus visual paired-comparison. **Dev. Psychobiol. 26:345-357.**

Overman, W.H., J. Bachevalier, M. Turner and A. Peuster (1992) Object recognition versus object discrimination: Comparison between human infants and infant monkeys. **Behav. Neurosci. 106:15-29.**

Pandya, D.N., P. Dye and N. Butters (1971) Efferent corticocortical projections of the prefrontal cortex in the rhesus monkey. **Brain Res. 31:35-46.**

Pandya, D.N. and H.G.J.M. Kuypers (1969) Cortical-cortical connections in the rhesus monkey. **Brain Res. 13:13-36.**

Pandya, D.N. and E.H. Yeterian (1990) Prefrontal cortex in relation to other cortical areas in rhesus monkey: Architecture and connections. **In Uylings, H.B.M. et al (Eds) Progress in Brain Research, Vol. 85, Elsevier Science Publishers BV, Amsterdam, pp 63-94.**

Pandya, D.N. and E.H. Yeterian (1996a) Morphological correlation's of human and monkey frontal lobe. **In Damasio, A.R. et al (Eds) Neurobiology of Decision Making. Springer-Verlag, Berlin pp 13-46.**

Pandya, D.N. and E.H. Yeterian (1996b) Comparison of prefrontal architecture and connections. **Phil. Trans. R. Soc. Lond. B. 351:1423-1432.**

Parnavelas, J.G., H.C. Moises and S.G. Speciale (1985) The monoaminergic innervation of the rat visual cortex. **Proc. R. Soc. Lond. B. 223:319-329.**

Passingham. R.E. (1972a) Visual discrimination learning after selective prefrontal ablations in monkeys (*Macaca Mulatta*). **Neuropsychol. 10:27-39.**

Passingham, R.E. (1972b) Non-reversal shifts after selective prefrontal ablations in monkeys (*Macaca Mulatta*). **Neuropsychol. 10:41-46.**

Passingham, R.E. (1978) Information about movements in monkeys (*Macaca Mulatta*) with lesions of dorsal prefrontal cortex. **Brain Res. 152:313-328.**

Passingham, R.E. (1993) **The Frontal Lobes and Voluntary Action. Oxford Psychology Series No. 21, Oxford University Press, Oxford.**

Pehek, E. (1996) Local infusion of the serotonin antagonists ritanserin or ICS 205,930 increases *in vivo* dopamine release in the rat medial prefrontal cortex. **Synapse 24:12-18.**

Peters, A. (1984) Chandelier cells. **In Peters, A. and E.G. Jones (Eds) Cerebral Cortex. Vol. 1: Cellular components of the cerebral cortex. New York, NY: Plenum Press, pp 361-380.**

Petrides, M. (1991a) Monitoring of selections of visual stimuli and the primate frontal cortex. **Proc. R. Soc. Lond. B. 246:293-298.**

Petrides, M. (1991b) Functional specialisation within the dorsolateral frontal cortex for serial order memory. **Proc. R. Soc. Lond. B. 246:299-306.**

Petrides, M. (1995) Impairments on non-spatial self-ordered and externally ordered working memory tasks after lesions of the mid-dorsal part of the lateral frontal cortex in the monkey. **J. Neurosci. 15:359-375.**

Petrides, M. (1996) Specialised systems for the processing of mnemonic information within the primate frontal cortex. **Phil. Trans. R. Soc. Lond. B. 351:1455-1462.**

Petrides, M. and D.N. Pandya (1984) Projections to the frontal cortex from the posterior parietal region in the rhesus monkey. **J. Comp. Neurol. 228:105-116.**

Petrides, M. and D.N. Pandya (1988) Association fibre pathways to the frontal cortex from the superior temporal region in the rhesus monkey. **J. Comp. Neurol. 273:52-66.**

Petrides, M and D.N. Pandya (1994) Comparative architectonic analysis of the human and macaque frontal cortex. **In Grafman, J. and F. Boller (Eds) Handbook of Neuropsychology. Elsevier Science Publishers BV, Amsterdam, pp 17-58.**

Plant, T. (1988) Neuroendocrine basis of puberty in the rhesus monkey (*Macaca Mulatta*). **In Martini, L. and W.F. Ganong (Eds) Frontiers in Endocrinology. Raven Press, Ltd., New York. 10:215-238.**

Porrino, L.J. and P.S. Goldman-Rakic (1982) Brainstem innervation of prefrontal cortex and anterior cingulate cortex in the rhesus monkey revealed by retrograde transport of HRP. **J. Comp. Neurol. 205:63-76.**

Preuss, T.M. and P.S. Goldman-Rakic (1991) Myelo- and cytoarchitecture of the granular frontal cortex and surrounding regions in the strepsirhine primate Galago and the anthropoid primate *Macaca*. **J. Comp. Neurol. 310:429-474.**

Pucak, M.L., J. B. Levitt, J.S. Lund and D.A. Lewis (1996) Patterns of intrinsic and associational circuitry in monkey prefrontal cortex. **J. Comp. Neurol. 376:614-630.**

Quencer, R.M. (1982) Maturation of normal primate white matter: Computed tomographic correlation. **Am. J. Roentgenol. 139:561-568.**

Rakic, P., J-P. Bourgeois, M.F. Eckenhoff, N. Zecevic and P.S. Goldman-Rakic (1986) Concurrent overproduction of synapses in diverse regions of the primate cerebral cortex. **Science 232:232-234.**

Rakic, P., J-P. Bourgeois and P.S. Goldman-Rakic (1994) Synaptic development of the cerebral cortex: Implications for learning, memory, and mental illness. **Brain Res. 102:227-243.**

Raleigh, M.J., G.L. Brammer, M.T. McGuire and A. Yuwiler (1985) Dominant social status facilitates the behavioural effects of serotonergic agonists. **Brain Res. 348:274-282.**

Raleigh, M.J., M.T. McGuire, G.L. Brammer and A. Yuwiler (1984) Social and environmental influences on blood serotonin concentrations in monkeys. **Arch. Gen. Psychiat. 41:405-410.**

Raleigh, M.J., M.T. McGuire, G.L. Brammer, D.B. Pollack and A. Yuwiler (1991) Serotonergic mechanisms promote dominance acquisition in adult male vervet monkeys. **Brain Res. 559:181-190.**

Raleigh, M.J., M.T. McGuire, W.P. Melega, S. Cherry, S.-C. Huang and M.E. Phelps (1996a) Neural mechanisms supporting successful social decisions in simians. **In Damasio, A.R. et al (Eds) Neurobiology of Decision-Making, Springer-Verlag, Berlin. pp 63-82.**

Raleigh, M.J., W.P. Melega, S.-C. Huang, S. Cherry, M.T. McGuire, M. Burton-Jones and M.E. Phelps (1996b) Enrichment during development induces enduring increases in resting cerebral glucose metabolism in monkey. **Soc. Neurosci. Abstr. 22:1133.**

Raleigh, M.J., W.P. Melega, S.-C. Huang, S. Cherry, M.T. McGuire and M.E. Phelps (1995) Sex differences in resting cerebral glucose metabolism in monkeys. **Soc. Neurosci. Abstr. 21:2022.**

Reader, T.A., A. Ferron, L. Descarries and H.H. Jasper (1979) Modulatory role for biogenic amines in the cerebral cortex microiontophoretic studies. **Brain Res. 160:217-229.**

Reiss, A.L., M.T. Abrams, H.S. Singer, J.L. Ross and M.B. Denckla (1996) Brain development, gender and IQ in children - a volumetric imaging study. **Brain 119:1763-1774.**

Rhoades, R.W., C.A. Bennett-Clarke, N.L. Chiaia, F.L. White, G.J. McDonald, J.H. Haring and M.F. Jacquin. (1990) Development and lesion induced reorganisation of the cortical representation of the rat's body surface as revealed by immunocytochemistry for serotonin. **J. Comp. Neurol. 293:190-207.**

Rogers, J. (1989) Calcium-binding proteins: The search for functions. **Nature 339:661-662.**

Romanski, L.M., M. Giguere, J.F. Bates and P.S. Goldman-Rakic (1997) Topographic organisation of medial pulvinar connections with the prefrontal cortex in the rhesus monkey. **J. Comp. Neurol. 379:313-332.**

Rörig, B., G. Klausa and B. Sutor (1995a) Modulatory neurotransmitters reduce dye-coupling between developing lamina II/III pyramidal neurons in rat neocortex. **Soc. Neurosci. Abstr. 21:1509.**

Rörig, B., G. Klausa and B. Sutor (1995b) Dye coupling between pyramidal neurons in developing rat and frontal cortex is reduced by protein kinase A activation and dopamine. **J. Neurosci. 15:7386-7400.**

Rörig, B. and B. Sutor (1996) Serotonin regulates gap junction coupling in the developing rat somatosensory cortex. **Eur. J. Neurosci. 8:1685-1695.**

Rosenberg, D.R. and D.A. Lewis (1994) Changes in the dopaminergic innervation of monkey prefrontal cortex during late postnatal development: A tyrosine hydroxylase immunohistochemical study. **Biol. Psychiat. 36:272-277.**

Rosenberg, D.R. and D.A. Lewis (1995) Postnatal maturation of the dopaminergic innervation of monkey prefrontal and motor cortices: A tyrosine hydroxylase immunohistochemical analysis. **J. Comp. Neurol. 358:383-400.**

Sakai, M. (1974) Prefrontal unit activity during visually-guided lever pressing reaction in the monkey. **Brain Res. 81:297-309.**

Saugstad, L.F. (1994) The maturational theory of brain development and cerebral excitability in the multifactorially inherited manic-depressive and schizophrenia. **Int. J. Psychophysiol. 18:187-188.**

Sawaguchi, T. (1987a) Properties of neuronal activity related to a visual reaction time task in the monkey prefrontal cortex. **J. Neurophysiol. 58:1080-1099.**

Sawaguchi, T. (1987b) Catecholamine sensitivities of neurons related to a visual reaction time task in the monkey prefrontal cortex. **J. Neurophysiol. 58:1100-1122.**

Sawaguchi, T. and P.S. Goldman-Rakic (1991) D_1-dopamine receptors in prefrontal cortex: Involvement in working memory. **Science 251:947-950.**

Sawaguchi, T. and P.S. Goldman-Rakic (1994) The role of D_1-dopamine receptors in working memory: Local injections of dopamine antagonists into the prefrontal cortex of rhesus monkeys performing on oculomotor delayed-response task. **J. Neurophysiol. 71:515-528.**

Sawaguchi, T, M. Matsumura and K.Kubota (1986) Dopamine modulates neuronal activities related to motor performance in the monkey prefrontal cortex. **Brain Res. 371:404-408.**

Sawaguchi, T., M. Matsumura and K. Kubota (1988) Delayed response deficit in monkeys by locally disturbed prefrontal neuronal activity by bicuculline. **Behav. Brain Res. 31:193-198.**

Sawaguchi, T., M. Matsumura and K. Kubota (1990a) Catecholaminergic effects on neuronal activity related to a delayed response task in monkey prefrontal cortex. **J. Neurophysiol. 63:1385-1400.**

Sawaguchi, T., M. Matsumura and K. Kubota (1990b) Effects of dopamine antagonists on neuronal activity related to a delayed response task in monkey prefrontal cortex. **J. Neurophysiol. 63:1401-1412.**

Schall, J.D., A. Morel, D.J. King and J. Bullier (1995) Topography of visual cortex connections with frontal eye field in macaque: Convergence and segregation of processing streams. **J. Neurosci. 15:4464-4487.**

Schmidt, C.J., S.M. Sorensen, J.H. Kehne, A.A. Carr and M.G. Palfreyman (1995) The role of 5-HT_{2A} receptors in antipsychotic activity. **Life Sci. 56:2209-2222.**

Schwartz, M.L. and L. Mrzljak (1992) Serotoninergic, noradrenergic and dopaminergic innervation of the primate mediodorsal thalamic nucleus. **Soc. Neurosci. Abstr. 18:1418.**

Selemon, L.D. and P.S. Goldman-Rakic (1985) Longitudinal topography and interdigitation of corticostriatal projections in the rhesus monkey. **J. Neurosci. 5:776-794.**

Seltzer, B. and D.N. Pandya (1984) Further observations on parieto-temporal connections in the rhesus monkey. **Exp. Brain. Res. 55:301-312.**

Seltzer, B. and D.N. Pandya (1989) Frontal lobe connections of the superior temporal sulcus in the rhesus monkey. **J. Comp. Neurol. 281:97-113.**

Seltzer, B. and D.N. Pandya (1994) Parietal, temporal, and occipital projections to cortex of the superior temporal sulcus in the rhesus monkey: A retrograde tracer study. **J. Comp. Neurol. 343:445-463.**

Sesack, S.R., C.N. Bressler and D.A. Lewis (1995a) Ultrastructural associations between dopamine terminals and local circuit neurons in the monkey prefrontal cortex: A study of calretinin-immunoreactive cells. **Neurosci. Letts. 200:9-12.**

Sesack, S.R., S.W. King, C.N. Bressler, S.J. Watson and D.A. Lewis (1995b) Electron microscopic visualisation of dopamine D_2 receptors in the forebrain: Cellular, regional and species comparisons. **Soc. Neurosci. Abstr. 21:150.**

Sholl, D.A. (1953) Dendritic organisation in the neurons of the visual and motor cortices of the cat. **J. Anat. 87:387-406.**

Sirvio, J., P. Riekkinen, Jr, P.J. Jakala and PJ. Riekkinen. (1994) Experimental studies on the role of

serotonin in cognition. **Prog. Neurobiol. 43:363-379.**

Siwek, D.F. and D.N. Pandya (1991) Prefrontal projections to the mediodorsal nucleus of the thalamus in the rhesus monkey. **J. Comp. Neurol. 312:509-524.**

Smiley, J.F. and P.S. Goldman-Rakic (1993) Heterogeneous targets of dopamine synapses in monkey prefrontal cortex demonstrated by serial section electron microscopy: A laminar analysis using the silver-enhanced diaminobenzidine sulphide (SEDS) immunolabelling technique. **Cerebral Cortex 3:223-238.**

Smiley, J.F. and P.S. Goldman-Rakic (1996) Serotonergic axons in monkey prefrontal cerebral cortex synapse predominantly on interneurons as demonstrated by serial section electron microscopy. **J. Comp. Neurol. 367:431-443.**

Smith, G.S., S.L. Dewey, J.D. Brodie, J. Logan, S.A. Vitkun, P. Simkowitz, R. Schloesser, D.A. Alexoff, A. Hurley, T. Cooper and N.D. Volkow (1997) Serotonergic modulation of dopamine measured with [^{11}C]-raclopride and PET in normal human subjects. **Am. J. Psychiat. 490-496.**

Somogyi, P. (1977) A specific "axo-axonal" interneuron in the visual cortex of the rat. **Brain. Res. 136:345-350.**

Somogyi, P. (1979) An interneurone making synapses specifically on the axon initial segment of pyramidal cells in the cerebral cortex of the cat. **J. Physiol. 296:18p-19p.**

Somogyi, P. and A. Cowey (1984) Double bouquet cells. **In Peters, A. and E.G. Jones (Eds) Cerebral Cortex. Vol. 1: Cellular components of the cerebral cortex. New York, NY: Plenum Press, pp 337-360.**

Somogyi, P., A. Cowey, N. Halasz and T.F. Freund (1981) Vertical organisation of neurons accumulating [^{3}H]-GABA in visual cortex of rhesus monkey. **Nature 294:761-763.**

Somogyi, P., A. Cowey, Z.F. Kisvárday, T.F. Freund and J. Szentogothai (1983) Retrograde transport of γ-amino-[^{3}H]-butyric acid reveals specific interlaminar connections in the striate cortex of monkey. **Proc. Natl. Acad. Sci. USA. 80:2385-2389.**

Somogyi, P., T. F. Freund and A. Cowey (1982) The axo-axonic interneuron in the cerebral cortex of the rat, cat and monkey. **Neurosci. 7:2577-2607.**

Spoont, M.R. (1992) Modulatory role of serotonin in neural information processing: Implications for human psychopathology. **Psycholog. Bull. 112:330-350.**

Takeuchi, Y. and Y. Sano (1983) Immunohistochemical demonstration of serotonin nerve fibres in the neocortex of the monkey (*Macaca fuscata*). **Anat. Embryol. 166:155-168.**

Thatcher, R.W., R.A. Walker and S. Giudice (1987) Human cerebral hemispheres develop at different rates and ages. **Science 236:1110-1113.**

Tiihonen, J., M. Kuoppamäki, K. Någren, J. Bergman, E. Eronen, E. Syvälahti and J. Hietala (1996) Serotonergic modulation of striatal D_2 dopamine receptor binding in humans measured with positron emission tomography. **Psychopharmacol.126:277-280.**

Trojanowski, J.Q. and S. Jacobson (1976) Areal and laminar distribution of some pulvinar cortical efferents in rhesus monkey. **J. Comp. Neurol. 169:371-392.**

Turlejski, K. and R. Djavadian (1996) Impaired developmental elimination of callosal and claustral projections to cortical areas 17 and 18 in cats neonatally depleted of serotonin. **Soc. Neurosci. Abstr. 22:605.**

Uylings, H.B.M., L. Mrzljak, M.J.T. Koenderink and R.J.K. Kramers (1995) Neural maturation and transient phases in development of human prefrontal cortex. **Eur. J. Morphol. 33:222-223.**

Van Brederode, J.F.M., K.A. Mulligan and A.E. Hendrickson (1990) Calcium-binding proteins as markers for sub-populations of GABAergic neurons in monkey striate cortex. **J. Comp. Neurol. 298:1-22.**

Varela, J., K. Richards and S.B. Nelson (1995) Modulation of synaptic inputs to visual cortical neurons by adenosine and 5-HT. **Soc. Neurosci. Abstr. 21:1654.**

Vogt, C. and O. Vogt (1919) Allgemeine ergebnisse unserer hirnforschung. **J. Psychol. Neurol. 25:279-462.**

Voigt, T. and A.D. De Lima (1991) Serotoninergic innervation of the ferret cerebral cortex I. Adult pattern. **J. Comp. Neurol. 314:403-414.**

Vu, D.H. and I. Tork (1992) Differential development of the dual serotoninergic fibre system in the cerebral cortex of the cat. **J. Comp. Neurol. 317:156-174.**

Walker, A.E. (1940) A cytoarchitectural study of the prefrontal area of the macaque monkey **J. Comp. Neurol. 73:59-86.**

Wang, Y.C., Q. Gu, Y.L. Liu, R. Douglas and M. Cynader (1994) Electrophysiological evidence of neuronal activities of cells in kitten visual cortex: *In vivo* and *in vitro* studies. **Soc. Neurosci. Abstr. 20:321.**

Watanabe, M. (1981) Prefrontal unit activity during delayed conditional discriminations in the monkey. **Brain Res. 225:51-65.**

Weinberger, D.R. (1988) Schizophrenia and the frontal lobe. **Trends Neurosci. 11:367-370.**

Weinberger, D.R. (1995) Schizophrenia: From neuropathology to neurodevelopment. **The Lancet 346:552-557.**

Weinberger, D.R. (1996) On the plausibility of "the neurodevelopmental hypothesis" of schizophrenia. **Neuropsychopharmacol. 14:1S-11S.**

Weinberger, D.R. and K.F. Berman (1996) Prefrontal function in schizophrenia: Confounds and controversies. **Phil. Trans. R. Soc. Lond. B. 351:1495-1503.**

Whitaker-Azmitia P.M., A. Borella and J. Muneyyici (1995) Depletion of serotonin during peak synaptogenesis in immature rats leads to loss of a dendritic marker (MAP-2) and learning disabilities as adults. **Soc. Neurosci. Abstr. 21:863.**

Whitaker-Azmitia P.M., M. Druse, P. Walker and J.M. Lauder (1996) Serotonin as a developmental signal. **Behav. Brain Res. 73:19-29.**

Williams, G.V. and P.S. Goldman-Rakic (1995) Modulation of memory fields by dopamine D_1 receptors in prefrontal cortex. **Nature 376:572-575.**

Williams, G.V., P.S. Goldman-Rakic and C. Leranth (1990) Characterisation of parvalbumin neurons and axons in the primate prefrontal cortex. **Soc. Neurosci. Abstr. 16:106.**

Williams, G.V., S.G. Rao, M. Franowitz, L. Romanski and P.S. Goldman-Rakic (1996) Ritanserin reduces activity of prefrontal neurons recorded during working memory tasks. **Soc. Neurosci. Abstr. 22:1936.**

Williams, S.M. and P.S. Goldman-Rakic (1993) Characterisation of the dopaminergic innervation of the primate frontal cortex using a dopamine-specific antibody. **Cerebral Cortex 3:199-222.**

Williams, S.M., P.S. Goldman-Rakic and C. Leranth (1992) The synaptology of parvalbumin-immunoreactive neurons in the primate prefrontal cortex. **J. Comp. Neurol. 320:353-369.**

Wilson, M.A. and M.E. Molliver (1986) Serotonin innervation patterns in primate cerebral cortex: Specific local ablations. **Soc. Neurosci. Abstr. 12:120.**

Wilson, M.A. and M.E. Molliver (1991a) The organisation of serotonergic projections to cerebral cortex in primates: Regional distribution of axon terminals. **Neurosci. 44:537-553.**

Wilson, M.A. and M.E. Molliver (1991b) The organisation of serotonergic projections to cerebral cortex in primates: Retrograde transport studies. **Neurosci. 44:555-570.**

Wilson, M.A., G.A. Ricaurte and M.E. Molliver (1989) Distinct morphologic classes of serotonergic axons in primates exhibit differential vulnerability to the psychotropic drug-3,4-methylenedioxymethamphetamine. **Neurosci. 28:121-137.**

Woo, T.-U., M.L. Pucak, C.H. Kye, C.V. Matus and D.A. Lewis (1997) Peripubertal refinement of the intrinsic and associational circuitry in monkey prefrontal cortex. **Neurosci. 80:1149-1158.**

Yakovlev and Lecours (1967) The myelogenetic cycles of regional maturation of the brain. **In: Minowski, A. (Ed) Regional development of the brain in early life, pp 3-70, Oxford: Blackwell.**

Yan, W., C.C. Wilson, W.M. Panneton and J.H. Haring (1995) Neonatal 5-HT depletion reduces dentate granule cell spine density. **Soc. Neurosci. Abstr. 21:862.**

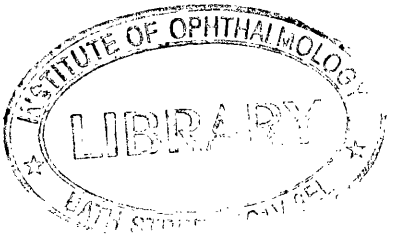

17.0: Acknowledgements.

During the course of this thesis many people have been of assistance to me and without them it would have been impossible to complete the finished work. I would first of all like to thank my supervisor, Professor. Jennifer Lund for giving me the opportunity to undertake my PhD studies at the Institute of Ophthalmology, for her grant support and for much incisive discussion and critical comment, along the way. The financial support for the work within this thesis was provided by NIMH (USA NIH) grant (code FA/R1).

Also I am grateful to Professor. David Lewis at the Department of Psychiatry and Neuroscience in the University of Pittsburgh, for providing much of the animal tissue and for useful discussions.

In addition, I would like to extend gratitude to Richard Whitehead in Professor Lewis' laboratory for histological assistance in the 5-HT study during my visit to Pittsburgh.

For photographic assistance and advice I would like to thank Stephen Griffiths in our lab and Mary Brady in Professor Lewis' lab.

Dr. Jonathan Levitt, Professor. James Bowmaker and Dr. Glenn Jeffrey have been invaluable sources of discussion and reassurance during the progress of the work.

Finally, last but certainly not least, I would like to thank my wife, Suzanne Claxton for being a tower of strength and understanding during the long course of this thesis. I am eternally grateful to her for her superlative organising skills in the closing stages of writing-up.

18.0: Abbreviations.

ACh	Acetylcholine
AIS	Axon initial segment
AMPA	α-amino-3-hydroxy-5-methyl-4-isoxazolepropanoic acid
AS	Arcuate sulcus
BDA	Biotinylated dextran amine
c	Caudal
CalB	Calbindin-positive
CalR	Calretinin-positive
CBP	Calcium-binding protein
CCK	Cholecystokinin
ChAT	Cholineacetyltransferase
CS	Central sulcus
CtB	Cholera toxin subunit-B
d	Dorsal
DA	Dopamine
2DG	2-[^{14}C]-deoxyglucose
DLPFC	Dorsolateral prefrontal cortex
DR	Delayed response task
DRN	Dorsal raphe nucleus
E	Embryonic
EEG	Electroencephalography
EM	Electron microscopy
fMRI	functional magnetic resonance imaging
GABA	Gamma-aminobutyric acid
5-HT	5-hydroxytryptamine (serotonin)
5-HTP	5-hydroxytryptophan
5-HTr	5-HT receptor
5-HIAA	5-hydroxyindoleacetic acid
Ia-p	Insula, agranular periallocortical
Idg	Insula, dysgranular
Ig	Insula, granular
IP	Intraparietal
IPa	Anterior inferior parietal area
IPL	Inferior parietal lobule
IPS	Intraparietal sulcus
IR	Immunoreactive
KA	Koniocortex
LCGU	Local cerebral glucose uptake
LIP	Lateral intraparietal area
LOS	Lateral orbital sulcus
LM	Light microscopy
LTD	Long term depression
LTP	Long term potentiation
mc	Magnocellular
MD	Mediodorsal nucleus
MDmf	Mediodorsal nucleus multiform subdivision
MOS	Medial orbital sulcus
MRI	Magnetic resonance imaging (structural)
MRN	Median raphe nucleus
MT	Middle temporal area
NA	Noradrenaline
NMDA	N-methyl-D-aspartate
NMDAR1	NMDA receptor 1
OA	area 19 (lower bank of STS)
OAa	Caudal depth and ventral bank of STS
OBF	Orbitofrontal cortex
ODR	Oculomotor delayed response
Opt	Caudalmost IPL
P	Pyramidal

Pa-Alt	Lateral parakoniocortex zone (in caudal dorsal STG)
pc	Parvocellular
PET	Positron emission tomography
PE	Caudal-dorsal parietal region
PF	Rostral-most IPL
PFC	Prefrontal cortex
PFG	Rostral middle IPL
PG	Caudal middle IPL
PI	Inferior pulvinar nucleus
PL	Lateral pulvinar nucleus
PM	Medial pulvinar nucleus
POa	Ventral bank of IPS
POa-e	External portion of ventral of IPS
ProA	Prokoniocortex
ProM	Rostral premotor cortex
PS	Principal sulcus
PV	Parvalbumin-positive
r	Rostral
S	Smooth, interneuron
S-I	Primary somatosensory cortex
SN	Substantia nigra
ST	Superior temporal region
STG	Superior temporal gyrus
STP	Superior temporal polysensory cortex
STS	Superior temporal sulcus
TAa	Rostro-caudally extensive strip of cortex in dorsal bank of STS
TEa	Rostral portion of ventral bank of STS
TEm	Middle dorsal inferior temporal cortex on lip of ventral bank of STS
TH	Tyrosine hydroxylase
TPO-1/2/3/4	Rostral, rostral middle, caudal middle and caudal sectors of dorsal STS (STP)
Tpt	Temporoparietal zone (caudal STG)
Ts1/2/3	Temporalis superior zones (anterior, middle and posterior portions of rostral dorsal STG)
v	ventral
V1	Primary visual cortex (area 17)
VTA	Ventral tegmental area
WBS	Whole blood serotonin

19.0: Published work resulting from this thesis.

1. Anderson, S.A., J.D. Classey, D.A. Lewis and J.S. Lund. (1993) Postnatal developmental changes in dendritic spine density on layer III pyramidal neurons in monkey prefrontal cortex. **Soc. Neurosci. Abs. 19:1445.**

2. Classey, J.D., S.A. Anderson, D.A. Lewis and J.S. Lund (1994) Postnatal developmental changes in dendritic spine density on layer III pyramidal neurons in monkey prefrontal cortex. **Brain Res. Assoc. Abstr. 11:28.4.**

3. Pucak, M.L., J.B. Levitt, J.D. Classey, J.S. Lund and D.A. Lewis (1994) Comparison of intra- and interareal patterns of connectivity in monkey prefrontal cortex. **Soc. Neurosci. Abs. 20:1416.**

4. Andersen, S.A., J.D. Classey, J.S. Lund, F. Condé and D.A. Lewis (1994) Postnatal remodelling of monkey prefrontal cortical circuitry. **Biol. Psychiatr. 35:706.**

5. Anderson, S.A., J.D. Classey, F. Condé, J.S. Lund and D.A. Lewis (1995) Synchronous development of markers of excitatory and inhibitory input to layer III pyramidal neurons in macaque prefrontal cortex. **Proc. Austral. Neurosci. Soc., Singer Symposium, Perth, Australia.**

6. Anderson, S.A., J.D. Classey, F. Condé, J.S. Lund and D.A. Lewis (1995) Synchronous development of pyramidal neuron dendritic spines and parvalbumin-immunoreactive chandelier neuron axon terminals in layer III of monkey prefrontal cortex. **Neuroscience 67:7-22.**